Novel approaches using human induced pluripotent stem cells and microRNAs in the development of relevant human hepatocyte models for drug-induced liver injury

Thesis submitted in accordance with the requirements of the University of Liverpool for the degree of Doctor in Philosophy

By

Richard Yin Kit Kia

October 2014

DECLARATION

This thesis is the result of my own work. The material contained within this thesis has not been presented, nor is currently being presented wholly, or in part, for any other degree of qualification.

Richard Yin Kit Kia

This research was undertaken at the Department of Molecular and Clinical Pharmacology and the MRC Centre for Drug Safety Science of the University of Liverpool.

TABLE OF CONTENTS

ABSTRACT

Novel approaches using human induced pluripotent stem cells and microRNAs in the development of relevant human hepatocyte models for drug-induced liver injury.

Richard Yin Kit Kia

Drug-induced liver injury (DILI) remains a prominent cause of patient morbidity and mortality, partly due to the lack of relevant *in vitro* hepatic models for accurate screening for drug-induced hepatotoxicity at the early stages of drug development, and also the lack of sophisticated *in vitro* model systems to mechanistically understand the pathways that are perturbed following drug exposure. This thesis describes our endeavour to develop more relevant *in vitro* human hepatocyte models via novel investigative approaches using insights gained from the rapidly advancing research areas of human induced pluripotent stem cells and microRNAs (miRs).

An emerging hepatic model is hepatocyte-like cells (HLCs) generated from human induced pluripotent stem cells (hiPSCs), though the functional phenotype of HLCs in general remains limited in comparison with the gold standard *in vitro* model of human primary hepatocytes (hPHs). As studies have shown that hiPSCs retain transient epigenetic memories of the donor cells despite cellular reprogramming with a resultant skewed propensity to differentiate towards the cell-type of origin, we evaluated the contribution of epigenetic memory towards hepatic differentiation by comparing HLCs generated from hPH- and non-hPH-derived hiPSC lines derived from a single donor. Our findings suggested that they were functionally similar, although comparison using hiPSC lines derived from other donors is still required to be conclusive.

Although hPHs remain the gold standard *in vitro* model for DILI, they are commonly harvested from liver tissue of poor quality and rapidly lose their *in vivo* phenotype during extended *in vitro* culture, limiting its utility to acute toxicity studies only. Using an unbiased miR expression profiling approach, we identified a set of differentially-expressed miRs in dedifferentiating hPHs which are associated with many of the previously delineated perturbed pathways and biological functions. However, validation experiments are now required to confirm our findings from the bioinformatics analyses.

Another approach taken to develop relevant and functional hepatic models includes efforts to better emulate the *in vivo* liver tissue environment by using complex hepatic models co-cultured with non-parenchymal cells. However, for the application of these models in the study of drug-induced toxicity, a hepatocyte-specific marker of hepatocyte perturbation is needed to discriminate non-specific cellular toxicity contributed by non-hepatocyte cell types present within the model. We demonstrated that the detection of miR-122 in cell culture media can be applied as a hepatocyte-enriched marker of toxicity in heterogeneous cultures of hepatic cells.

In summary, this thesis describes our contribution towards the continuing efforts to develop new and improve on existing hepatic models for DILI by evaluating the contribution of epigenetic memory towards the functional phenotype of HLCs, delineating the changing miR profile of dedifferentiating hPHs, and introduced the concept of using miR-122 as a cell-type specific marker of hepatocyte perturbation with a potential to bridge *in vitro* and *in vivo* findings.

ACKNOWLEDGEMENTS

First and foremost, I would like to express my utmost gratitude to my supervisors and mentors Dr. Chris Goldring, Dr. Neil Kitteringham, Professor Neil Hanley and Professor Kevin Park for their wisdom, patience and constant encouragement during my MRC fellowship and PhD study, without which this thesis would not have been at all possible. Thank you for this huge opportunity which undoubtedly has greatly influenced my clinical career and expanded my own belief in what I can attain.

I would also like to acknowledge my many MRC CDSS colleagues who selflessly guided a novice who had never previously held a pipette, and for sharing the joys and pains of experimental outcomes. More specifically, many thanks to James Heslop whose initials will be rightly immortalised in the name of our long-awaited first liver-derived hiPSC line, for his unwavering optimism, endless discussions and weekend shifts. I would also like to specifically thank Drs. Cliff Rowe and Rowena Sison-Young who helped in getting so many projects off the ground, but mainly for their kind friendship and prescient advice. Many thanks as well to all my collaborators who have contributed in various forms and capacity.

I would also like to acknowledge the Medical Research Council for its gracious award of the Clinical Training Fellowship and for generously funding my PhD study.

Lastly, as a formal record of my gratitude to the sacrifices of my wife Ai-Wei – thank you for being so accommodating and strong all these years. I dedicate this thesis to Isaac, who taught me to constantly inquire; and to Caitlin, who taught me perseverance.

LIST OF PUBLICATIONS

Kia, R., Sison, R. L., Heslop, J., Kitteringham, N. R., Hanley, N., Mills, J. S., Park, B. K. and Goldring, C. E. (2013). Stem cell-derived hepatocytes as a predictive model for drug-induced liver injury: are we there yet? *Br J Clin Pharmacol* **75**, 885-96.

Sison-Young, R. L.*, **Kia, R.***, Heslop, J.*, Kelly, L., Rowe, C., Cross, M. J., Kitteringham, N. R., Hanley, N., Park, B. K. and Goldring, C. E. (2012). Human pluripotent stem cells for modeling toxicity. *Adv Pharmacol* **63**, 207-56. **Joint first authorship*

Kia, R., Kelly, L., Sison-Young, R. L. C., Zhang, F., Pridgeon, C. S., Heslop, J. A., Metcalfe, P., Kitteringham, N. R., Baxter, M., Harrison, S., Hanley, N. A., Burke, Z. D., Storm, M. P., Welham, M. J., Tosh, D., Küppers-Munther B., Edsbagge, J., Bonner, F., Harpur, E., Sidaway, J., Bowes, J., Fenwick, S. W., Malik, H., Goldring, C. E. P. and Park, B. K. (2014). MicroRNA-122: a novel hepatocyte-enriched *in vitro* marker of drug-induced cellular toxicity. *Manuscript under review.*

Kia, R., Heslop, J., Rowe, C., Dudek, K., Bushell, M., Kitteringham, N. R., Hanley, N.A., Fenwick, S. W., Malik, H., Goldring, C. E. P. and Park, B. K. The global microRNA profiles of human primary hepatocytes in extended *in vitro* culture. *Manuscript in preparation.*

Goldring, C., Norris, A., Kitteringham N., Aleo, M. D., Antoine, D., Heslop, J., Howell, B. A., Ingelman-Sundberg, M., **Kia, R.**, Kamalian, L., Martinou, J-C., Mercer, A., Moggs, J., Naisbitt, D., Powell, C., Sidaway, J., Sison-Young, R., Snoeys, J., van der Water, B., Watkins, P. B., Weaver, R. J., Wolf, A., Zhang, F and Park, K. (2014). Mechanism-based markers of drug-induced liver injury to improve the physiological relevance and predictivity of *in vitro* models. *Manuscript under review.*

Kia, R., Sison, R. L., Heslop, J., Kitteringham, N. R., Hanley, N., Mills, J. S., Löwenadler, B., Malik, H., Fenwick, S., Goldring, C. and Park, K. (2014). Phenotypic comparison of hepatocyte-like cells differentiated from human induced pluripotent stem cells derived by cellular reprogramming of primary hepatocytes and dermal fibroblasts obtained from the same donor. *Gastroenterology* **146**(Suppl1), S-919.

LIST OF ABBREVIATIONS

α-SMA	alpha smooth muscle actin
A1AT	alpha-1 antitrypsin
AFP	alpha fetoprotein
ALB	albumin
ATP	adenosine triphosphate
CK18	cytokeratin-18
CYP	cytochrome-P450
DE	definitive endoderm
DILI	drug-induced liver injury
DNMT	DNA methyltransferase
EB	embryoid body
EGF	epidermal growth factor
HDAC	histone deacetylase
hDF	human dermal fibroblast
HE	hepatic endoderm
hESC	human embryonic stem cell
HGF	hepatocyte growth factor
hiPSC	human induced pluripotent stem cell
HLA	human leucocyte antigen
HLC	hepatocyte-like cell
HMGB1	high mobility group box-1
HNF4A	hepatic nuclear factor 4 alpha
hPSC	human pluripotent stem cell
hPH	human primary hepatocyte
ICC	Immunocytochemistry
LDH	lactate dehydrogenase

LETF	liver-enriched transcription factor
MAPK	mitogen-activated protein kinase
MEF	mouse embryonic fibroblast
miR	microRNA
MOI	multiplicity of infection
mRNA	messenger RNA
NF-κβ	nuclear factor kappa-light-chain-enhancer of activated B
OCT4	octamer-binding transcription factor 4
PI3K/AKT	phosphoinositide-3-kinase–protein kinase B/Akt
PXR	pregnane X receptor
qRT-PCR	quantitative reverse transcription polymerase chain reaction
RBP	RNA-binding protein
RNA	ribonucleic acid
SeV	Sendai virus
SOX2	sex determining region Y-box 2
SOX17	sex determining region Y-box 17
SSEA-4	stage-specific embryonic antigen-4
STAT3	signal transducer and activator of transcription 3
UGT	UDP-glucuronosyltransferase

CHAPTER 1

GENERAL INTRODUCTION

1.1 INTRODUCTION

Amongst the different types of adverse drug reactions, drug-induced liver injury (DILI) remains a prominent cause of patient morbidity and mortality, and confers major concerns to the pharmaceutical industry and regulatory agencies (Olsen and Whalen, 2009; Russo *et al.*, 2004; Sgro *et al.*, 2002). One of the major reasons for this is due to the lack of relevant *in vitro* hepatic models for accurate screening for drug-induced hepatotoxicity at the early stages of drug development, and also the lack of sophisticated *in vitro* model systems to mechanistically understand the pathways that are perturbed following drug exposure, especially after chronic low-dose regimes (Godoy *et al.*, 2013; LeCluyse *et al.*, 2012). Consequently, there continues to be major gaps in the extrapolation of findings from *in vitro* hepatic systems to the *in vivo* environment (LeCluyse*, et al.*, 2012).

This thesis describes our endeavour to develop more relevant *in vitro* human hepatocyte models via novel investigative approaches using insights gained from the rapidly advancing research areas of human induced pluripotent stem cells and microRNAs.

1.2 DRUG-INDUCED LIVER INJURY

1.2.1 Clinical aspects of drug-induced liver injury

The clinical presentation of DILI can mimic any type of acute or chronic liver disease. Hence, DILI is largely a clinical diagnosis of exclusion based on the overall findings from the clinical features, the clinical course of suspected DILI cases, presence or absence of patient risk factors, exclusion of other diagnoses and the reported hepatotoxicity profile of the suspected culprit drug (Fontana *et al.*, 2010). Therefore, it is not surprising that its diagnosis remains challenging with expert opinion in causality assessment still widely regarded as the gold standard, despite non-standardisation of what constitutes an expert, and how assimilation of information should be done to come to a diagnosis of DILI (Fontana*, et al.*, 2010). Nevertheless, much progress has been achieved in addressing these issues via the refinement of causality instruments such as the Roussel Uclaf Causality Assessment Method (Danan and Benichou, 1993; Maria and Victorino, 1997), and efforts to standardize the nomenclature used for defining clinical phenotypes of DILI (Fontana*, et al.*, 2010).

1.2.2 Burden of drug-induced liver injury

The incidence of DILI in the general population remains largely unknown. In a French population-based study, the annual incidence of DILI was estimated to be as high as 13.9 per 1,000,000 inhabitants (Sgro*, et al.*, 2002). The true incidence was also suggested to be underestimated, as the incidence found in the prospective study was 16 times higher than the number derived from spontaneous reporting of DILI cases to the French regulatory authorities. Meanwhile, the incidence of DILI developing among patients who were hospitalised was estimated to be 1.4% (Meier *et al.*, 2005), and 15% of liver transplants for acute liver failure deemed to be caused by DILI (Russo*, et al.*, 2004). DILI is also a major concern to the pharmaceutical industry and the regulatory authorities as it is the leading cause of costly drug withdrawal from the market post-licensing, restriction of prescribing

indications and the main reason for drug attrition during pre-clinical drug development (Watkins, 2005; Wilke *et al.*, 2007).

1.2.3 The role of drug metabolism in drug-induced liver injury

Amongst its many unique functions, the liver is the main organ where drugs or xenobiotics undergo biotransformation via a series of enzymatic reactions classified as phase I and II processes (Figure 1.1), primarily to reduce their biological activity and increase hydrophilicity to facilitate drug clearance (Fraczek *et al.*, 2013). Important phase I reactions include oxidation, reduction and hydrolysis and are facilitated by the various catalytic enzymes including cytochrome-P450 monooxygenases (CYPs) and alcohol dehydrogenases (ADH) (Guengerich, 2008). However, a few select CYP isoforms – namely CYP3A4, CYP2D6, CYP2C9 and CYP2C19 – are responsible for the biotransformation of the majority of marketed drugs (Hewitt *et al.*, 2007). The phase I metabolites are then conjugated with water-soluble endogenous substances in phase II reactions mediated by various transferases, though predominantly by UDP-glucuronosyltransferases (UGTs) (Fraczek*, et al.*, 2013). Excretion of the xenobiotics into the bile and urine is then facilitated through various transmembrane transporter proteins – the process being termed as phase III of xenobiotic biotransformation (Malarkey *et al.*, 2005).

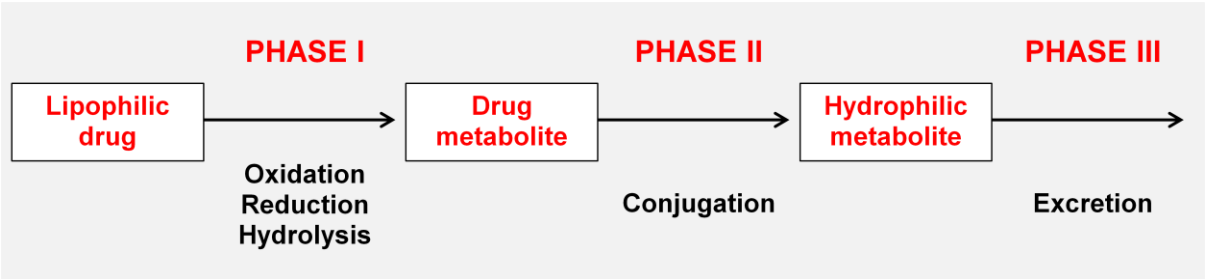

Figure 1.1 Schematic diagram showing the important reactions in each phase of drug metabolism.

However, some xenobiotics can undergo metabolic bioactivation during the biotransformation process, resulting in chemically reactive metabolites that is thought to have the potential to form adducts with cellular proteins (Park *et al.*, 2011). This covalent binding to biological macromolecules is then thought to cause cellular and organelle dysfunction via various poorly defined mechanisms including oxidative stress, DNA damage and protein dysfunction, which cumulatively manifests clinically as DILI (Park*, et al.*, 2011).

1.3 CONVENTIONAL HEPATIC MODELS FOR THE STUDY OF DRUG-INDUCED HEPATOTOXICITY

In view of the massive costs of unpredicted DILI to society, early detection of hepatotoxicity potential of a candidate drug during the early pre-clinical stages of drug discovery, and further mechanistic understanding of DILI is paramount. For these reasons, *in vitro* and *in vivo* hepatic models are important investigative tools, and are currently used throughout the pre-clinical phases of drug discovery to aid in the lead optimisation process and satisfy regulatory requirements before clinical development of a candidate drug can be pursued (Bass *et al.*, 2009). Although 40% of cells in the liver consist of many other cell-types including non-parenchymal cells such as endothelial cells, stellate cells, Kupffer cells, biliary epithelial cells and lymphoid cells (Godoy*, et al.*, 2013), most liver-specific functions are performed by the hepatocyte, including xenobiotic biotransformation (Fraczek*, et al.*, 2013). Therefore, most of the hepatic models currently used in safety pharmacology and toxicology research to understand the mechanisms of DILI, are based on hepatocytes.

The main hepatic models available for studies into the pathophysiology of DILI include primary hepatocytes, immortalised cell lines and animal models, though their utility and relevance for such purposes are somewhat limited as discussed below (Godoy*, et al.*, 2013; Kia *et al.*, 2013).

1.3.1 Human primary hepatocytes

The gold standard *in vitro* model for the study of DILI in humans is freshly-isolated human primary hepatocytes (hPHs) (Gomez-Lechon *et al.*, 2004). However, the use of hPHs is impeded by their limited availability, phenotypic differences between donors, variable viability and attachment of hPHs to tissue culture vessels following isolation and rapid dedifferentiation of the hepatocyte phenotype in culture, particularly in the loss of expression of CYP enzymes (Gomez-Lechon*, et al.*, 2004; Guguen-Guillouzo and Guillouzo, 2010; LeCluyse, 2001). Furthermore, hPHs are commonly harvested from diseased liver tissue which is not suitable for transplantation and likely to have experienced complex drug regimes, resulting in a skewed population of hPHs being used. The problem of hepatocyte dedifferentiation resulting in a short duration of optimal hepatocyte function also limits the utility of the hPH model to acute toxicity studies only, and compromises their use in mechanistic studies of DILI which often occurs following prolonged exposure to drugs (Guguen-Guillouzo and Guillouzo, 2010; Kalgutkar and Soglia, 2005; LeCluyse, 2001). The phenotypic characterisation of dedifferentiating primary hepatocytes has been extensively performed previously, though various efforts to reverse and prevent this process have proved limited in success (Elaut *et al.*, 2006; Fraczek*, et al.*, 2013). This will be discussed further in Chapter 3, which also describes our contribution towards better mechanistic understanding of dedifferentiation in hPHs by delineating the change in its global microRNA (miR) profile.

1.3.2 Immortalised human cell lines

Immortalised cell lines such as HepG2 (derived from liver tissue containing well-differentiated hepatocellular carcinoma), Fa2N-4 (immortalised hPHs) and HepaRG (derived from hepatocellular carcinoma) have been used to overcome some of these problems mainly as their proliferation is unlimited and are readily available (LeCluyse*, et al.*, 2012). However,

they generally are not representative systems for recapitulating hepatocyte function, do not contain all the families of metabolic enzymes required for drug metabolism, while expressed enzymes display reduced activity (Guguen-Guillouzo and Guillouzo, 2010; LeCluyse*, et al.*, 2012). Transfection methods to enable overexpression of CYP enzymes in these cells have been adopted, but this approach is still limited to the expression of one CYP isoform per cell line and therefore does not fully recapitulate the metabolic capacity and physiology of a fully functional hepatocyte (Chen and Cederbaum, 1998; Dai *et al.*, 1993; Goldring *et al.*, 2006; Pfeifer *et al.*, 1993).

1.3.3 Animal models

Although the use of animal models is a more amenable approach for *in vivo* studies, experimentation on animals raises ethical concerns, and public pressure to use animal-free assays has been reinforced with legislative changes that limit the use of animals for research and regulatory testing – most evidently exemplified in the cosmetic industry in Europe, which has an absolute ban on animal testing since 2013 (Fraczek*, et al.*, 2013). Furthermore, cross-species extrapolation of *in vivo* findings using animal models to humans is also variable due to interspecies differences in life histories, tissue-specific gene expression and variations in toxic responses to xenobiotics, including possession of higher levels of CYP enzymes in comparison to humans (Celander *et al.*, 2011; Lee *et al.*, 2006; Saldana-Ruiz *et al.*, 2012).

1.4 HUMAN PLURIPOTENT STEM CELL-DERIVED HEPATOCYTES

In view of the difficulties in procuring the gold standard *in vitro* model of hPHs and the functional limitations of the currently used hepatic models, new hepatic models with potential for better prediction and understanding of the mechanisms causing DILI will need to be explored. With the rapidly advancing stem cell technology, it is hoped that progress will be made in bridging this gap in toxicology research through the use of human pluripotent stem cells (hPSCs). hPSCs consist of human embryonic stem cells (hESCs) – derived from human embryos, and human induced pluripotent stem cells (hiPSCs) – reprogrammed from differentiated cells; both characterised by their pluripotency – ability to differentiate into cells from all three germ layers – and their potential to proliferate indefinitely (Kia*, et al.*, 2013). These unique features of hPSCs make them an attractive solution in safety pharmacology and toxicology research, as well as in the fields of regenerative medicine, tissue engineering and cell therapy (Bielby *et al.*, 2004; Hamazaki *et al.*, 2001; Lumelsky *et al.*, 2001; Vittet *et al.*, 1996; Wobus *et al.*, 2002). Directed differentiation of hPSCs to somatic cells with mature phenotypes in the laboratory could potentially provide a readily available source of metabolically competent cells such as mature hepatocytes as a relevant and functional hepatic model (Figure 1.2).

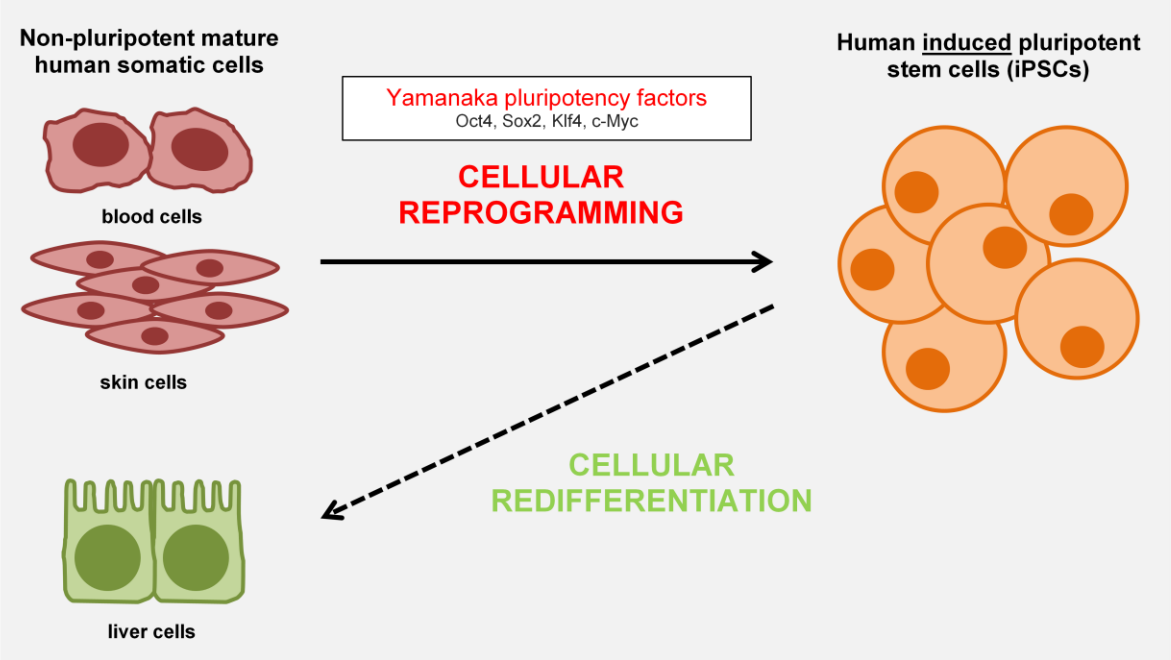

Figure 1.2 The potential utility of human induced pluripotent stem cells reprogrammed *(solid line)* **from easily accessible human somatic cells** *(red)* **to provide a readily available source of difficult to access cells such as hepatocytes** *(green)* **via directed differentiation in the laboratory** *(dashed lines)***.**

1.4.1 Human induced pluripotent stem cells

The successful generation of hiPSCs from mature somatic cells by cellular reprogramming (Takahashi and Yamanaka, 2006), have provided an increasingly attractive source of hPSCs; avoiding the use of human embryonic tissue-derived stem cell lines for research, while providing a unique opportunity for *in vitro* modelling of normal and variant phenotypes from pre-selected adult donors for safety pharmacology and toxicology evaluations (Kia*, et al.*, 2013). iPSCs were first generated by cellular reprogramming of murine fibroblasts using a retroviral vector that expressed transcription factors noted to be abundant in embryonic stem cells – namely Oct4, Sox2, Klf4, and c-Myc; collectively termed as the Yamanaka factors in recognition of the lead researcher who pioneered iPSC generation (Takahashi and Yamanaka, 2006). Since then, many reports using a variety of reprogramming techniques on various human somatic cells to induce pluripotency have been published, albeit with variable reprogramming efficiencies (Gonzalez *et al.*, 2011). These methods include viral-free

approaches to deliver the pluripotency gene set expressing the essential transcription factors into target somatic cells using episomal vectors, piggyBac transposons or minicircle vectors (Jia *et al.*, 2010; Kaji *et al.*, 2009; Woltjen *et al.*, 2009; Yu *et al.*, 2009; Yusa *et al.*, 2009). Reprogramming somatic cells via delivery of the reprogramming factors in their protein or messenger ribonucleic acid (RNA) form have also been reported (Kim *et al.*, 2009; Warren *et al.*, 2010; Zhou *et al.*, 2009). Small molecules have also been used solely or with all or some of the Yamanaka factors in a bid to improve the efficiency of induction (Hou *et al.*, 2013; Huangfu *et al.*, 2008; Mikkelsen *et al.*, 2008; Zhu *et al.*, 2010). Reprogramming using miRs that were shown to be abundant in ESCs and known to play important roles during the process were also reported to be successful (Anokye-Danso *et al.*, 2011; Miyoshi *et al.*, 2011). However, many of these latter approaches have not been widely adopted and cellular reprogramming using the Yamanaka factors remain the most robust thus far.

1.4.2 Generation of hepatocyte-like cells from hPSCs

Problems associated with freshly-isolated hPHs namely their limited availability, inter-donor differences and technical challenges of the isolation process, can theoretically be overcome by the use of a standard protocol-driven derivation of hepatocytes with batch-to-batch consistency and purity. In general, studies reporting on "hepatocytes" derived from hPSCs have been focussed on generating a closer representation of a freshly-isolated hPH phenotype. However, as no reports to date have confirmed complete recapitulation of a freshly isolated hPH, the term hepatocyte-like cells (HLCs) has been used to describe them.

The *in vitro* direct differentiation of hPSCs towards HLCs largely mimics the developmental pathway of the liver *in vivo* during embryogenesis (Baxter *et al.*, 2010). The aim is to derive mature hepatocytes from hPSCs using differentiation protocols encompassing the three main stages of hepatic development: induction of definitive endoderm, specification of hepatic endoderm and maturation of the HLCs (Baxter*, et al.*, 2010; Hay *et al.*, 2008;

Sullivan *et al.*, 2010). However, the differentiation efficiency in generating a pure culture of HLCs as defined by the presence of cells positive for hepatocyte-associated markers such as albumin and alpha-1-antitrypsin, has been reported to be variable (Kia*, et al.*, 2013). To date however, the perfect differentiation protocol has remained elusive. This is also compounded by the lack of standardisation of methods used to characterise these HLCs and in assessing their differentiation efficiency, though helpful recommendations for minimal criteria to allow comparison of protocols have been proposed (Sancho-Bru *et al.*, 2009).

1.4.2.1 Functional assessment of hPSC-derived hepatocyte-like cells

Although gene expression profiling of HLCs is useful for characterisation, ultimately it is the dynamic functional capabilities of these differentiated HLCs when compared to hPHs that will determine their suitability for use in safety pharmacology and toxicology. These functional assessments include drug metabolising enzyme activity, albumin secretion, glycogen storage, uptake of indocyanine green and uptake of low density lipoprotein (Kia*, et al.*, 2013).

As drug-induced hepatotoxicity and clinically apparent DILI is widely accepted to be associated with the formation of reactive metabolites following metabolism by phase I and II catalytic enzymes, especially CYPs, one of the key tests for the functional relevance of HLCs as a model for pharmaco-toxicology would be the demonstration of CYP activity at levels similar to freshly-isolated hPHs. However, when the CYP activity profile of HLCs has been compared to hPHs, the results have been variable – ranging from 0-100% of the hPH comparator (Duan *et al.*, 2010; Ek *et al.*, 2007; Yildirimman *et al.*, 2011). Comparison between studies is difficult due to major differences in the experimental factors such as different hPSC lines used as starting cell source, the differences in the multi-stage differentiation protocols employed, the difference in methods used to measure CYP activity and most pertinently, the variable quality of the reference hPHs being used in different

studies (Kia*, et al.*, 2013; Wobus and Loser, 2011). It is also important to note that full description of the hPH comparators used in all of these studies were not reported, making it difficult to judge the quality of the hPHs and their metabolic capacity. In contrast to efforts to assess the activity of phase I enzymes in HLCs, only one study have reported the presence and activity of phase II enzymes (Soderdahl *et al.*, 2007). In this study, glutathione-S-transferases (GSTs) were found to have overall comparable activity to that of the reference hPHs, though again the quality of the reference hPHs used was not characterised. The albumin secretion capability of HLCs has also been compared infrequently with hPHs, and has ranged from 23-75% of the hPH comparators (Basma *et al.*, 2009; Bone *et al.*, 2011). Nevertheless, in a recent study evaluating HLCs as an *in vitro* hepatic model for drug-induced hepatotoxicity (Szkolnicka *et al.*, 2014), hESC-derived HLCs and cryopreserved hPHs were shown to have comparable accuracy in predicting toxicity induced by a series of known hepatotoxicants, although the authors also reported variable metabolic and inducible CYP activities between HLCs generated from the two hESC and hiPSC lines examined, of which the reason(s) was unclear.

Overall, none of the reports of HLCs generated have claimed full functional recapitulation of the hPH phenotype. Instead, HLCs are currently widely recognised as more similar to a foetal hepatocyte, especially with its persistent expression of the proto-typical marker alpha-fetoprotein (Yi *et al.*, 2012). More recently, the CYP1A and CYP3A activities of HLCs have also been shown to be akin to that of hPHs with a dedifferentiated phenotype following 48 hours of *in vitro* culture (Ulvestad *et al.*, 2013).

1.4.2.2 Variations in hepatic differentiation from hPSCs

The reason(s) for the variation in the hepatic differentiation efficiency reported in the literature (Kia*, et al.*, 2013), is currently unclear and is likely to be at least due to the variations in the differentiation propensity of individual hPSC lines towards certain lineages

(Bock *et al.*, 2011; Osafune *et al.*, 2008; Ramos-Mejia *et al.*, 2010), which in turn potentially contributed by a myriad of factors. These include the heterogeneous genetic background of the donors, the differences in culture conditions, and variations in the methods for hiPSC generation (Kajiwara *et al.*, 2012). However, another potential factor could be the retention of epigenetic memory of the donor cells in hiPSCs despite cellular reprogramming, with a resultant skewed propensity to differentiate towards the cell-type of origin (Kim *et al.*, 2010; Kim *et al.*, 2011; Polo *et al.*, 2010), which to date has only been partially explored in the differentiation of hiPSCs towards HLCs. This will be discussed in more detail in Chapter 2, where we also describe our contribution to this conundrum by focussing on the potential impact of epigenetic memory in hepatic differentiation by comparing HLCs generated from isogenic hPH- and human dermal fibroblast-derived hiPSCs (Figure 1.3).

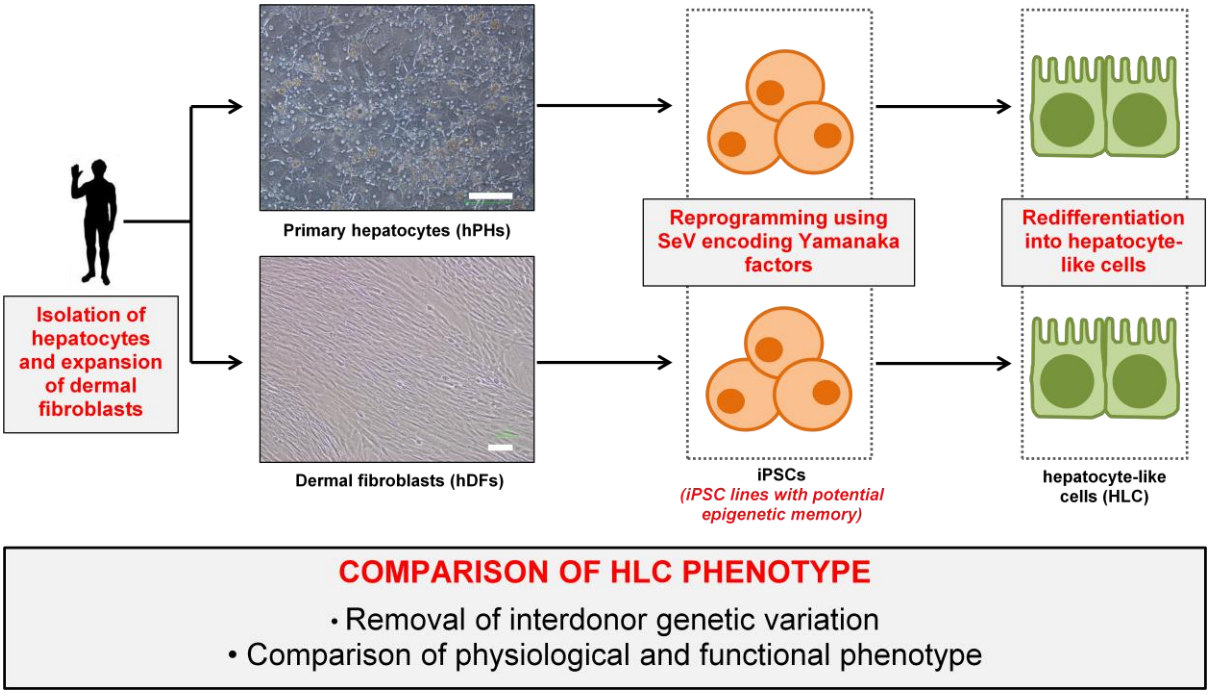

Figure 1.3 Schematic diagram of plan for comparison of isogenic hepatocyte-like cells generated from human primary hepatocytes and human dermal fibroblasts derived from the same donor. Scale bar, 100 μm.

1.5 microRNA

MicroRNAs (miRs) which are small non-coding RNAs consisting of 18-24 nucleotides (nt), were first discovered in 1993 (Lee *et al.*, 1993), and have since been found to play crucial roles in almost every facet of cellular biology and human disease (Li and Rana, 2014; Pritchard *et al.*, 2012). Although there is only approximately 2500 mature miRs in humans (Griffiths-Jones, 2004) compared to approximately 30000 mRNAs (Pritchard*, et al.*, 2012), one miR may regulate hundreds of mRNAs whilst each mRNA may in turn be regulated by many different miRs (Szabo and Bala, 2013). As a result, miR expression patterns convey a huge amount of biological information as variation in gene expression patterns can potentially be captured by the expression patterns of just one or a few miRs that regulate them. Therefore, there has been intense interest in the study of miR expression patterns for potential targets for manipulation as a means to influence biological functions and correct pathophysiological processes. Our effort in delineating the changing global miR profile of dedifferentiating hPHs as described in Chapter 3 of this thesis, is one example of this approach.

1.5.1 Biogenesis and function of miRs

Most of the miR genes lie within intronic regions of protein-coding genes and therefore the expression of miRs subjected to similar transcriptional control as these genes (Li and Rana, 2014). The major mechanism governing tissue- and cell-type-specific expression of miRs has been suggested to be due to transcriptional regulation, although many of the factors and catalytic enzymes involved in miR biogenesis are also tightly regulated (Krol *et al.*, 2010; Li and Rana, 2014).

Each miR is first transcribed by RNA polymerase II as a long primary transcript (termed as pri-miR), and is then processed into mature miR via canonical or non-canonical pathways (Figure 1.4) (Li and Rana, 2014). In the canonical pathway, the pri-miR stem-loop structure

is digested by an RNase III family member, Drosha into precursor miR (termed as pre-miR), while in the non-canonical pathway, the pre-miR is generated by the mRNA splicing machinery without the need for Drosha. Following the generation of the pre-miR via either pathway in the nucleus, it is then exported into the cytoplasm and further processed by another RNase III enzyme, Dicer into a double-stranded miR duplex which contains the mature miR strand and the passenger strand. The mature miR is then incorporated into a RNA-induced silencing complex (RISC) containing Argonaute 2 proteins, which function as key catalytic enzymes within the complex for miR-mediated post-transcriptional gene silencing (Chen, 2009). In most cases, the miR-RISC complex bind to their mRNA targets by complementary interaction between the 3' untranslated region (UTR) of the mRNA with a sequence of 2-8 nt, known as the seed region, at the 5' end of the mature miR. This miR-mRNA interaction then results in the regulation of gene expression via translational repression, inhibition of translation initiation or induction of endonucleolytic cleavage of the target mRNAs, although the exact mechanisms involved remain unclear (Chen, 2009; Li and Rana, 2014).

1.5.2 Nomenclature of miRs

The latest nomenclature of miR is widely-accepted to be based on miRBase (www.mirbase.org), which serves as the definitive repository of published miR sequences and annotation, with links to databases of predicted mRNA targets. Currently, the total number of listed entries of human pre-miR is 1881, while the total number of listed entries of mature miRs is 2588 (miRBase 21, accessed 22 August 2014). Important points to note is that distinct species of mature miRs can be produced from the 3' and 5' arms of the pre-miR duplex and either species could be the mature miR strand dependent on its stability in the double-stranded miR duplex (Szabo and Bala, 2013). In addition, sequencing studies have

shown that a given mature miR can vary from 15-23 nt, although the majority are of 22-23 nt, due to 3' or 5' end post-transcriptional modifications (Pritchard*, et al.*, 2012).

1.5.3 Liver-enriched miR-122

miR-122 (denoting the mature strand of miR-122-5p) was first identified in various mouse tissue samples and was found to be highly-enriched in the liver (Lagos-Quintana *et al.*, 2002). Its seed sequence was then subsequently demonstrated to be highly conserved in many species (Chang *et al.*, 2004), and are currently detected in 30 species (miRBase 21, accessed 22 August 2014). miR-122 has since been shown to be highly enriched and abundant in adult and foetal liver as well (Liu *et al.*, 2009; Sempere *et al.*, 2004).

1.5.3.1 The role of miR-122 in the liver

The human miR-122 genomic locus is situated on chromosome 18 in a non-coding RNA exon (Jopling, 2012), with a highly conserved core promoter region containing the target site for the liver-enriched transcription factor, hepatic nuclear factor 4 alpha, which positively-regulates its expression and involvement in hepatic differentiation (Laudadio *et al.*, 2012; Li *et al.*, 2011). miR-122 have been shown to play a major role in maintaining homeostasis of hepatic cholesterol and lipid metabolism through studies which involved inhibition of miR-122 using antisense oligonucleotides, although the exact pathways involved have not yet been delineated (Esau *et al.*, 2006; Krutzfeldt *et al.*, 2005). miR-122 has also been shown to regulate iron homeostasis in mice via translational repression of the activators of hepcidin – a major regulatory hormone (Castoldi *et al.*, 2011; Rossi, 2005). It also appears to be a tumour suppressor gene as miR-122 levels were found to be reduced in human hepatocellular carcinoma (HCC) compared to normal liver (Kutay *et al.*, 2006), while overexpression of miR-122 in HCC cell lines reduced their tumorigenic properties (Bai *et al.*,

2009), and sensitised their responses to chemotherapeutic agents (Bai*, et al.*, 2009; Fornari *et al.*, 2009).

1.5.3.2 miR-122 as a biomarker of DILI

Previous studies have also documented the presence of miRs in various forms in the plasma and other bodily fluids (Weber *et al.*, 2010), although the processes underlying their release from the intracellular compartment and postulations regarding their role in extracellular communication between tissues and organs remain unclear (Szabo and Bala, 2013). Due to their stability in the serum and plasma (Szabo and Bala, 2013), circulating miRs are seen as attractive biomarkers of various diseases; including the notion of miR-122 as a potential marker of liver injury in general. Increased plasma/serum levels of miR-122 have been found in patients with liver diseases of different aetiologies, including chronic viral hepatitis C, hepatocellular carcinoma and non-alcoholic fatty liver disease (Cermelli *et al.*, 2011; Xu *et al.*, 2011).

Several studies have also demonstrated the value of circulating miR-122 as a hepatocyte-specific biomarker of DILI in rodents and humans caused by drugs such as acetaminophen and heparin (Antoine *et al.*, 2013; Harrill *et al.*, 2012; Starkey Lewis *et al.*, 2011; Wang *et al.*, 2009). The decrease in the level of miR-122 in the livers of mice administered toxic doses of acetaminophen (Wang*, et al.*, 2009), added to the presumption that the liver-enriched miR-122 was released from injured hepatocytes into the circulation, although exact mechanisms have yet to be reported. Additionally, as miR-122 is highly conserved across many species (Chang*, et al.*, 2004), it has the potential to be used in pharmaco-toxicology studies as a relevant and liver-specific biomarker for extrapolation of *in vivo* findings from animal models to humans.

Similarly, a hepatocyte-specific biomarker of hepatocyte perturbation for *in vitro* pharmaco-toxicology studies that could be used to bridge *in vivo* and clinical studies would be

invaluable. Therefore, in Chapter 4 of this thesis, we describe our evaluation of miR-122 as a hepatocyte-enriched *in vitro* marker of drug-induced hepatotoxicity using the prototypical hepatotoxicants acetaminophen and diclofenac.

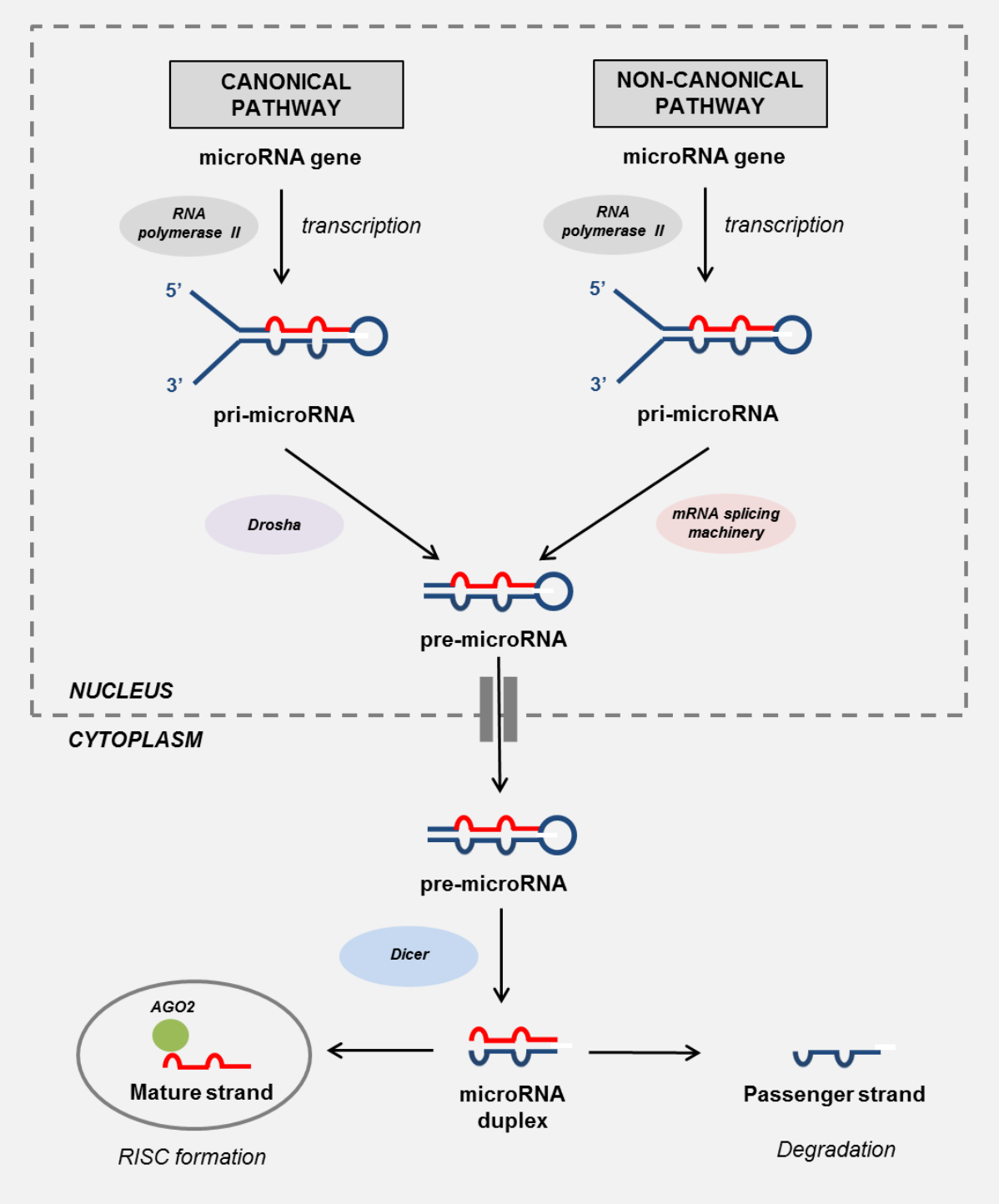

Figure 1.4 Biogenesis of microRNAs.

The microRNA (miR) gene is first transcribed by RNA polymerase II into a pri-miR stem-loop structure, which is then processed into a shorter precursor-miR (pre-miR) via both canonical and non-canonical pathways. The pre-miR molecule is then exported into the cytoplasm where it is further processed by Dicer into miR duplexes. The mature miR strand is then loaded together with Argonaute 2 (AGO2) proteins into RNA-induced silencing complexes (RISCs) which then bind to their target messenger RNAs causing gene silencing. The passenger strand meanwhile undergoes degradation.

1.6 AIMS OF THESIS

Relevant and functional human hepatic models are urgently required for the mechanistic study and prediction of drug-induced liver injury. hiPSC-derived HLCs represent an exciting hepatic model with a unique potential to capture the inherent genetic polymorphisms present in the population for the purposes of pharmaco-toxicology evaluations. However, the functional limitation of HLCs remains a hindrance despite great strides being made in refining differentiation protocols. One potential approach to increase the functional capacity of HLCs is by harnessing the epigenetic memory in hiPSCs of its cell-type of origin, although its contribution in the propensity for hepatic differentiation of hiPSCs has not been evaluated fully so far.

At the same time, understanding the process of dedifferentiation of hPHs, may help to enhance its functional lifespan for toxicology studies, especially in chronic toxicity of which there are currently no suitable models. As miR expression patterns capture a huge amount of biological information with potential for manipulation, studying the changing miR profile of hPHs may provide novel insights to reverse or prevent the detrimental process, with concomitant utility to enhance hepatic differentiation from hPSCs.

On the other hand, improving the translatability of results from pre-clinical studies to the human cohort and *vice versa*, would be immensely useful for the study of DILI. One way of doing so would be the use of cell-type specific biomarkers in *in vitro* assays, as opposed to generic cellular markers *e.g.* adenosine triphosphate (ATP), used in most conventional *in vitro* toxicity assays which have limited potential to bridge *in vitro* and *in vivo* findings. miR-122 which is also highly expressed in the liver of other species commonly used in *in vivo* studies is one example.

Therefore, this thesis will set about addressing the following hypotheses in relation to the issues explained above:

Hypothesis 1

- HLCs generated from hPH-derived hiPSCs display a closer resemblance to the hPH phenotype compared to HLCs generated from isogenic human dermal fibroblast-derived hiPSCs.

Hypothesis 2

- Novel insights into the process of hPH dedifferentiation can be gained by investigating the changing global miR profiles of hPHs in extended *in vitro* culture.

Hypothesis 3

- miR-122 can be utilised as a relevant *in vitro* marker of drug-induced hepatotoxicity in hepatic models expressing high levels of miR-122

CHAPTER 2

PHENOTYPIC COMPARISON OF ISOGENIC HEPATOCYTE-LIKE CELLS GENERATED FROM HEPATOCYTE- AND FIBROBLAST-DERIVED HUMAN IPSCS

2.1 INTRODUCTION

Drug-induced liver injury (DILI) in humans persists as a significant cause of patient morbidity and mortality, and unpredicted hepatotoxicity during drug development continues to be a major problem for the pharmaceutical industry and the regulatory authorities (Davies *et al.*, 2010; Olsen and Whalen, 2009). Due to a lack of alternative *in vitro* hepatic models, human primary hepatocytes (hPHs) remain the most relevant and the most metabolically active *in vitro* model, although a myriad of issues limit their application in the *in vitro* study of drug-induced toxicity and safety screening – most notably their limited availability, large donor variations and their limited preservation of their functional capabilities (Godoy *et al.*, 2013; Rodriguez-Antona *et al.*, 2002; Rowe *et al.*, 2010; Sison-Young *et al.*, 2012).

A potentially new hepatic model and an inexhaustible source of metabolically competent cells for the use in drug screening and the mechanistic study of DILI, is hepatocytes generated from human pluripotent stem cells (hPSCs), typically called hepatocyte-like cells (HLCs) (Baxter *et al.*, 2010). The generation of HLCs from both human embryonic stem cells and human induced pluripotent stem cells (hiPSCs) have been reported using multiple hepatic differentiation protocols which mimic the process of hepatogenesis during human embryonic development (Rashid *et al.*, 2010; Sullivan *et al.*, 2010; Szkolnicka *et al.*, 2014). However, the reported hepatic differentiation efficiencies in various studies were widely variable and the functional phenotype of HLCs in general remains limited in comparison with the gold standard *in vitro* hepatic model of hPH (Kia *et al.*, 2013).

This may be partially due to the variations in the differentiation propensity of hPSCs towards certain lineages (Bock *et al.*, 2011; Osafune *et al.*, 2008; Ramos-Mejia *et al.*, 2010), and the differences in turn potentially contributed by a myriad of factors. These include the heterogeneous genetic background of the donors, the differences in culture conditions, and variations in the methods for hiPSC generation (Kajiwara *et al.*, 2012).

In recent years, various studies have also shown that iPSCs retain transient epigenetic memories of the donor cells despite cellular reprogramming, with a resultant skewed propensity to differentiate towards the cell-type of origin (Kim *et al.*, 2010; Kim *et al.*, 2011; Polo *et al.*, 2010). The potential translational importance of these findings were then highlighted in a study where human iPSCs derived from pancreatic beta-cells were shown to have a greater propensity to differentiate back towards beta-cells when compared to isogenic hiPSCs derived from non-beta-cells (Bar-Nur *et al.*, 2011).

However, the contribution of epigenetic memory in the differentiation of hiPSCs towards HLCs has only been partially explored. In a mouse study, HLCs generated from mouse iPSCs (miPSCs) derived from hepatoblasts and hepatocytes possess a more functional hepatic phenotype compared to HLCs generated from isogenic foetal fibroblast-derived miPSCs (Lee *et al.*, 2012), though these findings have yet to be replicated in human studies. Another study of human donors compared the functional phenotype of HLCs generated from hiPSCs derived from cell-types from all three germ layers, including hPH-derived hiPSCs, and found their albumin secretion capacity and cytochrome-P450 enzyme activities to be similar (Liu *et al.*, 2011). However, in this study all the hiPSC lines were from different donors, hence the influence of genetic background was a confounding factor that was not controlled. Another study which did compare the functional phenotype of HLCs generated from isogenic hiPSC lines however did not include hPH-derived hiPSCs (Kajiwara*, et al.*, 2012). The paucity of studies of hepatic differentiation involving hPH-derived hiPSCs is likely to be related to the fact that only two reports from separate laboratories (Hansel *et al.*, 2014; Liu *et al.*, 2010) that have reported successful derivation of hiPSCs from hPHs, including the group that published the first study described above (Liu*, et al.*, 2010).

Therefore in this chapter, we aimed to investigate the hypothesis that HLCs generated from hPH-derived hiPSCs have a better hepatic differentiation capacity compared to HLCs generated from isogenic non-hPH-derived hiPSCs. To explore the contribution of epigenetic memory of the cell-type of origin in hiPSCs with minimal confounding factors, we used

genetically-matched hPHs and human dermal fibroblasts (hDFs) from the same adult donors. We derived hiPSCs from these starting cell types using the same reprogramming method and subsequently generated HLCs from them using the same differentiation protocol for comparison. Our comparison of HLCs generated from 1 clone of hPH-derived hiPSC against 3 clones of hDF-derived hiPSCs is described here.

2.2 MATERIALS AND METHODS

2.2.1 Human subjects and tissue

Human liver resections from surgical waste tissue were obtained from adult patients undergoing hepatobiliary surgery. For each donor, a full-thickness elliptical skin excision measuring about 1 – 2 cm in maximum length was also obtained by our surgical colleagues from the abdomen along the edge of the laparotomy incision undertaken for the hepatobiliary surgery. All tissue collection was undertaken with full informed consent and ethical approval from the relevant institutional review boards (National Research Ethics Service REC reference: 11/NW/0327).

2.2.2 Human primary hepatocyte isolation and culture

Human primary hepatocytes (hPHs) were isolated using a previously described method with minor modifications (LeCluyse *et al.*, 2005). Briefly, liver resections were received as surgical waste tissue immediately post-resection (Aintree University Hospital, Liverpool, United Kingdom) and transferred on ice in N-(2-Hydroxyethyl)piperazine-N′-(2-ethanesulfonic acid) (HEPES) buffer (10 mM HEPES, 136 mM NaCl, 5 mM KCl, 0.5% (w/v) glucose, pH 7.6) to the laboratory. The liver resection specimens were then perfused with HEPES-buffered saline (HBS) followed by digestion with collagenase A (Roche) or collagenase IV (Sigma-Aldrich) in HBS containing calcium. The suspension containing isolated hepatocytes was then filtered through a nylon gauze and purified by centrifugation twice at 80x g for 5 minutes at 4^{o}C, before the pellet was resuspended in an appropriate medium.

hPHs used for reprogramming into hiPSCs were resuspended in Williams E medium (WEM, Sigma-Aldrich) containing 10^{-7} M dexamethasone (Sigma-Aldrich), 5% (v/v) foetal bovine serum (FBS, Life Technologies), 2 mM L-glutamine (Sigma-Aldrich), 15 mM HEPES solution

(Sigma-Aldrich), 0.4% (v/v) insulin-transferrin-selenium (from 100x stock, Life Technologies), 1% (v/v) penicillin-streptomycin (Sigma-Aldrich), 50 ng/mL hepatocyte growth factor (HGF, PeproTech) and 50 ng/mL epidermal growth factor (EGF, PeproTech) before being seeded onto a Matrigel (hESC-Qualified matrix, Corning) -coated 6-well plate (Greiner Bio-One) and cultured at 5% CO_2 and 37°C. hPHs used as control were resuspended in WEM supplemented with 1% (v/v) insulin-transferrin-selenium, 2 mM L-glutamine, 10^{-7} M dexamethasone and 1% (v/v) penicillin-streptomycin and seeded onto a collagen-I coated 24-well plate (BD Beckinson) and cultured at 5% CO_2 and 37°C.

After 3 hours, non-attached cells were washed away and replaced with fresh medium before overnight incubation. The medium was replaced again the next day, and lysates and media for the control hPHs collected for analysis 48 hours later.

2.2.3 Propagation of human dermal fibroblasts (hDFs)

hDFs were established from the skin excisions of donors based on published methods with some minor modifications (Aasen and Izpisua Belmonte, 2010; Neely *et al.*, 2011). Briefly, following excision, the skin tissue was received immediately (Aintree University Hospital, Liverpool, United Kingdom) and transferred on ice in a 50 mL centrifuge tube (Greiner Bio-One) containing 15 mL of Dulbecco's modified Eagle's medium (DMEM, Sigma-Aldrich) supplemented with 2 mM L-glutamine (Sigma-Aldrich), 10% (v/v) foetal bovine serum (FBS; Life Technologies) and 1% (v/v) penicillin-streptomycin (Sigma-Aldrich).

The skin excisions were then transferred to a cell culture hood and rinsed with complete DMEM before separating the epidermis from the dermal layer using a scalpel (Fisher Scientific) and/or sterile scissors (Fisher Scientific). The dermis was then cut into 0.5 – 1.0 mm pieces and a maximum of 3 pieces placed directly into a single well of a 6-well tissue culture plate (Corning) using tweezers. A few drops of complete DMEM were placed onto each piece of dermal tissue, making sure that there was adequate contact with the surface

of the culture well. The dermal tissue pieces were then incubated overnight at 5% CO_2 and 37°C. For the next 2-3 days, the media was carefully replaced with new drops of complete DMEM daily to ensure that they did not dry out completely. When the dermal tissue pieces have attached to the surface of the culture well, the total volume of complete DMEM was gradually increased from 500 µL/well to 2 ml/well. The medium was replaced every 2-3 days and unattached pieces were removed.

After 7-10 days of placing the dermal tissues into the tissue culture well, outgrowths of fibroblasts appeared and the culture expanded for a further 7-10 days until a confluency of about 80% was reached. The fibroblasts were then rinsed twice with Dulbecco's Phosphate Buffered Saline (DPBS, Life Technologies) and then incubated with 500 µL of 0.05% trypsin-EDTA solution (Life Technologies) at 37°C for 3-5 minutes. The trypsinisation process was then stopped with complete DMEM and the detached fibroblasts collected into a 15 ml centrifuge tube (Greiner Bio-One) before centrifugation at 1000 rpm for 5 minutes at room temperature. The cell pellet was then resuspended and the fibroblast culture from each well of a 6-well plate passaged onto a 100 mm tissue culture dish (Greiner Bio-One) for expansion.

2.2.4 Derivation of hiPSCs from human primary hepatocytes

Following plating of the hPHs onto Matrigel (hESC-Qualified matrix, Corning) –coated tissue culture wells, the hPHs were cultured for 3 days in WEM (Sigma-Aldrich) containing 10^{-7} M dexamethasone (Sigma-Aldrich), 5% (v/v) FBS (Life Technologies), 2 mM L-glutamine (Sigma-Aldrich), 15 mM HEPES solution (Sigma-Aldrich), 0.4% (v/v) insulin-transferrin-selenium (from 100x stock, Life Technologies), 1% (v/v) penicillin-streptomycin (Sigma-Aldrich), 50 ng/mL HGF (PeproTech) and 50 ng/mL EGF (PeproTech), which was replaced daily. This medium composition, termed as the hPH reprogramming medium, and the

following hPH reprogramming protocol was adapted and modified based on a previously reported protocol of hiPSC generation from hPHs (Liu*, et al.*, 2010) (Figure 2.2) .

After 3 days post-seeding (designated Day 0), the hPHs were transduced with the CytoTune-iPS Sendai Reprogramming Kit (Life Technologies) containing four Sendai viral-based reprogramming vectors, each expressing one of the four Yamanaka factors (*i.e.* Oct4, Sox2, Klf4, and c-Myc) (Fusaki *et al.*, 2009) at a multiplicity of infection (MOI) of 3 to 7, in WEM. After 24 hours of transduction, the medium was replaced daily with fresh hPH reprogramming medium until Day 3 post-transduction when the medium was replaced with Essential 6 (E6, Life Technologies) medium supplemented with 100 ng/mL of recombinant basic fibroblast growth factor (bFGF, Life Technologies). The E6 medium was then replaced daily and the culture closely monitored for the appearance of hiPSC colonies, typically around Day 25-30.

2.2.4.1 Manual passaging of hPH-derived hiPSC colonies

When the colonies were ready to be transferred, the colonies were manually picked with the aid of a light microscope (EVOS XL Core Cell Imaging System, Life Technologies) in the cell culture hood. Each colony was then cut into 8-10 pieces in a grid-like pattern using a disposable surgical blade (Swann-Morton), and the pieces from a single colony transferred using a 100 µL pipette to a well of a 24-well plate (Greiner Bio-One) prepared with mitotically-inactivated murine embryonic fibroblast (MEFs, CF-1 strain, GlobalStem) containing Dulbecco's Modified Eagle Medium: Nutrient Mixture F-12 (DMEM/F12, Life Technologies) supplemented with 20% (v/v) KnockOut Serum Replacement (KOSR, Life Technologies), 100 µM minimum essential medium non-essential amino acids (MEM NEAA, Life Technologies), 50 µM 2-mercaptoethanol (2-ME, Life Technologies), 4 ng/ µL bFGF (Life Technologies) and 0.5% (v/v) penicillin-streptomycin (Life Technologies). The MEF culture plate containing the picked colonies was then incubated overnight at 37°C to allow

attachment before replacing the medium daily with fresh complete DMEM/F12 medium. The reprogrammed colonies were then expanded and maintained as described in Section 2.2.6.

2.2.5 Derivation of hiPSCs from human dermal fibroblasts

The reprogramming of human dermal fibroblasts (hDFs) was performed using the CytoTune-iPS Sendai Reprogramming Kit (Life Technologies) as per protocol. Briefly, hDFs at passage 5 or less were plated onto a 6-well plate (Corning) and cultured for 48 hours in DMEM (Life Technologies) supplemented with 2 mM L-glutamine (Sigma-Aldrich), 10% (v/v) FBS (embryonic stem cell-qualified, Life Technologies) and 0.5% (v/v) penicillin-streptomycin (Life Technologies), aiming for a confluency of 80-90% and ensuring the fibroblasts have extended and adhered. On the day of transduction (Day 0), each well containing hDFs was transduced with the CytoTune-iPS Sendai Reprogramming Kit (Life Technologies) containing the four Sendai viral-based reprogramming vectors at a MOI of 3 to 5 in fresh complete DMEM. After 24 hours of viral transduction, the medium was replaced with fresh complete DMEM and the culture continued until Day 7 with a medium change every other day. The transduced fibroblasts were then trypsinised with 0.05% trypsin-EDTA (Life Technologies) as described in Section 2.2.3 and centrifuged at 200x g for 5 minutes. The cell pellet was then resuspended with fresh complete DMEM and the cell concentration determined using a haemocytometer. The derivation of hiPSCs from the transduced fibroblasts was then continued using either a feeder-dependent method or a feeder-free method.

2.2.5.1 Feeder-dependent method of reprogramming hDFs

For the feeder-dependent method, the transduced fibroblasts were seeded onto 100 mm tissue culture dishes (Greiner Bio-One) prepared with MEFs (CF-1 strain, GlobalStem) at

densities of 5 x 10^4 – 2 x 10^5 cells/dish and incubated at 37°C for 24 hours. At Day 8, the medium was then replaced with DMEM/F12 (Life Technologies) supplemented with 20% (v/v) KnockOut Serum Replacement (KOSR, Life Technologies), 100 µM MEM NEAA (Life Technologies), 100 µM 2-ME (Life Technologies), 4 ng/ µL bFGF (Life Technologies) and 0.5% (v/v) penicillin-streptomycin (Life Technologies). The medium was then replaced daily and the culture closely monitored for the appearance of hiPSC colonies, typically at Day 20-25. Colonies that were ready for transfer were manually picked as described in Section 2.2.4.1 onto 24-well plates coated with MEFs for further expansion.

2.2.5.2 Feeder-free method of reprogramming hDFs

For the feeder-free method, the transduced fibroblasts were seeded onto a 6-well plate (Corning) coated with Matrigel (hESC-Qualified matrix, Corning) at densities of 2.5 x 10^4 - 5 x 10^5 cells/well and incubated at 37°C for 24 hours. At Day 8, the medium was then replaced with E6 medium (Life Technologies) supplemented with 100 ng/mL of bFGF (Life Technologies). The medium was then replaced daily and the culture closely monitored for the appearance of hiPSC colonies, typically at Day 25-30. Colonies that were ready for transfer were manually picked as described in Section 2.2.4.1 onto 24-well plates (Corning) coated with Matrigel (Corning) in Essential 8 medium (E8, Life Technologies) for further expansion.

2.2.6 Human induced pluripotent stem cell culture

2.2.6.1 Maintenance matrices and media for hiPSCs

The hiPSC lines were maintained on either MEFs (CF-1 strain, GlobalStem) in DMEM/F12 (Life Technologies) supplemented with 20% (v/v) KnockOut Serum Replacement (KOSR, Life Technologies), 100 µM MEM NEAA (Life Technologies), 50 µM 2-ME (Life

Technologies), 4 ng/ µL bFGF (Life Technologies) and 0.5% (v/v) penicillin-streptomycin (Life Technologies), or on Matrigel (Corning) in E8 medium (Life Technologies) supplemented with 0.5% (v/v) penicillin-streptomycin (Life Technologies).

2.2.6.2 Enzyme-free passaging of hiPSCs

All the hiPSC lines were passaged every 4-7 days at a ratio of 1:3 to 1:6 using an enzyme-free Gentle Cell Dissociation Reagent (GCDR, STEMCELL Technologies) based on a previously described protocol (Chen *et al.*, 2011). Briefly, for each well of a 6-well format tissue culture plate, the confluent culture was first washed gently with 1 ml of GCDR, before incubation with 1 mL of fresh GCDR for 2-5 minutes at room temperature. The culture was observed closely under a light microscope with phase contrast (100x magnification, ECLIPSE TS100/100-F, Nikon) for the appearance of junctions within colonies. At this point, the dissociation was stopped by removing the GCDR and adding 2 mL of the appropriate complete hPSC medium. The colonies were gently detached with a cell scraper (Greiner Bio-One), and the cell aggregates transferred to a 15 mL centrifuge tube (Greiner Bio-One). The mixture was gently pipetted to break up the aggregates to create a uniform suspension of aggregates of approximately 100 µm. The aggregate mixture was allowed to stand at room temperature for about 1 minute to separate out larger aggregates and the dense MEF feeder layer which would sink faster to the bottom of the centrifuge tube. The suspension containing aggregates with optimal size was then added to fresh matrix-coated wells in the appropriate passage ratio and incubated overnight at 37°C. Once attachment of the aggregates to the fresh matrix-coated well was confirmed, the medium was replaced with fresh complete hiPSC medium.

2.2.6.3 Preparation of MEF feeder layers

MEF feeder layers were prepared by seeding mitotically-inactivated MEFs (CF-1 strain, GlobalStem) at the recommended density by the manufacturer, onto tissue culture vessels pre-coated with Attachment Factor (AF, Life Technologies) in DMEM (Life Technologies) supplemented with 15% (v/v) FBS (embryonic stem cell-qualified, Life Technologies), 2 mM L-glutamine (Life Technologies) and 1% (v/v) penicillin-streptomycin (Life Technologies). The MEFs were then incubated overnight at 37°C, and rinsed a few times with DPBS (Life Technologies) before use.

2.2.7 Directed hepatic differentiation of hiPSCs

The directed differentiation of all the hiPSC lines towards hepatocyte-like cells was performed using a common protocol adapted from a combination of previously published protocols (Kajiwara*, et al.*, 2012; Sullivan*, et al.*, 2010; Szkolnicka*, et al.*, 2014). The directed differentiation protocol is summarised in Figure 1. All the hiPSCs used for directed differentiation towards hepatocyte-like cells (HLCs) were from feeder-free cultures maintained on Matrigel (Corning); hence hiPSC lines maintained on MEFs were first transitioned to feeder-free Matrigel matrix and maintained for at least 2 passages before being used for differentiation towards HLCs.

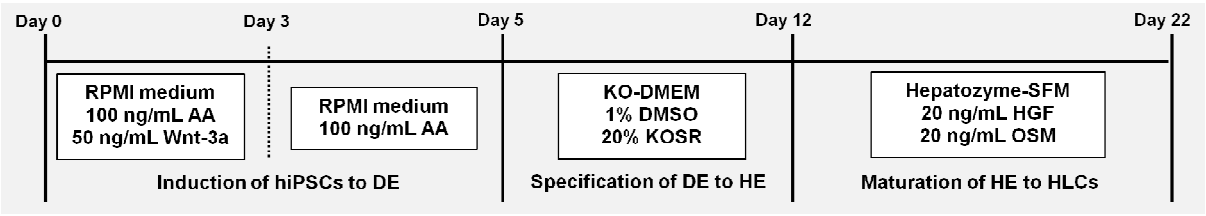

Figure 2.1 Protocol for directed differentiation of hiPSCs towards HLCs using growth factors and small molecules.

RPMI, Roswell Park Memorial Institute; AA, activin A; Wnt-3a, wingless-type MMTV integration site family, member 3A; KO-DMEM, KnockOut Dulbecco's Modified Eagle's Medium; DMSO, dimethyl sulfoxide; KOSR, KnockOut Serum Replacement; HGF, hepatocyte growth factor; OSM, oncostatin M; hiPSCs, human induced pluripotent stem cells; DE, definitive endoderm; HE, hepatic endoderm; HLCs, hepatocyte-like cells.

2.2.7.1 Induction of hiPSCs to definitive endoderm

For the differentiation of the hiPSCs towards definitive endoderm (DE), the feeder-free hiPSC cultures were first dissociated into single cell suspensions by incubating the cultures with Accutase (Life Technologies) at 37^{o}C for 2-5 minutes. Once detachment of the hiPSCs was observed, the dissociation reaction was stopped by diluting the Accutase with complete E8 medium (Life Technologies) and dissociated into single cells by pipetting. The cell concentration of the suspension was determined using a haemocytometer, centrifuged at 200x g for 4 minutes at room temperature, and resuspended with Roswell Park Memorial Institute (RPMI, Life Technologies) medium supplemented with 1% (v/v) B27 (from 50x stock, Life Technologies), 0.5% (v/v) penicillin-streptomycin (Life Technologies), 100 ng/mL activin A (AA, R&D Systems) and 50 ng/mL Wnt-3a (R&D Systems) and 10 µM of the selective inhibitor of Rho-associated protein kinase, InSolution Y-27632 (Merck Millipore). The hiPSCs were then seeded onto Matrigel (Corning) at a density of 2.5 x10^{5} cells/cm^{2} and incubated overnight at 37°C. The medium was then replaced on the first day of differentiation (designated Day 0) with RPMI medium supplemented with 1% (v/v) B27, 0.5% (v/v) penicillin-streptomycin, 100 ng/mL AA and 50 ng/mL Wnt-3a for 72 hours, followed by a further 48 hours of the same medium composition but without Wnt-3a. The medium was replaced daily for this stage.

2.2.7.2 Specification of DE to hepatic endoderm (HE)

Hepatic specification was then carried out for seven days in KnockOut DMEM (Life Technologies) supplemented with 20% (v/v) KnockOut Serum Replacement (KOSR, Life Technologies), 1 mM L-glutamine (Sigma-Aldrich), 100 µM MEM NEAA (Life Technologies), 200 µM beta-ME (Life Technologies), 1% (v/v) dimethyl sulfoxide (DMSO, Fisher Scientific) and 0.5% (v/v) penicillin-streptomycin (Life Technologies), which was changed every two days.

2.2.7.3 Maturation of HE to hepatocyte-like cells (HLCs)

To allow for maturation, HLCs were cultured for a further seven days in Hepatozyme-SFM medium (Life Technologies) supplemented with 0.5% (v/v) penicillin-streptomycin (Life Technologies), 2 mM L-glutamine (Sigma-Aldrich), 10^{-7} M dexamethasone (Sigma-Aldrich), 20 ng/mL oncostatin M (OSM, PeproTech) and 20 ng/mL hepatocyte growth factor (HGF, PeproTech), which was changed every two days. Cells were lysed at Days 5, 12 and 22 of differentiation in 700 µL of QIAzol (Qiagen) as per manufacturer's instructions before being stored at -80°C.

2.2.8 Embryoid body formation and spontaneous differentiation into cells of three germ layers

For the embryoid formation assay, the hiPSC colonies were first dissociated using GCDR (STEMCELL Technologies) as described in Section 2.2.6, and the cell aggregates seeded on non-tissue culture treated plates (Corning) at a passaging ratio of 2:1 in differentiation medium consisting of DMEM/F12 (Life Technologies) supplemented with 20% (v/v) KOSR (Life Technologies), 2 mM L-glutamine (Sigma-Aldrich), 100 µM MEM NEAA (Life Technologies), 100 µM 2-ME (Life Technologies) and 0.5% (v/v) penicillin-streptomycin (Life Technologies). 50% of the medium was replaced with fresh medium every two days. After seven days, the embryoid bodies (EBs) were collected and transferred to tissue culture treated plates coated with 0.1% AF (Life Technologies) and cultured for another 5-7 days with the medium changed every two days before the cells were fixed for indirect immunocytochemistry analysis. Some embryoid bodies were also lysed in 700 µL of QIAzol (Qiagen) as per manufacturer's instructions before being stored at -80°C.

2.2.9 Immunocytochemistry

2.2.9.1 Indirect immunocytochemistry

For indirect immunocytochemistry analysis, cells were fixed in 4% (w/v) paraformaldehyde (Sigma-Aldrich) for 10 minutes at room temperature followed by repeated washes in Dulbecco's Phosphate Buffered Saline (DPBS, with magnesium chloride and calcium chloride, Life Technologies). The fixed cells were then incubated in DPBS (Life Technologies) containing 10% (v/v) donkey serum (Sigma-Aldrich) and 0.1% (v/v) Triton X-100 (Sigma-Aldrich) for 30 minutes followed by overnight incubation with the relevant primary antibody at 4°C. After three washes in DPBS (Life Technologies), the fixed cells were incubated with the appropriate secondary antibody for 2 hours in the dark, at room temperature, before the cells were washed three times again with DPBS. The cells were then incubated with Hoechst 33342 (1:7500, from stock solution of 1 mg/ml, Sigma–Aldrich) for 15 minutes at room temperature before further washes with DPBS. Primary and secondary antibodies were diluted in DPBS (Life Technologies) containing 10% (v/v) donkey serum (Sigma-Aldrich) and 0.1% (v/v) TritonX-100 (Sigma-Aldrich), which was then centrifuged at 13000 rpm for 6 minutes at room temperature. The following primary and secondary antibodies were used: rabbit anti-Oct4 (1:100, ab18976, Abcam), rabbit anti-Sox2 (1:100, ab75627, Abcam), rabbit anti-Nanog (1:200, ab21624, Abcam), rabbit anti-albumin (1:20, ab135575, Abcam), rabbit anti-alpha smooth muscle actin (1:100, ab5694, Abcam), rabbit anti-beta-III tubulin (1:500, ab18207, Abcam), rabbit anti-alpha fetoprotein (1:100, A0008, Dako), goat anti-Sox17 (1:20, AF1924, R&D Systems), rabbit anti-HNF-4α (1:50, sc-8987, Santa Cruz Biotechnology), donkey Alexa Fluor 488-anti-rabbit IgG (1:1000, A-21206, Life Technologies) and donkey Alexa Fluor 568-anti-goat IgG (1:1000, A-11057, Life Technologies). Technical control stainings without primary antibodies were performed for all indirect immunocytochemical stainings (data not shown).

2.2.9.2 Direct immunocytochemistry

For direct immunocytochemistry analysis, the fixed cells were incubated with conjugated primary antibodies diluted in DPBS (Sigma-Aldrich) for 90 minutes at 37°C before repeated washes with DMEM/F12. The cells were then incubated with Hoechst 33342 (1:7500, from stock solution of 1 mg/ml, Sigma–Aldrich) for 15 minutes at 37°C before further washes with DMEM/F12. The following conjugated primary antibodies were used: Alexa Fluor 488-anti-TRA-1-60 (1:10, 560173, BD Biosciences) and Alexa Fluor 555-anti-SSEA-4 (1:10, 560218, BD Biosciences).

The immunocytochemical stainings were analysed using a fluorescence microscope (Axio Observer.Z1, Carl Zeiss), a digital camera (AxioCam MR, Carl Zeiss) and corresponding software (ZEN, Carl Zeiss).

2.2.10 Flow cytometry

For flow cytometric analysis of albumin-positive cells in hPH cultures, the hPHs were first dissociated into a cell suspension using TrypLE Select Enzyme (Life Technologies) as per manufacturer's protocol. The cells were then fixed and permeabilised using the Cytofix/Cytoperm Fixation/Permeabilization Solution Kit (BD Biosciences) as per manufacturer's protocol, before being labelled with rabbit anti-albumin (1:20, ab135575, Abcam) in a volume of 100 µL on ice for 30 minutes. The cell was then pelleted and labelled with donkey Alexa Fluor 488-anti-rabbit IgG (1:2000, A-21206, Life Technologies) on ice for 20 minutes. A minimum of 10000 cells were analysed by flow cytometry using the BD FACSCanto II (BD Biosciences) cell analyser and the data analysed using Cyflogic (CyFlo). Technical controls using unlabelled hPHs and hPHs labelled with the secondary antibody only were also used. The technical assistance of Dr. Lee Faulkner (University of Liverpool) with the flow cytometric analysis is gratefully acknowledged.

2.2.11 Real-time quantitative RT-PCR (qRT-PCR)

2.2.11.1 Purification of total RNA

The purification of total RNA from cellular lysates was performed using the miRNeasy mini kit (Qiagen), as per the manufacturer's instructions. Briefly, each lysate was thawed at room temperature and thoroughly mixed before the addition of 140 µL of chloroform. The samples were then mixed vigorously for 15 seconds and left at room temperature for 3 minutes. The homogenates were then centrifuged at 12000x g for 15 minutes at 4°C. 350 µL of the upper aqueous phase and 525 µL of 100% ethanol were then mixed thoroughly in a new collection tube before transferring to a miRNeasy Mini spin column. The column was then sequentially centrifuged and washed with supplied buffers at room temperature, before the column was placed into a new collection tube. 30 µL of RNase-free water was then added directly onto the column membrane and centrifuged for 1 minute at 10000x g to elute the total RNA which also contained the small RNA fraction. Quantification and the quality of the total RNA extracts was then analysed using the NanoDrop spectrophotometer (Thermo Scientific).

2.2.11.2 Gene expression analysis

For the analysis of mRNA expression, first strand complementary DNA (cDNA) was synthesized from equal amounts of total RNA with ImProm-II Reverse Transcription System (Promega) as per manufacturer’s instructions. Briefly, a total RNA and primer mixture was first prepared as instructed in a total volume of 25 µL and incubated for 5 minutes at 70°C before being chilled on ice for at least 5 minutes. A reverse transcription (RT) reaction mixture was then prepared as instructed and added to the 25 µL of the total RNA and primer mixture for complementary DNA (cDNA) synthesis in a total volume of 50 µL, before being heated sequentially in a GeneAmp PCR System 9700 thermal cycler (Applied Biosystems) for 5 minutes at 25°C, 60 minutes at 42°C and 15 minutes at 70°C. The cDNA was then

chilled at 4°C before storage at -20°C or proceeding to real-time quantitative RT-PCR (qRT-PCR) which was performed using SYBRGreen JumpStart Taq ReadyMix (Sigma-Aldrich) as per manufacturer's instructions. Briefly, 5 µL of cDNA was mixed with a PCR mixture containing 10 µM of PCR primers in a total volume of 25 µL. PCR amplification was then performed in duplicates with the ABI Prism 7000 or ViiA 7 Real-Time PCR instruments (Applied Biosystems) using a 2-step thermal cycling protocol of 95°C for 10 minutes followed by 40 cycles of 95°C for 15 seconds and 60°C for 60 seconds. C_t values were determined using the fluorescent signal produced from the SYBR Green I dye. The gene expression was normalized against the reference gene glyceraldehyde 3-phosphate dehydrogenase (GAPDH), and fold changes were calculated using a calibrator sample using the relative quantification method.

2.2.11.4 Design of real-time qRT-PCR primers

Primers for real-time qRT-PCR analysis of mRNA expression were designed using Primer-BLAST with their default parameters (Ye *et al.*, 2012). The mRNA targets were based on the latest NCBI RefSeq annotations and the specificity of primers checked against the RefSeq human mRNA database. All the designed primers span an exon-exon junction to exclude the possibility of genomic DNA amplification. The primers were also assessed for the likelihood for self-complementarity, hairpin and primer-dimer formations using OligoCalc (Kibbe, 2007). The primer sequences used for qRT-PCR analysis of mRNA expression reported in this chapter are listed in Table 1.

Table 1.1 Primer sequences for real-time qRT-PCR.

For gene name abbreviations, please see http://www.ncbi.nlm.nih.gov/gene/. Commonly known aliases are listed in parentheses.

Gene	Real-time qRT-PCR primers	Sequence (5' – 3')
ALB	ALB mRNA-F	CCTGTTGCCAAAGCTCGATG
	ALB mRNA-R	ATCTCCATGGCAGCATTCCG
SERPINA1 *(A1AT)*	A1AT mRNA-F	TCCGATAACTGGGGTGACCT
	A1AT mRNA-R	AGACGGCATTGTCGATTCACT
CYP3A4	CYP3A4 mRNA-F	AGAAATCTGAGGCGGGAAGC
	CYP3A4 mRNA-R	GGAATGGAAAGACTGTTATTGAGAG
KRT18 *(CK18)*	CK18 mRNA-F	ACATCCGGGCCCAATATGAC
	CK18 mRNA-R	GGTGCTCTCCTCAATCTGCT
GAPDH	GAPDH mRNA-F	CTATAAATTGAGCCCGCAGCC
	GAPDH mRNA-R	GCCCAATACGACCAAATCCGT
HNF4A	HNF4A mRNA-F	GTTGACGATGGGCAATGACAC
	HNF4A mRNA-R	TCTTTGTCCACCACGCACTG
AFP	AFP mRNA-F	GCGGCCTCTTCCAGAAACTA
	AFP mRNA-R	AATAATGTCAGCCGCTCCCT
SOX17	SOX17 mRNA-F	GGATACGCCAGTGACGACCA
	SOX17 mRNA-R	GACTTGCCCAGCATCTTGCTC
NANOG	NANOG mRNA-F	GGCTCTGTTTTGCTATATCCCCTAAA
	NANOG mRNA-R	CATTACGATGCAGCAAATACGAGA

2.2.12 Enzyme-linked immunosorbent assay (ELISA) for albumin detection

For the measurement of albumin secretion, the culture media of HLCs and hPHs were collected and stored at -80°C until further analysis using the Human Albumin ELISA Quantitation Set (Bethyl Laboratories) as per manufacturer's protocol. Briefly, 96-well format plates were first coated with supplied goat anti-human albumin antibody and prepared according to instructions. A standard curve was also prepared using recommended dilutions of supplied human reference serum. Diluted media samples in a total volume of 100 µL were

then loaded in duplicates and incubated at room temperature for 1 hour. The plates were then washed five times with a wash buffer, and incubated with the supplied goat HRP-conjugated anti-human albumin detection antibody for a further 1 hour. Following washes, the supplied 3,3′,5,5′-Tetramethylbenzidine (TMB) Substrate Solution was then added, and the colour enzymatic reaction allowed to develop at room temperature in the dark for 15 minutes. The reaction was then stopped using 0.18M of sulphuric acid and its absorbance measured using the MRX^{e} Microplate Reader (Dynex Technologies) at 450 nm. The albumin concentration in the samples was then estimated using values obtained from the prepared standard curve.

2.2.13 Phase contrast microscopy

Cell morphology was analysed by light microscopy using a phase contrast microscope (ECLIPSE TS100/100-F, Nikon), and photographs captured using a digital camera head (DS-Vi1, Nikon) and a stand-alone controller and display unit (DS-L3, Nikon).

2.2.13 Statistical analysis

For pairwise comparisons between HLCs generated from different hiPSC lines, the unpaired t-test was used. For all tests, $p < 0.05$ was considered significant. Statistical analyses were performed using GraphPad Prism 6 (GraphPad Software).

2.3 RESULTS

2.3.1 Isogenic hiPSC lines were successfully derived from hepatocytes and fibroblasts using Sendai viral vectors encoding the Yamanaka pluripotency factors

Corresponding sets of isogenic human iPSC lines (hiPSCs) were derived from human primary hepatocytes (hPHs) and human dermal fibroblasts (hDFs) originating from the same patients, using commercially-available Sendai episomal viral vectors encoding the Yamanaka pluripotency factors *i.e.* Oct4, Sox2, Klf4 and c-Myc (Fusaki*, et al.*, 2009; Takahashi *et al.*, 2007). The demographic and clinical details of the adult donor from which the tissues were obtained from are shown in Table 2.2

Table 2.2 Demographic and clinical details of the adult donor of hPHs and hDFs

	DONOR 1	DONOR 2
Age at surgery	66	63
BMI	27.9	31.2
Sex	Male	Female
Diagnosis	Colorectal carcinoma with liver metastases	Colorectal carcinoma with liver metastases
Co-morbidity	Type II diabetes mellitus	Hypertension Chronic liver disease Type II diabetes mellitus

2.3.1.1 Derivation of hiPSCs from adult human primary hepatocytes

The reprogramming of hPHs from adult donors was performed using the protocol described in Section 2.2.4, and summarised in Figure 2.2. The purity of the hPH culture in terms of cells expressing the hepatic marker albumin was also assessed using cultures of hPHs isolated from both donors. Following plating of the hPHs and prior to the reprogramming of the culture at Day 0, the hPH cultures were analysed using immunocytochemical (n = 2

donors) and flow cytometric methods (n = 1 donor). Using immunocytochemistry, we estimated that >90% of the plated hPHs were positive for albumin, while flow cytometric quantification showed that 85.1% of the cells were positive (Figure 2.3). The cell viability of hPHs isolated from both donors was >80%.

The morphology of the hPH culture in the medium containing hepatocyte growth factor (HGF) and epidermal growth factor (EGF) was also noted to change prior to reprogramming from its initial typical cuboidal shape with distinct borders to flattened cells with multiple projections (Figure 2.4A and 2.4B). Following transduction of the plated hPHs, the culture was monitored closely for the appearance of nascent hiPSC colonies with daily replacement of the medium. At Day 2, the morphology of the culture was noted to have changed further with the presence of apoptotic cells, presumably due to the SeV transduction, and also the presence of cells which were noted to be smaller than a typical hPH which has lost its distinct borders (Figure 2.5A and 2.5B). Whether these latter cells were transduced hPHs undergoing early reprogramming or hPHs merely transformed by the presence of SeV is unclear. The number of cells present in the culture continued to noticeably decrease until about Day 7, before the eventual emergence and expansion of homogenous colonies of epithelial-like cells (Figure 2.5C and 2.5D). By about Day 18, the morphology of some these homogenous colonies was also noted to change and distinct cells with a high ratio of nucleus to cytoplasm resembling human embryonic stem cells (hESCs), started to emerge within these homogeneous colonies (Figure 2.5E and 2.5F). Concomitantly, there were also colonies of cells resembling typical hESC-like colonies which appeared separate from the homogeneous colonies of flat small cells and typically appeared later during the reprogramming process (Figure 2.5G, 2.5H and 2.5I). hiPSC lines were successfully established from both types of colonies containing hESC-like cells. There were also numerous colonies which were non-hESC-like and most probably represent incompletely reprogrammed cells. Between Day 25 to Day 40, the hESC-like colonies of sufficient size

were then manually passaged separately onto either Matrigel-coated wells or MEF feeder layers for expansion.

The manually picked colonies were then expanded as described in Section 2.2.6. However, only colonies which were plated onto MEF feeder layers were successfully established as hiPSC lines (Figure 2.6A and 2.6B). Details of successful hiPSC derivation from hPHs obtained from the 2 adult donors are shown in Table 2.3.

Overall, from our experience of reprogramming hPHs (n = 4 separate donors of hPHs), we found that the optimal conditions required to successfully derive hiPSC lines include using a multiplicity of infection (MOI) of 5-7, avoiding the use of thawed SeV particles, the use of feeder layers to support picked colonies and using a starting cell density of at least 2 x10^5 cells/well of a 6-well plate format to obtain adequate hESC-like colonies for isolation.

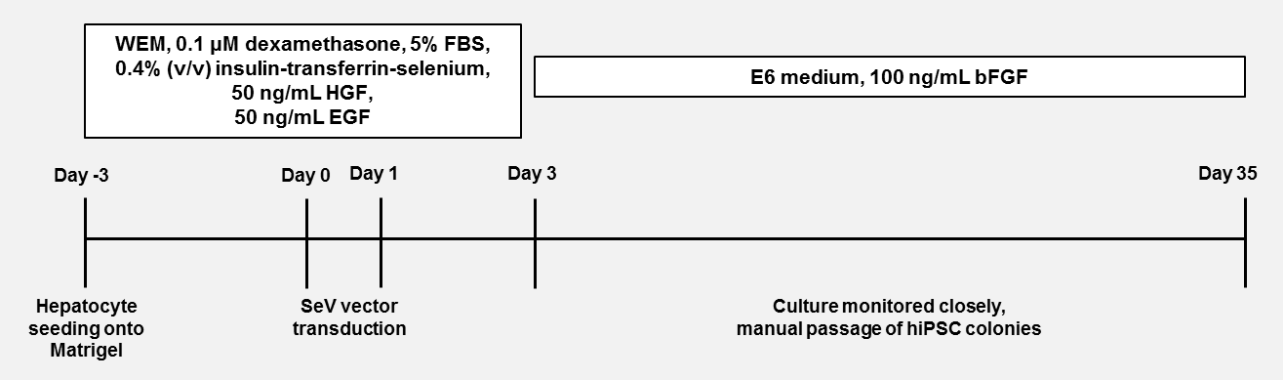

Figure 2.2 Protocol of reprogramming hPHs into hiPSCs.

WEM, Williams E medium; FBS, foetal bovine serum; HGF, hepatocyte growth factor; EGF, epidermal growth factor; E6, essential 6; bFGF, basic fibroblast growth factor; SeV, Sendai virus; hiPSC, human induced pluripotent stem cell.

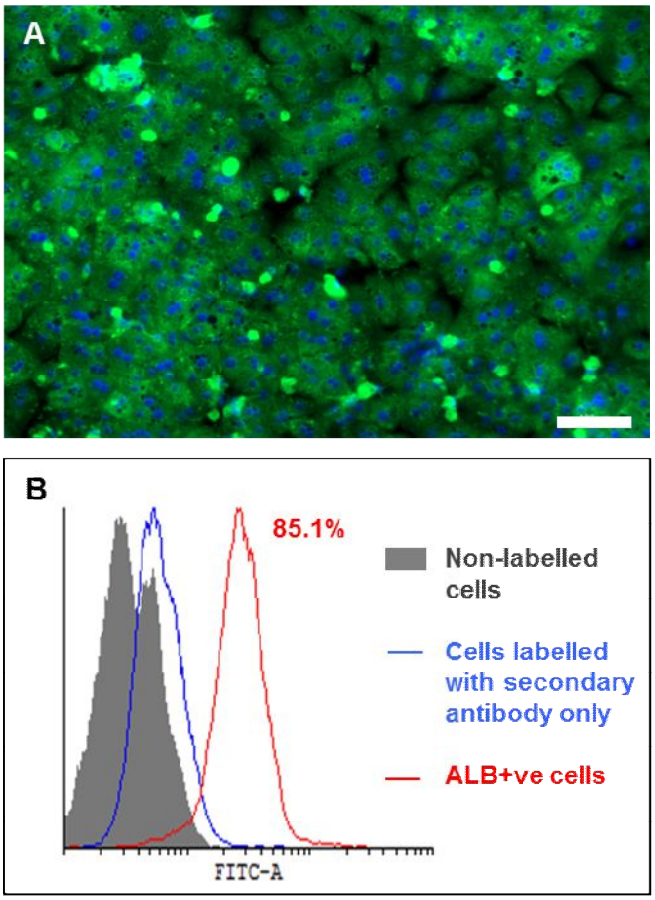

Figure 2.3 Characterisation of the hPH cultures for ALB-positive cells

Representative results for hPHs obtained from Donor 1: (A) Immunocytochemical analysis of ALB in combination with Hoescht 33342 (nuclear stain in blue) for hPHs at Day 0. Magnification: 200x; scale bar, 100 µm. (B) ALB expression of cells from the hPH culture at Day 0, analysed using flow cytometry.

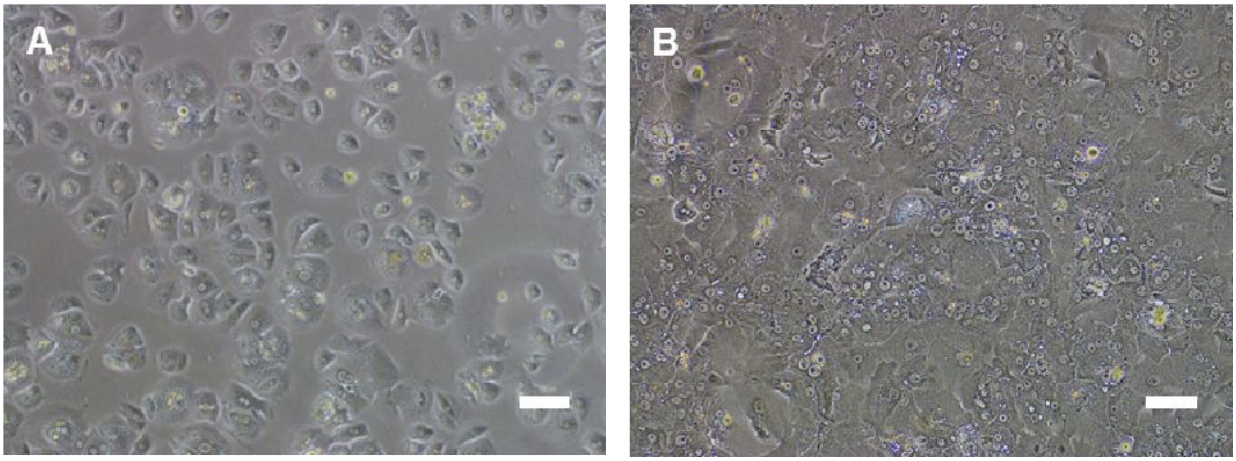

Figure 2.4 Morphological changes of the hPH culture before reprogramming.

Phase contrast microscopy showing morphology of plated hPHs pre-transduction at (A) Day -3, and (B) Day 0. Magnification: 100x; scale bar, 100 µm.

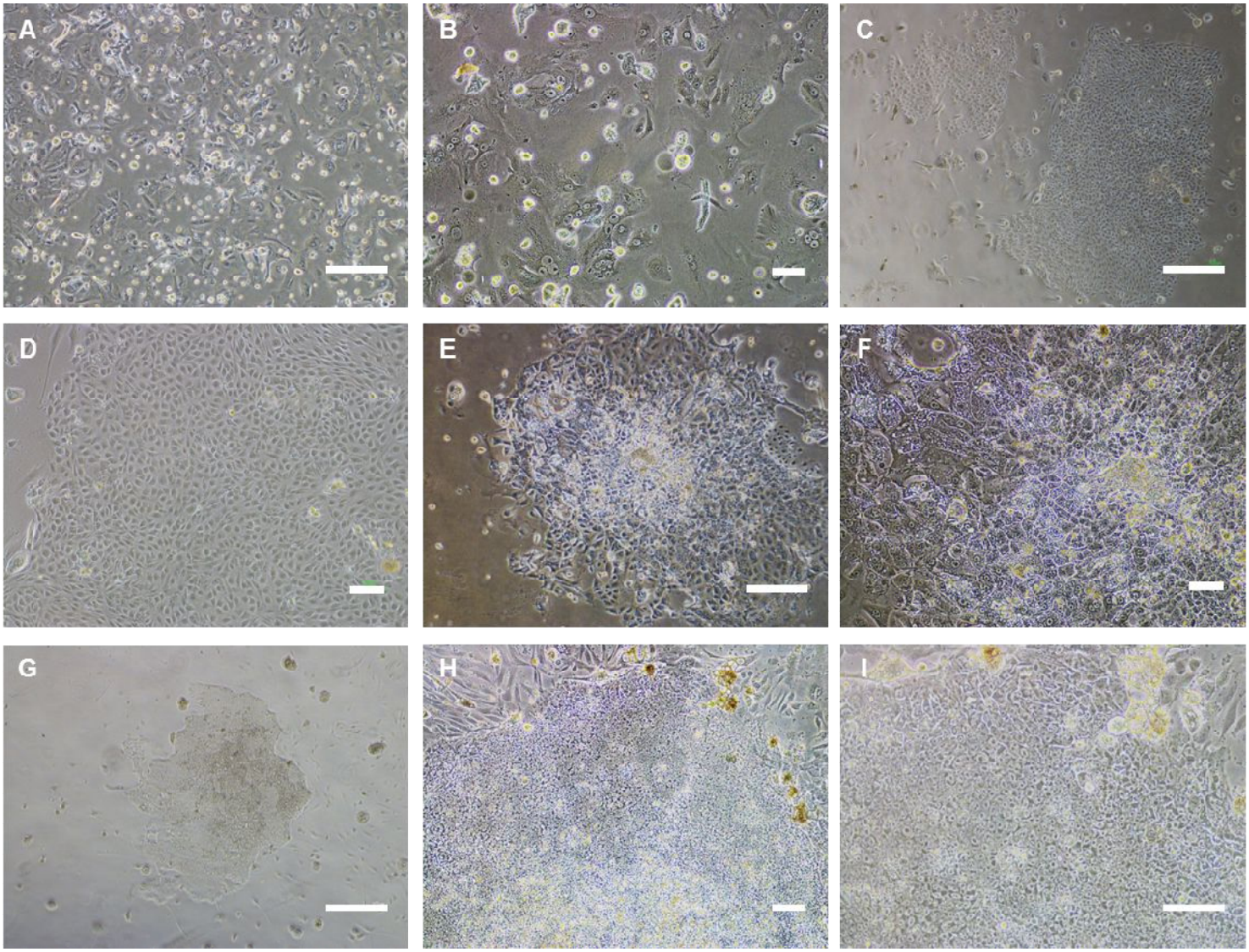

Figure 2.5 Morphological changes of the hPH culture during reprogramming.

Phase contrast microscopy showing morphology of plated hPHs at Day 2, imaged with magnification of (A) 40x; scale bar, 500 µm and (B) 100x; scale bar, 100 µm. Appearance of a typical homogeneous colony of small flat cells with high ratio of nucleus to cytoplasm at Day 13, imaged with magnification of (C) 40x; scale bar, 500 µm and (D) 100x; scale bar, 100 µm. Typical morphology of hESC-like cells emerging within the homogenous colony of small cells observed at Day 23, imaged with magnification of (E) 40x; scale bar, 500 µm and (F) 100x; scale bar, 100 µm. A typical hESC-like colony observed at Day 36, imaged with magnification of (G) 40x; scale bar, 500 µm, (H) 100x; scale bar, 100 µm and (I) 200x; scale bar, 100 µm. hESC, human embryonic stem cell.

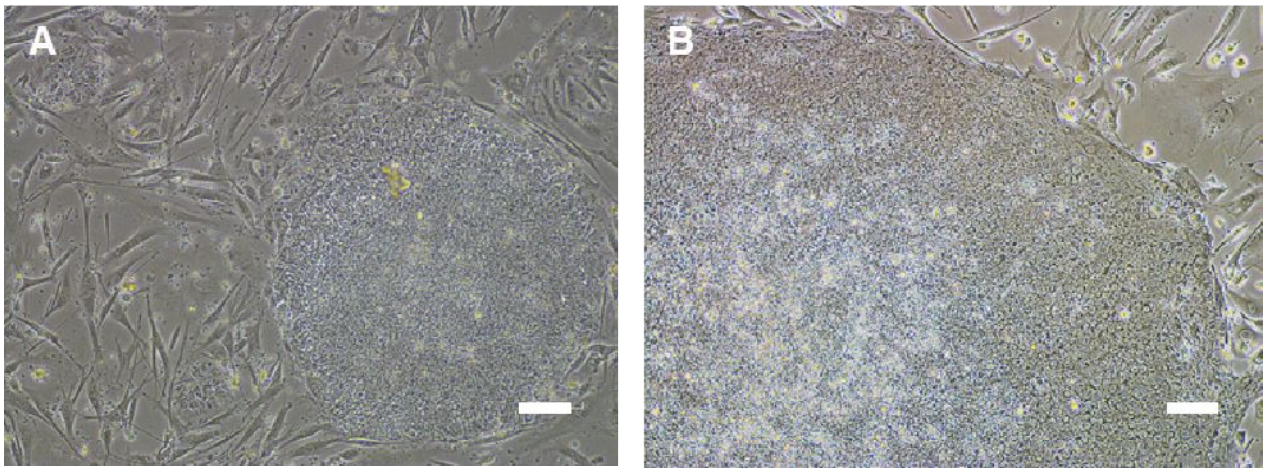

Figure 2.6 Representative established hiPSC lines derived from hPHs of 2 different adult donors

Phase contrast microscopy showing morphology of (A) Liv4HJ derived from hPHs of Donor 1 and (B) Liv6HD derived from hPHs of Donor 2. Magnification: 100x; scale bar, 100 µm.

Table 2.3 Details of hiPSC derivation from adult donors of hPHs.

* Reprogramming efficiency for each donor-batch of hPH was calculated as: (number of hiPSC lines established/total number of hPHs seeded) x100%.

Donor	Number of hPHs seeded	hESC-like colonies picked	hiPSC lines established	Reprogramming efficiency (%)*
1	2.0×10^5	8	1	0.0005
2	4.0×10^5	7	5	0.00125

2.3.1.2 Derivation of hiPSCs from adult human dermal fibroblasts

hDFs from the corresponding adult donors of hPHs were first propagated from the skin excisions (Figure 2.7) and reprogrammed only when at least one hiPSC line was successfully derived from hPHs isolated from the donor. The hDFs used for reprogramming were passaged less than four times from initial propagation from the dermal tissue pieces.

The derivation of hiPSCs from hDFs of Donors 1 and 2 were both performed using the same SeV vectors encoding the Yamanaka pluripotency factors (Figure 2.8). The hDFs were reprogrammed as per manufacturer's protocol and as previously described (Fusaki*, et al.*, 2009), with the main difference compared to the protocol used for reprogramming hPHs being that the culture of transduced hDFs was split and replated at Day 7 to prevent the culture from being too confluent due to the proliferation of the hDFs (Figure 2.8C).

The transduced hDFs were then transferred onto MEF feeder layers or Matrigel and the cultures monitored for the emergence of nascent hiPSC colonies (Figure 2.8D). hESC-like colonies were seen from Day 15 onwards and the colonies manually passaged onto fresh MEF feeder layer or Matrigel respectively between Day 25 to Day 35. In contrast to hiPSCs derived from hPHs, hiPSC lines derived from hDFs were successfully established on both feeder-dependent and feeder-free cultures (Figure 2.9). The reprogramming efficiency of hDFs was notably much higher than hPHs, as there were many other colonies in the reprogramming cultures with typical hESC-like appearances which were not picked as we only manually isolated enough colonies (>10 per donor-batch of hDFs from both feeder-dependent and feeder-free cultures) to ensure successful establishment of at least 3 hDF-derived hiPSC lines.

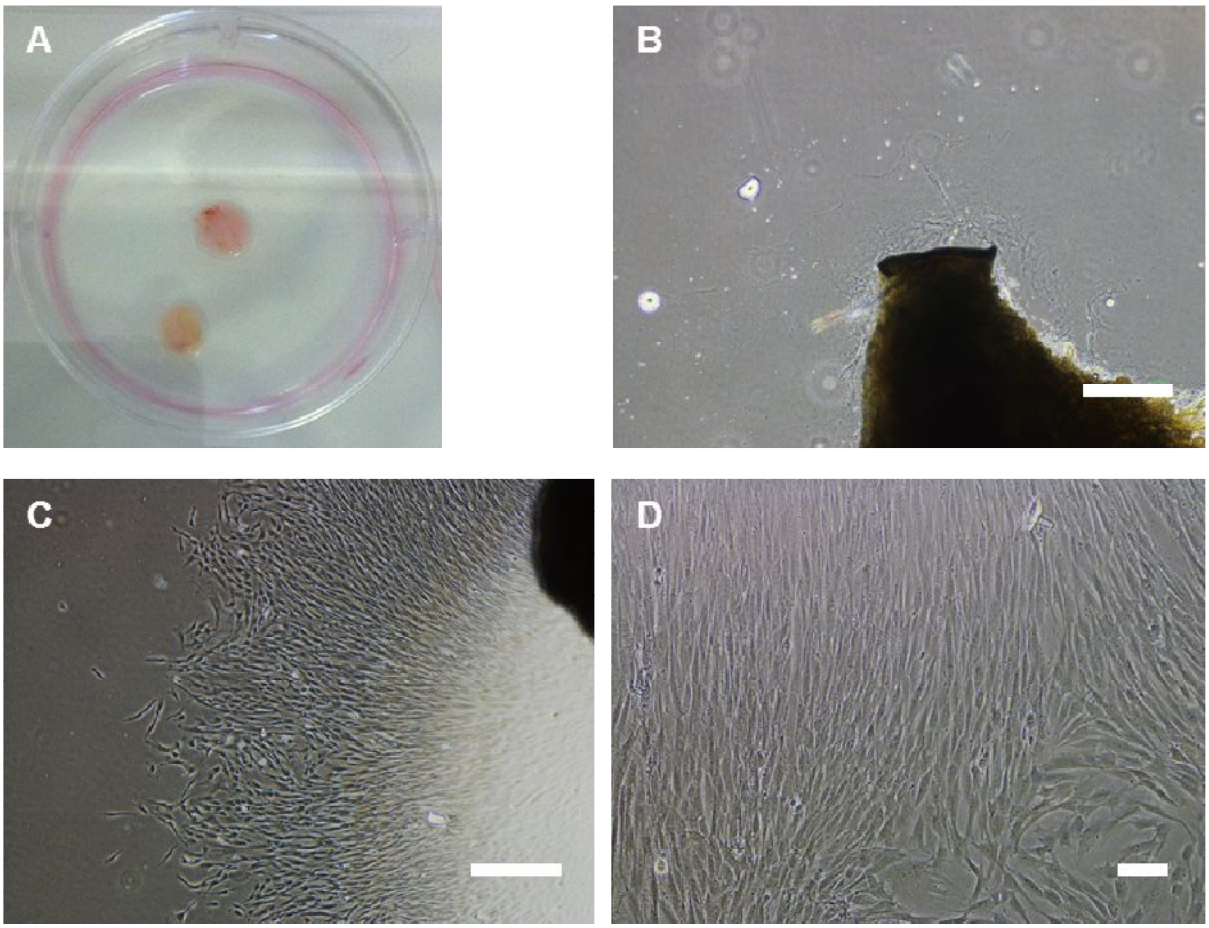

Figure 2.7 Propagation of hDFs from skin excisions.

(A) Close-up view of pieces of dermis placed in a single well of a 6-well tissue culture plate. Phase contrast microscopy showing (B) a piece of dermal tissue on the surface of the tissue-culture plate, imaged with magnification of 40x; scale bar, 500 µm. Appearance of hDFs growing out from the edge of the dermal tissue 17 days after initial propagation, imaged with (C) magnification of 40x; scale bar, 500 µm, and (D) magnification of 100x; scale bar, 100 µm.

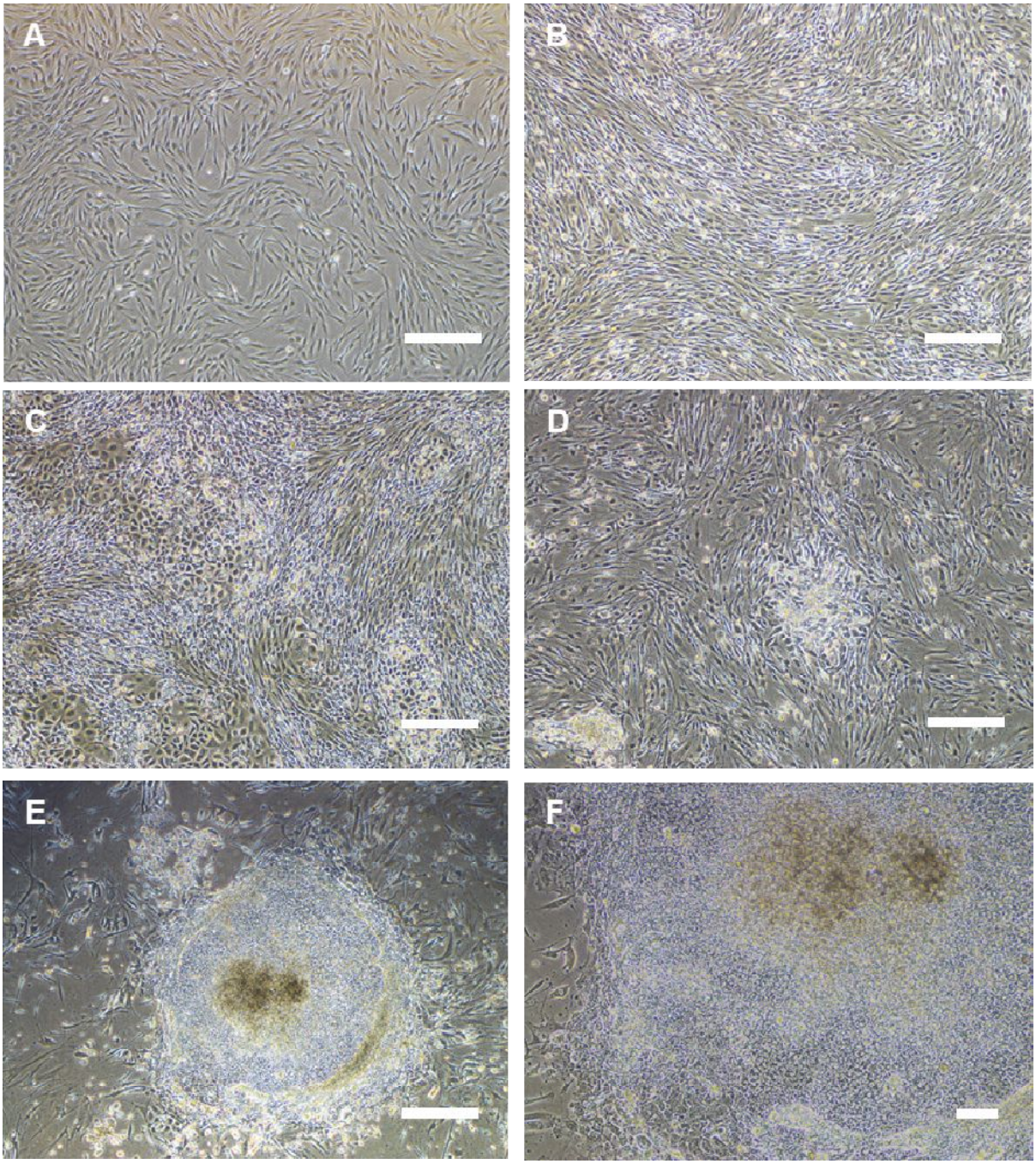

Figure 2.8 Morphological changes of the hDF culture during reprogramming.

Phase contrast microscopy showing (A) plated hDFs at Day 0 prior to transduction of SeV vectors, seen with magnification of 40x; scale bar, 500 µm. Morphology of transduced hDFs at (B) Day 4 and (C) Day 7 prior to splitting of the culture, both seen with magnification of 40x; scale bar, 500 µm. (D) Appearance of hESC-like colony observed at Day 16 for the culture of transduced hDFs transferred onto a MEF feeder layer, seen with magnification of 40x; scale bar, 500 µm. Typical appearance of a hiPSC colony ready for manual passaging, observed at Day 31, seen with magnification of (E) 40x; scale bar, 500 µm and (F) 100x; scale bar, 100 µm.

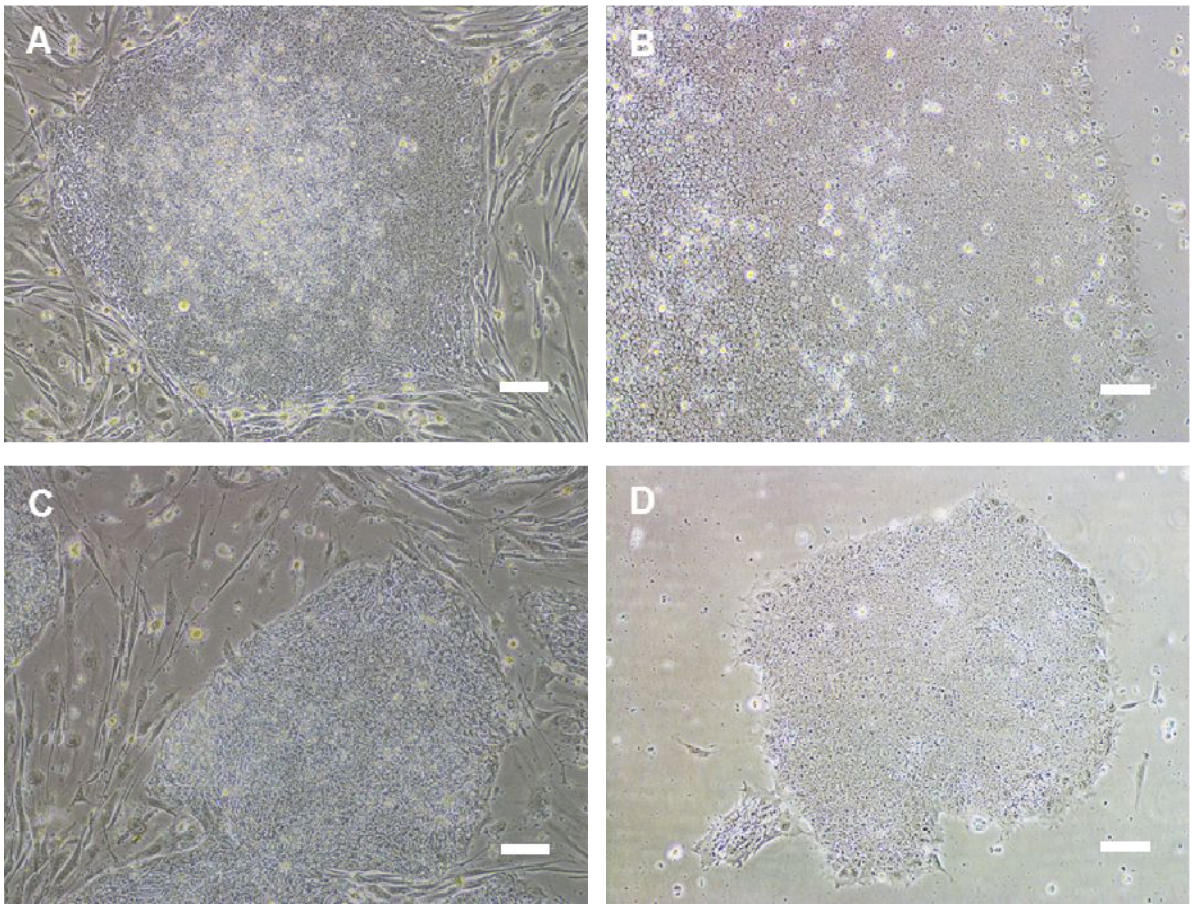

Figure 2.9 Representative established hiPSC lines derived from hDFs of 2 different adult donors.

Phase contrast microscopy showing morphology of (A) Liv4FA and (B) Liv4FB derived from hDFs of Donor 1; (C) Liv6FP and (B) Liv6FC derived from hDFs of Donor 2. Magnification for all images: 100x; scale bar, 100 µm.

2.3.2 Characterisation of isogenic hiPSC lines derived from hepatocytes and dermal fibroblasts

At the time of preparation for the thesis, only HLCs differentiated from hiPSC lines derived from Donor 1 was available for comparison. Therefore, the rest of the following chapter will only describe the characterisation of the hiPSC lines derived from Donor 1 and also the respective HLCs generated from these lines.

2.3.1.1 Derived hiPSC lines express pluripotency markers

All the hiPSC lines derived from both hPHs and hDFs which were used for subsequent directed differentiation towards HLCs were confirmed for their pluripotency using immunocytochemistry with antibodies against a panel of pluripotency markers: octamer-binding transcription factor 4 (OCT4), sex determining region Y-box 2 (SOX2), NANOG, TRA-1-60 and stage-specific embryonic antigen-4 (SSEA-4) (Figure 2.10). The hiPSC lines were cultured as monolayers and maintained their undifferentiated state, as observed by their morphology.

2.3.1.2 Derived hiPSC lines spontaneously differentiate into cells of three germ layers

All the hiPSC lines were also assessed for their ability to spontaneously differentiate *in vitro* into cells of all three germ layers using the embryoid body formation assay (Figure 2.11). After 7 days in suspension culture, the embryoid bodies were plated onto gelatin-coated plates and culture continued for a further 5-7 days. The attached cells showed various morphology when analysed using phase contrast microscopy, and immunocytochemistry detected cells positive for beta-III tubulin (marker of ectodermal cells), alpha smooth muscle actin (α-SMA, marker of mesodermal cells) and alpha fetoprotein (AFP, marker of

endodermal cells) in all the hiPSC lines assessed (Figure 2.12). This confirmed that the hiPSCs could spontaneously differentiate into cells from all three germ layers *in vitro*.

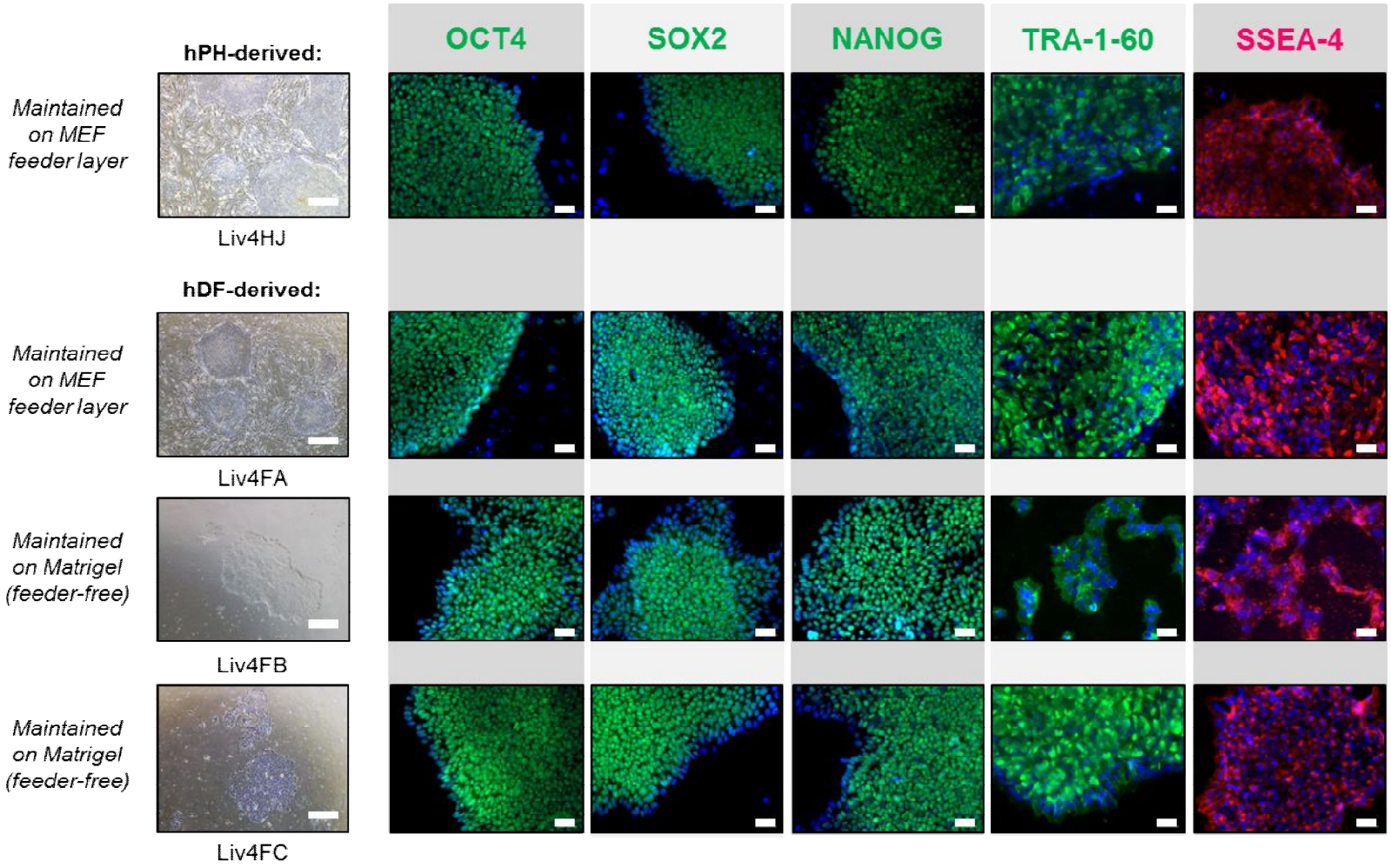

Figure 2.10 Immunocytochemistry for pluripotency markers in isogenic hiPSCs derived from hPHs and hDFs.

For all the ICC images (coloured panels), the nuclei were counterstained with Hoescht 33342 (blue) and imaged with magnification of 200x; scale bar, 100 µm. The left panel shows corresponding phase contrast microscopy images of the hiPSC colonies, imaged with magnification of 40x; scale bar 500 µm.

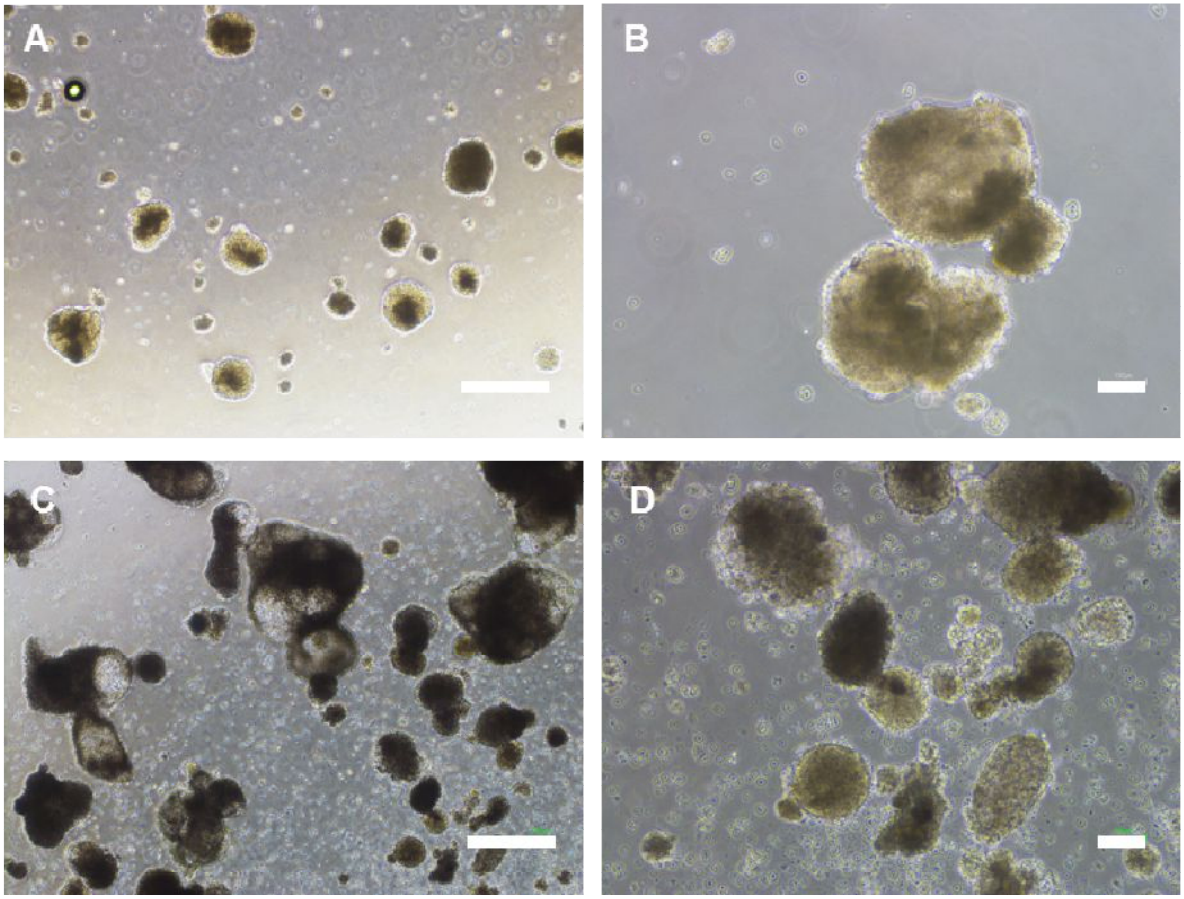

Figure 2.11 Embryoid body formation from hiPSCs.

Representative phase contrast microscopy images of embryoid bodies of various sizes formed from Liv4HJ (A, B) and Liv4FA (C, D) in suspension culture. Magnification of (A, B) 40x; scale bar 500 µm and (C, D) 100x; scale bar 100 µm.

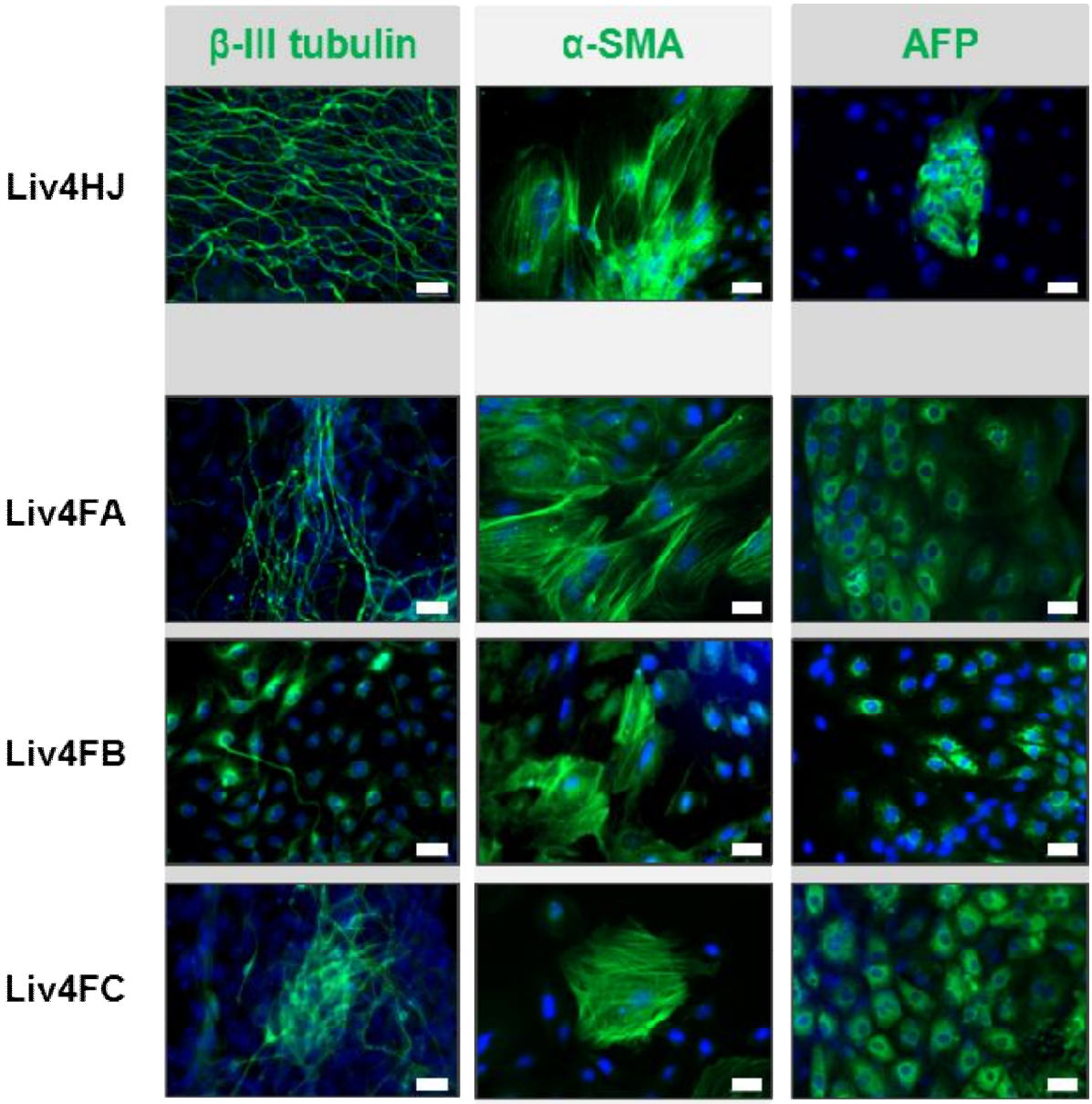

Figure 2.12 Immunocytochemistry for multi-lineage markers of spontaneously differentiated cells from embryoid bodies formed from isogenic hiPSCs derived from hPHs and hDFs.

The ICC images show cells positive (green) for β-III tubulin (left column), alpha-smooth muscle actin (α-SMA, middle column) and alpha fetoprotein (AFP, right column) with the nuclei counterstained with Hoescht 33342 (blue), imaged with magnification of 200x; scale bar, 100 μm. The images were representative of cells spontaneously differentiated from both hPH-derived hiPSCs (Liv4HJ, first row) and hDF-derived hiPSCs (Liv4FA, second row; Liv4FB, third row; and Liv4FC, fourth row).

2.3.3 HLCs generated from multiple hepatocyte- and fibroblast-derived hiPSC lines using a modified multistage hepatic differentiation protocol

To examine the potential contribution of epigenetic memory inherent in the hiPSC lines towards the propensity for hepatic differentiation, we generated HLCs from all the hiPSC lines which were at the early-passage stage (passaged less than 10 times) to avoid the abrogation of epigenetic memory in late-passage hiPSCs as previously reported (Kim*, et al.*, 2011; Polo*, et al.*, 2010). We also applied the same directed hepatic differentiation protocol to all the hiPSC lines examined and used a modified protocol (Figure 2.1) adapted from previously reported ones which were shown to allow for effective hepatic differentiation for multiple hiPSC lines (Kajiwara*, et al.*, 2012; Sullivan*, et al.*, 2010; Szkolnicka*, et al.*, 2014).

All the hiPSC lines were able to undergo hepatic differentiation towards HLCs using the three-step protocol. Briefly, all the hiPSCs were initially dissociated into single cells to allow for greater reproducibility of the cellular responses to growth factors and cell-cell to interactions as opposed to the more conventional method of hepatic differentiation using hiPSC clusters of variable and undefined sizes (Kajiwara*, et al.*, 2012). The induction of hiPSCs into definitive endodermal (DE) cells was confirmed by immunocytochemistry using the DE marker, sex determining region Y-box 17 (SOX17) (Cai *et al.*, 2007; Yasunaga *et al.*, 2005) while hepatic nuclear factor 4 alpha (HNF4A) and albumin was used as hepatic markers at the hepatic endodermal (Day 12, denoting 12 days after the start of differentiation) and mature stages (Day 22) of the differentiation process respectively (Figure 2.13) (Cai*, et al.*, 2007; Hay *et al.*, 2008; Hengstler *et al.*, 2005). There were also sequential morphological changes during the differentiation process and the HLCs at Day 22 generally assumed a polyglonal shape though the resemblance to hPHs was more pronounced with Liv4HJ- and Liv4FB-derived HLCs (Figure 2.13).

The hepatic differentiation of the hiPSCs was also confirmed using real-time qRT-PCR to analyse the expression of the hepatic markers *SOX17* and *AFP*. There was a temporal up-

regulation of the DE marker *SOX17* for all the hiPSC lines at Day 5, compared to their respective undifferentiated hiPSC counterparts (Figure 2.14A), while the expression of *AFP,* gradually increased for all the hiPSC lines and peaked at the HLC stage (Figure 2.14B). Concomitantly, all the hiPSC lines also had down-regulation of the pluripotency marker *NANOG* during the differentiation process (Figure 2.14C).

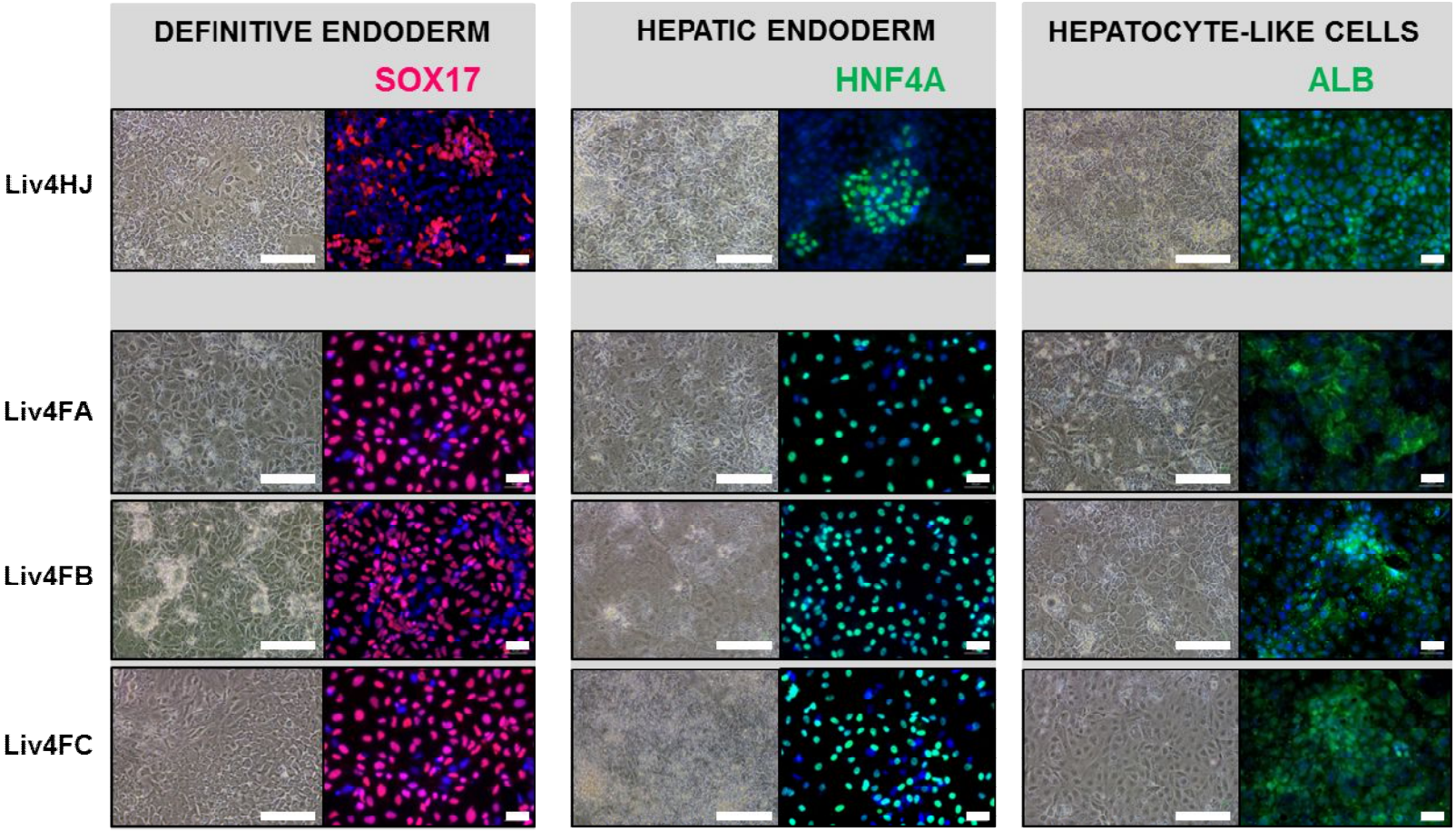

Figure 2.13 Immunocytochemistry for protein markers of key stages of the hepatic differentiation of hiPSCs.

The representative ICC images (right panel of each column) show cells positive (magenta for Sox17, green for HNF4α and albumin) with the nuclei counterstained with Hoescht 33342 (blue), imaged with magnification of 200x; scale bar, 100 µm. The images were representative of cells differentiated from both hPH-derived hiPSCs (Liv4HJ, first row) and hDF-derived hiPSCs (Liv4FA, second row; Liv4FB, third row; and Liv4FC, fourth row). Phase contrast microscopy images of the cells in corresponding stages of hepatic differentiation are shown in the left panel of each column – magnification: 200x; scale bar, 100 µm.

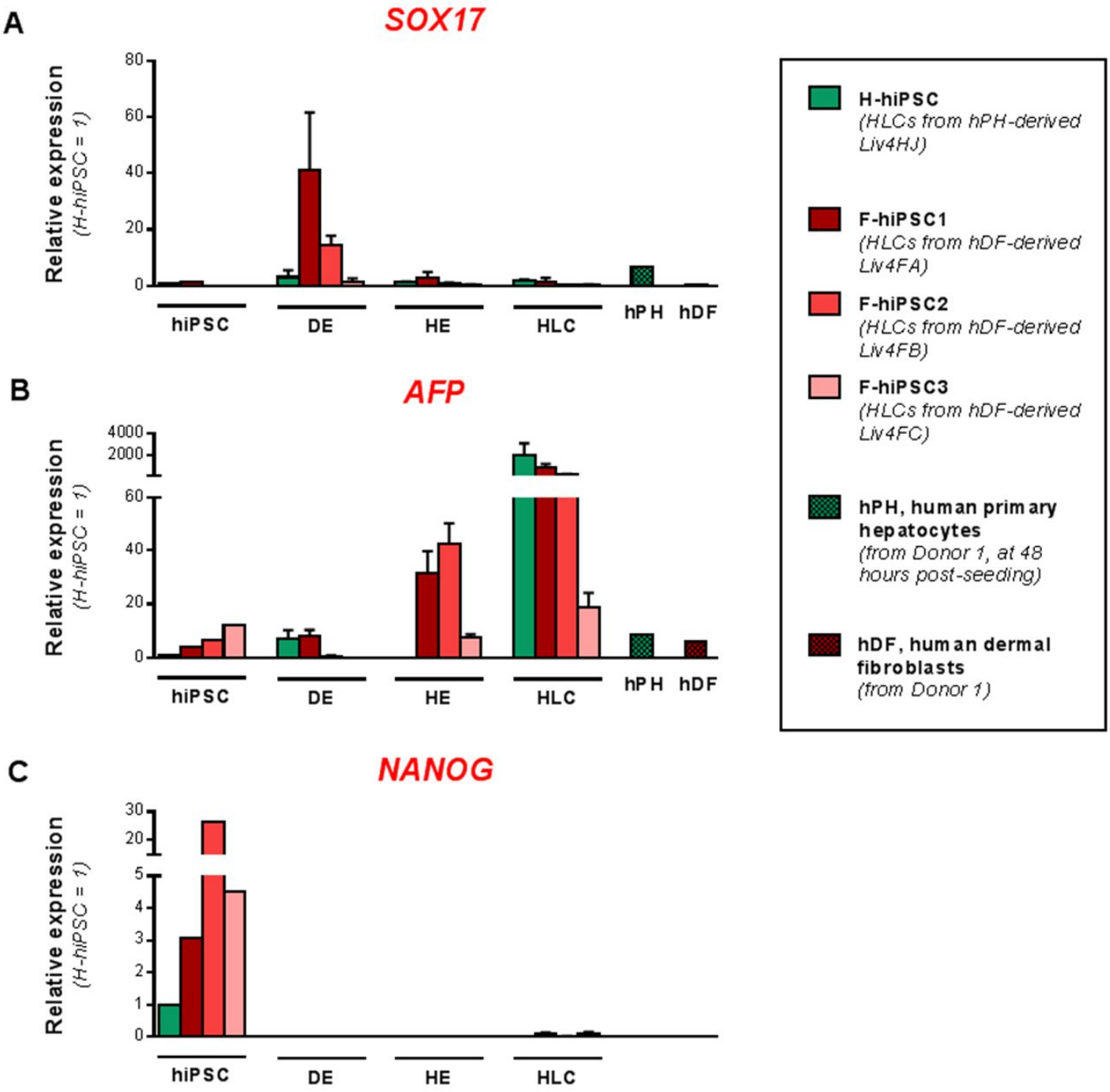

Figure 2.14 Real-time qRT-PCR gene expression analyses of hepatic markers and the pluripotency marker *NANOG* during hepatic differentiation.

Data is presented as the mean fold change of gene expression relative to H-hiPSC. The error bars for the endodermal derivatives represent the standard error of the mean (SEM) for three individual replicate cultures performed in parallel for each hiPSC line. For each sample, the real-time qRT-PCR reactions were performed in duplicates. DE, definitive endoderm; HE, hepatic endoderm; HLC, hepatocyte-like cell; SOX17, sex determining region Y-box 17; AFP, alpha fetoprotein.

2.3.3 Comparison of liver-related gene expression between isogenic HLCs

Following successful generation of HLCs from all the hiPSC lines derived from both primary hepatocytes and dermal fibroblasts, we then quantitatively compared their expression of commonly accepted hepatocyte-specific genes (Cai*, et al.*, 2007; Hay*, et al.*, 2008; Hengstler*, et al.*, 2005). For this comparison, we used the same donor's hPHs as the ideal comparator to exclude the effect of genetic variability in the expression of liver-related genes between different donors.

Overall, we found that the gene expression profile of the HLCs generated from hPH-derived hiPSCs was largely similar to the HLCs generated from hDF-derived hiPSCs (Figure 2.15). In fact, it was HLCs generated from one of the hDF-derived hiPSC line (Liv4FA) that had the highest gene expression of albumin *(ALB)* and alpha-1 antitrypsin *(A1AT)*, hepatic markers that are frequently used to denote the differentiation efficiency of HLC cultures (Kia*, et al.*, 2013). There were also no significant differences in the expression of the liver-enriched transcription factor *HNF4A* and the most abundant cytochrome-P450 enzyme in the human liver *CYP3A4* (Rodriguez-Antona, et al., 2002), between the HLCs generated from the examined hiPSC lines. The HLCs generated from the hPH-derived hiPSC line also expressed significantly higher levels of *ALB, A1AT* and the hepatocyte lineage marker keratin-18 (*CK18)* compared to HLCs generated from of the hDF-derived hiPSC line (Liv4FC). There were also differences in the expression of the hepatic genes between the HLCs generated from the various hDF-derived hiPSC lines.

Therefore, based on these results obtained using hiPSC lines derived from a single donor, there did not seem to be a higher propensity of HLCs generated from hPH-derived hiPSCs to express a hepatic transcription profile comparable to hPHs, and differences in the hepatic gene expression profile was also seen between HLCs generated from hiPSCs derived from the same tissue type, in this case hDFs.

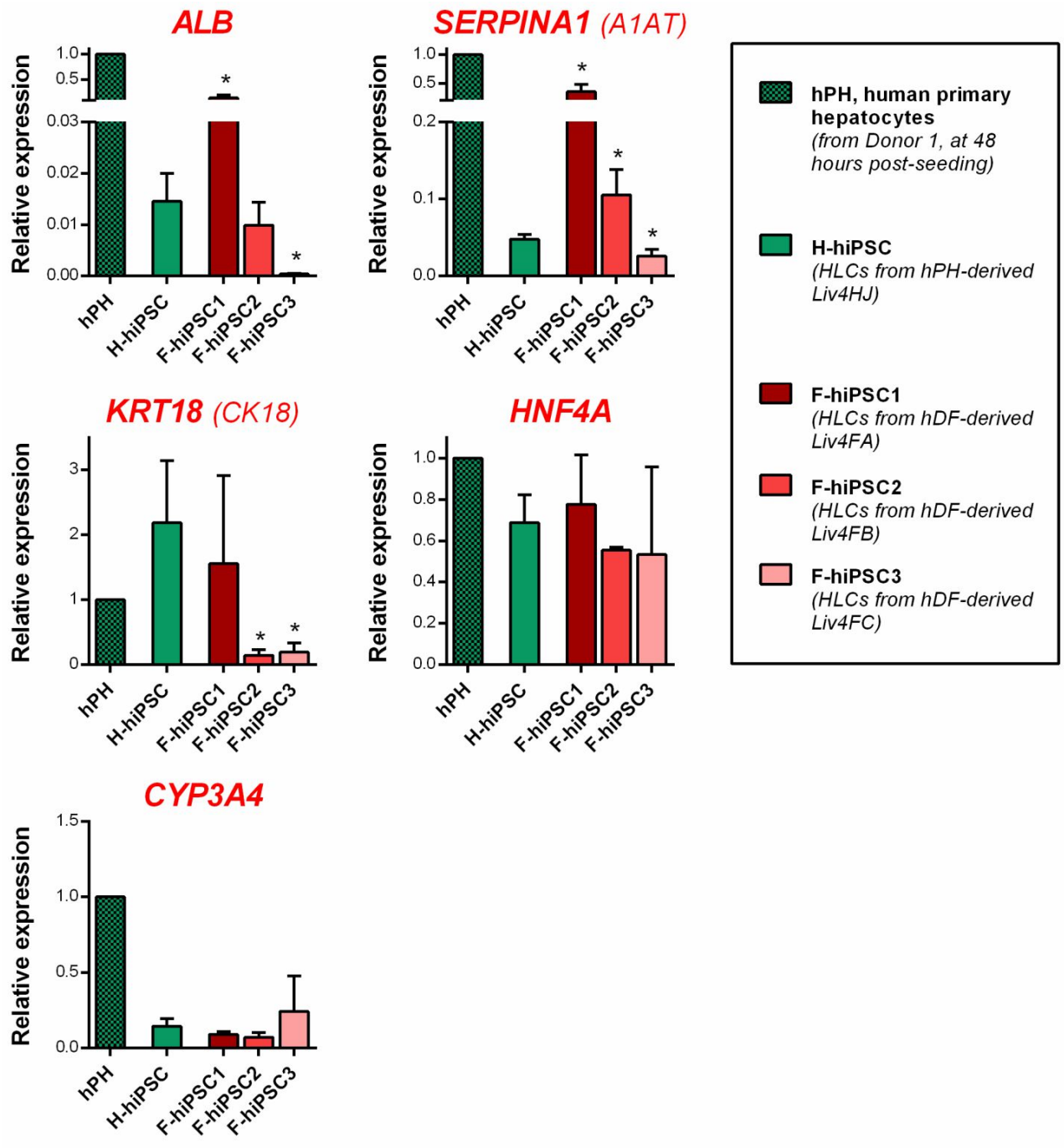

Figure 2.15 Real-time qRT-PCR gene expression analyses of hepatic markers in isogenic HLCs generated from hPH- and hDF-derived hiPSCs of the same adult donor.

Data is presented as the mean fold change of gene expression relative to the donor's hPHs. The error bars for the HLCs represent the standard error of the mean (SEM) for three individual replicate cultures performed in parallel for each hiPSC line. For each sample, the real-time qRT-PCR reactions were performed in duplicates. The unpaired t-test was used to compare the statistical significance of the mean fold change of each gene for the hDF-derived hiPSC lines (F-hiPSC1, F-hiPSCS2 and F-hiPSCS3) against the hPH-derived hiPSC line (H-hiPSC). * denotes $p < 0.05$. For gene name abbreviations, please see http://www.ncbi.nlm.nih.gov/gene/. Commonly known aliases are listed in parentheses. Selected descriptions of gene name abbreviations: SERPINA1 *(A1AT)*, serpin peptidase inhibitor, clade A (alpha-1 antiproteinase, antitrypsin), member 1; CYP3A4, cytochrome P450, family 3, subfamily A, polypeptide 4; KRT18 *(CK18)*, keratin-18.

2.3.4 Comparison of albumin secretion capacity between isogenic HLCs

We then chose to examine the functional phenotype of the HLC cultures by examining the amount of albumin secreted into the media. Hepatocytes are the only cell-type that secretes albumin (Hengstler*, et al.*, 2005) and the capacity for albumin secretion in HLCs is frequently used as a surrogate for quantitative comparison of "maturity" of their phenotype (Hay*, et al.*, 2008; Kajiwara*, et al.*, 2012; Shan *et al.*, 2013)

The media was collected serially from the same well of the respective cultures of HLCs and the concentration of albumin measured. In parallel to the *ALB* expression data shown in (Figure 2.15), the HLC cultures generated from Liv4FA, a hDF-derived hiPSC line, had the highest amount of albumin in the media, while the culture of HLCs generated from Liv4FC which had the lowest relative expression of *ALB*, had the least albumin in the media (Figure 2.16A).

When the mean concentration of albumin in the media of the respective cultures at Day 22 was normalised to the amount of total protein of HLCs from the same wells of cultures used as a surrogate for cell count, the mean concentration of albumin in the media of HLC cultures generated from Liv4FA was 16-fold higher than that of the HLCs generated from the hPH-derived Liv4HJ, and about 2-fold lower than that in the media of the donor's primary hepatocytes which has been plated for 48 hours (Figure 2.16B). Again, based on the comparison of albumin secretion, HLCs generated from hPH-derived hiPSCs did not result in a better functional phenotype compared to HLCs generated from hDF-derived hiPSCs, with variable albumin secretion seen also between HLCs generated from different hiPSC lines derived from hDFs.

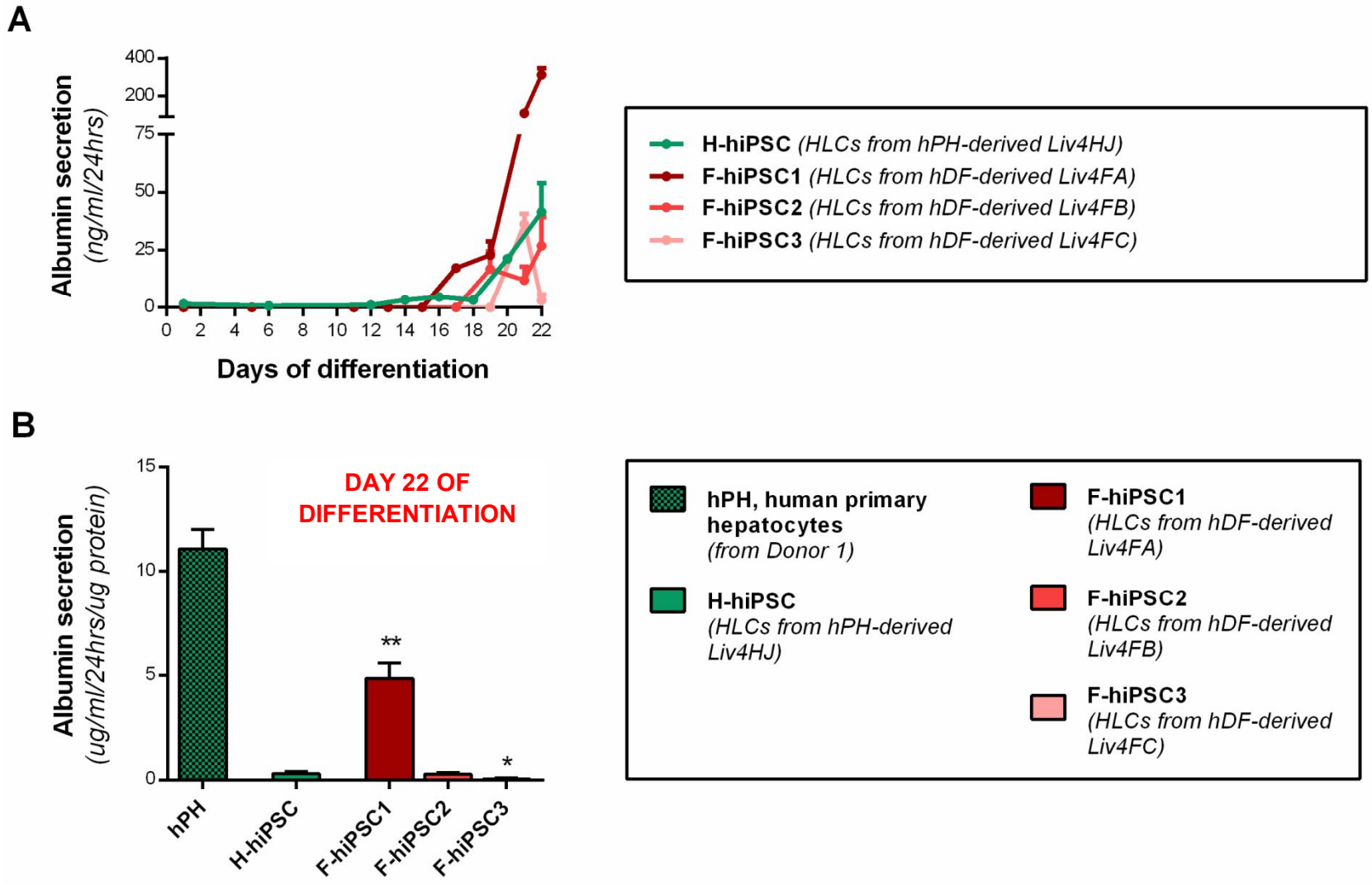

Figure 2.16 Comparison of albumin secretion between isogenic HLCs generated from hPH- and hDF-derived hiPSCs of the same adult donor.

(A) Data is presented as the mean secretion of albumin into the media of HLCs per 24 hours and the error bars represent the standard error of the mean (SEM) for three individual replicate cultures performed in parallel for each hiPSC line. The trend of albumin secretion for each culture of HLC was analysed using serial media samples from each respective well. (B) Data is presented as the mean secretion of albumin into the media per 24 hours normalised to the amount of total protein of the culture, and the error bars represent the standard error of the mean (SEM) for three individual replicate cultures performed in parallel for each hiPSC line and hPHs. The media used for comparison was collected at Day 22 for the HLCs and at 48 hours post-plating for the hPHs. For each media sample, the ELISA reactions were performed in duplicates. The unpaired t-test was used to compare the statistical significance of the mean albumin secretion for the hDF-derived hiPSC lines (F-hiPSC1, F-hiPSCS2 and F-hiPSCS3) against the hPH-derived hiPSC line (H-hiPSC). * denotes $p < 0.05$, ** denotes $p < 0.01$.

2.4 DISCUSSION

To investigate our hypothesis in this chapter, we first had to derive hiPSCs from hPHs which had previously only been reported twice in the literature (Hansel*, et al.*, 2014; Liu*, et al.*, 2010). Both reports were contrasting in their experience with reprogramming hPHs though the methods used were not directly comparable. Liu *et al*. reported rapid and efficient reprogramming of hPHs using retroviral delivery of the Yamanaka factors, in contrast to Hansel *et al*. who reported a very low reprogramming efficiency of hepatocytes from children. The latter group managed to derive three hiPSC lines from a 13-month-old and 12-year-old donor, while reprogramming attempts of hPHs from 12 other donors including adults failed to generate any hESC-like colonies. They also required delivery using lentiviral vectors of two additional reprogramming factors (Lin-28 and Nanog) in addition to the conventional Yamanaka factors used in our study (Hansel*, et al.*, 2014). Therefore, as successful derivation of hiPSC lines from adult hPH donors would be the critical component in our study, we therefore adapted our own reprogramming protocol largely based on the experience reported by Liu *et al* (Figure 2.2).

For this study, we chose to use the Sendai viral (SeV) vectors to deliver the transcription factors for two main reasons: 1. The vectors are non-integrative - they replicate as negative single-stranded RNA in the cytoplasm of infected cells and do not integrate into the host genome, unlike retroviral or lentiviral vectors which result in viral transgene insertions into the host genome that may affect terminal differentiating potential (Bitzer *et al.*, 2003; Macarthur *et al.*, 2012; Okita *et al.*, 2007); and 2. They are efficient in delivering foreign genes into a wide spectrum of host cells (Bitzer*, et al.*, 2003; Tokusumi *et al.*, 2002) – an important factor in the design of the study, as a standardised method of efficient reprogramming both hPHs and hDFs with minimal variation was required to minimise confounding factors that influence the phenotype of hiPSCs and subsequent differentiated HLCs. Although efficient reprogramming of hDFs and blood cells using the SeV vectors encoding the Yamanaka pluripotency factors have been reported (Fusaki*, et al.*, 2009; Seki

et al., 2012), the application of SeV vectors in reprogramming hepatocytes have not been reported until now. Therefore, we show that the use of SeV vectors is a robust and reproducible non-integrative method for reprogramming adult hPHs.

To explore the contribution of epigenetic memory of the cell-type of origin in hiPSCs with minimal confounding factors, we also generated HLCs from multiple hiPSC lines using the same differentiation protocol for comparison (Figure 2.2). Despite successful generation of HLCs from multiple hiPSC lines for comparison, the differentiation efficiency was not high, ranging from an estimated 20-40% as determined by immunocytochemistry for albumin-positive cells at the end of differentiation (data not shown). Furthermore, as we only used the described protocol to ensure a standardised approach to generating HLCs from multiple hiPSC lines, it is possible that a different differentiation protocol may yield different efficiencies and propensities of the various hiPSC lines towards hepatic differentiation. However, we feel that our choice of protocol was justifiable as it was adapted from previously published protocols that were shown to be robust in generating HLCs from various hiPSC clones derived from multiple cell-types (Kajiwara*, et al.*, 2012; Sullivan*, et al.*, 2010; Szkolnicka *et al.*, 2013).

Our results stemming from the comparison of HLCs generated from hepatocyte- and fibroblast-derived hiPSC lines of a single donor suggest that there is no advantage in the use of hPHs as the starting cell-type for deriving hiPSCs to generate functional HLCs. However, there are caveats to our provisional results which require further exploration.

Firstly, the comparison between the HLCs was made using only a single hiPSC line derived from hPHs of Donor 1. This single clone may not be truly representative of the effect of epigenetic memory as clonal variations in the propensity for hepatic differentiation has been reported in sibling hiPSC clones derived from non-hPH cell-types of origin (Kajiwara*, et al.*, 2012). In fact, analysis of the expression of *SOX17* among the three hDF-derived hiPSC lines (Figure 2.14) suggests that clonal differences may be manifested early in the

differentiation process as the hDF-derived hiPSC lines demonstrated variable response to induction towards definitive endoderm which also loosely correlated with their corresponding albumin secretion capacity. Therefore, future comparisons using at least 3 of the 5 established hPH-derived hiPSC lines from Donor 2 should help to clarify this limitation.

Secondly, the influence of donor differences in ultimately being of more importance in generating functional HLCs cannot be discounted. This specific issue was addressed partially by Kajiwara *et al.*, where they showed that the variations in the hepatic differentiation of isogenic peripheral blood-derived and hDF-derived hiPSC lines were small in contrast to larger variations seen between hiPSC lines derived from different donors (Kajiwara*, et al.*, 2012). However, to truly answer the relative contribution of epigenetic memory of the cell-type of origin in isogenic hiPSC lines and donor differences towards hepatic differentiation, the inclusion of hPH-derived hiPSC lines is vital. Therefore, further comparisons using corresponding sets of hPH- and hDF-derived hiPSC lines from Donor 2 and future donors will hopefully clarify this question.

Thirdly, the HLCs generated in this study were still relatively "immature" with limited expression of most hepatocyte-specific genes including *CYP3A4* as well as albumin secretion compared to the donor hPHs (Figure 2.15 and 2.16B). There were also high levels of expression of *AFP*, a prototypical marker of hepatoblasts and foetal hepatocytes undergoing maturation (Figure 2.14) (Kuhlmann and Peschke, 2006). Overall, this characterisation data is not dissimilar to the phenotype of HLCs reported by various groups in the literature using different protocols (Kia*, et al.*, 2013). However, it is possible that the potential advantage of using hiPSC lines derived from hPHs to generate functional HLCs may never be fully evaluated pending the availability of a robust and validated hepatic differentiation protocol to generate HLCs with a functional phenotype more akin to a freshly-isolated hPH phenotype.

In summary, this chapter describes our attempt to evaluate the contribution of epigenetic memory towards hepatic differentiation. Our results using hiPSC lines derived from a single donor suggests that our null hypothesis of HLCs generated from hPH-derived hiPSC line is more functional compared to HLCs generated from non-hPH-derived hiPSC is false, although comparison using hiPSC lines derived from other donors are required to be conclusive.

CHAPTER 3

THE GLOBAL MICRORNA PROFILES OF HUMAN PRIMARY HEPATOCYTES IN EXTENDED *IN VITRO* CULTURE

3.1 INTRODUCTION

Despite longstanding efforts to develop novel *in vitro* hepatic models which are functional and relevant for mechanistic studies of drug-induced liver injury, freshly-isolated human primary hepatocytes (hPHs) remain largely unsurpassed as the gold standard *in vitro* model (LeCluyse, 2001), though Szkolnicka *et al.* had recently showed that hESC-derived HLCs has equivalence with cryopreserved hPHs, albeit not tested with hepatotoxicants (Szkolnicka, 2014). hPHs maintain a level of functionality during short-term cultures and are thus widely used for *in vitro* studies on drug metabolism and acute toxicity (Godoy *et al.*, 2013). However, they rapidly lose their *in vivo* phenotype during extended *in vitro* culture, including the capacity for xenobiotic biotransformation, thereby preventing its use for the study of chronic toxicity which commonly precedes clinical presentations of idiosyncratic drug-induced liver injury (Rodriguez-Antona *et al.*, 2002; Rowe *et al.*, 2013; Verma and Kaplowitz, 2009). This detrimental process, termed as "dedifferentiation", results in a short duration of optimal hepatocyte function which limits the utility of the hPH model to acute toxicity studies only, and compromises their use in mechanistic studies of DILI which often occurs following prolonged exposure to drugs (Guguen-Guillouzo and Guillouzo, 2010; Kalgutkar and Soglia, 2005; LeCluyse, 2001). Therefore, reversal or prevention of the dedifferentiation process would result in a more relevant hepatic model for pharmaco-toxicology studies. Furthermore, it is hoped that by better understanding the mechanisms involved in hPH dedifferentiation, new insights can be gained to improve the differentiation process of human pluripotent stem cells towards hepatocyte-like cells.

Dedifferentiation of hPHs has been described to begin during the isolation procedure, and is shown to be a consequence of the activation of proliferative and inflammatory signalling pathways, resulting in a shift of the isolated hepatocytes towards a "proliferation-primed state" in expense of its functional phenotype (Paine and Andreakos, 2004; Vinken *et al.*, 2006). Various strategies employed to prevent or reverse hepatocyte dedifferentiation, include the modification of the *in vitro* culture systems (Fraczek *et al.*, 2013), overexpression

of liver-enriched transcription factors (Naiki *et al.*, 2004) and manipulation of the epigenetic mechanisms to counter the underlying gene expression changes (Bolleyn *et al.*, 2011). However, the existence of fully functional hPHs in long-term *in vitro* culture remains elusive.

MicroRNAs (miRs), a group of endogenous non-coding RNAs which has been shown to play an important role in post-transcriptional gene silencing by either inhibiting protein translation or facilitating protein degradation of their target messenger RNAs (mRNAs) (Bartel, 2004), have also been recently investigated for its role in the dedifferentiation process in rat primary hepatocytes (Bolleyn*, et al.*, 2011). Currently, more than 2500 mature miRs have been described in humans in the latest version of the miRBase database (miRBase 21) of published miR sequences and annotation (Griffiths-Jones, 2004), and about 50% of human mRNAs were estimated to be miR targets (Lewis *et al.*, 2005). As each miR may regulate hundreds of mRNAs, substantial effects on the gene expression pattern may result from the change of expression of just a few miRs that regulate them. Indeed, miRs have been demonstrated to play a role in all basic biological processes including metabolism (Krutzfeldt and Stoffel, 2006), cell proliferation (Bueno *et al.*, 2008) and tissue differentiation (Shi *et al.*, 2006). Similarly, altered miR expression was also implicated in various human diseases (Jiang *et al.*, 2009), including in hepatocellular carcinoma (HCC) (Fornari *et al.*, 2008). This realisation has prompted intense research into therapeutic targeting of miRs using various approaches particularly antisense oligonucleotides (ASOs) that target miRs directly (Li and Rana, 2014). In fact, there are currently many miR-targeting ASOs that are in clinical and preclinical trials (Li and Rana, 2014), with promising early results in the treatment of chronic hepatitis C virus infection and hypercholesterolaemia (Lindow and Kauppinen, 2012; Li and Rana, 2014). On the other hand, a miR-34 mimic as replacement therapy to normalise its reduced levels in patients with HCC or metastatic cancer involving the liver, has also entered a Phase I clinical trial (Bouchie, 2013).

Genome-wide or global unbiased miR expression profiling using high-throughput platforms have further enriched our understanding of the role of miRs in biological and pathological

processes, for example, through the identification of a set of differentially-expressed miRs involved in the differentiation of human embryonic stem cells towards hepatocyte-like cells (Kim *et al.*, 2011) and in the dedifferentiation of rat hepatocytes (Bolleyn*, et al.*, 2011). Therefore, it is conceivable that similar global miR profiling studies could help in further delineating the process of dedifferentiation in hPHs. However, miR profiling studies have never been performed in isolated hPHs previously, although various studies using human adult and foetal liver tissue have been reported (Barad *et al.*, 2004; Fu *et al.*, 2005; Landgraf *et al.*, 2007). Therefore, we hypothesised that by investigating the miR profiles of freshly-isolated hPHs in extended *in vitro* culture, potential miRs as targets for modulation may be identified, and fresh insights may be gained into the complex molecular cascades involved.

3.2 MATERIALS AND METHODS

3.2.1 Human subjects and tissue

Human liver resections from surgical waste tissue were obtained from adult patients undergoing hepatobiliary surgery with full informed consent and ethical approval from the relevant institutional review boards (National Research Ethics Service REC reference: 11/NW/0327).

3.2.2 Human primary hepatocyte isolation

Human primary hepatocytes (hPHs) were isolated using a previously described method with minor modifications (LeCluyse *et al.*, 2005). Briefly, liver resections were received as surgical waste tissue immediately post-resection (Aintree University Hospital, Liverpool, United Kingdom) and transferred on ice in N-(2-Hydroxyethyl)piperazine-N′-(2-ethanesulfonic acid) (HEPES) buffer (10 mM HEPES, 136 mM NaCl, 5 mM KCl, 0.5% (w/v) glucose, pH 7.6) to the laboratory. The liver resection specimens were then perfused with HEPES-buffered saline (HBS) followed by digestion with collagenase A (Roche) or collagenase IV (Sigma-Aldrich) in HBS containing calcium. The suspension containing isolated hepatocytes was then filtered through a nylon gauze and purified by centrifugation twice at 80x g for 5 minutes at 4^{o}C, before the pellet was resuspended in Williams E medium (Sigma-Aldrich). The hPHs were then seeded onto collagen-I coated 24-well plates (BD Beckinson) at 2.5 x 10^5 cells/cm^2 and cultured in Williams E medium supplemented with 1% (v/v) insulin-transferrin-selenium (from 100x stock, Life Technologies), 2 mM L-glutamine (Sigma-Aldrich), 10^{-7} M dexamethasone (Sigma-Aldrich) and 1% (v/v) penicillin-streptomycin (Sigma-Aldrich) at 5% CO_2 and 37°C. After 3 hours, non-attached cells were washed away and replaced with fresh Williams E medium before overnight incubation. The medium was replaced again the next day at the start of the experiments.

3.2.3 Human primary hepatocyte culture

The plated hPHs were cultured in Williams E medium supplemented with 1% (v/v) insulin-transferrin-selenium (from 100x stock, Life Technologies), 2 mM L-glutamine (Sigma-Aldrich), 10^{-7} M dexamethasone (Sigma-Aldrich) and 1% (v/v) penicillin-streptomycin (Sigma-Aldrich) up to seven days without any additional matrix overlay to promote dedifferentiation (Rowe*, et al.*, 2013). The media was changed daily for the duration of the study, and the cells were lysed in QIAzol (Qiagen) according to the manufacturer's protocol at 24 hours, 48 hours and 168 hours post-plating. Pellets of freshly-isolated hPHs were also lysed in QIAzol (Qiagen) as baseline reference samples. The lysates were stored immediately in -80°C.

3.2.4 Total RNA extraction

The purification of total RNA containing the miR fraction from media or lysate samples was performed using the miRNeasy mini kit (Qiagen), as per the manufacturer's instructions. Briefly, each lysate was thawed at room temperature and thoroughly mixed before the addition of 140 µL of chloroform. The samples were then mixed vigorously for 15 seconds and left at room temperature for 3 minutes. The homogenates were then centrifuged at 12000x g for 15 minutes at 4°C. 350 µL of the upper aqueous phase and 525 µL of 100% ethanol were then mixed thoroughly in a new collection tube before transferring to a miRNeasy Mini spin column. The column was then sequentially centrifuged and washed with supplied buffers at room temperature, before the column was placed into a new collection tube. 30 µL of RNase-free water was then added directly onto the column membrane and centrifuged for 1 minute at 10000x g to elute the total RNA containing the small RNA fraction.

To ensure removal of residual organic solvent contamination which may result in inaccurate quantification of the total RNA, each total RNA elute was further purified using additional chloroform extractions as recommended by the microarray system manufacturer (Agilent

Technologies). Briefly, 100 µL of a 1:1 mixture of acid phenol (Sigma-Aldrich) and chloroform (Sigma-Aldrich) was added to the total RNA elute and thoroughly mixed before being centrifuged at maximum speed for 15 minutes at 4°C. The aqueous phase was then collected in a new tube. 100 µL of RNase-free water was added to the remaining acid phenol/chloroform mixture, thoroughly mixed and centrifuged as before, and the aqueous phase added to the previously recovered portion. 1 µL of glycogen (20 µg/µL stock solution, Life Technologies), 10% (v/v) of 3M sodium acetate (pH 5.2, Sigma-Aldrich) and 500 µL of a 2:1 mixture of ethanol and isopropanol was then added to the total volume of recovered aqueous phase, and the mixture incubated overnight at -20°C, before being centrifuged for 15 minutes at maximum speed at 4°C. The supernatant was discarded and the pellet rinsed with cold 75% ethanol. The pellet was spun down at 7500x g for 5 minutes before the supernatant was again discarded and air-dried at room temperature for 10 minutes. The total RNA precipitate was then dissolved in an appropriate amount of RNase-free water. Quantification and the quality of the total RNA extracts was analysed using the NanoDrop spectrophotometer (Thermo Scientific) and Agilent 2100 bioanalyser (using the RNA 6000 Nano kit, Agilent Technologies) respectively. Only samples which had a RNA Integrity Number (RIN) of $\geq$ 7 were used as input samples for microarray analysis.

3.2.5 MicroRNA microarray analysis

MicroRNA (miR) microarray analysis was performed using the miRNA Complete Labeling and Hyb kit (Agilent Technologies) according to the manufacturer's protocol. Briefly, 100 ng of total RNA was incubated with calf intestinal alkaline phosphatase (CIP) reaction mixture consisting of 0.4 µL 10x CIP buffer, 0.5 µL CIP and 1.1 µL labelling spike-in solution, at 37°C for 30 minutes to dephosphorylate the RNA. The samples were then denatured with 2.8 µL of DMSO at 100°C for 5 min. A ligation master mixture consisting of 3 µL of Cyanine3-pCp, 1 µL of 10x T4 RNA ligase buffer and 0.5 µL of T4 RNA ligase was then added to each sample

and incubated at 16°C for 2 hours. The labelled RNA was then purified using Micro Bio-Spin 6 columns (Bio-Rad), according to the manufacturer's protocol. Briefly, each sample was transferred into the column and centrifuged at 1000x g at room temperature for 4 minutes. The RNA samples were then dried for 1 hour using a DNA SpeedVac (Thermo Scientific), before being resuspended in a mixture consisting of 17 µL of RNase-free water, 22.5 µL of 2x Hi-RPM hybridisation buffer, 4.5 µL of 10x blocking agent and 1 µL of hybridisation spike-in solution. The samples were then incubated at 100°C for 5 minutes before being chilled on ice. The samples were then loaded onto the human miRNA Microarray Release 16.0, 8x60k microarrays (G4872A-031181, Agilent Technologies), of which 1347 human miRs were represented based on miRBase 16 (http://www.mirbase.org/). The hybridisation step was performed at 55°C for a minimum of 20 hours in a rotating chamber at 20 rpm. The hybridized miR arrays were then washed using proprietary buffers and according to protocol, and the hybridized images scanned using a G2505C Agilent Microarray Scanner (scan control version A.8.4.1, Agilent Technologies).

3.2.6 Data pre-processing and statistical analysis of microRNA microarray data

The images provided by the scanner were analysed using the Agilent Feature Extraction (AFE) software (version 10.7.3.1, Agilent Technologies) with default settings, of which a quality control report was produced for each scanned image. All microarrays used for downstream analysis passed the defined quality control parameters. The AFE algorithms estimated a summarised signal for each miR termed as the total gene signal (TGS) which was then used by the bioinformatics tool AgiMicroRna (open-source software available from the Bioconducter project - http://www.bioconductor.org) for further pre-processing and differential expression analysis of the microRNA microarray data (Lopez-Romero, 2011).

The AFE-processed TGS was first normalised between microarrays using the quantile method integrated in AgiMicroRna and the default filtering algorithm applied to remove

control features and genes not detected in any of the samples in the study. The *limma* package was used to fit a linear model to each miR (Smyth, 2004), to analyse statistically significant differential expression between the samples collected at various time-points in comparison to baseline. Using this model, the differential expressions were calculated using moderated t-test (Bayesian approach) and miRs exhibiting a significant fold change (p value of ≤ 0.05) were selected for further analysis. For each time-point of sample collection, 4-6 biological replicates from different donors were used for this study (*i.e.* 4 donors had corresponding samples with RIN ≥ 7 for all time-points, while 2 donors had corresponding samples with RIN ≥ 7 for only the baseline and 48-hour time-points).

3.2.7 MicroRNA target prediction

The miR targets of the differentially-expressed miRs (see criteria above) were analysed using the MicroRNA Target Filter module of Ingenuity Pathway Analysis (IPA; Qiagen, Redwood City, CA, www.qiagen.com/ingenuity) which enabled identification of experimentally validated and predicted messenger RNA (mRNA) targets. The databases referred to by this IPA module were Tarbase5.0 (Vergoulis *et al.*, 2012), miRecords (Xiao *et al.*, 2009), TargetScan (Friedman *et al.*, 2009) and the Ingenuity manually curated database (available through IPA). For the predicted miR-mRNA target interactions, only predictions with high confidence as deemed by TargetScan were included for further analyses of functional term enrichment and canonical pathway involvement using the Core Analysis module of IPA. In the analyses of mRNA targets of liver-enriched transcription factors and genes associated with liver-specific functions, predicted miR-mRNA target interactions with moderate confidence as deemed by TargetScan were also included. The sequence of all the detected mature miR were mapped to the annotations used in miRBase 19 (latest version available during the commencement of the study, www.mirbase.org/index.shtml).

3.2.8 Real-time quantitative RT-PCR (qRT-PCR)

The level of expression of selected differentially-expressed miRs as analysed by microarray analysis (Section 3.2.5 and 3.2.6) were determined via a multiplexed reverse transcriptase (RT) step followed by real-time PCR reactions using the TaqMan miRNA assays (Applied Biosystems) according to the manufacturer's protocol. The TaqMan MicroRNA Assays used were for hsa-miR-122-5p (assay ID: 002245), hsa-miR-4284 (assay ID: 241828_mat), hsa-miR-21-5p (assay ID: 000397), hsa-miR-885-5p (assay ID: 002296) and U6 (assay ID: 001973).

Briefly, a RT primer pool consisting of each individual 5x RT primer was mixed with 1x TE Buffer (Sigma-Aldrich) to a final volume of 1 ml. The RT reaction mix is then prepared using the TaqMan MicroRNA RT Kit (Applied Biosystems) with an appropriate volume of the RT primer pool. 12 µL of the RT reaction mix was then added to each well of a 96-well plate before 3 µL of total RNA (350 ng per reaction) extracted from the samples used for the microarray analysis was added, prior to incubation on ice for 5 minutes. Reverse transcription was then performed using the GeneAmp PCR System 9700 thermal cycler (Applied Biosystems) using the recommended thermal-cycling conditions.

For the real-time PCR reaction, the PCR reaction mix was first prepared by mixing the TaqMan Universal Master Mix II, No AmpErase UNG (2X) (Applied Biosystems) with the appropriate volume of 20x TaqMan MicroRNA Assay (Applied Biosystems), the relevant RT product and nuclease-free water (Qiagen) as per the manufacturer's instructions. 10 µL of the PCR reaction mix was then added to each well of a 384-well plate before being sealed with an adhesive film and briefly centrifuged. Real-time PCR was then performed in duplicates with the ViiA 7 Real-Time PCR instruments (Applied Biosystems) using a 2-step thermal cycling protocol of 95°C for 10 minutes followed by 40 cycles of 95°C for 15 seconds and 60°C for 60 seconds. Ct values were determined using the fluorescent signal produced from the TaqMan probes. U6 snRNA was used as endogenous control for normalisation and

the fold change of expression of the respective miR relative to baseline expression at the 0 hour time-point were calculated using the $2^{-\Delta\Delta Ct}$ method (Livak and Schmittgen, 2001). The expression of each miR at each time-point was expressed as the mean fold change +/- standard deviation of three biological replicates (n =3). The real-time qRT-PCR experiments were analysed with the unpaired t-test using GraphPad Prism 6 (GraphPad Software), with $p < 0.05$ considered significant.

3.2.9 Cell morphology

Cell morphology was analysed by light microscopy using a phase contrast microscope (ECLIPSE TS100/100-F, Nikon), and photographs captured using a digital camera head (DS-Vi1, Nikon) and a stand-alone controller and display unit (DS-L3, Nikon).

3.3 RESULTS

3.3.1 Morphological changes of human primary hepatocytes during *in vitro* culture

During the extended culture of plated human primary hepatocytes (hPHs) on collagen-coated plates, the cell morphology was noted to change (Figure 3.1). Following overnight incubation post-seeding, the confluent cultures of attached hPHs were noted to display a cuboidal shape with distinct borders and bile canaliculi were observed. However, following *in vitro* culture up to 7 days, the hPH cultures were noted to progressively lose their distinct cuboidal shapes, appeared generally more disorganised and flattened with the presence of more cellular projections, with the loss of distinct bile canaliculi. These morphological changes were most noticeable after 48 hours of *in vitro* culture, and were most pronounced at the end of the study. The above changes were generally similar for hPH cultures from multiple human donors, with no obvious increase in cell detachment, cell death or proliferation during *in vitro* culture of up to 168 hours in this study, although these processes were not formally assessed using cell viability and cell proliferation assays.

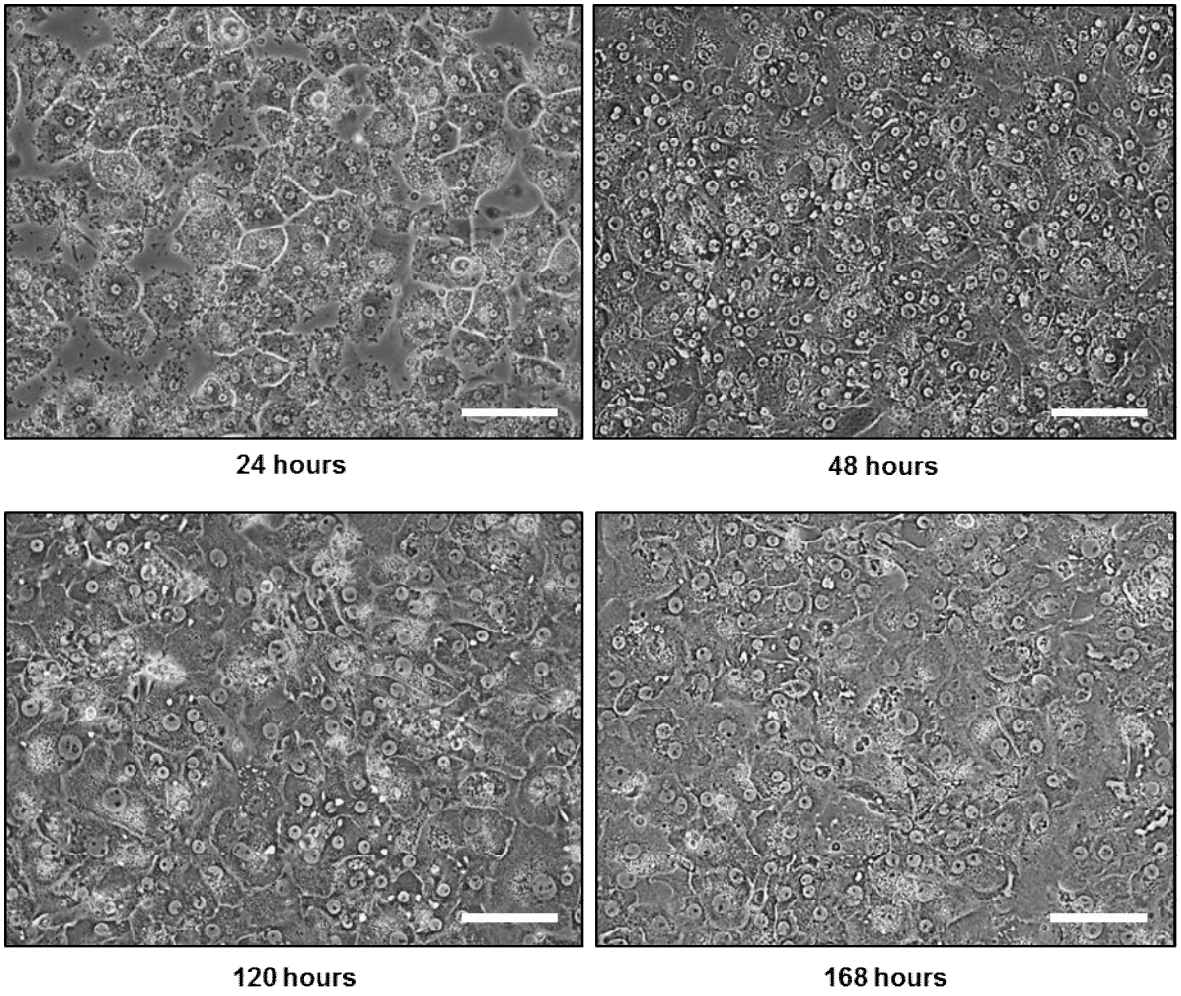

Figure 3.1 Morphological changes of collagen-plated hPHs over time in culture.

The series of pictures above were hPHs isolated from a single donor and representative of typical changes in 6 different donors, as analysed by phase contrast microscopy (magnification: 200x; scale bar, 100 µm).

3.3.2 Global microRNA expression profile of freshly-isolated human primary hepatocytes

The global miR expression profile of freshly-isolated hPHs in isolation from the other non-parenchymal cell counterparts present in the human liver, have not been previously reported. Using data from the miR microarray analysis of freshly-isolated hPHs (n = 6 different donors), 117 unique human miRs were detected. Each miR was considered present only if it was detected in at least 3 individual donors.

Enrichment analysis of the most abundantly expressed miRs in hPHs was performed using the normalised intensity values of the detected miRs of which the 30 most abundantly expressed miRs are shown in Figure 3.2. Based on the analysis of the mean normalised intensity values of all detected miRs, the most enriched miR in hPHs were miR-122-5p, which is estimated to constitute around 21% of all detected miRs in hPHs, while the 5 most abundant miRs constitute 56% of the total miR content in hPHs.

Overall, the miR profile consisting of 117 detected miRs in our series of hPHs isolated from 6 different donors, represent the first characterisation of the “miR-ome” of the hPH.

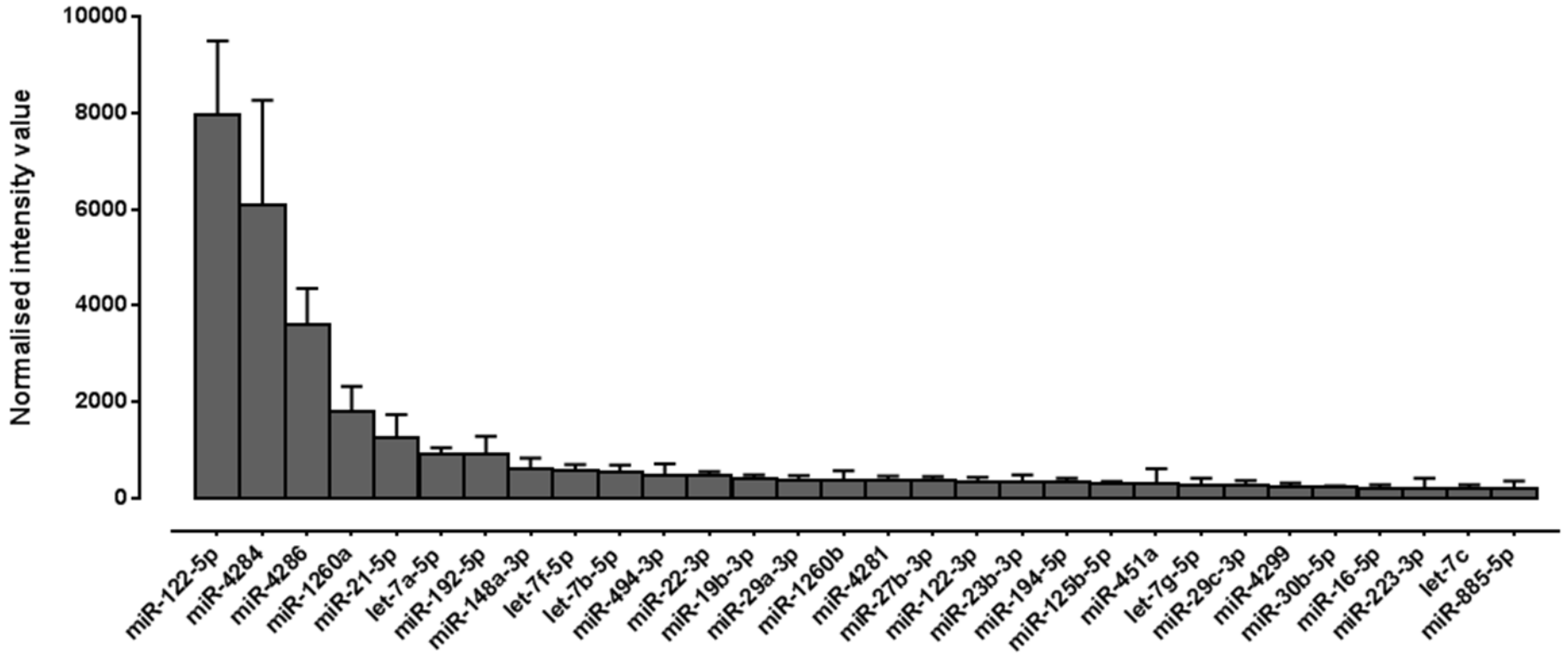

Figure 3.2 Enriched miRs in freshly-isolated human primary hepatocytes.

Data is presented as the mean normalised intensity value of the 30 most abundant miRs obtained from individual microarray analysis of human primary hepatocytes isolated from 6 different donors. Error bars represent the standard deviation of the mean for each data point. Each miR was included in analysis only if detected in 3 individual donors or more.

3.3.3 The global microRNA expression profiles of human primary hepatocytes in extended *in vitro* culture

We then investigated the miR profiles of the hPHs during conventional *in vitro* culture by analysing their global profiles using microarray analysis at 24 hours, 48 hours and 168 hours post-plating, in comparison with freshly-isolated hepatocytes. We specifically chose to culture the hPHs without any additional extracellular matrix overlay to promote hepatocyte dedifferentiation (Fraczek*, et al.*, 2013) and hypothesised that the miR expression profile changes over time during extended *in vitro* culture.

For the fold-change analysis, we included all miRs which were detected (defined as miRs detected from at least 3 individual adult hPH donors) at all time-points of the study. The results are summarised as a heatmap showing the mean log fold-change of each analysed miR at each time-point in comparison to the baseline levels in freshly-isolated hepatocyte samples, defined as 0 hours in culture (Figure 3.3A). We also separately analysed a set of miRs which were detected at baseline (definition of detected miR as above) but were otherwise not detected at *all* time-points during extended *in vitro* culture (Figure 3.3B). In general, most of the miRs showed a trend of either increasing up- or down-regulation of their expression over time, with the notable exception of the let-7 family of miRs of which their expression was generally unchanged (Figures 3.3A and 3.3B). The number of miRs which were differentially-expressed also increased with the duration of culture (Table 3.1).

Using linear modelling and moderated t-test (Bayesian approach), the differential expression of miRs at each time-point in comparison to baseline was analysed for significance. All miRs which exhibited a significant fold change (p value of < 0.05) at each time-point are shown in Table 3.1, of which 22 out of 117 detected miRs were found to be differentially-expressed compared to the baseline samples of freshly-isolated hPHs (Table 3.1 and Figure 3.4). This list also included miR-122-3p which is recognised as the inactive counterpart of miR-122-5p, or more precisely the passenger strand of their RNA complex (Chen, 2009; Jopling, 2012),

and has no predicted targets according to the databases used in this study (Section 3.2.7). The magnitude of change of expression of these miRs over time in culture were also analysed in Figure 3.4.

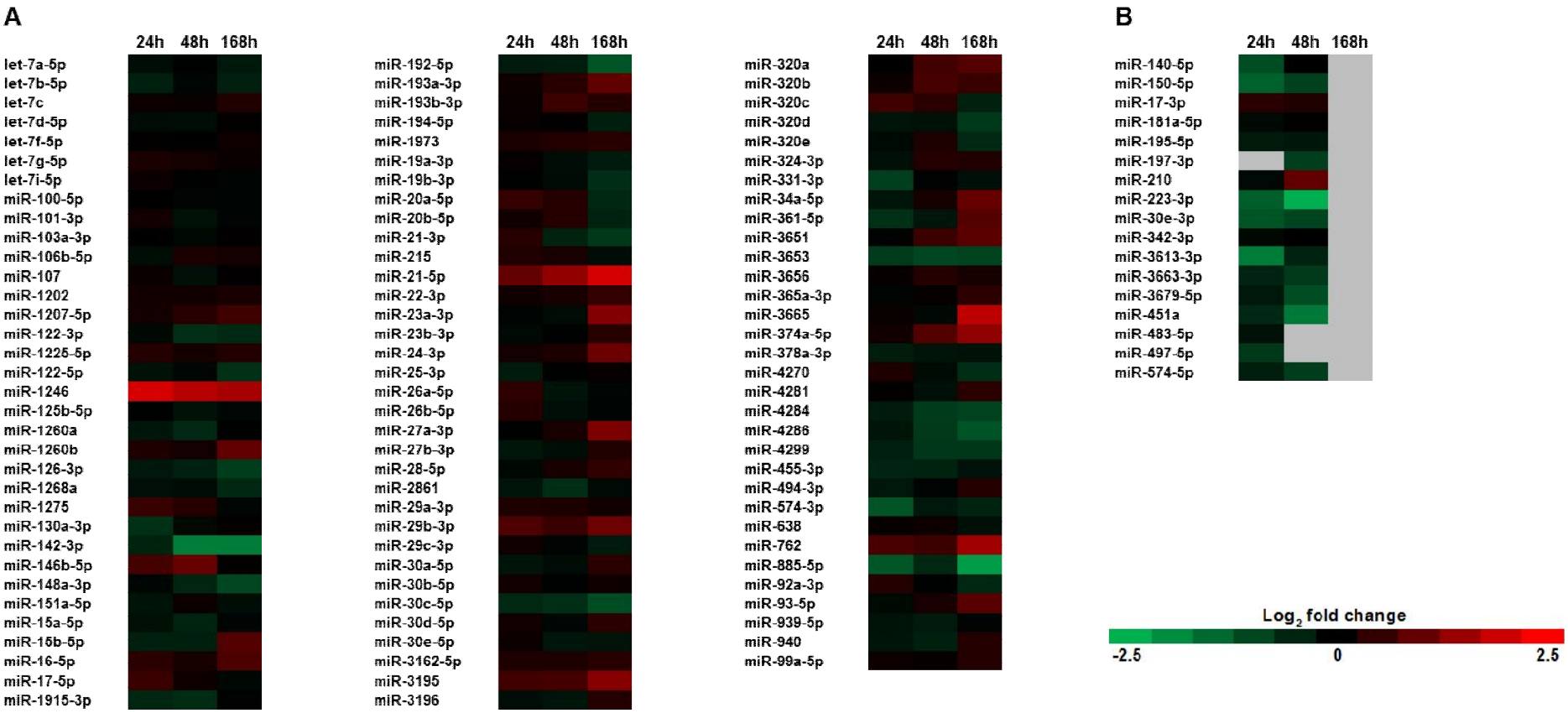

Figure 3.3 Heatmap showing change of expression of miRs in extended *in vitro* culture of hPHs.

Data is presented as mean $\log_2$ fold change of normalised intensity value of each detected miR in hPHs, compared to baseline (freshly-isolated hepatocytes at 0 hours), at 24 hours, 48 hours, and 168 hours in culture respectively. Each row represents a miR detected and the fold changes in the expression of miRs are represented by red colour for up-regulation compared to baseline (0 hours in culture), green colour for down-regulation and grey colour for non-detection. (A) miRs which were detected in samples from 3 donors or more in *every* time-point (n = 100 individual miRs), and (B) miRs which were detected in samples from 3 donors or more at baseline, but *not* in every time-point (n = 17 individual miRs).

Table 3.1 Differentially-expressed miRs at each time-point of extended *in vitro* culture of hPHs, compared to baseline at 0 hours.

All mean fold-change (FC) between 0 and 1 were transposed to a range of -1 until -infinity. The direction of change of expression is indicated by the symbol + for up-regulation, and – for down-regulation.

miRNA	Up / down regulation	Mean FC	p-value
24 h compared to 0 h			
miR-1246	+	4.37	1.44E-02
miR-21-5p	+	2.13	1.16E-02
miR-29b-3p	+	1.73	4.00E-02
48 h compared to 0 h			
miR-21-5p	+	2.83	2.27E-04
miR-193b-3p	+	1.53	7.72E-03
miR-223-3p	-	4.74	9.14E-03
miR-4284	-	1.77	1.91E-02
miR-4286	-	1.65	1.48E-02
miR-122-3p	-	1.41	4.64E-02
168 h compared to 0 h			
miR-21-5p	+	4.53	2.30E-05
miR-3665	+	3.76	1.81E-02
miR-1246	+	3.21	2.67E-02
miR-762	+	3.00	2.72E-02
miR-3195	+	2.57	4.37E-02
miR-29b-3p	+	2.19	9.32E-03
miR-24-3p	+	2.11	1.29E-02
miR-34a-5p	+	2.03	9.08E-03
miR-1260b	+	1.97	2.97E-02
miR-193a-3p	+	1.94	3.58E-03
miR-16-5p	+	1.69	1.47E-02
miR-885-5p	-	3.94	3.12E-02
miR-192-5p	-	2.24	3.59E-02
miR-4286	-	2.15	1.19E-02
miR-30c-5p	-	1.98	4.50E-02
miR-148a-3p	-	1.92	1.37E-02
miR-4284	-	1.89	5.50E-03
miR-19b-3p	-	1.55	4.23E-03
miR-122-5p	-	1.53	8.80E-03

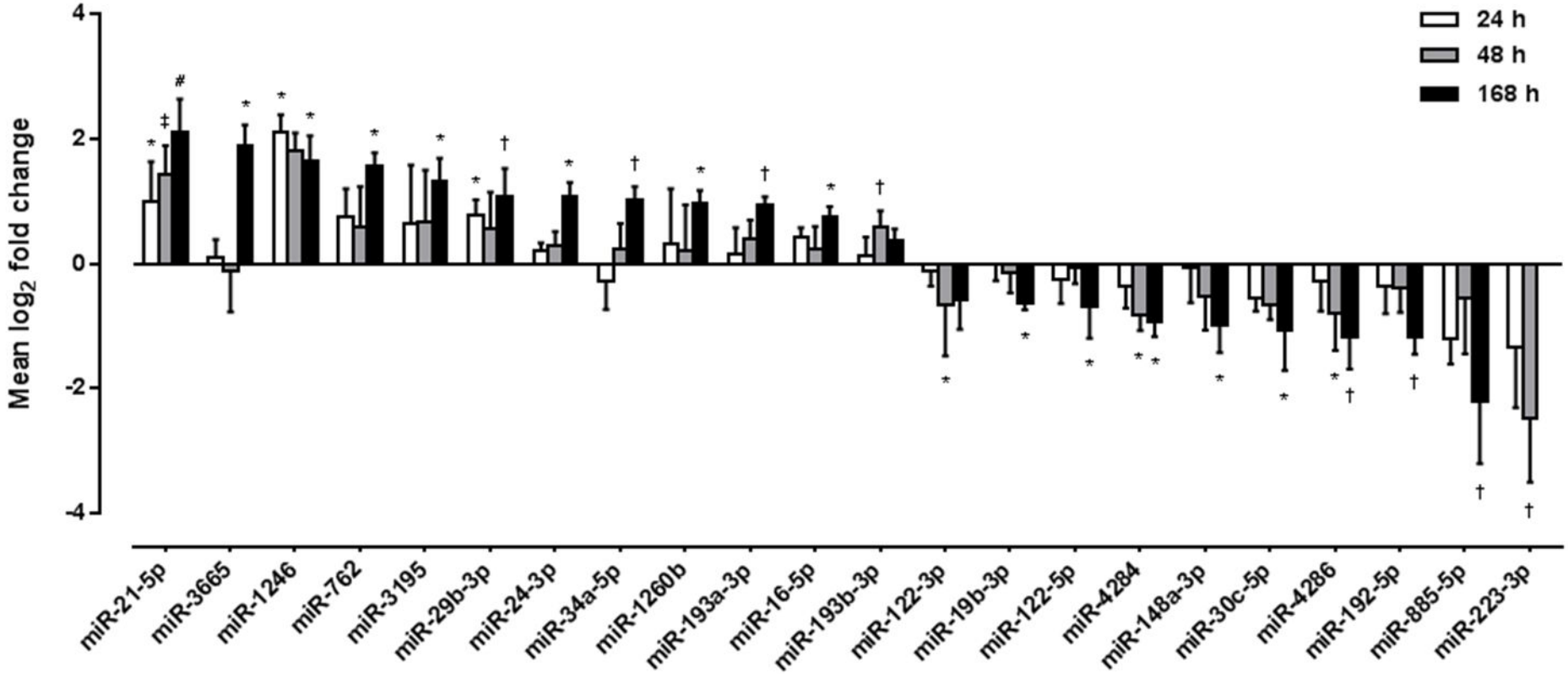

Figure 3.4 Fold-change of differentially-expressed miRs at each time-point of extended *in vitro* culture of hPHs, compared to baseline at 0 hours.

Data is presented as the mean log_2 fold change of normalised intensity value of each miR compared to baseline (freshly-isolated hepatocytes at 0 h), at 24 hours, 48 hours, and 168 hours in culture respectively, from 6 individual donors of hPHs. For each miR, a time-point was included in analysis only if detected in 3 donors or more. Error bars represent the standard deviation of the mean log_2 fold-change for each data point. * denotes $p < 0.05$, † denotes $p < 0.01$, ‡ denotes $p < 0.001$, # denotes $P < 0.0001$.

3.3.4 Real-time quantitative RT-PCR (qRT-PCR) validation of microarray microRNA expression profiles

To verify the miR expression profiles of hPHs obtained from the microarray analysis, qRT-PCR analysis on selected differentially-expressed miRs identified from the microarray analysis was performed. The expression profiles of four selected miRs were analysed further by qRT-PCR using the same samples of donor hPHs used in the microarray analysis. For this purpose, samples of extracted total RNA from three of the four donors which had corresponding RIN > 7 for all the time-points, as determined by the Agilent 2100 bioanalyser (using the RNA 6000 Nano kit, Agilent Technologies), were analysed.

The rationale for the selection of the four miRs for validation using qRT-PCR were as follows: miR-122-5p as it was the most abundantly-expressed miR in freshly-isolated hPHs (Figure 3.2); miR-4284 as it was the second most abundantly-expressed miR in freshly-isolated hPHs and was not previously detected in adult liver tissue (Figure 3.2); miR-21-5p as it was the most up-regulated miR at the 168 hour time-point (Table 3.1); and miR-885-5p as it was the most down-regulated miR at the 168 hour time-point (Table 3.1). A fold-change analysis of the selected miRs was then performed at each time-point in comparison to the baseline levels in freshly-isolated hepatocyte samples for each individual miR, similar to the fold-change analysis done for all the miRs detected in hPHs from the microarray analysis (Figure 3.3, Table 3.1, Figure 3.4).

As shown in Figure 3.5, similar expression profiles of all the selected miRs compared to the microarray analysis were seen with a matching trend towards up- or down-regulation compared to baseline at the 168 hour time-points, with similar magnitude of mean fold changes. All the time-points with significant difference to the baseline values for each miR when analysed by microarray analysis, were also similarly observed with the same trend of expression when analysed by the qRT-PCR method, apart from the 48 hour time-point for miR-4284 which had no significant difference. Therefore, we concluded that the global miR

expression profiles of human primary hepatocytes in extended *in vitro* culture as analysed by the microarray platform, were robust and reliable for further detailed analyses.

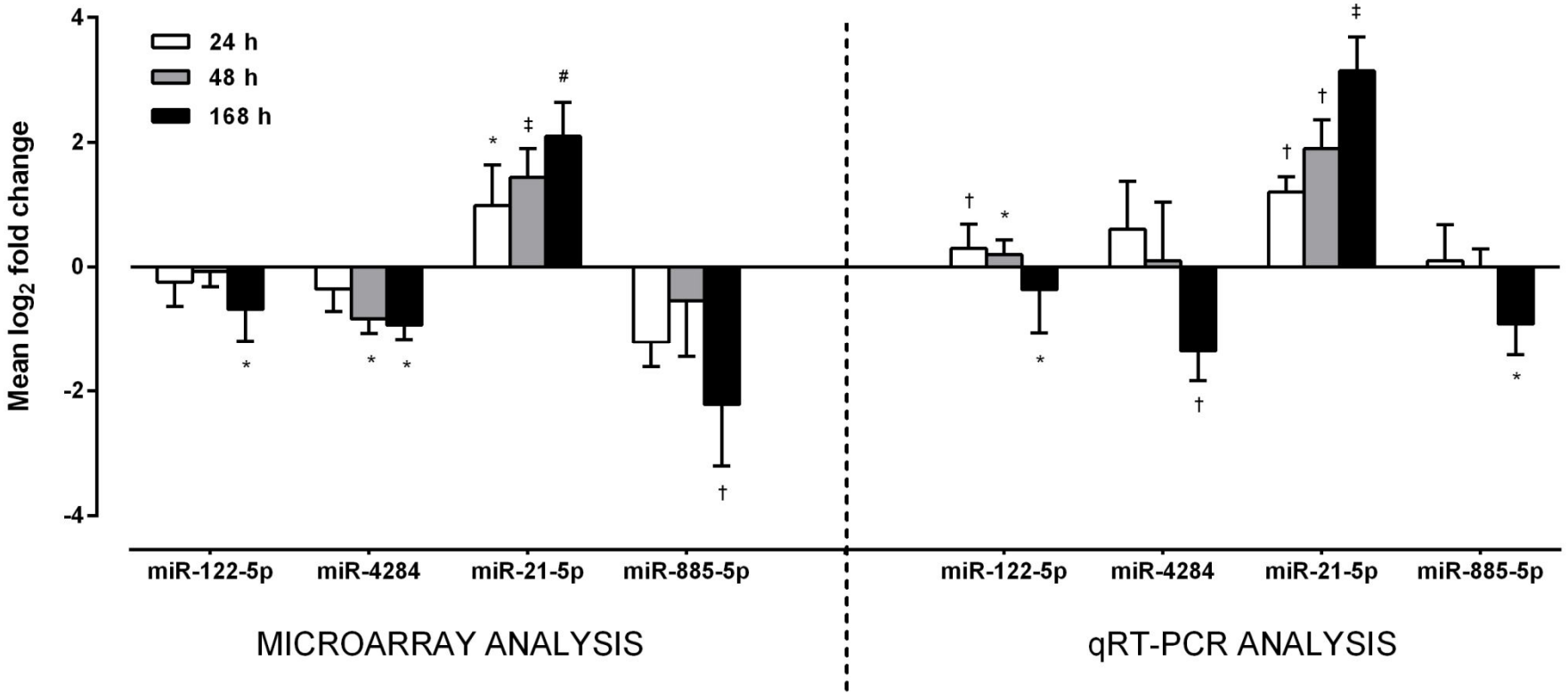

Figure 3.5 Comparison of expression profiles of selected miRs of hPHs in extended *in vitro* culture as analysed by microarray analysis and real-time quantitative RT-PCR

Data is presented as the mean log_2 fold change of expression for each miR compared to baseline (freshly-isolated hepatocytes at 0 h), at 24 hours, 48 hours, and 168 hours in culture respectively, as per (left panel) microarray analysis, and (right panel) real-time quantitative RT-PCR. Error bars represent the standard deviation of the mean log_2 fold-change for each data point. * denotes $p < 0.05$, † denotes $p < 0.01$, ‡ denotes $p < 0.001$, # denotes $P < 0.0001$.

3.3.5 Perturbed biological functions and canonical pathways of human primary hepatocytes in extended *in vitro* culture

The target mRNAs of the differentially-expressed miRs were then identified, and subsequent analyses of their involvement in biological functions and canonical pathways were performed for each set of differentially-expressed miRs at each time-point, using Ingenuity Pathway Analysis (IPA; Qiagen).

In general, as early as 24 hours after plating of hPHs, many biological functions were significantly affected via the targeting of specific genes by the differentially-expressed miRs (Figure 3.6). More detailed analysis of the processes involved with each perturbed biological function was also interrogated by analysing the function annotation terms for the gene targets, which gave more biological insight into the changes that occur in hPHs during extended *in vitro* culture (Tables 3.2A, 3.2B and 3.2C).

We found that the most significantly perturbed biological function at each time-point was related to gene expression (Figure 3.6). Biological functions relating to cell motility, cellular proliferation, cellular organisation and cytoskeletal integrity were also perturbed throughout extended *in vitro* culture, with increasing significance and number of mRNAs targeted by differentially-expressed miRs at the 168 hour time-point (Tables 3.2A, 3.2B and 3.2C), which supports the morphological changes seen with the hPH cultures (Figure 3.1). Processes involved in cell death and survival such as apoptosis and necrosis were also among the five most significantly perturbed functions after 48 hours of culture (Table 3.2B and 3.2C) while processes involved in cell cycle were also more significantly perturbed at the 168 hour time-point (Figure 3.6). At 7 days post-plating of the hPHs, functions relating to metabolism and environmental information processing were also noted to have higher significance values compared to earlier time-points of *in vitro* culture (Figure 3.6).

The canonical pathways that were significantly perturbed during the process of hepatocyte dedifferentiation were also examined (Figure 3.7).

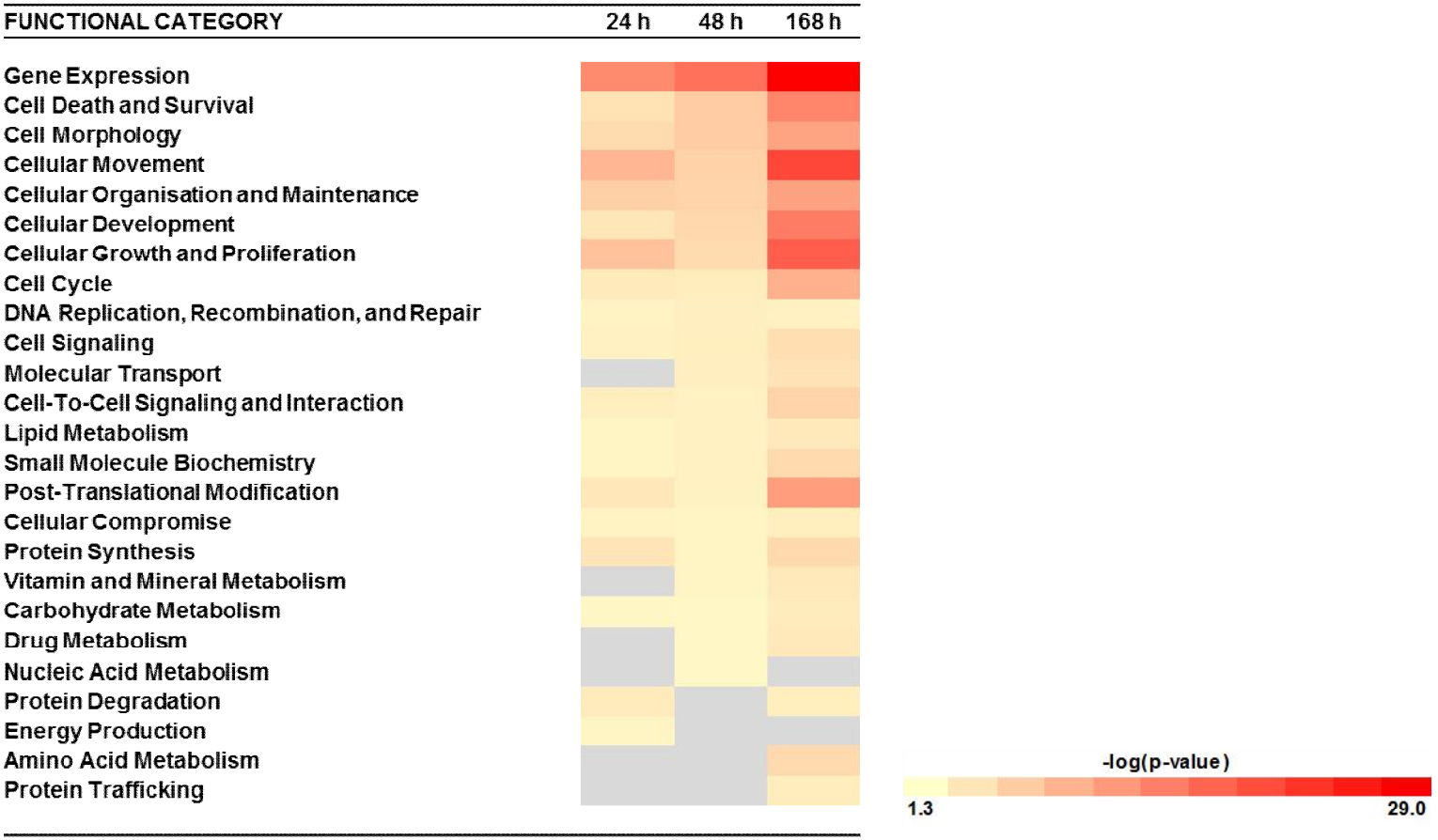

Figure 3.6 Heatmap showing the high-level functional category enrichment for gene targets of differentially-expressed miRs at each time-point of extended *in vitro* culture of hPHs, compared to baseline at 0 hours.

Data is presented as the significance value of the most relevant function for each high-level category, which indicates the probability of association between the dataset of predicted mRNA targets of differentially-expressed miRs at each time-point, and the function is due to random chance alone. The categories are ranked according to the highest values at 48 hours. The significance is expressed as the negative exponent of the p-value ($-\log_{10}$ p-value) as calculated by Fisher's exact test right tailed. Red and yellow colour denotes high and low significance levels respectively, while grey colour denotes non-significant values ($p > 0.05$).

Table 3.2 Analysis of function annotation term enrichment for gene targets of differentially-expressed miRs at (A) 24 hours, (B) 48 hours and (C) 168 hours, compared to baseline at 0 hours.

Differentially-expressed miRs were analysed with IPA using the microRNA Target Filter module, and the predicted gene targets were analysed with the IPA Core Analysis module. The top 5 most significantly perturbed categories of molecular and cellular function denoted by their representative function annotations are shown below with their corresponding p-value *(calculated by Fisher's exact test right tailed)* and number of predicted mRNA targets.

(A) 24 hours

Category	Representative function annotations	p-value *(with multiple testing correction)*	Number of mRNA targets
GENE EXPRESSION	**Transcription of RNA**	2.02E-13	186
	Transcription of DNA	4.99E-09	135
	Activation of DNA endogenous promoter	1.06E-05	86
	Binding of DNA	7.76E-04	45
CELLULAR MOVEMENT	**Cell movement**	5.86E-10	167
	Migration of cells	8.67E-08	144
CELLULAR GROWTH AND PROLIFERATION	**Proliferation of cells**	9.44E-09	302
	Cytostasis	6.09E-06	33
CELLULAR ORGANISATION AND MAINTENANCE	**Development of cytoplasm**	3.08E-07	40
	Formation of filaments	5.45E-07	37
	Formation of cytoskeleton	2.71E-06	33
CELL MORPHOLOGY	**Morphology of cells**	7.05E-06	64
	Necrosis	3.10E-04	16

(B) 48 hours

Category	Representative function annotations	p-value *(with multiple testing correction)*	Number of mRNA targets
GENE EXPRESSION	**Transcription of RNA**	2.69E-17	200
	Transcription of DNA	1.48E-11	145
	Activation of DNA endogenous promoter	4.28E-07	92
	Transactivation of RNA	2.78E-06	62
	Binding of DNA	3.76E-05	50
CELL DEATH AND SURVIVAL	**Apoptosis**	1.23E-07	211
	Necrosis	5.47E-07	223
CELL MORPHOLOGY	**Morphology of cells**	1.29E-07	70
	Autophagy	9.34E-04	29
CELULAR MOVEMENT	**Cell movement**	6.42E-07	155
	Migration of cells	2.90E-05	133
CELLULAR ORGANISATION AND MAINTENANCE	**Development of cytoplasm**	1.06E-06	39
	Quantity of lipid droplets	1.14E-05	13
	Formation of cytoskeleton	5.96E-05	30
	Depolarization of mitochondrial membrane	1.86E-04	7
	Remodelling of chromatin	6.34E-04	9

(C) 168 hours

Category	Representative function annotations	p-value *(with multiple testing correction)*	Number of mRNA targets
GENE EXPRESSION	**Transcription of RNA**	9.74E-30	698
	Transcription of DNA	5.37E-23	526
	Transactivation of RNA	8.59E-15	231
	Activation of DNA endogenous promoter	5.87E-12	331
	Repression of RNA	1.52E-06	51
	Binding of DNA	6.67E-06	165
	Binding of protein binding site	9.87E-05	81
CELLULAR MOVEMENT	**Cell movement**	4.46E-22	642
	Migration of cells	6.92E-17	560
CELLULAR GROWTH AND PROLIFERATION	**Proliferation of cells**	1.60E-19	1230
	Colony formation of cells	8.72E-09	185
	Arrest in growth of cells	1.67E-06	65
CELLULAR DEVELOPMENT	**Differentiation of cells**	2.80E-16	379
	Epithelial-mesenchymal transition	9.99E-07	66
	Immortalization	3.22E-04	13
CELL DEATH AND SURVIVAL	**Apoptosis**	3.30E-15	832
	Necrosis	2.22E-14	893
	Cell viability	1.87E-11	456
	Anoikis	6.92E-05	37

Figure 3.7 Heatmap showing the most significantly perturbed canonical pathways at each time-point of extended *in vitro* culture of hPHs, compared to baseline at 0 hours.

Data is presented as the significance value of the canonical pathway, which indicates the probability of association between the dataset of mRNA targets of differentially-expressed miRs at each time-point with the canonical pathway is due to random chance alone. The top 50 pathways are ranked according to the highest values at 48 hours. The significance is expressed as the negative exponent of the p-value ($-\log_{10}$ p-value) as calculated by Fisher's exact test right tailed. Red and yellow colour denotes high and low significance levels respectively, while grey colour denotes non-significant values ($p > 0.05$).

3.3.6 Targets of up-regulated microRNAs in dedifferentiating hPHs include liver-specific genes and liver-enriched transcription factors

During extended *in vitro* culture of hPHs, liver-specific features progressively decline (Elaut *et al.*, 2006), and the reduction of the mRNA levels of phase I/II xenobiotic biotransformation enzymes and drug transporters as well as liver-enriched transcription factors have been shown to occur during hepatocyte dedifferentiation (Elaut*, et al.*, 2006; Mizuguchi *et al.*, 1998; Padgham *et al.*, 1993; Rodriguez-Antona*, et al.*, 2002).

In this study, we found that the targets of many of the up-regulated miRs include genes involved in all phases of xenobiotic biotransformation (Table 3.3). Some of these genes were targeted by both up- and down-regulated miRs, though interestingly for the phase I enzymes including the cytochrome-P450s, they were almost exclusively targeted by miRs which were up-regulated during extended *in vitro* culture (Table 3.3). Three liver-enriched transcription factors (LETFs) and two nuclear factors that play important roles in the transcriptional control of liver-specific gene expression were also found to be targets of up-regulated miRs (Tables 3.4 and 3.5). Corresponding fold-change values for down-regulated miRs which target the listed factors were also included to provide a more balanced picture, though the overall net effect of all the associated miRs on the function of each factor is unknown.

Table 3.3 Selected genes that are important for xenobiotic biotransformation which are targeted by up-regulated miRs.

Liver-specific function	Liver-specific genes	miRs targeting liver-specific genes	Up / down regulation	Mean FC at 168 h
Phase I xenobiotic biotransformation	ALDH1A1	miR-21-5p	+	4.53
	CYP1A2	*miR-762*	+	3.00
		miR-4284	-	1.89
	CYP1B1	miR-1260b	+	1.97
		miR-16-5p	+	1.69
	CYP2B6	*miR-29b-3p*	+	2.19
	CYP2C18	miR-3665	+	3.76
	CYP2C8	miR-3665	+	3.76
	CYP3A4	*miR-762*	+	3.00
	CYP3A5	*miR-21-5p*	+	4.53
	DPYD	miR-34a-5p	+	2.03
	PTGS2 *(COX2)*	**miR-16-5p**	+	1.69
Phase II xenobiotic biotransformation	COMT	*miR-3665*	+	3.76
		miR-762	+	3.00
		miR-16-5p	+	1.69
		miR-30c-5p	-	1.98
	NQO1	*miR-34a-5p*	+	2.03
	SULT1A1	*miR-1260b*	+	1.97
	SULT1C2	*miR-1260b*	+	1.97
		miR-148a-3p	-	1.92
	SULT4A1	*miR-29b-3p*	+	2.19
		miR-34a-5p	+	2.03
		**miR-193a-3p*	+	1.94
Phase III xenobiotic biotransformation	ABCB6	miR-29b-3p	+	2.19
	ABCC6 *(MRP6)*	*miR-762*	+	3.00
		miR-122-5p	-	1.53
	SLC15A1	*miR-193a-3p	+	1.94
		miR-122-5p	-	1.53
	SLC22A7 *(OAT2)*	miR-29b-3p	+	2.19
	SLC22A9 *(OAT4)*	*miR-24-3p*	+	2.11
		miR-4284	-	1.89
	SLCO2B1 *(OATP2B1)*	miR-762	+	3.00
		miR-4284	-	1.89

For gene name abbreviations, please see http://www.ncbi.nlm.nih.gov/gene/. Commonly known aliases are listed in parentheses. Selected descriptions of gene name abbreviations: ALDH1A1, aldehyde dehydrogenase 1 family, member A1; DPYD, dihydropyrimidine dehydrogenase; PTGS2 *(COX2)*, prostaglandin-endoperoxide synthase 2 *(cyclooxygenase 2;*

COMT, catechol-O-methyltransferase; NQO1, NAD(P)H dehydrogenase, quinone 1; SLC15A1, solute carrier family 15, member 1; OAT2, organic anion transporter 2; SLCO2B1 *(OATP2B1)*, solute carrier organic anion transporter family, member 2B1 *(organic anion transporting polypeptide, member 2B1)*. miRs highlighted in bold represent miR-mRNA interaction that have been experimentally observed, miRs in normal font represent predicted miR-mRNA interaction with high confidence *(as defined by TargetScan)* and miRs in italics represent predicted miR-mRNA interaction with moderate confidence *(as defined by TargetScan).*The mean fold change (FC) of miRs which were between 0 and 1 at 168 hours, compared to baseline at 0 hours, was transposed to a range of -1 until -infinity. The direction of change of expression for all miRs listed is indicated by the symbol + for up-regulation, and – for down-regulation. * miR-193a-3p and miR-193b-3p share the same seed sequence of ACUGGCC used for downstream analysis of mRNA targets.

Table 3.4 Liver-enriched transcription factors (LETFs) targeted by up-regulated miRs, and their roles in liver-specific functions.

LETF	Liver-specific function	Liver-specific genes regulated by LETF	miRs targeting LETF	Up / down regulation	Mean FC at 168 h
HNF1A	**Xenobiotic biotransformation**	CYP1A2, CYP2C11, CYP2E1, CYP7A1, GSTA2, SULT2A1, UGT1A1, UGT1A3, UGT1A4, UGT1A6, UGT1A7, UGT2B1, UGT2B7, UGT2B17	*miR-34a-5p*	+	2.03
	Carbohydrate and lipid metabolism	PCK2 *(PEPCK)*, ALDOB, APOA1, APOB			
	Protein synthesis	ALB, AFP, TTR, SERPINA1 *(A1AT)*			
HNF4A	**Xenobiotic biotransformation**	CYP2A6, CYP2C2, CYP2C8, CYP2C9, CYP2D6, CYP3A4, CYP3A5, UGT1A9	miR-34a-5p	+	2.03
	Carbohydrate and lipid metabolism	ALDH2, APOA1, APOC3			
	Protein synthesis and urea cycle	TTR, TF, SERPINA1 *(AAT)*, OTC			
CEBPA	**Xenobiotic biotransformation**	CYP2A6, CYP2B6, CYP2C9, CYP2D6, CYP3A4 GSTA1, UGT2B1, UGT2B7	*miR-762*	+	3.00
	Carbohydrate and lipid metabolism	PCK2 (PEPCK), ALDOB, APOB			
	Protein synthesis	ALB, AFP, TTR, TF, SERPINA1 *(A1AT)*			

For gene name abbreviations, please see http://www.ncbi.nlm.nih.gov/gene/. Commonly known aliases are listed in parentheses. Selected descriptions of gene name abbreviations: HNF1A, hepatocyte nuclear factor 1, alpha; PCK2 *(PEPCK)*, phosphoenolpyruvate carboxykinase 2; ALDOB, aldolase B, fructose-bisphosphate; APOA1, apolipoprotein A-1; APOB, apolipoprotein B; ALB, albumin; AFP, alpha-fetoprotein; TTR,

transthryretin; SERPINA1 *(A1AT)*, serpin peptidase inhibitor, clade A (alpha-1 antiproteinase, antitrypsin), member 1; ALDH2, aldehyde dehydrogenase 2 family; APOC3, apolipoprotein C-III; OTC, ornithine transcarbamoyltransferase; TF, transferrin; CEBPA, CCAAT/enhancer binding protein (C/EBP), alpha. miRs in normal font represent predicted miR-mRNA interaction with high confidence *(as defined by TargetScan)* and miRs in italics represent predicted miR-mRNA interaction with moderate confidence *(as defined by TargetScan).* The direction of change of expression for all miRs listed is indicated by the symbol + for up-regulation, and – for down-regulation. References for the associated genes regulated by the LETFs are listed in Fraczek *et al.*, 2013.

Table 3.5 Nuclear receptors (NRs) targeted by up-regulated miRs, and their roles in liver-specific functions.

NR	Liver-specific function	Associated genes regulated by nuclear receptor‡	miRs targeting NR	Up / down regulation	Mean FC at 168 h
NR1I2 *(PXR)*	**Xenobiotic biotransformation**	CYP2B, CYP3A4, UGT1A1, UGT1A6, ABCC2	*miR-34a-5p*	+	2.03
			miR-148a-3p	-	1.92
	Bile acid homeostasis	CYP7A1, ABCC2, SLC21A6			
PPARA	**Carbohydrate and lipid metabolism**	CPT1A, ACOX1, HMGCS1	miR-21-5p	+	4.53
		GPD1, GPD2, GK	miR-24-3p	+	2.11
			miR-16-5p	+	1.69
			miR-19b-3p	-	1.55
			miR-223-3p	-	4.74*

For gene name abbreviations, please see http://www.ncbi.nlm.nih.gov/gene/. Selected descriptions of gene name abbreviations: NR1I2 *(PXR)*, nuclear receptor subfamily 1, group I, member 2 *(also known as pregnane X receptor)*; PPARA, peroxisome proliferator-activated receptor alpha; CPT1A, carnitine palmitoyltransferase 1A ; ACOX1, acyl-CoA oxidase 1, palmitoyl; HMGCS1, 3-hydroxy-3-methylglutaryl-CoA synthase 1; GPD1, glycerol-3-phosphate dehydrogenase 1; GK, glycerol kinase. miRs highlighted in bold represent miR-mRNA interaction that have been experimentally observed, miRs in normal font represent predicted miR-mRNA interaction with high confidence (as defined by TargetScan) and miRs in italics represent predicted miR-mRNA interaction with moderate confidence (as defined by TargetScan).The mean fold change (FC) of miRs which were between 0 and 1 at 168 hours, compared to baseline at 0 hours, was transposed to a range of -1 until -infinity. The direction of change of expression for all miRs listed is indicated by the symbol + for up-regulation, and – for down-regulation. * The mean FC shown for miR-223-3p was at 48 hours post-plating, as it was not detected at 168 hours post-plating. ‡ References for the associated genes regulated by the NRs: (Jigorel *et al.*, 2006; Kakizaki *et al.*, 2011; Lefebvre *et al.*, 2006; Staudinger *et al.*, 2003; Takagi *et al.*, 2008)

3.4 DISCUSSION

Dedifferentiation of hPHs, which are currently used as the gold standard *in vitro* hepatic model (LeCluyse, 2001), remains a major limitation of its application in pharmaco-toxicology studies, especially in chronic toxicity studies that aim to mimic the clinical presentations of DILI which often occurs following prolonged exposure to drugs (Guguen-Guillouzo and Guillouzo, 2010; Kalgutkar and Soglia, 2005; LeCluyse, 2001). Therefore, better understanding of the dedifferentiation process is vitally important to develop a more relevant hepatic model of drug-induced hepatotoxicity and could additionally reveal novel insights for better hepatic differentiation of human pluripotent stem cells towards hepatocyte-like cells.

The global miR profile of human primary hepatocytes (hPHs) has not been previously reported, although the global miR expression of liver tissue has been updated over the years with newly-discovered mature miRs being included as part of the repertoire of miRs detectable by high-throughput platforms. However, as up to 40% of hepatic cells consist of many other cell-types including non-parenchymal cells such as endothelial cells, stellate cells, Kupffer cells, biliary epithelial cells and lymphoid cells (Godoy*, et al.*, 2013), the miR expression profile of the liver tissue actually represents the composite miR profiles of all the above cell-types. For the purposes of understanding the process of dedifferentiation of hPHs, the distinct global miR expression of a human hepatocyte is more relevant as opposed to the profile of the liver tissue.

Using samples of freshly-isolated hPHs from six different adult donors, we found that in general, the global miR profile of a typical hPH include previously identified enriched miRs (miR-122-5p, miR-21-5p, miR-22-3p, miR-125b-5p, miR-27b-3p and the let-7 family of miRs) in earlier studies using human liver tissue profiled using small RNA library sequencing (Landgraf*, et al.*, 2007) and oligonucleotide microarray techniques (Barad*, et al.*, 2004) (Figure 3.2). Our list of enriched miRs in hPHs also includes some miRs (miR-1260a, miR-4286, miR-30b-5p and miR-223-3p) reported in the latest study which included a list of all

detected miRs in healthy liver tissue using PCR arrays capable of detecting 372 pre-chosen miRs (Ward *et al.*, 2014).

Similar to human liver tissue, miR-122-5p was the most abundant in isolated hPHs (Figure 3.2), which is not surprising given that hepatocytes constitute 81% of the total liver cell mass (Kmiec, 2001; Landgraf*, et al.*, 2007). However, based on the analysis of the mean normalised intensity values of all detected miRs in this study, the relative abundance of miR-122-5p was estimated to constitute around 21% of all detected miRs in hPHs. This is a striking contrast to the often-quoted figure of approximately 70% relative abundance of miR-122-5p in mouse liver tissue (Jopling, 2012; Lagos-Quintana *et al.*, 2002), although many methodological differences between our studies prevent any conclusive direct comparisons. The study by Lagos-Quintana *et al.*, which was based on the identification of miRs which were cloned and sequenced, only detected 11 distinct miR sequences in the mouse liver tissue, including 2 other less common sequence variants of miR-122-5p which were also included in the estimation of the relative abundance of miR-122-5p. In addition, only less than 100 miRs were previously reported in the literature at the time of that study. Furthermore, if only the sequence of miR-122-5p with the highest mean number of reads per million was used for estimation, the relative abundance of miR-122-5p from that study would be lower at 45%. Nevertheless, further quantitative estimation of miR-122-5p in the human liver in comparison to isolated hPHs would be interesting to exclude the possibility of significant change with its level during the process of isolation, which may be related to early events in the dedifferentiation process.

There were also differences between the global miR profile of an isolated hPH delineated in our study in comparison to previously published miR profiles of human liver tissue. Firstly, within the list of the 30 most abundant miRs detected (Figure 3.2), there were novel miRs (miR-494-3p, miR-4284, miR-4281, and miR-4299) which were not previously reported in adult liver tissue. The discovery of the latter three miRs were only first reported in 2009 in human embryonic stem cells and neural precursors (Goff *et al.*, 2009), following the

publication of the earlier studies (Barad*, et al.*, 2004; Landgraf*, et al.*, 2007) and these miRs were also not included as part of the analysis in the latest study using human liver tissue (Ward*, et al.*, 2014).

Furthermore, there were also differences with the relative abundance of the miRs detected in hPHs and human liver tissue (Table 3.6). The latest published study using normal liver tissue was used for comparison against results from our study as it used a list of miR assays which were most comparable to our study, although caution should be applied due to the different methods used for miR analysis (PCR array versus oligonucleotide microarray) and the coverage of miRs detectable (372 versus 1204). Nevertheless, this comparison allows for unique contextual analysis of the miR profile of isolated hPHs. 13 of the top 30 most abundant miRs detected in hPHs were also detected in the top 30 most abundant miRs in human liver tissue, though conversely, 15 of the top 30 most abundant miRs detected in human liver tissue were found to be of much lower abundance in hPHs, outwith the top 30 most abundant miRs. Therefore, it is quite possible that many of the miRs detected at much higher abundance in the liver tissue compared to hPHs are miRs which are more enriched in non-parenchymal cells, and the list of top 30 most abundant miRs in hPHs shown in Figure 3.2 represents the first unencumbered definition of human hepatocyte-enriched miRs.

However, it is currently unclear if the miR profile of the isolated hPH reported in this study is truly representative of the hPH residing in the *in vivo* liver niche, and whether the “true” miR profile was altered by the isolation process. Therefore, further validation studies by other groups using freshly-isolated hPHs and possibly parallel global analysis of hPHs microdissected from liver tissue will be required to confirm our findings.

To specifically study the role of miRs in the dedifferentiation process of hPHs, the miR profiles were analysed using hPHs which were maintained as two-dimensional monolayer culture in conventional conditions up to 168 hours (termed Day 7). The combined effect of these differentially-expressed miRs was then interrogated by the analyses of the perturbed

biological functions (Figure 3.6) and canonical pathways (Figure 3.7). Strikingly, gene expression was the most significantly perturbed function identified at every time-point of the study (Figure 3.6) with the number of mRNAs targeted by differentially-expressed miRs increasing by more than 3-fold at Day 7 compared to Day 1 (Table 3.2A and 3.2C).

Further analysis of the function annotations related to gene expression suggested that during extended *in vitro* culture the gene expression hPHs was perturbed at both the pre- and post-transcriptional levels due to dysfunction to the processes of binding of protein binding sites, transactivation of RNA, binding of DNA and activation of DNA endogenous promoter (Table 3.2C). Therefore, delineating in more detail the additional mechanisms of how the differentially-expressed miRs can regulate the global regulators of gene expression in dedifferentiating hPHs, may provide new approaches to counter hepatocyte dedifferentiation.

Besides its widely studied role in the translational repression of protein-coding genes via direct binding to the 3′ untranslated region (UTR) of target mRNAs (Bartel, 2004), miRs have also been found to regulate gene expression by binding to and disrupting the function of RNA-binding proteins (RBPs), which have been suggested recently to be the main drivers of gene expression (Kechavarzi and Janga, 2014) by acting as transcriptional activators or repressors (Beitzinger and Meister, 2010). With this in mind, we found that 4 out of 10 RBPs with the highest gene expression values reported in human liver tissue (Kechavarzi and Janga, 2014), were targeted by 6 of the differentially-expressed miRs in our study (Table 3.7). Further comprehensive analysis of the 850 genes experimentally characterised as RBPs in the human genome (Castello *et al.*, 2012) may of course yield more potential targets. Furthermore, there is evidence that miRs target directly and indirectly effectors of the epigenetic machinery. Increased expression of the miR-29 family, including miR-29b-3p which was upregulated in our study (Table 3.1), was shown to directly and indirectly target the family members of DNA methyltransferases (DNMTs; DNMT1, 3A and 3B) (Fabbri *et al.*, 2007; Garzon *et al.*, 2009), which play important roles in maintaining the cell and tissue-

specific epigenetic fingerprint of their methylation pattern (Cheng and Blumenthal, 2008), resulting in a global reduction of DNA methylation. Similarly, overexpression of miR-21-5p, which was also up-regulated in our study, was also shown to result in the down-regulation of DNMT1 (Pan *et al.*, 2010). In addition, many of the histone deacetylases (HDACs), which are typically associated with transcriptional repression by their role in the reconstitution of a dense chromatin (Eberharter and Becker, 2002), were also noted to be targets of our set of differentially-expressed miRs (Table 3.8). These included HDAC-1 and HDAC-4 targeted by the up-regulated miR-34a-5p and miR-29b-3p respectively, of which the interactions were experimentally observed (Winbanks *et al.*, 2011; Zhao *et al.*, 2013). Therefore, our findings add a further dimension to the increasing recognition that the modulation of epigenetic mechanisms using HDAC and DNMT inhibitors may be a promising strategy to prevent or restore the dedifferentiated phenotype (Fraczek*, et al.*, 2013). However, targeting all of the HDAC and DNMT isozymes with a broad spectrum inhibitor may not be ideal, as our current knowledge of their individual roles in specific hepatocellular processes are still lacking (Fraczek*, et al.*, 2013). Perhaps by modulating the differentially-expressed miRs either in isolation or in a considered combinatorial approach that target individual isozymes of HDACs and DNMTs as well as RBPs, a more targeted assessment of the contribution of dysregulated effectors of gene expression towards hepatic dedifferentiation could be evaluated.

Dedifferentiation of hepatocytes has been described to begin during the hepatocyte isolation process partly due to the proliferative response, mediated by the mitogen-activated protein kinase (MAPK) pathway (Elaut*, et al.*, 2006; Fraczek*, et al.*, 2013). Adult hepatocytes are usually highly differentiated and mitotically quiescent at the G0 phase, though they retain the potential for high proliferative capacity (Fausto, 2001; Fraczek*, et al.*, 2013). However, following the isolation process, the hepatocytes were reported to rapidly and synchronously re-enter the G1 phase of the cell cycle and primed to respond to growth signals, with a consequent negative effect on the expression of liver-specific genes, particularly those

related to phase I and II xenobiotic transformation and the liver-enriched transcription factors (LETFs) (Beigel *et al.*, 2008; de Longueville *et al.*, 2003; Fraczek*, et al.*, 2013; Paine and Andreakos, 2004). In our study, two of the most significantly perturbed pathways associated with the differentially-expressed miRs at the 48 hour time-point, were the extracellular signal-regulated kinases (ERK)/MAPK signalling pathway and the pathway governing cyclins and cell cycle regulation (Figure 3.7), which suggests that miRs also play an early and important role in hepatocytes entering the "proliferation-primed state". Cellular proliferation was also noted to be a significantly perturbed biological function from Day 1 (Figure 3.6). Therefore, another approach to prevent the occurrence of hepatocyte dedifferentiation could be the early modulation of differentially-expressed miRs associated with cellular proliferation at the early time-points. Indeed, miR-21-5p which was up-regulated from Day 1 and was the most up-regulated miR at Day 2 and Day 7 (Table 3.1), similar to the findings in a dedifferentiating rat hepatocyte model (Bolleyn*, et al.*, 2011), was also previously shown to be up-regulated during the proliferative phase of liver regeneration in rat and mice models (Castro *et al.*, 2010; Marquez *et al.*, 2010). miR-1246 which was the most up-regulated miR at Day 1 and remaining significantly up-regulated at Day 7 (Table 3.1), was previously reported to promote cell proliferation and migration in a human cervical cancer cell line (Chen *et al.*, 2014). Meanwhile, miR-885-5p which was the most down-regulated miR at Day 7 (Table 3.1), was shown to inhibit proliferation of neuroblastoma cell lines through the activation of the p53 pathway (Afanasyeva *et al.*, 2011). Modulation of the miRs that target components of the MAPK pathway could also be considered.

In addition, many of the pathways that were previously reported to be involved in the process of hepatocyte dedifferentiation (Elaut*, et al.*, 2006; Fraczek*, et al.*, 2013) such as the phosphoinositide-3-kinase–protein kinase B/Akt (PI3K/AKT) pathway, apoptosis signalling pathways, the signal transducer and activator of transcription 3 (STAT3) pathway and the nuclear factor kappa-light-chain-enhancer of activated B cells (NF-κβ) pathway, were also noted to be perturbed in our study (Figure 3.7). By modulating a small set of miRs that target

multiple components of a pathway as exemplified in the STAT3 pathway (Figure 3.8), which play a major role in the expression of liver-specific genes (Kyriakis and Avruch, 2001), the negative consequences of the perturbation of a specific pathway may be nullified.

One of the major hallmark of a dedifferentiated hPH in *in vitro* culture is the reduction in the expression of genes and associated proteins involved in xenobiotic biotransformation (Rowe*, et al.*, 2013; Ulvestad *et al.*, 2013), as well as liver-enriched transcription factors (LETFs) (Rodriguez-Antona*, et al.*, 2002) which play crucial roles in the transcriptional regulation of a myriad of liver-specific genes (Elaut*, et al.*, 2006; Fraczek*, et al.*, 2013). Therefore, it is interesting to note from our study that many of these genes and LETFs, are direct targets of the up-regulated miRs (Table 3.3 and 3.4). The nuclear receptor, pregnane X receptor (PXR), which regulates the expression of enzymes involved in phase I-III drug metabolism and transport (Elaut*, et al.*, 2006), was also a target (Table 3.5). Therefore, one further anti-dedifferentiating strategy to produce a relevant human hepatic *in vitro* model for the purposes of pharmaco-toxicology where drug metabolising capability is important, could be selective inhibition of the identified differentially-expressed miRs that target the genes involved in xenobiotic biotransformation and LETFs.

In summary, we have shown that our hypothesis of using a global approach in identifying the changing miR profiles of dedifferentiating hPHs to gain novel insights is valid. We have shown that differentially-expressed miRs in dedifferentiating hPHs were associated with many of the previously delineated perturbed pathways, biological functions and genes, and highlighted a potential major effect of miRs in the dedifferentiation process via perturbation of gene expression at the pre- and post-transcriptional levels. However, validation experiments are now required to confirm our findings from the bioinformatics analyses, and it still remains to be answered whether miRs are mere silent observers or active participants in the process of hepatic dedifferentiation. Nevertheless, our study added to the ongoing efforts in overcoming the dedifferentiation of hPHs in *in vitro* culture by providing a narrow list of targets for manipulation in the form of the differentially-expressed miRs, which could in turn

result in simultaneous manipulation of numerous biological processes and pathways governed by these miRs.

Table 3.6 Comparison of the top 30 most abundant miRs in human primary hepatocytes with human liver tissue.

* The miRs were ranked according to the mean normalised intensity value obtained from individual microarray analysis of hPHs isolated from 6 different donors. ‡ The miRs were ranked according to raw CT values as reported in Ward, et al., 2014, excluding miRs which were considered tRNA fragments, from 3 healthy donors. The slash denotes miRs which were not assayed, while blank values represent miRs which were detected but not within the top 30 most abundant miRs.

microRNA	Top 30 most abundant miRs in hPHs* *(values denote rank)*	Top 30 most abundant miRs in human liver tissue‡ *(values denote rank)*
miR-122-5p	1	1
miR-4284	2	/
miR-4286	3	4
miR-1260a	4	2
miR-21-5p	5	7
let-7a-5p	6	
miR-192-5p	7	16
miR-148a-3p	8	15
let-7f-5p	9	
let-7b-5p	10	
miR-494-3p	11	/
miR-22-3p	12	9
miR-19b-3p	13	
miR-29a-3p	14	17
miR-1260b	15	
miR-4281	16	/
miR-27b-3p	17	
miR-122-3p	18	/
miR-23b-3p	19	
miR-194-5p	20	11
miR-125b-5p	21	14
miR-451a	22	5
let-7g-5p	23	
miR-29c-3p	24	8
miR-4299	25	/
miR-30b-5p	26	
miR-16-5p	27	12
miR-223-3p	28	
let-7c	29	
miR-885-5p	30	
miR-4454	/	3
miR-4516	/	6
miR-126-3p		10
miR-26a-5p		13
miR-4301		18
miR-195-5p		19
miR-99a-5p		20
miR-100-5p		21
miR-101-3p		22
miR-30e-5p		23
miR-24-3p		24
miR-148b-3p		25
miR-30a-5p		26
miR-145-5p		27
miR-27a-3p		28
miR-20a-5p		29
miR-199a-5p		30

Table 3.7 Selection of RNA-binding proteins (RBPs) and differentially-expressed miRs in dedifferentiating hPHs that target their mRNA.

The 10 most highly expressed genes classified as RBPs in human liver tissue as reported by Kechavarzi *et al.*, 2014, were analysed as potential targets of differentially-expressed miRs detected in our study. miRs in normal font represent predicted miR-mRNA interaction with high confidence (as defined by TargetScan) and miRs in italics represent predicted miR-mRNA interaction with moderate confidence (as defined by TargetScan).The mean fold change (FC) of miRs which were between 0 and 1 at 168 hours, compared to baseline at 0 hours, was transposed to a range of -1 until -infinity. The direction of change of expression for all miRs listed is indicated by the symbol + for up-regulation, and – for down-regulation.

RNA-binding protein (RBP)	miRs targeting RBP	Up / down regulation	Mean FC at 168 h
EEF1A1 *(eukaryotic translation elongation factor 1 alpha 1)*	*miR-3665*	+	3.76
	miR-30c-5p	-	1.98
PDIA3 *(protein disulfide isomerase family A, member 3)*	miR-148a-3p	-	1.92
CANX *(calnexin)*	miR-29b-3p	+	2.19
	miR-148a-3p	-	1.92
	miR-122-5p	-	1.53
P4HB *(prolyl 4-hydroxylase, beta polypeptide)*	*miR-762*	+	3.00

Table 3.8 Histone deacetylases (HDACs) and differentially-expressed miRs in dedifferentiating hPHs that target their mRNA.

miRs highlighted in bold represent miR-mRNA interaction that have been experimentally observed, miRs in normal font represent predicted miR-mRNA interaction with high confidence (as defined by TargetScan) and miRs in italics represent predicted miR-mRNA interaction with moderate confidence (as defined by TargetScan).The mean fold change (FC) of miRs which were between 0 and 1 at 168 hours, compared to baseline at 0 hours, was transposed to a range of -1 until -infinity. The direction of change of expression for all miRs listed is indicated by the symbol + for up-regulation, and – for down-regulation. * The mean FC shown for miR-223-3p was at 48 hours post-plating, as it was not detected at 168 hours post-plating.

Class	HDAC	miRs targeting HDAC	Up / down regulation	Mean FC at 168 h
I	**HDAC-1**	**miR-34a-5p**	+	2.03
		miR-4284	-	1.89
	HDAC-2	*miR-24-3p*	+	2.11
		miR-192-5p	-	2.24
	HDAC-8	*miR-1260b*	+	1.97
IIa	**HDAC-4**	**miR-29b-3p**	+	2.19
		miR-19b-3p	-	1.55
		miR-223-3p	-	4.74*
	HDAC-5	miR-762	+	3.00
		miR-30c-5p	-	1.98
	HDAC-7	miR-19b-3p	-	1.55
		miR-4286	-	2.15
	HDAC-9	miR-30c-5p	-	1.98
IIb	**HDAC-6**	miR-762	+	3.00
IV	**HDAC-11**	miR-762	+	3.00
		miR-1260b	+	1.97

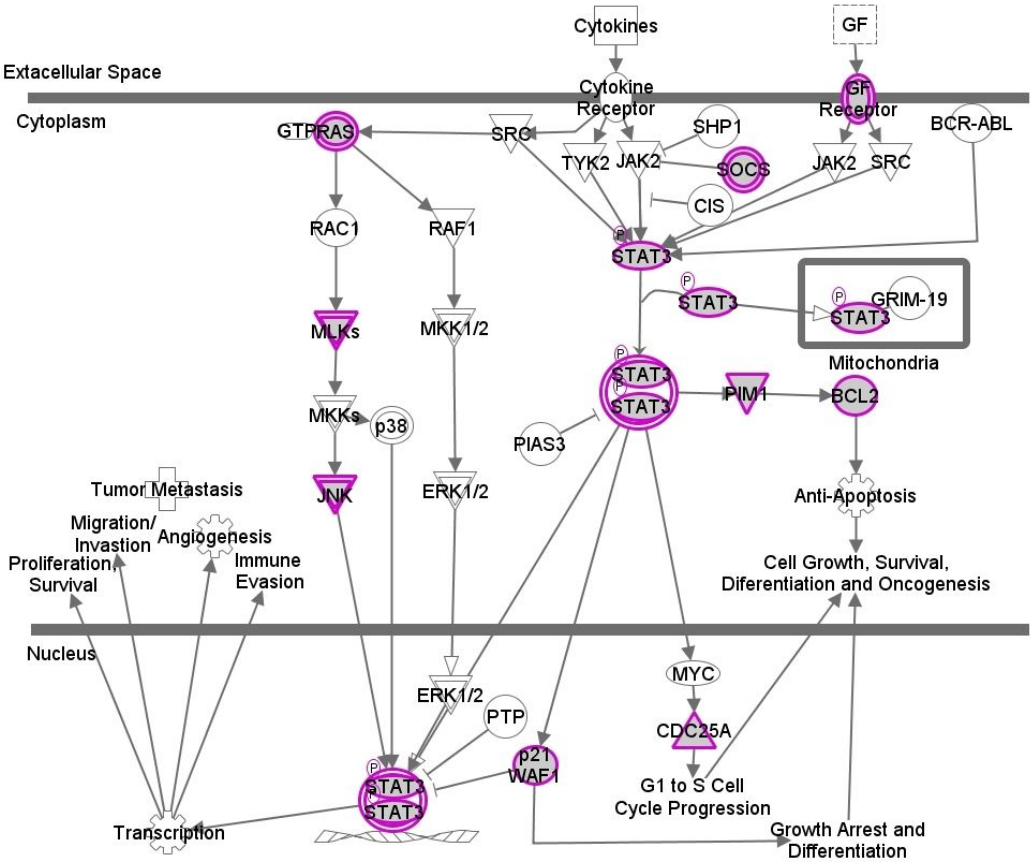

Pathway	miRNA	Up / down regulation	Mean FC at 48 h	mRNA targets
STAT3	miR-21-5p	+	2.8	BCL2, **BMPR2**, **CDC25A**, **CDKN1A**, MAPK10, SOCS5, SOCS6, STAT3, TGFBR2
	miR-193b-3p	+	1.5	KRAS, MAPK10, TGFBR3
	miR-223-3p	-	4.7	FGFR2, IGF1R, RRAS2, TGFBR3
	miR-4284	-	1.8	MAP3K9
	miR-4286	-	1.6	PIM1

Figure 3.8 (A) Schematic representation of the STAT3 pathway, with constituents of which the mRNAs are targeted *(outlined in purple)* **by differentially-expressed miRs at 48 hours of hPH culture, compared to baseline at 0 hours. (B) Pathway mRNA targets of differentially-expressed miRs at 48 hours of hPH culture.**

mRNA targets highlighted in bold represent miR-mRNA interaction that have been experimentally observed and mRNA targets in normal font represent predicted miR-mRNA interaction with high confidence (as defined by TargetScan). All mean fold change (FC) of miRs between 0 and 1 were transposed to a range of -1 until -infinity. The direction of change of expression is indicated by the symbol + for up-regulation, and – for down-regulation. For gene name abbreviations, please see http://www.ncbi.nlm.nih.gov/gene/.

CHAPTER 4

MICRORNA-122: A NOVEL HEPATOCYTE-ENRICHED *IN VITRO* MARKER OF DRUG-INDUCED HEPATOTOXICITY

4.1 INTRODUCTION

Despite the development of various hepatic models for use in screening for adverse effects of new drugs and to aid mechanistic understanding of hepatotoxicity, drug-induced liver injury (DILI) in humans remains a significant cause of patient morbidity and mortality, and confers a major burden to the pharmaceutical industry and the regulatory authorities (Davies *et al.*, 2010; Olsen and Whalen, 2009). This is partly due to the major limitations of currently available hepatic models in recapitulating *in vivo* functional and metabolic capabilities of the human hepatocyte, most notably the expression of drug metabolising proteins such as cytochrome-P450 (CYP) enzymes, and drug transporters which are important for a mechanistic understanding of drug-induced toxicity (Godoy *et al.*, 2013). The most metabolically active *in vitro* hepatic model is freshly-isolated human primary hepatocytes, although a myriad of issues limit their application in the *in vitro* study of drug-induced toxicity and safety screening (Kia *et al.*, 2013). Human primary hepatocytes are not readily available, they are expensive, exhibit large donor variations, and rapidly lose their functional phenotype over time in *in vitro* culture, leading to reduced expression of the majority of CYP enzymes (Godoy*, et al.*, 2013; Rodriguez-Antona *et al.*, 2002; Rowe *et al.*, 2010).

A potential new hepatic model is the use of human pluripotent stem cells to generate hepatocytes *in vitro* (Baxter *et al.*, 2010; Bone *et al.*, 2011; Brolen *et al.*, 2010). Directed differentiation of human pluripotent stem cells into hepatocytes, typically called hepatocyte-like cells (HLCs), with a mature functional phenotype, could in theory provide a readily available source of metabolically competent cells for use in drug screening (Greenhough *et al.*, 2010; Yildirimman *et al.*, 2011). However, the differentiation efficiency of HLCs from human pluripotent stem cells can be variable, which is believed to be mainly due to differences of the differentiation protocols being employed and the propensity of the selected pluripotent stem cell line to differentiate towards a hepatic lineage (Baxter*, et al.*, 2010; Bock *et al.*, 2011). The differentiation efficiency of HLCs from a starting culture of undifferentiated pluripotent stem cells can range from 9-90%, as determined by the percentage of cells in the

culture that express the hepatocyte protein marker albumin (Hay *et al.*, 2008; Rashid *et al.*, 2010; Shiraki *et al.*, 2008). Therefore, for the application of HLCs as an *in vitro* model for drug screening and toxicology, this heterogeneity of maturity needs to be accounted for.

Another approach taken to develop a relevant and functional hepatic model includes efforts to better emulate the *in vivo* liver tissue environment that mimics complex multicellular and cell-matrix interactions. Examples include the co-culture of primary hepatocytes with non-parenchymal cells such as hepatic sinusoidal endothelial cells and fibroblasts, in either conventional two dimensional (2D) platforms or as three dimensional (3D) spheroids (Bader *et al.*, 1996; Bhatia *et al.*, 1999). More recently, a complex 3D quasi-liver "bud" was also successfully engineered from a co-culture of human pluripotent stem cell-derived HLCs with non-hepatocyte cell lines, and this showed promising functional improvement of the HLCs compared to conventional 2D culture (Takebe *et al.*, 2013).

However, for the application of HLC cultures with heterogeneous maturity and complex hepatic co-culture models in the study of drug-induced toxicity, a hepatocyte-specific marker of hepatocyte perturbation is needed to discriminate non-specific cellular toxicity contributed by non-hepatocyte cell types present within the model. This is currently lacking as the cytotoxicity assays routinely used in *in vitro* toxicology research depend on intracellular molecules which are ubiquitously present in all eukaryotic cell types. Parameters commonly used in cytotoxicity assays include the release of the stable cytoplasmic molecule lactate dehydrogenase (LDH) from necrotic cells, or change in the metabolic activity of viable cells, by either relative quantification of intracellular adenosine triphosphate (ATP), or reduction of substrates such as tetrazolium salts by cellular oxidoreductase enzymes using the MTT or MTS colorimetric assays (Lappalainen *et al.*, 1994; Mosmann, 1983; Slater, 2001). These intracellular molecules and enzymes that are used in these assays are not cell-specific, and therefore the parameters described above to measure toxicity and cell viability can only be applied accurately in models incorporating homogeneous cultures. Therefore, in the emerging models of DILI which take the field beyond assaying simple single hepatocytes or

HLCs, current toxicological endpoints largely reflect the *global* toxicity of the different cell types in the culture, and are not able to specifically measure only the perturbation of the hepatocytes or HLCs.

In this chapter, the concept of using microRNA-122 (miR-122) as a potential hepatocyte-enriched marker of toxicity was explored. MicroRNAs (miRs) are highly-conserved small non-coding RNAs responsible for translational regulation of messenger RNAs (Chen and Rajewsky, 2007; Lagos-Quintana *et al.*, 2001). Some miR species demonstrate high tissue enrichment, with miR-122 shown to be highly enriched and abundant in adult and foetal liver (Liu *et al.*, 2009; Sempere *et al.*, 2004), constituting approximately 70% of the total mouse liver miR content in one of the earliest studies (Lagos-Quintana *et al.*, 2002). miR-122 is involved in hepatic differentiation via a feedback loop with the liver-enriched transcription factor network (Laudadio *et al.*, 2012), and is also highly upregulated in human embryonic stem cell-derived hepatocytes compared to undifferentiated stem cells and early endodermal lineage cells (Kim *et al.*, 2011). For these reasons, several studies have evaluated miR-122 in the plasma as a circulating hepatocyte-specific biomarker of various liver injuries, including DILI in rodents and humans caused by drugs such as acetaminophen and heparin (Antoine *et al.*, 2013; Harrill *et al.*, 2012; Starkey Lewis *et al.*, 2011; Wang *et al.*, 2009). Therefore, miR-122 could potentially be used as a bridging biomarker to translate findings from *in vitro* experiments to *in vivo* experiments and the clinical setting. However, to date, the utility of miR-122 as an *in vitro* hepatocyte-enriched marker of drug-induced toxicity has not been explored.

To explore the potential application of miR-122 as a hepatocyte-enriched biomarker in hepatic models, the prototypical hepatotoxicants acetaminophen and diclofenac were chosen as model compounds. Acetaminophen overdose which causes centrilobular hepatic necrosis (Prescott, 1980) remains a major clinical cause of acute liver failure (Lee, 2004; Litovitz *et al.*, 2002). When ingested, acetaminophen typically undergoes phase II drug metabolism to produce non-toxic conjugates which are then eliminated (James *et al.*, 2003).

However, acetaminophen-induced hepatotoxicity has been shown to be caused by reactive metabolites due to concomitant bioactivation of the analgesic by phase I cytochrome-P450 (CYP) enzymes, rather than direct effects of the parent compound (James*, et al.*, 2003; Mitchell *et al.*, 1973). The reactive metabolite has been identified as *N*-acetyl-*p*-benzoquinone imine (NAPQI) and is produced from the oxidation of acetaminophen by CYP2E1, 1A2, 3A4 and 2A6 (Chen *et al.*, 1998; Patten *et al.*, 1993; Thummel *et al.*, 1993). In cases of acetaminophen overdose, the hepatic reserve of glutathione which detoxifies NAPQI, is rapidly depleted, resulting in formation of acetaminophen-protein adducts which are then postulated to perturb key cellular proteins (Nelson, 1990). In contrast, diclofenac has been linked to rare, but clinically-relevant idiosyncratic hepatotoxicity with a predominantly hepatocellular pattern of injury (Banks *et al.*, 1995; de Abajo *et al.*, 2004). Similar to acetaminophen, metabolic activation of diclofenac resulting in reactive metabolites and protein adducts which subsequently lead to diclofenac-induced liver injury is likely to be a factor (Aithal, 2011). The parent drug is metabolised by CYP2C9, 2C8, 3A4 and 2C19 while the accumulation of the reactive metabolites is also affected by the expression of the phase III efflux transporter multidrug resistance protein 2 (Aithal, 2011; Yan *et al.*, 2005). As acetaminophen and diclofenac-induced toxicity largely occurs in the event of bioactivation by drug metabolising enzymes which are predominantly expressed in hepatic tissue, both compounds have been widely adopted as model hepatotoxicants to evaluate the functional relevance of preclinical hepatic models being developed for drug-induced toxicity (Brolen*, et al.*, 2010; Leite *et al.*, 2012; Szkolnicka *et al.*, 2014).

Therefore, the hypothesis to be addressed in this chapter is that miR-122 can be utilised as a hepatocyte-enriched *in vitro* marker of drug-induced toxicity. We aimed to address this using human primary hepatocytes and human pluripotent stem cell-derived hepatocytes – hepatic models with high levels of intracellular miR-122, treated with the model hepatotoxicants and aimed to compare the sensitivity of the miR-122 toxicity assay in

comparison with conventional cytotoxicity assays in detecting drug-induced hepatocyte perturbation.

4.2 MATERIALS AND METHODS

4.2.1 Human subjects and tissue

Human liver resections from surgical waste tissue were obtained from adult patients undergoing hepatobiliary surgery with full informed consent and ethical approval from the relevant institutional review boards (National Research Ethics Service REC reference: 11/NW/0327).

4.2.2 Human primary hepatocyte isolation and culture

This work was and is an ongoing collaborative effort within the MRC Centre for Drug Safety Science, University of Liverpool. Human primary hepatocytes were isolated using a previously described method with minor modifications (LeCluyse *et al.*, 2005). Briefly, liver resections were received as surgical waste tissue immediately post-resection (Aintree University Hospital, Liverpool, United Kingdom) and transferred on ice in N-(2-Hydroxyethyl)piperazine-N′-(2-ethanesulfonic acid) (HEPES) buffer (10 mM HEPES, 136 mM NaCl, 5 mM KCl, 0.5% (w/v) glucose, pH 7.6) to the laboratory. The liver resection specimens were then perfused with HEPES-buffered saline (HBS) followed by digestion with collagenase A (Roche) or collagenase IV (Sigma-Aldrich) in HBS containing calcium. The suspension containing isolated hepatocytes was then filtered through a nylon gauze and purified by centrifugation twice at 80x g for 5 minutes at 4^{o}C, before the pellet was resuspended in Williams E medium (Sigma-Aldrich). The hepatocytes were then seeded onto collagen-I coated 24-well plates (BD Beckinson) at 2.5 x 10^5 cells/cm^2 and cultured in Williams E medium supplemented with 1% (v/v) insulin-transferrin-selenium (from 100x stock, Life Technologies), 2 mM L-glutamine (Sigma-Aldrich), 10^{-7} M dexamethasone (Sigma-Aldrich) and 1% (v/v) penicillin-streptomycin (Sigma-Aldrich) at 5% CO_2 and 37°C. After 3 hours, non-attached cells were washed away and overlaid with fresh ice-cold medium

containing 0.25 mg/ml of Matrigel (BD Beckinson). The media was replaced the next day at the start of the experiments.

4.2.3 Human cancer cell line culture

The human hepatoma cell lines (HepG2 and HuH7) and the pancreatic cancer cell line (Suit-2) were cultured in Dulbecco's modified Eagle's medium (DMEM) supplemented with 2 mM L-glutamine (Sigma-Aldrich), 10% (v/v) foetal bovine serum (FBS; Life Technologies) and 1% (v/v) penicillin-streptomycin (Sigma-Aldrich) at 5% CO2 and 37°C.

4.2.4 Human pluripotent stem cell (hPSC) culture

The hESC line HUES7 was maintained on mitotically-inactivated murine embryonic fibroblasts (MEFs) as previously reported (Baxter *et al.*, 2009), in KnockOut DMEM (KO-DMEM; Life Technologies) supplemented with 20% (v/v) KnockOut Serum Replacement (KOSR; Life Technologies), 0.1 mM non-essential amino acids (NEAA), 2 mM L-glutamine (Life Technologies), 1% (v/v) penicillin-streptomycin (Life Technologies), 1% (v/v) insulin-transferrin-selenium (from 100x stock, ITS; Life Technologies), 0.1 mM beta-mercaptoethanol (Life Technologies) and 4 ng/ml fibroblast growth factor 2 (FGF2; PeproTech). HUES7 hESCs in 96-well plate format were kindly gifted by Professor Hanley, University of Manchester as part of collaboration within the Stem Cells for Safer Medicines (SC4SM) consortium.

The human embryonic stem cell line (hESCs) Shef-3 was maintained on embryonic stem cell-qualified Matrigel (BD Beckinson) -coated plates as previously reported (Bone*, et al.*, 2011), in mTeSR1 (STEMCELL Technologies). Shef-3 hESCs in 96-well plate format were kindly gifted by Professor Tosh, University of Bath as part of collaboration within the Stem Cells for Safer Medicines (SC4SM) consortium.

Cell suspensions of human induced pluripotent stem cells, ChiPSC-18 (DEF-hiPSC™, Cellectis AB) were purchased and plated at a density of 70000 cells/cm^2 onto a proprietary matrix as per protocol, and maintained using a proprietary feeder-free and defined culture system, DEF-CS 500 (Cellectis AB). ChiPSC-18 were generated using polycistronic retrovirus technology (Edsbagge, 2014 – personal communication) based on the transduction of the transcription factors Oct3/4, Sox2, Klf4 and c-Myc (Takahashi *et al.*, 2007).

4.2.5 Differentiation of hPSCs into hepatocyte-like cells (HLCs)

4.2.5.1 Directed differentiation of HUES7 towards HLCs

The differentiation of HUES7 hESCs towards definitive endoderm was commenced 3-4 days post-passage onto fresh MEFs in Roswell Park Memorial Institute (RPMI) media (Sigma-Aldrich) supplemented with 0.5% (v/v) FBS (Life Technologies), 100 ng/ml activin A (AA, PeproTech) and 25 ng/ml Wnt-3a (R&D Systems) for 48 hours, followed by 0.5% (v/v) FBS (Life Technologies) and 100 ng/ml AA (PeproTech) without Wnt-3a for a further 48 hours. Hepatic specification was then carried out for 6 days in Hepatocyte Culture Medium (HCM; Lonza) supplemented with 20 ng/ml bone morphogenetic protein 2 (BMP2; R&D Systems) and 30 ng/ml fibroblast growth factor 2 (PeproTech). For the hepatocyte maturation stage, the HLCs were cultured in HCM supplemented with 20 ng/ml hepatocyte growth factor (HGF, PeproTech) for 5 days followed by HCM supplemented with 10 ng/ml oncostatin M (R&D Systems) and 10^{-7} M dexamethasone (Sigma-Aldrich) for a further 15 days. Differentiation of HUES7-derived HLCs in 96-well plate format were performed in the laboratory of Professor Hanley, University of Manchester, who kindly gifted us the material as part of collaboration within the Stem Cells for Safer Medicines (SC4SM) consortium.

4.2.5.2 Directed differentiation of Shef-3 towards HLCs

The differentiation of Shef-3 hESCs towards hepatocyte-like cells (HLCs) was performed using a 3-stage differentiation protocol. Briefly, to induce differentiation to definitive endoderm (DE), Shef-3 hESCs were cultured in RPMI media (Life Technologies) containing 100 ng/ml AA (PeproTech) and 2 µM 1m for 24 hours, followed by 100 ng/ml AA and 0.2% (v/v) HyClone FBS (Fisher Scientific) for 48 hours. DE cells were then passaged as single cells with Accutase (STEMCELL Technologies) onto Matrigel (BD Beckinson) -coated 96-well plates at a density of 18,000 cells/well. Hepatic specification was carried out for 7 days in KO-DMEM supplemented with L-glutamine (Life Technologies), 0.5% (v/v) penicillin-streptomycin (Life Technologies), 1 mM NEAA (Life Technologies), 2% (v/v) KnockOut Serum Replacement (Life Technologies), 10 ng/ml HGF (PeproTech) and 10 ng/ml fibroblast growth factor 4 (FGF4; PeproTech). To allow for maturation, HLCs were cultured for 14 days in Williams E medium supplemented with L-glutamine (Life Technologies), 0.5% (v/v) penicillin-streptomycin, 1% (v/v) ITS (from 100x stock, Life Technologies), 10 ng/ml oncostatin M (PeproTech), 10 ng/ml HGF (PeproTech), 10 ng/ml FGF4 (PeproTech), 10 ng/ml epidermal growth factor (PeproTech) and 10^{-7} M dexamethasone (Sigma-Aldrich). During hepatic induction and maturation, medium was replenished every other day. Differentiation of Shef-3-derived HLCs in 96-well plate format were performed in the laboratory of Professor Tosh, University of Bath, who kindly gifted us the material as part of collaboration within the Stem Cells for Safer Medicines (SC4SM) consortium.

4.2.5.3 Commercially-sourced HLCs

ChiPSC-18-derived HLCs were purchased in plated 96-well plate formats (HEP-104-0096, Cellectis AB) which was received at Day 23 of differentiation and maintained with proprietary media, HEP-104-SUP (Cellectis AB).

4.2.6 Cytotoxicity assays

Human primary hepatocytes, HLCs and undifferentiated human pluripotent stem cells were treated for up to 24 hours with acetaminophen (0 mM – 30 mM, Sigma-Aldrich) and diclofenac (0 mM – 1 mM, Sigma-Aldrich), which were dissolved and diluted to the final test concentrations in the appropriate culture media. The range of concentrations used in the cytotoxicity assays were chosen to incorporate the concentration of 30 times the reported efficacious concentration (C_{max}) for each compound in humans, which was suggested to be the optimal drug concentration for *in vitro* prediction of human toxicity (O'Brien *et al.*, 2006).

The human primary hepatocytes and the hiPSCs (ChiPSC-18) were treated with the test compounds 24 hours after seeding, while for the ChiPSC-18-derived HLCs, cytotoxicity assays were started on Day 31 of differentiation.

4.2.6.1 LDH activity assay

For the human primary hepatocyte samples, both the cellular lysates and media at the end of the experiments were collected and assayed separately for LDH using the Cytotoxicity Detection Kit (Roche). Briefly, the media was first collected and the cells lysed in medium containing 2% (v/v) Triton X-100 (Sigma-Aldrich). Both the media and cellular lysate were then stored in -80°C immediately. The level of LDH activity (a surrogate for the quantity of LDH molecules) in each sample was determined separately as per the manufacturer's instructions and the percentage of LDH activity in the media was expressed as a percentage of the combined total intracellular and extracellular LDH activity in the well.

4.2.6.2 Intracellular ATP assay

The quantification of intracellular ATP in HLCs and undifferentiated human pluripotent stem cells was performed using the CellTiter-Glo Luminescent Cell Viability Assay (Promega). Following dosing of the cells with acetaminophen and diclofenac for 24 hours, the media was collected first for miR-122 analysis and the remaining adherent cells used for ATP measurement. Briefly, 50 µL of Dulbecco's Phosphate Buffered Saline (Life Technologies) was added to each well followed by 50 µL of CellTiter-Glo reagent which was prepared according to the manufacturer's protocol. The contents were mixed in a plate shaker for 2 minutes to induce cell lysis and then incubated for 10 minutes at room temperature. The cellular lysate was then transferred to an opaque 96-well plate and the luminescent signal measured using a Varioskan Flash spectral scanning multimode reader (Thermo Scientific).

4.2.7 Total RNA extraction

The purification of total RNA containing the miR fraction from media or lysate samples was performed using the miRNeasy mini kit (Qiagen), as per the manufacturer's instructions, with some modifications. Briefly, a typical 40 µL of media or lysate diluted in RNAse-free water up to a total volume of 200 µL was used for RNA purification in each experiment. Following addition of 700 µL of QIAzol (Qiagen) to the diluted media or lysate, and incubation at room temperature for 10 minutes, 5 µL of a 5 fM solution of cel-lin-4 (Integrated DNA Technologies) was added as a spiked-in exogenous non-human miR to monitor for the efficiency of the miR extraction process by evaluation of the amount of recovered cel-lin-4 in each sample. 140 µL of chloroform was then added and the rest of the protocol was as per the manufacturer's instruction. The total RNA containing the miR fraction was eluted with RNase-free water and quantification performed using the NanoDrop spectrophotometer (Thermo Scientific). The fully automated platform QIAcube (Qiagen) was used in the extraction of total RNA containing miRs in the HLC media samples.

4.2.8 Real-time quantitative RT-PCR (qRT-PCR) analysis of miR-122

MiR-122 levels in each sample were determined using the TaqMan gene expression assay (Applied Biosystems) according to the manufacturer's protocol. Briefly, a reverse transcription (RT) cocktail mixture containing specific stem-loop RT primers for each target miR species (Applied Biosystems) was prepared as instructed and added to 5 µL of the total RNA elute for complementary DNA (cDNA) synthesis in a total volume of 15 µL using the GeneAmp PCR System 9700 thermal cycler (Applied Biosystems). 1.33 µL of cDNA was then mixed with a PCR mixture containing specific stem-loop PCR primers in a total volume of 20 µL. Real-time PCR was then performed in duplicates with the ABI Prism 7000 or ViiA 7 Real-Time PCR instruments (Applied Biosystems) using a 2-step thermal cycling protocol of 95°C for 10 minutes followed by 40 cycles of 95°C for 15 seconds and 60°C for 60 seconds. C_t values were determined using the fluorescent signal produced from the TaqMan probes. The number of copies of miR-122 in each PCR reaction was quantified using the absolute quantification method with a standard curve of cel-lin-4 cDNA used as a surrogate for miR-122 cDNA, due to its similar nucleotide length and to avoid contamination of PCR reactions with synthetic miR-122. The total number of copies of miR-122 in each sample was then extrapolated from this figure. For the human primary hepatocyte samples, both the total copies of miR-122 in the cellular and media components were determined separately, and the percentage of miR-122 in the media was expressed as a percentage of the combined total of intracellular and extracellular miR-122 copies in the well, analogous to the LDH cytotoxicity assay.

4.2.9 Statistical analysis

For comparison of the intracellular miR-122 level between models, the mean and the standard error of the mean of each model was determined. For comparisons between each model with human primary hepatocytes, the Mann-Whitney non-parametric test was used,

while the Dunn's multiple comparison test was used for comparison of more than two models. For the cytotoxicity assays, the unpaired t-test was used for pairwise comparisons, while correlation analyses were performed using the Pearson correlation test. For all tests, $p < 0.05$ was considered significant. Statistical analyses were performed using GraphPad Prism 6 (GraphPad Software).

4.3 RESULTS

4.3.1 Intracellular miR-122 levels reflect the physiological relevance of human hepatic models

Freshly-isolated human primary hepatocytes are currently considered to be the most physiologically-relevant single cell *in vitro* hepatic model, particularly due to their functional recapitulation of the *in vivo* metabolic processes such as phase I and II enzyme activities, glucose metabolism and ammonia detoxification (Godoy*, et al.*, 2013; Kia*, et al.*, 2013). Therefore, to investigate the relevance of miR-122 as a potential biomarker in *in vitro* hepatic models, we first performed quantification of the intracellular level of miR-122 among the commonly used hepatic models of liver cancer cell lines (HepG2 and HuH7) and human pluripotent stem cell-derived HLCs in direct comparison to freshly-isolated and plated human primary hepatocytes from adult donors.

We found that the mean intracellular miR-122 level normalised to the amount of total RNA used for qRT-PCR, is the highest in human primary hepatocytes, with a 9- to 41-fold lower expression in hPSC-derived HLCs, 410-fold lower in HepG2 and 2600-fold lower in HuH7 (Figure 4.1). Human primary hepatocytes also expressed significantly more miR-122 compared to undifferentiated hPSCs (3900- to 78000-fold lower) and the pancreatic cancer cell line Suit2 (17000-fold lower), which was included as part of the comparison as a negative control for non-hepatic cells of the endodermal lineage.

Overall, the results in Figure 4.1 confirm that miR-122 is highly enriched in human primary hepatocytes and provide a quantitative comparison of intracellular miR-122 among the most relevant human hepatic *in vitro* models currently used.

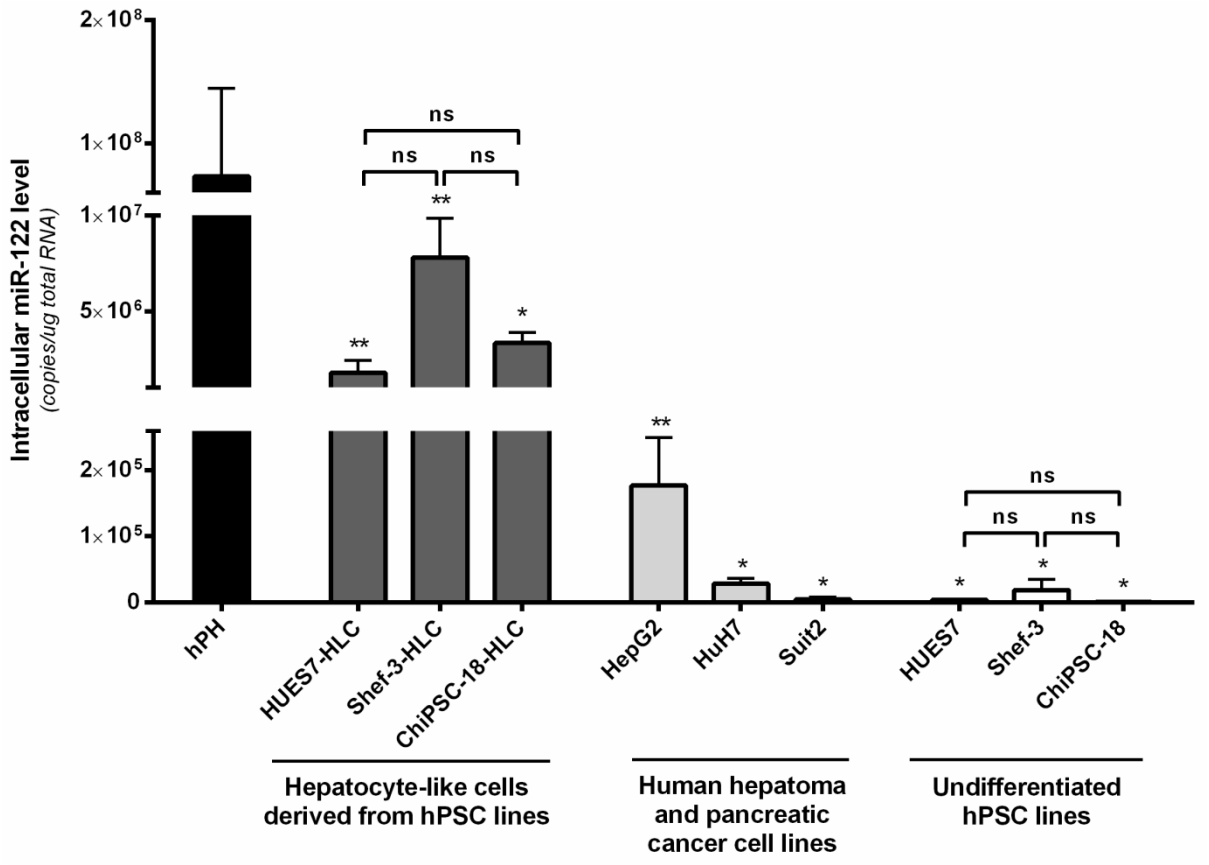

Figure 4.1 Quantitative comparison of intracellular miR-122 between human hepatic models.

Data is presented as the mean total number of copies of intracellular miR-122 per µg of total RNA +/- standard error of the mean (SEM) for human primary hepatocytes, hPH (n = 6 different donors), HLCs differentiated from HUES7 and Shef-3 hESC lines (n = 3 separate differentiation experiments each), HLCs differentiated from ChiPSC-18 hiPSC line (n = 3 separate differentiation experiments), HepG2 (n = 4 independent experiments), HuH7 (n = 3 biological replicates from one experiment), Suit2 (n = 3 biological replicates from one experiment) and undifferentiated human pluripotent stem cell (hPSC) lines (n = 3 independent experiments each). * denotes $p < 0.05$, ** denotes $p < 0.01$, ns denotes non-significance.

4.3.2 miR-122 expression increases during directed differentiation of hESCs and hiPSCs towards HLCs

The mean fold increase of miR-122 in HLCs differentiated from their respective hESC lines was similar (420- and 430- fold change respectively), in contrast to the varying basal levels of miR-122 in the undifferentiated hESCs, while in the HLCs differentiated from the hiPSC line (ChiPSC-18), the mean miR-122 level was 3500-fold higher (Figure 4.1). There was also no significant difference between the mean intracellular miR-122 levels among the HLCs derived from the two hESC lines and ChiPSC-18, or between the low levels of mean intracellular miR-122 detected in the undifferentiated pluripotent stem cell lines.

4.3.3 The relative level of miR-122 detected in the media correlates with the extracellular release of LDH in drug-induced toxicity of human primary hepatocytes

To explore the potential of miR-122 as an *in vitro* marker of drug-induced cellular perturbation, we first compared its performance against the conventional marker of cellular necrosis, LDH, using human primary hepatocytes. We chose to validate miR-122 against LDH, as the levels of LDH and miR-122 can be readily measured in both the cellular lysate and media component, which allows for direct comparison of the sensitivity of both markers in detecting drug-induced toxicity.

Dose-response experiments using human primary hepatocytes treated with the known hepatotoxicants acetaminophen and diclofenac (Figure 4.2A and 4.2B) were performed. The LDH activity in the media and cellular fraction of each well were separately measured to calculate the relative percentage of total LDH activity in the media. In parallel experiments, using the same donor-batch of human primary hepatocytes, we also quantified the number of copies of miR-122 in the media and cellular fraction in response to acetaminophen and diclofenac, and calculated the relative percentage of total miR-122 in the media (Figure 4.2A and 4.2B). We found that the level of miR-122 increased in the media with increasing

concentrations of acetaminophen and diclofenac, which paralleled the extracellular release of intracellular LDH, with significant levels of both molecules detected in the media at the maximal concentrations of acetaminophen and diclofenac used in this study (Figure 4.2A and 4.2B). By plotting the paired values of each biomarker obtained from the experiments using various concentrations of acetaminophen and diclofenac in a scatter graph, we confirmed that there was a high positive correlation between the levels of LDH and miR-122 in the media (Pearson's correlation coefficient, $r = 0.993$, $p < 0.0001$, 95% CI 0.974 to 0.998) (Figure 4.2C). This suggests that using the model of human primary hepatocytes, miR-122 is equivalent to LDH when used as an *in vitro* biomarker of drug-induced toxicity.

We also performed a time-course experiment on the hepatocytes treated with diclofenac over 24 hours and observed comparable trends in both biomarkers in the media with a concentration of 1 mM (Figure 4.3A and 4.3B). Increased levels of both biomarkers were detected in the media after 2 hours, although significant levels were only detected at 24 hours using either biomarker (Figure 4.3A and 4.3B). This suggests miR-122 is as sensitive as LDH when used as a toxicity marker for human primary hepatocytes but the time-course experiments using diclofenac as the test compound, did not point towards the possibility of miR-122 providing an earlier signal of hepatocyte perturbation compared to LDH.

We also observed that the miR-122 level in the media has a wider dynamic range compared to LDH. In both sets of dose-response experiments, the untreated human primary hepatocytes showed a baseline mean percentage of total LDH in the media at 24 hours of 6.4% and 6.9% respectively, compared to a baseline mean percentage of total miR-122 of 1.8% and 1.4% (Figure 4.2A and 4.2B). When a toxic concentration of 30 mM acetaminophen was used, the mean increase over baseline of LDH in the media was 6.8-fold compared to a higher mean increase of 25-fold for miR-122 (Figure 4.2A). Similarly, human primary hepatocytes treated with 1 mM diclofenac showed a mean increase over baseline of LDH in the media of only 8.9-fold compared to a higher mean increase of 53-fold for miR-122 (Figure 4.2B).

We then sought to simplify the miR-122 assay further and observed that the estimation of the total copies of miR-122 in the media alone is sufficiently predictive of the relative percentage of total miR-122 in the media. It has a wide dynamic range and the denominator of the total number of copies of miR-122 in both the cellular lysates and the media component remained fairly constant throughout the various validation experiments (Figure 4.4 and Figure 4.5). Using the experimental values obtained from the dose-response experiments of hepatocytes treated with various concentrations of acetaminophen and diclofenac, we found a high positive correlation between the mean *percentage* of total miR-122 and the mean *number* of copies of miR-122 in the media (Pearson's correlation coefficient, $r = 0.967$, $p < 0.0001$, 95% CI 0.882 to 0.991) (Figure 4.6A). There was also a similarly high positive correlation between the mean percentage of total LDH activity and the mean number of copies of miR-122 in the media (Pearson's correlation coefficient, $r = 0.945$, $p < 0.0001$, 95% CI 0.810 to 0.985) (Figure 4.6B). Therefore, by absolute quantification of the number of copies of miR-122 in the media alone, the miR-122 assay as a biomarker of toxicity is made simpler without the need to measure the miR-122 level in the cell lysate component. Drug-induced perturbation of the hepatic models can be evaluated using only the media component by relative comparison with the baseline levels of miR-122 in the media.

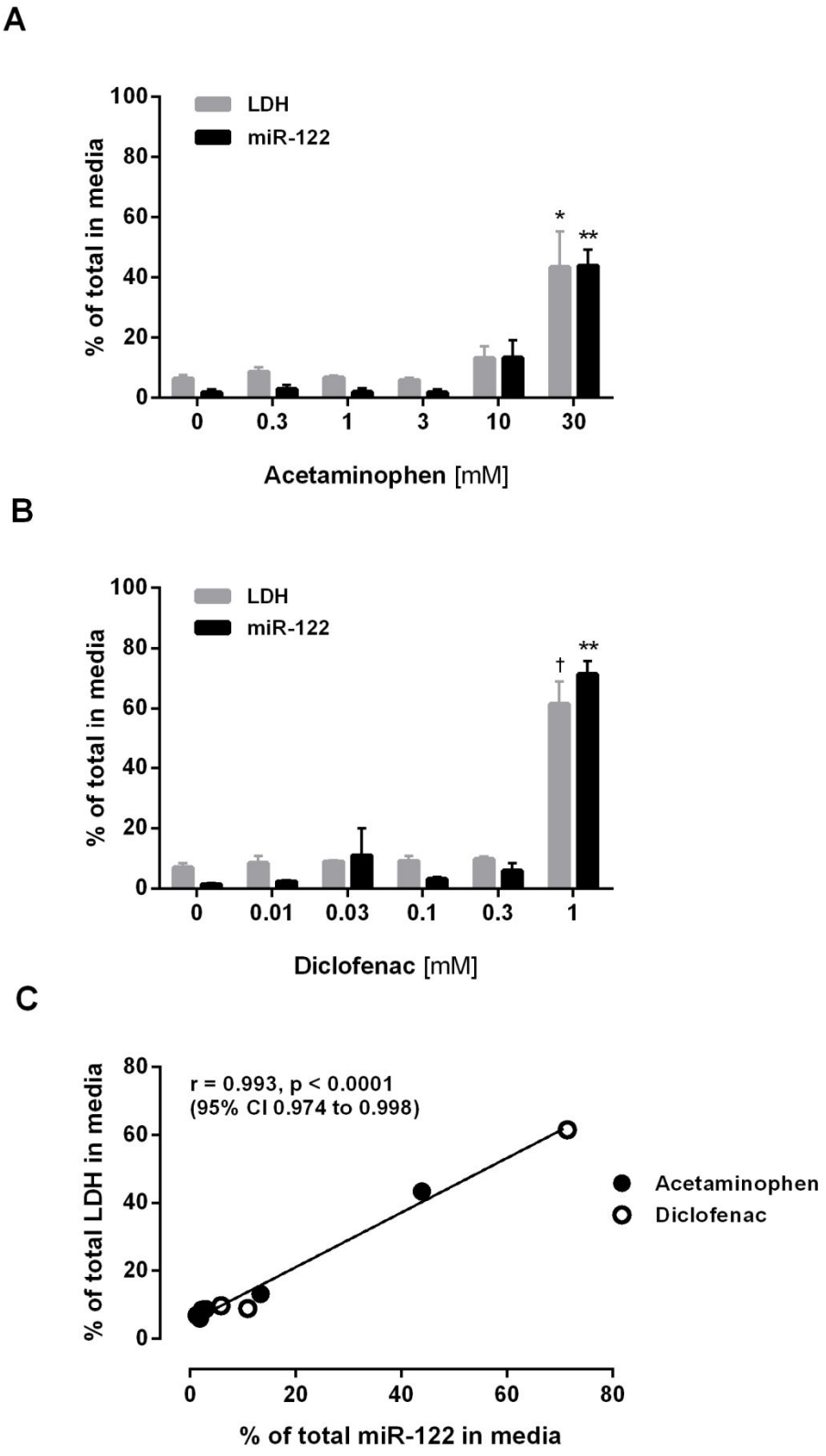

Figure 4.2 Dose-response of human primary hepatocytes after treatment with acetaminophen and diclofenac.

Percentage of total LDH and miR-122 in the media of human primary hepatocytes at 24 hours post-treatment with (A) acetaminophen and (B) diclofenac. Data is presented as the mean +/- SEM from 3 independent experiments using different donors of human primary

hepatocytes. For each donor batch of hepatocytes, parallel experiments were performed in duplicates to compare the sensitivity of LDH and miR-122 as biomarkers. The unpaired t-test was used to compare the statistical significance of the dose-response as measured by the percentage of total marker in the media for each concentration of hepatotoxicant against the respective untreated controls. * denotes $p < 0.05$, ** denotes $p < 0.01$, † denotes $p < 0.0001$. (C) Correlation of the percentage of total LDH in the media against the percentage of total miR-122 in the media, using paired mean values for each condition obtained from experimental results summarised in Figures 2A and 2B. r denotes Pearson's correlation coefficient, CI denotes the confidence interval of r.

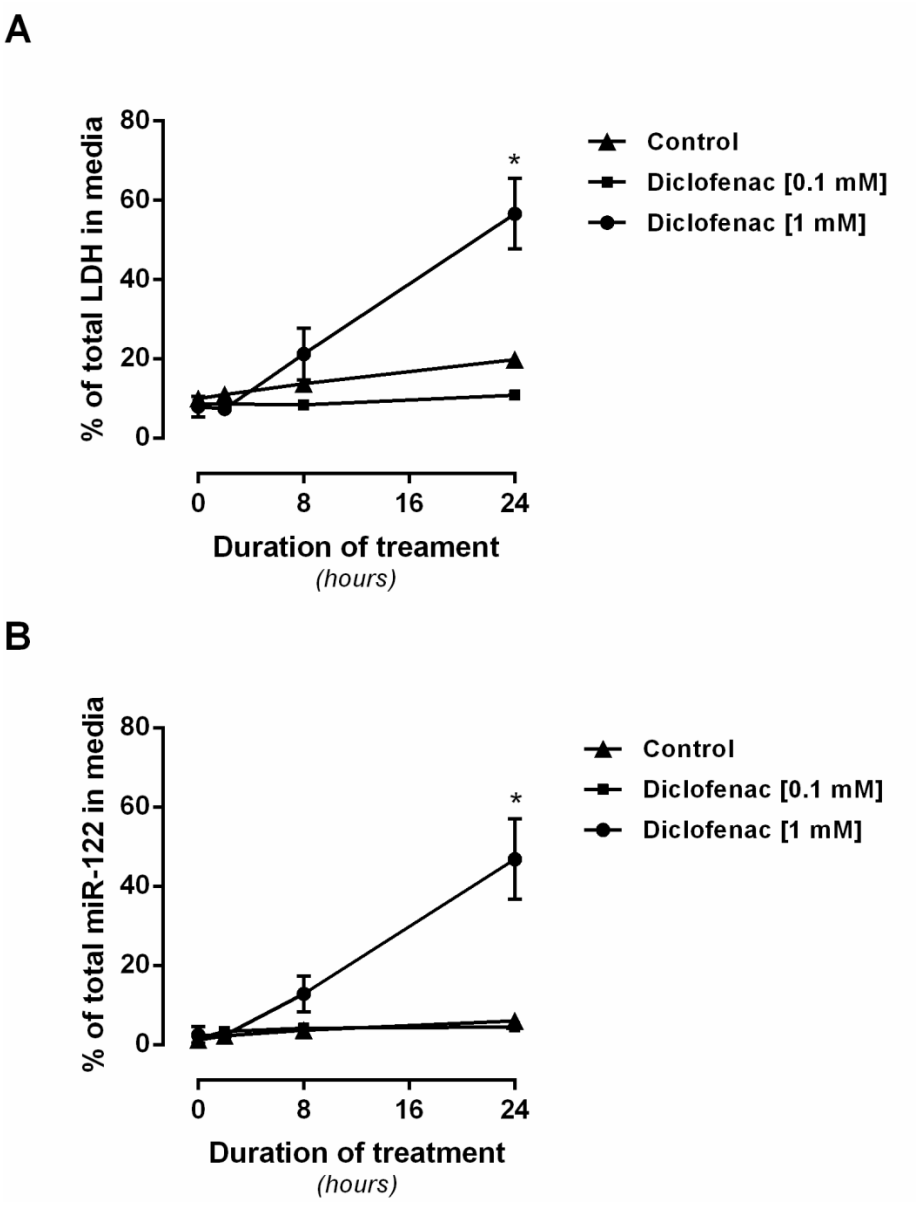

Figure 4.3 Hepatotoxicity of human primary hepatocytes treated with diclofenac up to 24 hours.

Time-course experiment of human primary hepatocytes treated with diclofenac up to 24 hours as measured by (A) percentage of total LDH in the media and (B) percentage of total miR-122 in the media. Data is presented as the mean +/- SEM from 3 independent experiments using different donors of human primary hepatocytes. For each donor batch of hepatocytes, parallel experiments were performed in duplicates to compare the sensitivity of LDH and miR-122 as biomarkers. The unpaired t-test was used to compare the statistical significance of the percentage of total marker in the media at each timepoint compared to untreated controls. * denotes $p < 0.05$

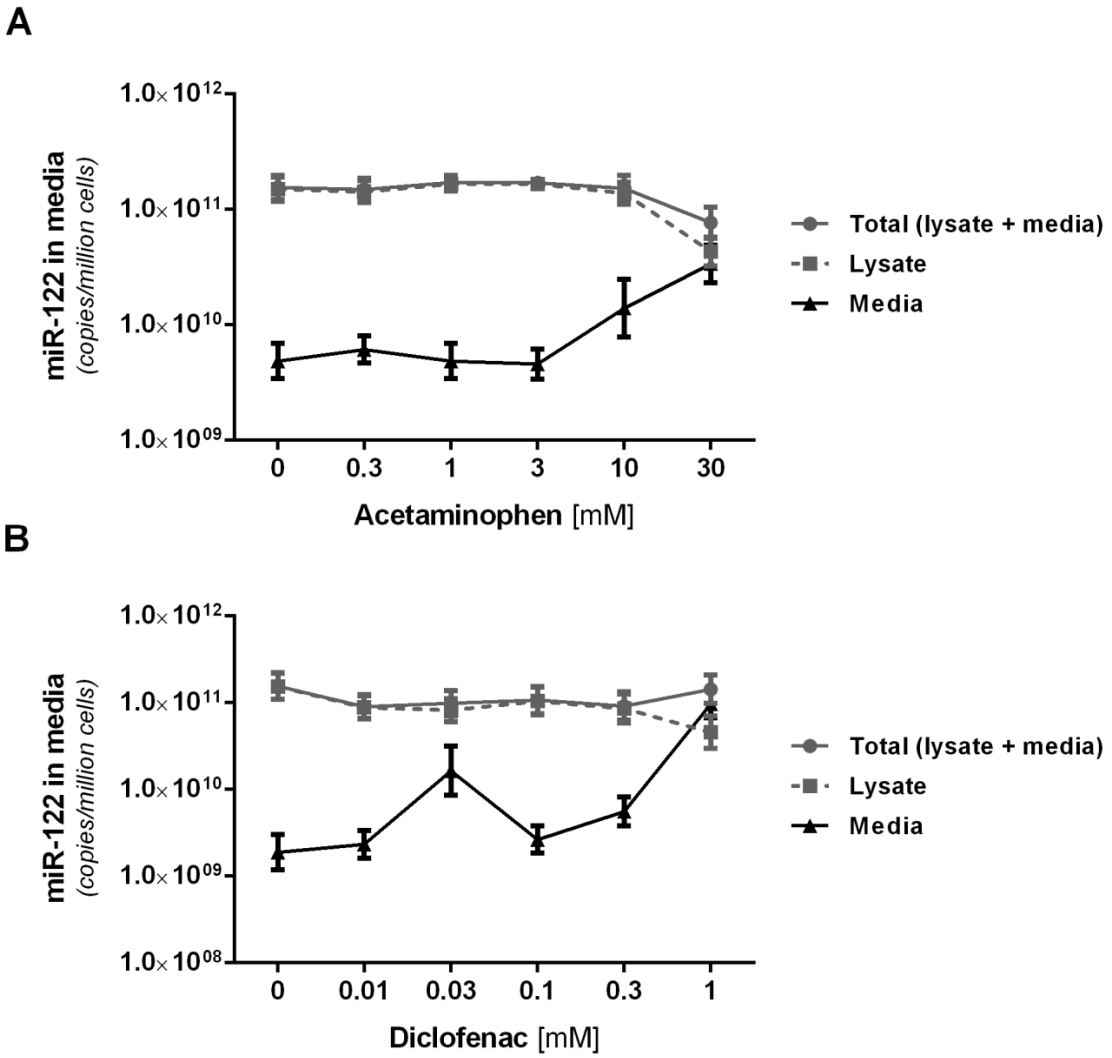

Figure 4.4 Analysis of the change in the number of copies of miR-122 in the lysate and media components of human primary hepatocyte cultures treated with acetaminophen and diclofenac.

Data is presented as the mean +/- SEM of the number of copies of miR-122 in the lysate and/or media components of the dose-response experiments of human primary hepatocytes treated with (A) acetaminophen and (B) diclofenac, from 3 independent experiments using different donors of human hepatocytes. The number of copies of miR-122 estimated in the media and lysates were normalised to the number of hepatocytes in the culture to allow for a direct comparison of absolute quantities of miR-122 in the media with other cell types used for similar cytotoxicity assays. The cytotoxicity assays were performed on hepatocytes plated in 24-well plates at a density of 5 x 10^5 hepatocytes per well. The same raw values from these graphs were used to calculate the percentage of total miR-122 in the media shown in Figure 4.2.

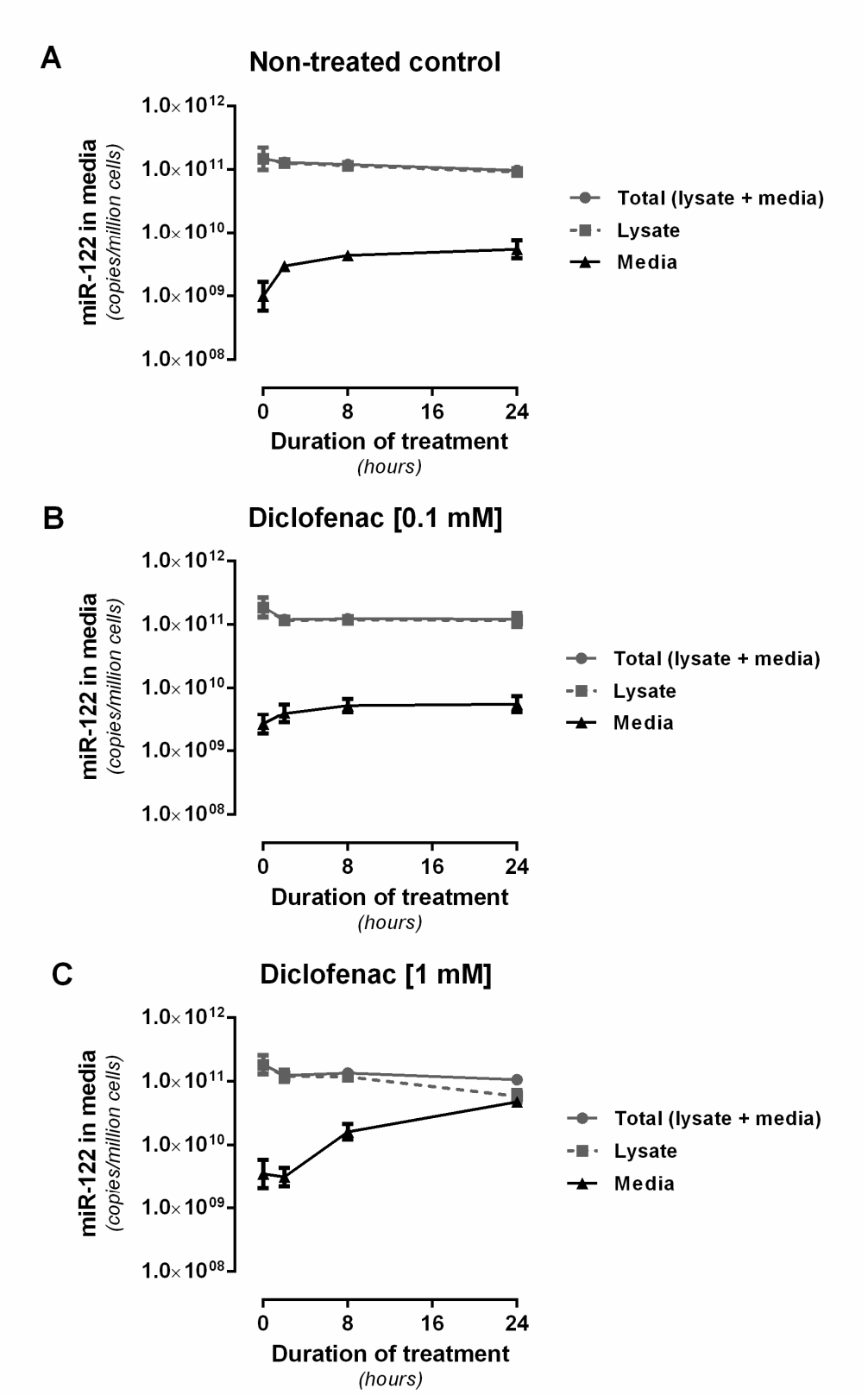

Figure 4.5 Analysis of the change in the number of copies of miR-122 over time in the lysate and media components of human primary hepatocyte cultures treated with non-toxic and toxic concentrations of diclofenac.

Data is presented as the mean number of copies of miR-122 in the lysate and/or media components of the time-course experiments of (A) Untreated human primary hepatocytes, and hepatocytes treated with (B) non-toxic concentration of 0.1 mM diclofenac and (C) toxic concentration of 1 mM diclofenac. Error bars indicate the SEM from 3 independent experiments using different donors of human primary hepatocytes. The same raw values from these graphs were used to calculate the percentage of total miR-122 in the media shown in Figure 4.3.

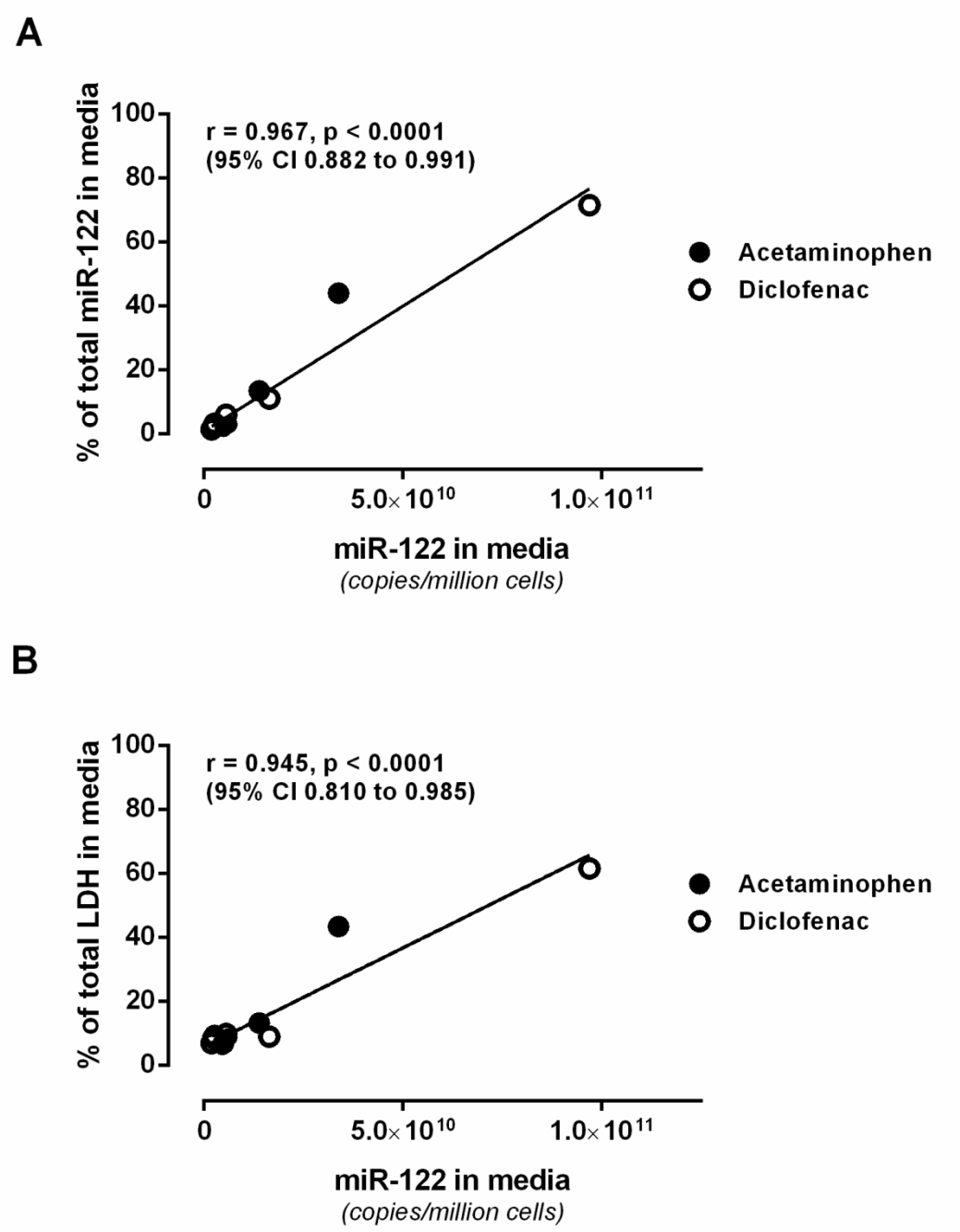

Figure 4.6 Correlation between absolute quantification of miR-122 copies in the media and the relative percentage levels of miR-122 and LDH in the media of human primary hepatocytes treated with acetaminophen and diclofenac

Experimental values from the dose-response experiments of human primary hepatocytes treated with acetaminophen and diclofenac for 24 hours (Figure 4.2) were used to examine the correlation of mean number of copies of miR-122 with (A) mean percentage of total miR-122 and (B) mean percentage of total LDH, in the media. r denotes Pearson's correlation coefficient, CI denotes the confidence interval of r.

4.3.4 The level of miR-122 in the media reflects hepatocyte-specific drug-induced toxicity in hiPSC-derived HLCs

We then explored the use of miR-122 in complex human hepatic models which may not be homogeneous such as cultures of HLCs, where the differentiation efficiency can be variable and not 100% predictable (Baxter*, et al.*, 2010; Kia*, et al.*, 2013). We hypothesised that the hepatocyte-enriched expression of miR-122 could be used to detect selectively drug-induced perturbation of the HLCs, without concomitant measurement of cellular toxicity of other non-hepatocyte cells present in the culture, as is the case with other simple cellular markers of toxicity such as LDH and ATP, and others used in multiparametric high content screening platforms (Rausch, 2006).

The use of miR-122 as an *in vitro* biomarker in hiPSC-derived HLCs (ChiPSC-18-derived HLCs) was explored using the same hepatotoxicants (acetaminophen and diclofenac), and compared against the sensitivity of intracellular ATP quantification by multiplexing both assays in the same experiments. We chose to use the intracellular ATP assay instead of the LDH activity assay to compare against the miR-122 assay for the cytotoxicity experiments utilising HLCs, as the much smaller volume of media available for each culture of HLCs (100 uL total volume per well in a 96-well plate format) did not allow for sufficient material for both extraction of miRs and quantification of the LDH activity in the media. However, the intracellular ATP assay has been separately validated by our group for assessment of drug-induced hepatocyte perturbation, using different donors of freshly-isolated adult human primary hepatocytes treated with a similar dose range of acetaminophen and diclofenac (n = 8 and n = 6 respectively). The endpoint of change in intracellular ATP level was confirmed to significantly correlate with the percentage of total LDH activity in the media, percentage of total miR-122 in the media and the number of copies of miR-122 per million cells in the media (unpublished data).

In parallel experiments, we also used the undifferentiated hiPSCs (ChiPSC-18) from which the HLCs were derived from, as a surrogate for poorly differentiated cells present in HLC cultures that do not possess a hepatic phenotype and express a very low level of intracellular miR-122 relative to hepatic cells, to examine the hepatic specificity of miR-122 as an *in vitro* marker of toxicity. Each batch of HLCs or hiPSCs were treated with acetaminophen or diclofenac over 24 hours, and the lysate was used for the ATP assay, whilst the media from the same well was collected in order to estimate the number of copies of miR-122 (Figure 4.7A to 4.7D). Using the ATP assay, perturbation of the HLCs was detected, with a mean reduction of ATP of 35% and 33% respectively at 24 hours, when the cells were treated with the highest concentrations of acetaminophen and diclofenac (Figure 4.7A and 4.7B). However, the non-hepatocyte model of hiPSCs displayed a higher reduction in ATP levels, with lower concentrations of acetaminophen (56% with 10 mM and 99% with 30 mM), confirming ATP as a generic and non-cell-type specific marker of cellular perturbation (Figure 4.7A). In contrast, the hiPSCs, when treated with diclofenac, displayed increased ATP levels of up to 196% of baseline (Figure 4.7B).

Using miR-122 as a marker for drug-induced toxicity in the same experiments, a trend towards an increase in the number of copies of miR-122 in the media of HLCs was noted with acetaminophen and diclofenac, with a mean 4-fold and 6-fold increase from baseline respectively, at the highest concentrations used in these experiments (Figure 4.7C and 4.7D). This suggested that when the miR-122 assay was used as a toxicity assay for the HLCs, its performance was as sensitive as the ATP assay. This was confirmed by a correlation analysis using the paired values of both assays from the experiments using HLCs treated with acetaminophen and diclofenac at various concentrations (Figure 4.8A). By plotting the values in a scatter graph, a significant negative correlation was found (Pearson's correlation coefficient, $r = -0.862$, $p < 0.001$, 95% CI -0.961 to -0.571).

However, in contrast to the varying intracellular ATP profile seen in the hiPSCs treated with acetaminophen and diclofenac (Figure 4.7A and 4.7B), the miR-122 level in the media did

not display any increasing trend and was fairly constant throughout the range of concentrations of the hepatotoxicants (Figure 4.7C and 4.7D). Analysis utilising the paired values of both biomarkers from the experiments using hiPSCs described above, also showed no correlation between the levels of miR-122 in the media and the change in intracellular ATP levels in the hiPSCs (Pearson's correlation coefficient, $r = 0.041$, $p = 0.901$, 95% CI -0.546 to 0.601) (Figure 4.8B).

The total number of copies of miR-122 expressed by an equivalent number of hiPSCs was also at least 78-fold less than that expressed by the HLCs, and therefore the potential contributory effect of miR-122 from the non-hepatocyte cells in HLC cultures towards the total number of copies of miR-122 measured in the media was negligible. More importantly, at the toxic concentrations of acetaminophen and diclofenac, where a reduction of intracellular ATP level and an increase in miR-122 in the media of treated HLCs was detected (Figure 4.7A to 4.7D), the corresponding miR-122 level in the media of hiPSCs treated with the same concentrations remained unchanged. This meant that the source of increased level of miR-122 in a heterogeneous culture such as HLCs treated with toxic concentrations of hepatotoxicants was likely to be from hepatic cells with a high level of intracellular miR-122 – in this case well-differentiated HLCs.

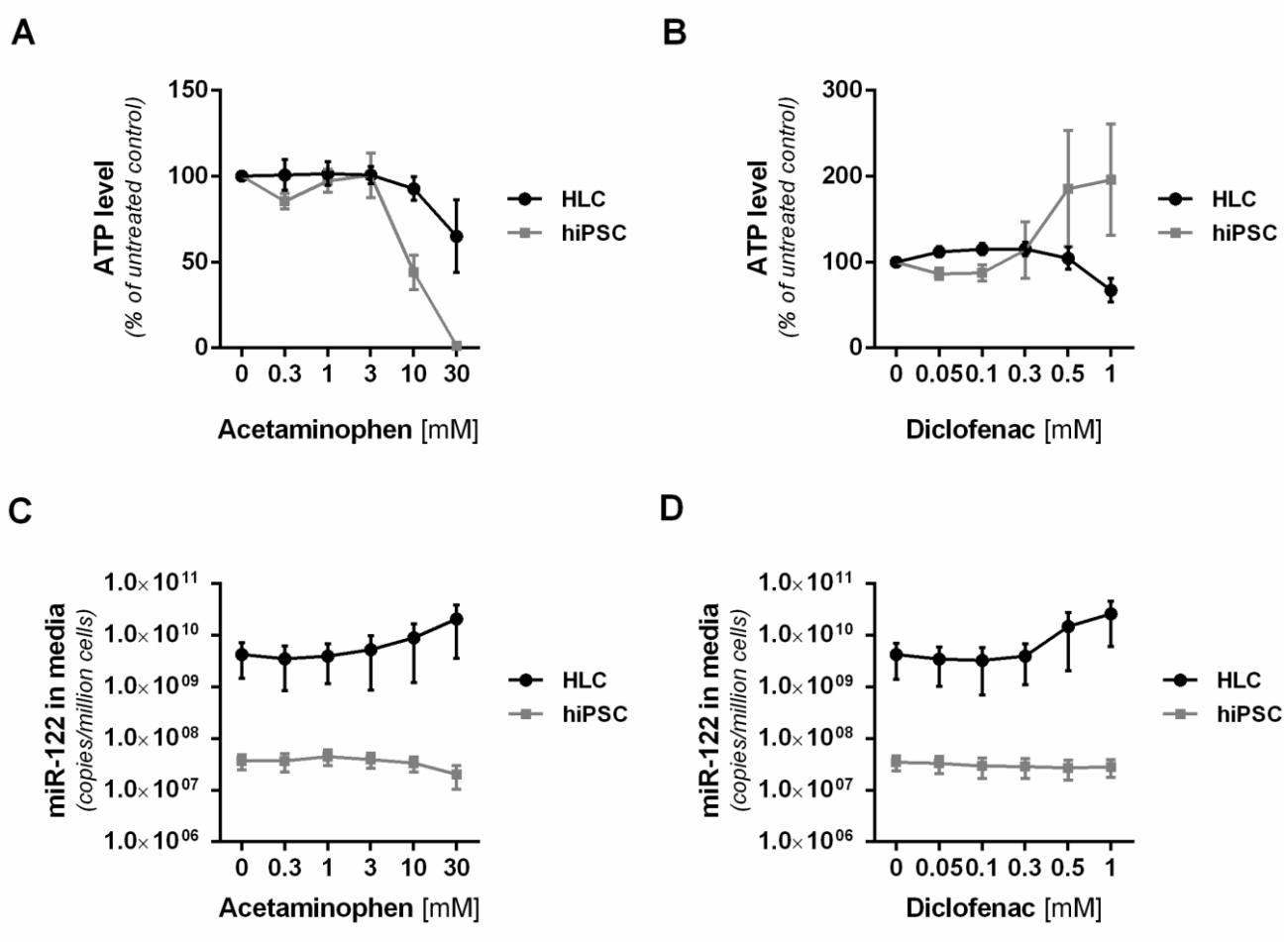

Figure 4.7 Dose-response of hepatocyte-like cells (ChiPSC-18-derived HLCs) and undifferentiated human induced pluripotent stem cells (ChiPSC-18) after treatment with acetaminophen and diclofenac.

(A, B) Intracellular ATP level (expressed as percentage of vehicle control) and (C, D) number of copies of miR-122 per million cells in the media of hiPSC-derived HLCs and undifferentiated hiPSCs treated with acetaminophen and diclofenac for 24 hours. Data is presented as the mean +/- SEM from 3 independent experiments. For the HLCs, each independent experiment represented HLCs from separate differentiation experiments, while for the hiPSCs, each independent experiment represented separate batches of hiPSCs plated on different days. The cytotoxicity assays were performed in at least two replicates on HLCs and hiPSCs cultured in 96-well plates. The number of copies of miR-122 estimated in the media was normalised to the number of cells estimated to be present in the HLC and hiPSC cultures to allow for a direct comparison of absolute quantities of miR-122 in the media. The density of HLCs present in a single well was estimated to be about 1 x 10^5 cells/cm^2 when the HLC culture was fixed and stained with the nuclear stain 4',6-diamidino-2-phenylindole (DAPI) (data not shown). As the total cell culture surface per well was 0.32 cm^2, a total number of 3.2 x 10^4 HLCs per well was obtained. For the hiPSCs, a total number of 2.2 x 10^4 hiPSCs per well was obtained using the plating density of 7 x 10^5 cells/cm^2.

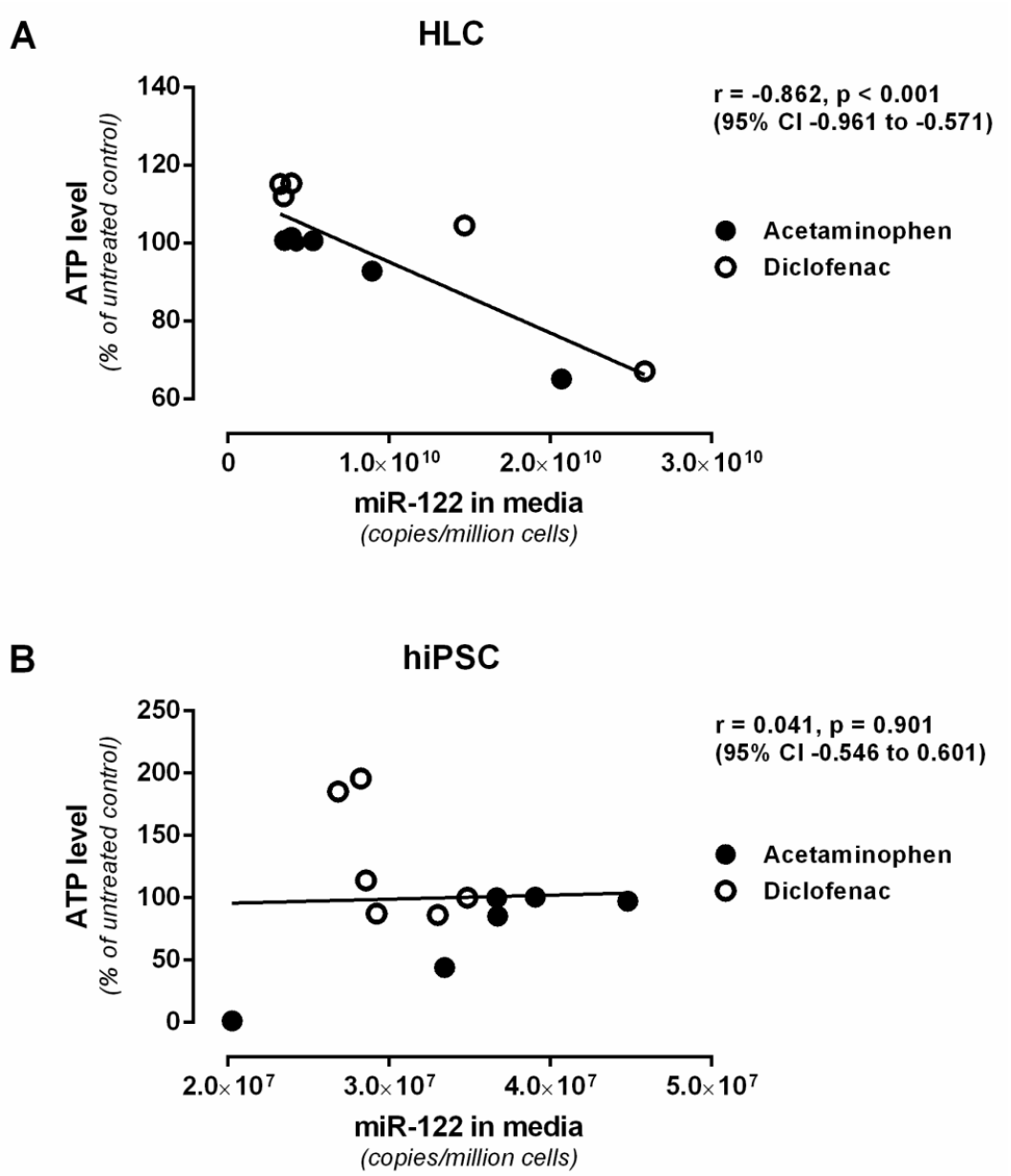

Figure 4.8 Correlation of intracellular ATP activity with miR-122 level in the media.

Correlation between intracellular ATP activity (expressed as percentage of vehicle control) and number of copies of miR-122 per million cells in the media of (A) hiPSC-derived HLCs and (B) undifferentiated hiPSCs, treated with acetaminophen and diclofenac over 24 hours using paired mean values obtained from experimental results summarised in Figure 4. r denotes Pearson's correlation coefficient, CI denotes the confidence interval of r.

4.4 DISCUSSION

MicroRNA-122 has been shown to be a liver-enriched and -abundant miR, which could be useful as a bridging biomarker of drug-induced hepatotoxicity to translate findings from *in vitro* experiments to *in vivo* experiments and the clinical setting.

However, quantitative evaluation of its abundance in various *in vitro* hepatic models currently used for the study of drug-induced hepatotoxicity in comparison to human primary hepatocytes has not been considered. For this study, we first confirmed that the *in vitro* hepatic models examined express high levels of miR-122, in contrast to the non-hepatic models (Figure 4.1). The lower intracellular miR-122 levels in the various models in comparison to freshly-isolated human primary hepatocytes, suggest that the quantity of intracellular miR-122 broadly reflects the models' degree of hepatic phenotype. HLCs differentiated in conventional two dimensional (2D) cultures have not yet been reported to display a full complement of drug metabolising enzymes at comparable levels to human primary hepatocytes (Kia*, et al.*, 2013; Sjogren *et al.*, 2014; Ulvestad *et al.*, 2013), while HLCs derived from pluripotent stem cell lines with normal genotypes would be expected to exhibit a physiologically more relevant hepatic phenotype compared to liver cancer cell lines, as shown by previous studies directly comparing the drug metabolising capacity of pluripotent stem cell-derived HLCs and the hepatocellular cancer cell lines, HepG2 and HuH7 (Brolen*, et al.*, 2010; Sjogren*, et al.*, 2014; Soderdahl *et al.*, 2007). Therefore, miR-122 can also be potentially exploited as a biomarker of physiological relevance of current and emerging *in vitro* hepatic models for mechanistic studies of DILI, by correlating their intracellular level of miR-122 to the biochemical and functional phenotype.

Figure 4.1 also supports a previous observation that the miR-122 expression increases during directed differentiation of hESCs towards HLCs (Kim*, et al.*, 2011). In that study, only a single hESC line was used for HLC generation using a different protocol to those used in this study. Hence our study adds to that finding as we used two different hESC lines,

maintained in both feeder and feeder-free culture conditions, and were differentiated towards HLCs using two disparate protocols. This study also demonstrates for the first time, that HLCs differentiated from hiPSCs also exhibit a similar trend of increase in miR-122 expression to hESC-derived HLCs, although only one hiPSC line was examined in this study.

In homogeneous hepatic models, such as plated human primary hepatocytes or HLC cultures derived with high differentiation efficiencies, we propose that the miR-122 cytotoxicity assay, which has marked concordance with the conventional assays utilising generic markers (Figures 4.2, 4.3 and 4.8), is a more relevant cell-type-specific assay to examine drug-induced toxicity of the hepatic cells. As alluded to earlier, one major advantage of using miR-122 as an *in vitro* biomarker is also the potential to translate such *in vitro* findings to *in vivo* animal models and human samples using the same assay, as miR-122 in the plasma has been shown to be an appropriate marker of acetaminophen-induced liver injury in a mouse model and in humans (Antoine*, et al.*, 2013; Harrill*, et al.*, 2012; Starkey Lewis*, et al.*, 2011; Wang*, et al.*, 2009). In other words, miR-122 can be used to bridge results in *in vitro* experiments to clinical findings, and conversely used to link findings from clinical studies to inform on the relevance of *in vitro* models being developed for the study of DILI, which the current conventional *in vitro* markers including LDH and ATP could not provide.

Similarly, in models where heterogeneity of the hepatic phenotype is present such as in HLC cultures with moderate or variable differentiation efficiencies, the miR-122 cytotoxicity assay may be essential as it allows for specific assessment of the effect of hepatotoxicants on the hepatic cells and the ability to discriminate from the “noise” of the surrounding non-hepatocytes. For example, determining the relative intracellular ATP levels between mature HLCs and poorly differentiated endodermal progenitors or differentiated cells of other lineages in a typical HLC culture would not be possible, as the ATP assay readout reflects the composite of *all* the ATP content present within a culture. Therefore, the dose-response

of mature HLCs specifically towards hepatotoxicants in a heterogeneous culture cannot be reliably measured using the ATP assay or any other assays utilising biomarkers ubiquitously present in all cells, such as LDH. This was borne out in our study where the non-hepatocyte model of hiPSCs displayed higher levels of toxicity as measured by the reduction of intracellular ATP levels at lower concentrations of acetaminophen, likely through non-CYP dependent mechanisms, confirming ATP as a generic and non-cell-type specific marker of cellular perturbation (Figure 4.7A). Conversely, the ATP levels in hiPSCs treated with diclofenac increased up to 196% of baseline (Figure 4.7B). Although the effect of diclofenac on human pluripotent stem cells have not been reported in the literature, this increase is likely to be an effect of hormesis.

The utility of the miR-122 cytotoxicity assay for the specific assessment of the effect of hepatotoxicants on hepatic cells is also potentially applicable in complex 2D or 3D hepatic models of human hepatocytes co-cultured with their non-parenchymal counterparts, which are widely considered to be the ideal *in vitro* hepatic models as they mimic the complex multicellular interactions that recapitulate the niche environment in the human liver (Godoy*, et al.*, 2013). Indeed, exciting progress has been reported in using human hepatocytes and pluripotent stem cell-derived HLCs in co-cultures with non-hepatocyte cells to produce *in vitro* hepatic models with improved functional phenotype (Bhatia*, et al.*, 1999; Takebe*, et al.*, 2013). Although the co-culture with non-hepatocyte cells enhances the functional phenotype of the hepatic cells, their concomitant presence could conceivably complicate the analysis of toxicity specifically targeting the hepatocytes, using the currently available conventional cytotoxicity assays. Indeed, one reported approach in a co-culture model of rat primary hepatocytes and murine stromal support cells to calculate the hepatocyte-only responses for non-hepatocyte-specific endpoints such as intracellular ATP and glutathione in response to drug-induced toxicity, was to perform simultaneous assays on cultures of the stromal cells alone and to subtract subsequent values from that obtained from the co-cultures (Ukairo *et al.*, 2013). However, this approach does not truly encompass the effect of the multicellular

interaction between the hepatocytes and the stromal cells in response to events causing cellular perturbation, such as drug-induced toxicity. An ideal biomarker in these co-cultures would be one which is specifically and dynamically changed only in the hepatic cells, and also measured directly in the co-cultures. We propose that miR-122 is one such hepatocyte-enriched marker that can be applied in hepatic models that incorporate hepatocytes or HLCs that express high levels of miR-122.

Although we have shown the utility of miR-122 in the human primary hepatocyte and HLC models, validation experiments of its predicted utility in complex co-culture hepatic models will still need to be conducted. Similarly, the utility of the miR-122 assay could be considered in high content cellular screening assays widely adopted by the pharmaceutical industry, which look at organelle-specific toxicity or screen for cellular perturbation events that are not hepatocyte-specific (Rausch, 2006). Therefore, changes in endpoints will be detected as readily in non-hepatocyte cells as in hepatocytes.

In a practical sense, as the miR-122 cytotoxicity assay described here uses quantitative RT-PCR, only a small amount of miR-122-containing media is required – we have extracted adequate miR-122 for analysis using as little as 50 µL of media from a total volume of 100 µL used to maintain 2.2 x 10^4 hiPSCs in a 96-well format. This assay can also be multiplexed simultaneously with other cytotoxicity assays that require a portion of the media and/or cellular lysate components. Furthermore, the miR-122 assay allows for repetitive sampling during chronic dosing experiments, which may be a more relevant approach to studying DILI in humans, and will also enable sampling of hepatocyte damage in complex 3D bioreactor cultures. A disadvantage of this assay compared to other conventional cytotoxicity assays that mainly use plate readers for end-point readouts, is that the quantification of miR-122 in the media for each sample involves multiple pre-processing steps of RNA extraction and reverse transcription. So far, the miR-122 cytotoxicity assay has not been applied as high-throughput readouts, but our workflow in using this assay benefits

from the availability of automated platforms of RNA extraction, an automated instrument for PCR setup and a PCR platform for analysing a 384-well PCR plate format.

Although the application of miR-122 for detecting drug-induced toxicity is shown in this study, the basis for the increase of miR-122 in the media during drug-induced toxicity is still unclear. However, our finding of a high correlation between the increases in LDH and miR-122 in the media of human primary hepatocytes treated with hepatotoxicants, suggest that miR-122 may be passively released from necrotic cells (Figures 4.2 and 4.3), which is in keeping with the finding of miR-122 predominantly increased in the protein-rich fraction compared to the exosome-rich fraction in the plasma/serum samples of a mouse model of acetaminophen-induced liver injury (Bala *et al.*, 2012). It was postulated that as acetaminophen-induced liver injury is severe and rapid, miRs may be released primarily through leakage from dying hepatocytes, as opposed to release through exosomes in liver injuries which are less severe and slower such as in alcoholic liver disease. However, increased cellular-mediated release of miR-122 in microparticles, exosomes or protein complexes as a response to toxic chemical exposure cannot be excluded (Salminen *et al.*, 2011). It is also unclear if drug-induced toxicity *per se* or individual drugs have any effect on the synthesis or degradation of mature miR-122, although data shown in Figure 4.4 and Figure 4.5 suggest that the hepatotoxicants examined in this study at least, have no effect on the steady state level or the total number of copies of miR-122 in the human primary hepatocyte cultures. Therefore, following on from the establishment of miR-122 as a useful *in vitro* marker of drug-induced toxicity, parallel bridging *in vitro* and *in vivo* studies can now be performed to define further the mechanism(s) of miR-122 release, which will further enhance the mechanism-based utility of miR-122 both as a quantitative and qualitative marker of liver injury.

In summary, this chapter tested the hypothesis that miR-122 can be utilised as a hepatocyte-enriched *in vitro* marker of drug-induced toxicity and our results confirmed this to be true in human primary hepatocytes and pluripotent stem cell-derived HLCs treated with the

prototypical hepatotoxicants acetaminophen and diclofenac. We have demonstrated that the detection of miR-122 in cell culture media can be used as an alternative *in vitro* marker of drug-induced cytotoxicity in homogeneous cultures of hepatic cells, and that this can be applied as a hepatocyte-enriched marker of toxicity in heterogeneous cultures of hepatic cells. The miR-122 cytotoxicity assay can also potentially be applied in hepatic models with co-culture of non-hepatocyte cells, where use of conventional cytotoxicity assays employing generic cellular markers may not be appropriate, though further validation experiments using in hepatic co-culture models will need to be conducted. We also showed that the sensitivity of the miR-122 cytotoxicity assay is similar to conventional assays measuring LDH activity and intracellular ATP levels in hepatic cultures, but further experiments with a more detailed dose-response of acetaminophen and diclofenac or with other model hepatotoxicants may clarify the potential of utilising the wider range of the miR-122 level to better discriminate the toxic concentration of a model hepatotoxicant, at least in comparison to LDH.

One limitation of this study was that the CYP activity profile was not determined of the ChiPSC-18-derived HLCs used for the toxicity experiments, although data communicated by the manufacturer suggested that they possess CYP1A, 3A and 2C9 activity comparable to cryopreserved human hepatocytes, as measured by liquid chromatography-mass spectrometry (personal communication, Cellectis AB, July 2014). Therefore, it was presumed that the toxicity seen in the HLCs were secondary to bioactivation of the compounds in the presence of the relevant CYP enzymes. For future experiments, it may be useful to quantify the CYP activity level of HLCs used to ensure that the findings from the miR-122 cytotoxicity assays are reproducible in HLCs generated from different lines possessing a similar profile of CYP activity. Future challenges also include unravelling the mechanisms by which miR-122 is released into the media and understanding the effect of drugs on miR-122 biogenesis and stability.

CHAPTER 5

CONCLUDING DISCUSSION

5.1 INTRODUCTION

As described throughout this thesis, our endeavour to develop relevant *in vitro* human hepatocyte models via novel investigative approaches was driven by the significant gaps in the availability of functional *in vitro* model systems to mechanistically understand DILI, and to screen for drug-induced hepatotoxicity at the early stages of drug development (Godoy *et al.*, 2013; LeCluyse *et al.*, 2012). Ultimately, this contributes to the persistent clinical problem of DILI as a cause of patient morbidity and mortality, with huge financial and societal burden to the pharmaceutical industry and regulatory agencies (Olsen and Whalen, 2009; Russo *et al.*, 2004; Sgro *et al.*, 2002).

We investigated the potential of exploiting the epigenetic memory inherently present in hiPSCs to generate a more functional phenotype of HLCs, by performing a series of carefully controlled experiments of hiPSC derivation and HLC generation using liver and skin tissue donated by the same donor, and also explored the phenomenon of hepatic dedifferentiation in the gold standard *in vitro* hepatic model of freshly-isolated hPHs, from the novel perspective of understanding the potential effects of changing global miR profiles, using an unbiased bioinformatics approach. We also aimed to improve the extrapolation of results between pre-clinical and clinical studies by developing and validating a real-time quantitative RT-PCR-based assay of hepatocyte-enriched biomarker of miR-122, which has the unique potential to be applied in complex hepatic co-culture models, currently not afforded by conventional generic cell-based markers.

This concluding chapter describes the implications of our findings and provides some future perspectives in relation to the ongoing multidisciplinary efforts to develop better hepatic models of DILI.

5.2 IMPLICATIONS OF FINDINGS AND FUTURE PERSPECTIVES

5.2.1 The ongoing evaluation of HLCs generated from hPH-derived hiPSCs

Results described in Chapter 2 which stemmed from the comparison of HLCs generated from isogenic hepatocyte- and fibroblast-derived hiPSC lines of a single donor, suggested that there is no advantage in the use of hPHs as the starting cell-type for deriving hiPSCs to generate functional HLCs (Figure 2.15 and 2.16), although it must be emphasised that further confirmation using tissue from other donors, preferably with at least three hPH-derived hiPSC lines, would be important to firstly confirm the findings, and secondly to clarify the relative importance of donor and clonal differences in the generation of functional HLCs. Therefore, future comparisons using at least 3 of the 5 established hPH-derived hiPSC lines from Donor 2 (Table 2.3), should help to clarify our experimental findings using hiPSC lines from Donor 1.

However, any potential definitive results from our ongoing experiments must be put into context in relation to our intended aim of improving the functional phenotype of HLCs for pharmaco-toxicology studies. Even if there is a proven advantage in using hPH-derived hiPSCs to generate HLCs, the peak functional phenotype of HLCs generated from hPH-derived hiPSC lines is unlikely to match that of the gold standard comparator of freshly-isolated hPHs using the current differentiation protocols. This is evidenced by the various reports of HLCs generated using different protocols from multiple starting cell-types, including hPHs (Liu *et al.*, 2010), which showed suboptimal CYP activity profiles in comparison to hPHs (Kia *et al.*, 2013), with limited information on Phase II and III enzymes and transporters. Furthermore, the generation of HLCs for pharmaco-toxicology studies is still hampered by the phenotypic instability of HLCs in extended *in vitro* culture (Baxter *et al.*, 2010; Hay *et al.*, 2011) – akin to the process of dedifferentiation of freshly-isolated hPH described in Chapter 3 – although promise has been shown in using novel polymer-based culture matrices to enhance stability (Hay*, et al.*, 2011).

Nevertheless, understanding the contribution of different factors, such as the contribution of epigenetic memory of hiPSCs (Kim *et al.*, 2010), causing variations in the hepatic differentiation propensity of hPSCs would be important. The attainment of a truly functional HLC phenotype suitable for pharmaco-toxicology studies is likely to require a combination of optimal conditions shown to positively influence HLC generation, starting from the choice of cell-types to use for hiPSC derivation, method of cellular reprogramming, culture conditions for hiPSC maintenance, variations of differentiation propensity between hiPSC clones, genetic variations between donors, to factors related to the hepatic differentiation process (Kajiwara *et al.*, 2012).

Conversely, if our hypothesis is proven to be false, our research would have contributed towards the conflicting findings about the role of epigenetic memory of iPSCs in influencing its hepatic differentiation propensity (Kajiwara*, et al.*, 2012; Kim *et al.*, 2011a; Lee *et al.*, 2012; Liu *et al.*, 2011). This would also mean that hepatic differentiation using hiPSCs derived from easily accessible tissue sources such as skin and peripheral blood would suffice, and simplify the practical considerations for *in vitro* modelling of normal and variant phenotypes from pre-selected adult donors, including donors who have suffered clinically relevant DILI (Kia*, et al.*, 2013).

Additionally, it is also possible that the potential advantage of using hiPSC lines derived from hPHs to generate functional HLCs may never be fully evaluated pending the availability of a robust and validated hepatic differentiation protocol to generate HLCs with a functional phenotype more akin to a freshly-isolated hPH phenotype. Future planned experiments that may help address our hypothesis further that circumvent the current limitations of directed hepatic differentiation in monolayer culture, include phenotypic comparison of the *spontaneous* differentiation propensity of isogenic hPH- and hDF-derived hiPSCs towards cells of hepatic lineages using embryoid bodies. This approach was used to show the contribution of epigenetic memory in pancreatic beta-cell-derived hiPSCs that skewed its spontaneous differentiation propensity towards cells of the endodermal lineages that

expressed beta-cell genes (Bar-Nur *et al.*, 2011). Alternatively, the "peak" functional phenotype of the HLCs may be more appropriately compared when matured further in three-dimensional culture systems which resulted in higher gene expression of hepatic lineage markers, higher functional capabilities and longer duration of culture in comparison to conventional two-dimensional maturation of HLCs (Gieseck *et al.*, 2014; Subramanian *et al.*, 2014).

5.2.2 Further definition of the utility of HLCs as a relevant model for DILI

However, in our quest to generate HLCs with higher capabilities of metabolic bioactivation of xenobiotics through enhanced expression and activity of drug metabolising enzymes, the unique capability of patient-derived hiPSCs for *in vitro* modelling to capture the genetic factors associated with DILI caused by drugs that undergo minimal or no bioactivation, should not be overlooked (Kia*, et al.*, 2013). One example is flucloxacillin-mediated liver injury, which is a type of idiosyncratic DILI (Godoy*, et al.*, 2013), highly associated with a specific human leucocyte antigen (HLA) allele – HLA-B*5701 (Daly *et al.*, 2009) – with clinical evidence of the immune component being involved (Park *et al.*, 2005). Only 10% of a standard dose of flucloxacillin is metabolised to reactive metabolites by CYP3A4 (Andrews *et al.*, 2010), and the parent compound have been shown to modify albumin and form drug-protein conjugates in antigen-presenting cells to stimulate the secretion of cytokines and cytolytic molecules from CD8+ T-lymphocytes in a HLA-restricted manner (Jenkins *et al.*, 2009; Monshi *et al.*, 2013). However, to mechanistically study how and why flucloxacillin-specific T-lymphocytes induce hepatocyte perturbation in a HLA-restricted manner, an *in vitro* model incorporating co-culture of isogenic hepatocytes and immune cells with HLA-B*5701 will be needed. The only practical approach in fact to develop such a model would be the use of isogenic hiPSC-generated HLCs and isolated T-cells from a pre-selected donor or patient with that particular HLA allele (Figure 5.1), which we have started exploring

as part of our overall aim to develop relevant human hepatic models for DILI. The possibility of an *in vitro* model of immune-mediated DILI based on HLCs with pre-selected genotypes described above, exemplified the notion that despite the functional limitations of HLCs in recapitulating the metabolic phenotype with most if not all, important drug metabolising enzymes and transporters required of a hepatic model for pharmaco-toxicology studies and drug screening in pre-clinical drug development, further refinement of what HLCs can and cannot be used for will be important, while continuing progress is made in improving its functional status.

For example, in a recent study which compared gene expression profiles between various *in vitro* hepatic models, HLCs have been suggested to be a good alternative to human cryopreserved hepatocytes for detection of compounds with direct apoptosis-driven cytotoxicity (Sjogren *et al.*, 2014). The authors and others have also highlighted the potential role of HLCs for chronic toxicity studies as the CYP enzymes and transporter proteins remained relatively stable for one week, albeit at lower levels than human cryopreserved hepatocytes (Sjogren*, et al.*, 2014; Ulvestad *et al.*, 2013). Although the CYP expression is lower compared to hPHs, the fact that its expression is stable and importantly do not display donor variations as exhibited by different batches of hPHs, may make HLCs of a single genetic background, a reliable *in vitro* model for application in the pharmaceutical industry for drug screening.

Additionally, instead of focussing on attaining a certain percentage of basal CYP protein level in HLCs that match that of freshly-isolated hPHs, in deciding if the HLCs generated from a certain hPSC line using a specific differentiation protocol is functionally relevant for pharmaco-toxicology studies, perhaps a more relevant characterisation criteria is their CYP levels *with* drug induction. This was shown in a study using HLCs generated from hESCs which showed an increase in CYP3A4 and 1A2 activities of more than four-fold following induction with phenobarbital, and subsequently shown to have a comparable accuracy to

human cryopreserved hepatocytes in predicting drug-induced hepatotoxicity following compound incubation up to seven days (Szkolnicka *et al.*, 2014).

Therefore, whilst efforts continue to understand the factors that influence the functional status of HLCs, it is clear that HLCs have an important and unique role to play in the field of *in vitro* toxicology – the more pertinent question right now is how and where.

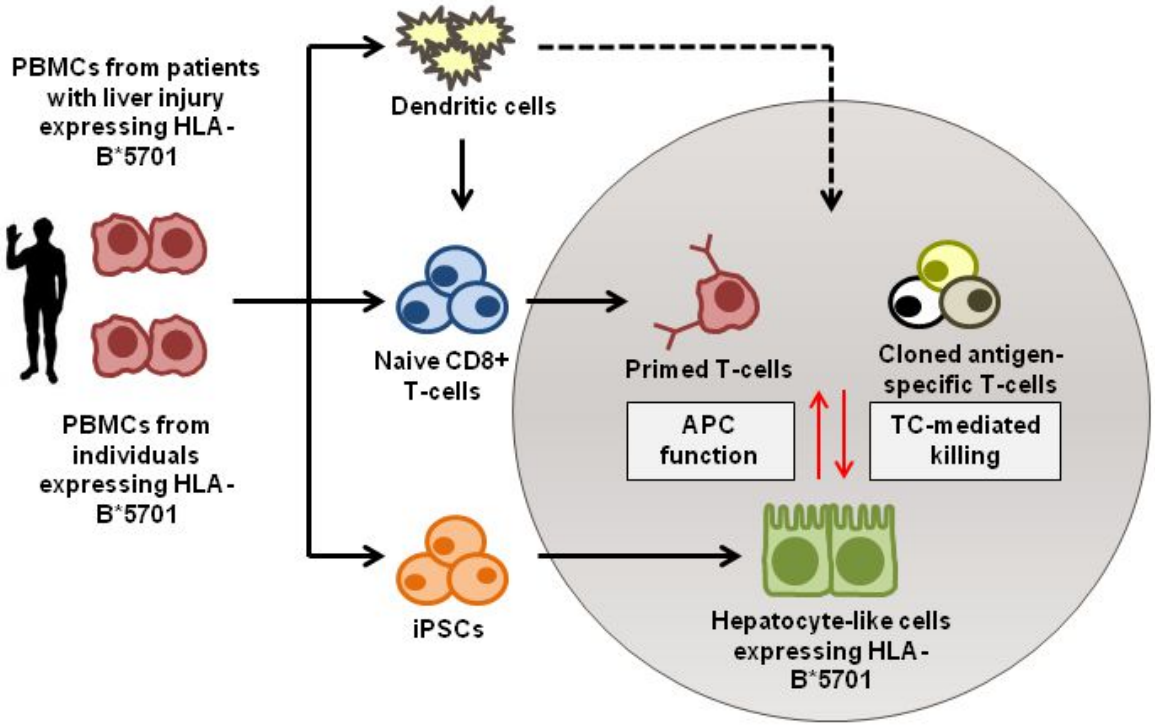

Figure 5.1 Schematic diagram of a complex co-culture of isogenic human iPSC-generated HLCs and isolated T-cells from a pre-selected donor or patient with HLA-B*5701 as a potential model to study flucloxacillin-mediated liver injury.

PBMC, peripheral blood mononuclear cells; HLA, human leucocyte antigen; iPSC, induced pluripotent stem cells; APC, antigen presenting cell; TC, T-cell.

5.2.3 Unlocking the value of global microRNA profiling of dedifferentiating hPHs

The detrimental process of dedifferentiation in the gold-standard *in vitro* model of hPH continue to limit its utility to acute toxicity studies only, and compromises their use in chronic toxicity studies with prolonged drug exposure, which would better reflect most clinical presentations of DILI (Guguen-Guillouzo and Guillouzo, 2010; Kalgutkar and Soglia, 2005;

LeCluyse, 2001). Although the process and its detrimental effect on the metabolic phenotype in hPHs has been characterised extensively (Paine and Andreakos, 2004; Vinken *et al.*, 2006), none of the strategies that aimed to reverse or prevent it have proved successful so far (Bolleyn *et al.*, 2011; Fraczek *et al.*, 2013; Naiki *et al.*, 2004).

Therefore, in Chapter 3, we described our contribution towards the understanding of this process from the novel perspective of global miR profiles of dedifferentiating hPHs. Broadly speaking, many of the perturbed biological processes and pathways that were linked to the differentially-expressed miRs have been described previously in the literature. For example, the ERK/MAPK and NF-κβ signalling pathways which are involved in proliferative and inflammatory responses – major mechanisms underlying hepatocyte dedifferentiation causing the loss of transcription of genes related to liver-specific functions – were identified as two of the most significantly perturbed pathways after 48 hours of *in vitro* culture (Figure 3.6) (Fraczek*, et al.*, 2013). The main implication of our study however, is the possibility of influencing these pathways by manipulating the expression of all or some of the relatively few differentially-expressed miRs that collectively target many of the genes involved in each pathway in a considered manner, using existing miR-targeting and/or miR replacement strategies (Li and Rana, 2014). Similarly, we also highlighted the fact that the differentially-expressed miRs target many of the genes important for xenobiotic biotransformation either directly (Table 3.3), or indirectly via targeting associated liver-enriched transcription factors (LETFs) and nuclear factors (Table 3.4 and 3.5) known to regulate their expression. Perhaps one “simple” strategy to ensure the hPHs maintain their basal level of CYP expression and are fit for utility as a relevant model for pharmaco-toxicology studies is to manipulate the expression of miRs that negatively affect the expression of their CYP gene targets.

Additionally, our study also identified that gene expression in general, is the most significantly perturbed function throughout the experiment with a large number of genes involved in the pre- and post-transcription levels being targeted by the differentially-expressed miRs (Figure 3.5, Table 3.2, 3.7 and 3.8). The targets include the histone

deacetylases (HDACs) (Table 3.8) which are typically associated with transcriptional repression, hence lending credence to using HDAC inhibitors as an anti-dedifferentiation strategy to facilitate the restoration and maintenance of the fully differentiated phenotype of hepatocytes (Fraczek *et al.*, 2009; Henkens *et al.*, 2007). However, as noted by some authors (Fraczek*, et al.*, 2013), using broad spectrum HDAC inhibitors may not be ideal as it does not allow for discrimination between isozymes of HDACs that may play differing roles in hepatocellular processes. On the contrary, manipulation of differentially-expressed miRs that target specific isozymes of HDAC could potentially be a more selective HDAC inhibition strategy.

However, validation studies will need to be performed to investigate the predicted effect(s) of targeted manipulation of the differentially-expressed miRs, and will be an ongoing focus of our group. Furthermore, it remains to be answered whether miRs are only silent observers or active participants in the process of hepatic dedifferentiation. To this end, as our group have also completed global proteomic profiling of dedifferentiating hPHs cultured *in vitro* using the same experimental design (n = 5 different donors, manuscript in preparation), systematic integration of information from both datasets will be useful to address this question. Similarly, concomitant analysis of previously published transcriptomic profiles of dedifferentiating hPHs (Richert *et al.*, 2006) will be informative, especially for interrogating gene sets which are not readily detected using a proteomics approach.

Another aim of our miR profiling study was to identify pattern(s) of miR changes that may inform new strategies for improved HLC functional capacity. Interestingly, the only study that had performed global miR profiling of the differentiation process of hPSCs towards HLCs (Kim *et al.*, 2011b), found that miR-21-5p, which was the most up-regulated miR during hPH dedifferentiation after 48 hours of culture (Table 3.1), was also increased during differentiation of definitive endoderm towards HLCs. miR-21-5p is known to target genes associated with proliferation and cancer metastasis (Krichevsky and Gabriely, 2009) and has been shown to be up-regulated during the proliferative phase of liver regeneration in rat and

mice models (Castro *et al.*, 2010; Marquez *et al.*, 2010). As the loss of the hepatic phenotype in hPHs during *in vitro* culture has been described to be partly due to its "proliferation-primed state" (Fraczek*, et al.*, 2009), the up-regulation of miR-21-5p during HLC differentiation may be an important link to the limited attainment of a functional phenotype of HLCs.

However, to truly draw parallels between the process of hPH dedifferentiation and HLC differentiation, future studies directly comparing the global miR, transcriptomic and/or proteomic profiles of HLCs, freshly-isolated hPHs and dedifferentiated hPHs would be needed to firstly delineate the biological functions and canonical pathways which are lacking or dysregulated in HLCs; and secondly to help formulate novel HLC differentiation strategies, such as possible miR targets for modulation. A similar transcriptomic approach had suggested that the CYP expression profile of HLCs were akin to that of hPHs cultured for 48 hours (Ulvestad*, et al.*, 2013), though a global analysis of the whole transcriptome was not employed. To reduce the confounding factor of genetic variability, perhaps our approach of using isogenic cells described in Chapter 2 could be combined by using hPHs and HLCs originating from the same donor(s) for comparative analyses.

5.2.4 Utility of microRNA-122 as a hepatocyte-enriched *in vitro* biomarker

In Chapter 4, we described the validation of miR-122 as a more relevant cell-type-specific assay to examine drug-induced toxicity of the hepatic cells, as opposed to conventional cytotoxicity assays which typically rely on the release of ubiquitous cellular enzymes or the measurement of generic cell health parameters (Sumantran, 2011). We also highlighted its potential utility in complex hepatic models when applied for toxicology research, where the miR-122 cytotoxicity assay may be essential as it allows for specific assessment of the effect of hepatotoxicants on the hepatic cells and the ability to discriminate from the "noise" of the surrounding non-hepatocyte cells. These non-hepatocyte cells could be in the form of poorly-

differentiated cells present within HLC cultures with low differentiation efficiency, or non-parenchymal cells used in co-cultures with hPHs and HLCs, which is increasingly applied as the basis for many novel two dimensional (2D) and 3D complex hepatic models (LeCluyse*, et al.*, 2012; Takebe *et al.*, 2013). This is mainly in response to the increasing recognition that the ideal *in vitro* hepatic models are those that recapitulate the niche environment in the human liver by mimicking the complex multicellular interactions (Godoy*, et al.*, 2013).

One example is a commercially-available system of 2D micro-patterned co-cultures of hepatocytes with murine stromal cells which have been reported to have greater drug metabolising capacity, longer viability and phenotypic stability compared to conventional monocellular culture models (Khetani and Bhatia, 2008; LeCluyse*, et al.*, 2012). However, as shown in a recent toxicology study that used this platform, the concomitant presence of the stromal cells complicated the analysis of toxicity specifically targeting the hepatocytes when conventional cytotoxicity assays were used (Ukairo *et al.*, 2013). The approach reported to calculate the hepatocyte-only toxicity using non-hepatocyte-specific endpoints such as ATP in response to hepatotoxicants, was to perform simultaneous assays on cultures of the stromal cells alone and to subtract subsequent values from that obtained from the co-cultures. This however, does not truly encompass the effect of the multicellular interaction between the hepatocytes and the stromal cells in response to cellular perturbation. In contrast, the detection of miR-122 as a hepatocyte-enriched marker of drug-induced toxicity in this situation would have been ideal, as it would have been measured directly in the co-cultures, and the endpoint specifically correlating with toxicity of the hepatocytes only. Furthermore, the miR-122 assay also allows for repetitive sampling during chronic dosing experiments, which may be a more relevant approach to studying DILI in humans, and will also enable sampling of hepatocyte damage in complex 3D bioreactor cultures. Therefore, the validation of miR-122 as a biomarker for drug-induced hepatotoxicity will hopefully help in the deployment of emerging complex hepatic models for pharmaco-toxicology studies that may have otherwise been limited by conventional cytotoxicity assays.

Another aspect which has greatly contributed to the huge societal burden caused by DILI is the lack of qualified bridging biomarkers that allow for accurate translation between pre-clinical and clinical studies (Antoine *et al.*, 2014). However, there has been tremendous progress in recent years in validating many novel translational biomarkers such as high mobility group box-1 (HMGB1) and keratin-18 (CK18) in *in vivo* and clinical studies which reflect the different mechanisms of DILI (Antoine *et al.*, 2009; Harrill *et al.*, 2012). This is also true for miR-122 which has been shown to be an appropriate marker of acetaminophen-induced liver injury in a mouse model and in humans (Antoine *et al.*, 2013; Harrill*, et al.*, 2012; Starkey Lewis *et al.*, 2011; Wang *et al.*, 2009).

Therefore, one further advantage of using miR-122 as an *in vitro* biomarker is its potential to bridge results in *in vitro* experiments to clinical findings using the same assay. Conversely, analysis of miR-122 release can also be used to assess the relevance of *in vitro* models being developed for the study of DILI by linkage with clinical findings, which the current conventional *in vitro* markers such as LDH and ATP could not provide. However, to fulfil its full potential, further studies are needed to delineate its mechanism(s) of miR-122 release during drug-induced toxicity, and are currently in progress in our group.

5.3 FINAL COMMENTS

In conclusion, the hypotheses addressed in this thesis will be commented on individually:

Hypothesis 1

- HLCs generated from hPH-derived hiPSCs display a closer resemblance to the hPH phenotype compared to HLCs generated from isogenic human dermal fibroblast-derived hiPSCs.

  Comment: *HLCs generated from a single clone of hPH-derived hiPSCs did not show greater resemblance to hPHs as assessed by its transcriptomic and functional profile, compared to HLCs generated from isogenic human dermal fibroblast-derived hiPSCs. However, further clarification of these results is required using HLCs originating from other donors, ideally with more hPH-derived hiPSC clones available for comparison. The use of other differentiation protocols should also be considered.*

Hypothesis 2

- Novel insights into the process of hPH dedifferentiation can be gained by investigating the changing global miR profiles of hPHs in extended *in vitro* culture.

  Comment: *The global miR profiling of hPHs in extended in vitro culture have provided novel insights into the role of miRs in the detrimental process of hepatic dedifferentiation. This approach also defined a list of differentially-expressed miRs which could be modulated as a anti-dedifferentiation strategy. Validation studies are now required to confirm our findings from the bioinformatics analyses using miR mimics and antagomirs.*

Hypothesis 3

- miR-122 can be utilised as a relevant *in vitro* marker of drug-induced hepatotoxicity in hepatic models expressing high levels of miR-122.

  Comment: *miR-122 was successfully validated as a hepatocyte-enriched in vitro marker of drug-induced hepatotoxicity in hPHs and HLCs generated from hiPSCs, which were both shown to have high intracellular levels of miR-122. Detection of miR-122 release may be a useful alternative to conventional cytotoxicity assays in complex co-culture hepatic models, and could be applied as a bridging biomarker of DILI between pre-clinical and clinical studies.*

BIBLIOGRAPHY

Aasen, T. and Izpisua Belmonte, J. C. (2010). Isolation and cultivation of human keratinocytes from skin or plucked hair for the generation of induced pluripotent stem cells. *Nat Protoc* **5**, 371-82.

Afanasyeva, E. A., Mestdagh, P., Kumps, C., Vandesompele, J., Ehemann, V., Theissen, J., Fischer, M., Zapatka, M., Brors, B., Savelyeva, L., Sagulenko, V., Speleman, F., Schwab, M. and Westermann, F. (2011). MicroRNA miR-885-5p targets CDK2 and MCM5, activates p53 and inhibits proliferation and survival. *Cell Death Differ* **18**, 974-84.

Aithal, G. P. (2011). Hepatotoxicity related to antirheumatic drugs. *Nat Rev Rheumatol* **7**, 139-50.

Andrews, E., Armstrong, M., Tugwood, J., Swan, D., Glaves, P., Pirmohamed, M., Aithal, G. P., Wright, M. C., Day, C. P. and Daly, A. K. (2010). A role for the pregnane X receptor in flucloxacillin-induced liver injury. *Hepatology* **51**, 1656-64.

Anokye-Danso, F., Trivedi, C. M., Juhr, D., Gupta, M., Cui, Z., Tian, Y., Zhang, Y., Yang, W., Gruber, P. J., Epstein, J. A. and Morrisey, E. E. (2011). Highly efficient miRNA-mediated reprogramming of mouse and human somatic cells to pluripotency. *Cell Stem Cell* **8**, 376-88.

Antoine, D. J., Williams, D. P., Kipar, A., Jenkins, R. E., Regan, S. L., Sathish, J. G., Kitteringham, N. R. and Park, B. K. (2009). High-mobility group box-1 protein and keratin-18, circulating serum proteins informative of acetaminophen-induced necrosis and apoptosis in vivo. *Toxicol Sci* **112**, 521-31.

Antoine, D. J., Dear, J. W., Lewis, P. S., Platt, V., Coyle, J., Masson, M., Thanacoody, R. H., Gray, A. J., Webb, D. J., Moggs, J. G., Bateman, D. N., Goldring, C. E. and Park, B. K. (2013). Mechanistic biomarkers provide early and sensitive detection of acetaminophen-induced acute liver injury at first presentation to hospital. *Hepatology* **58**, 777-87.

Antoine, D. J., Harrill, A. H., Watkins, P. B. and Park, B. K. (2014). Safety biomarkers for drug-induced liver injury - current status and future perspectives. *Toxicology Research* **3**, 75-85.

Bader, A., Knop, E., Kern, A., Boker, K., Fruhauf, N., Crome, O., Esselmann, H., Pape, C., Kempka, G. and Sewing, K. F. (1996). 3-D coculture of hepatic sinusoidal cells with primary hepatocytes-design of an organotypical model. *Exp Cell Res* **226**, 223-33.

Bai, S., Nasser, M. W., Wang, B., Hsu, S. H., Datta, J., Kutay, H., Yadav, A., Nuovo, G., Kumar, P. and Ghoshal, K. (2009). MicroRNA-122 inhibits tumorigenic properties of hepatocellular carcinoma cells and sensitizes these cells to sorafenib. *J Biol Chem* **284**, 32015-27.

Bala, S., Petrasek, J., Mundkur, S., Catalano, D., Levin, I., Ward, J., Alao, H., Kodys, K. and Szabo, G. (2012). Circulating microRNAs in exosomes indicate hepatocyte injury and inflammation in alcoholic, drug-induced, and inflammatory liver diseases. *Hepatology* **56**, 1946-57.

Banks, A. T., Zimmerman, H. J., Ishak, K. G. and Harter, J. G. (1995). Diclofenac-associated hepatotoxicity: analysis of 180 cases reported to the Food and Drug Administration as adverse reactions. *Hepatology* **22**, 820-7.

Barad, O., Meiri, E., Avniel, A., Aharonov, R., Barzilai, A., Bentwich, I., Einav, U., Gilad, S., Hurban, P., Karov, Y., Lobenhofer, E. K., Sharon, E., Shiboleth, Y. M., Shtutman, M., Bentwich, Z. and Einat, P. (2004). MicroRNA expression detected by oligonucleotide microarrays: system establishment and expression profiling in human tissues. *Genome Res* **14**, 2486-94.

Bar-Nur, O., Russ, H. A., Efrat, S. and Benvenisty, N. (2011). Epigenetic memory and preferential lineage-specific differentiation in induced pluripotent stem cells derived from human pancreatic islet beta cells. *Cell Stem Cell* **9**, 17-23.

Bartel, D. P. (2004). MicroRNAs: genomics, biogenesis, mechanism, and function. *Cell* **116**, 281-97.

Basma, H., Soto-Gutierrez, A., Yannam, G. R., Liu, L., Ito, R., Yamamoto, T., Ellis, E., Carson, S. D., Sato, S., Chen, Y., Muirhead, D., Navarro-Alvarez, N., Wong, R. J., Roy-Chowdhury, J., Platt, J. L., Mercer, D. F., Miller, J. D., Strom, S. C., Kobayashi, N. and Fox, I. J. (2009). Differentiation and transplantation of human embryonic stem cell-derived hepatocytes. *Gastroenterology* **136**, 990-9.

Bass, A. S., Cartwright, M. E., Mahon, C., Morrison, R., Snyder, R., McNamara, P., Bradley, P., Zhou, Y. Y. and Hunter, J. (2009). Exploratory drug safety: a discovery strategy to reduce attrition in development. *J Pharmacol Toxicol Methods* **60**, 69-78.

Baxter, M. A., Camarasa, M. V., Bates, N., Small, F., Murray, P., Edgar, D. and Kimber, S. J. (2009). Analysis of the distinct functions of growth factors and tissue culture substrates necessary for the long-term self-renewal of human embryonic stem cell lines. *Stem Cell Res* **3**, 28-38.

Baxter, M. A., Rowe, C., Alder, J., Harrison, S., Hanley, K. P., Park, B. K., Kitteringham, N. R., Goldring, C. E. and Hanley, N. A. (2010). Generating hepatic cell lineages from pluripotent stem cells for drug toxicity screening. *Stem Cell Res* **5**, 4-22.

Beigel, J., Fella, K., Kramer, P. J., Kroeger, M. and Hewitt, P. (2008). Genomics and proteomics analysis of cultured primary rat hepatocytes. *Toxicol In Vitro* **22**, 171-81.

Beitzinger, M. and Meister, G. (2010). Preview. MicroRNAs: from decay to decoy. *Cell* **140**, 612-4.

Bhatia, S. N., Balis, U. J., Yarmush, M. L. and Toner, M. (1999). Effect of cell-cell interactions in preservation of cellular phenotype: cocultivation of hepatocytes and nonparenchymal cells. *FASEB J* **13**, 1883-900.

Bielby, R. C., Boccaccini, A. R., Polak, J. M. and Buttery, L. D. (2004). In vitro differentiation and in vivo mineralization of osteogenic cells derived from human embryonic stem cells. *Tissue Eng* **10**, 1518-25.

Bitzer, M., Armeanu, S., Lauer, U. M. and Neubert, W. J. (2003). Sendai virus vectors as an emerging negative-strand RNA viral vector system. *J Gene Med* **5**, 543-53.

Bock, C., Kiskinis, E., Verstappen, G., Gu, H., Boulting, G., Smith, Z. D., Ziller, M., Croft, G. F., Amoroso, M. W., Oakley, D. H., Gnirke, A., Eggan, K. and Meissner, A. (2011). Reference Maps of human ES and iPS cell variation enable high-throughput characterization of pluripotent cell lines. *Cell* **144**, 439-52.

Bolleyn, J., Fraczek, J., Vinken, M., Lizarraga, D., Gaj, S., van Delft, J. H., Rogiers, V. and Vanhaecke, T. (2011). Effect of Trichostatin A on miRNA expression in cultures of primary rat hepatocytes. *Toxicol In Vitro* **25**, 1173-82.

Bone, H. K., Nelson, A. S., Goldring, C. E., Tosh, D. and Welham, M. J. (2011). A novel chemically directed route for the generation of definitive endoderm from human embryonic stem cells based on inhibition of GSK-3. *J Cell Sci* **124**, 1992-2000.

Bouchie, A. (2013). First microRNA mimic enters clinic. *Nat Biotechnol* **31**, 577.

Brolen, G., Sivertsson, L., Bjorquist, P., Eriksson, G., Ek, M., Semb, H., Johansson, I., Andersson, T. B., Ingelman-Sundberg, M. and Heins, N. (2010). Hepatocyte-like cells derived from human embryonic stem cells specifically via definitive endoderm and a progenitor stage. *J Biotechnol* **145**, 284-94.

Bueno, M. J., Perez de Castro, I. and Malumbres, M. (2008). Control of cell proliferation pathways by microRNAs. *Cell Cycle* **7**, 3143-8.

Cai, J., Zhao, Y., Liu, Y., Ye, F., Song, Z., Qin, H., Meng, S., Chen, Y., Zhou, R., Song, X., Guo, Y., Ding, M. and Deng, H. (2007). Directed differentiation of human embryonic stem cells into functional hepatic cells. *Hepatology* **45**, 1229-39.

Castello, A., Fischer, B., Eichelbaum, K., Horos, R., Beckmann, B. M., Strein, C., Davey, N. E., Humphreys, D. T., Preiss, T., Steinmetz, L. M., Krijgsveld, J. and Hentze, M. W. (2012). Insights into RNA biology from an atlas of mammalian mRNA-binding proteins. *Cell* **149**, 1393-406.

Castoldi, M., Vujic Spasic, M., Altamura, S., Elmen, J., Lindow, M., Kiss, J., Stolte, J., Sparla, R., D'Alessandro, L. A., Klingmuller, U., Fleming, R. E., Longerich, T., Grone, H. J., Benes, V., Kauppinen, S., Hentze, M. W. and Muckenthaler, M. U. (2011). The liver-specific microRNA miR-122 controls systemic iron homeostasis in mice. *J Clin Invest* **121**, 1386-96.

Castro, R. E., Ferreira, D. M., Zhang, X., Borralho, P. M., Sarver, A. L., Zeng, Y., Steer, C. J., Kren, B. T. and Rodrigues, C. M. (2010). Identification of microRNAs during rat liver regeneration after partial hepatectomy and modulation by ursodeoxycholic acid. *Am J Physiol Gastrointest Liver Physiol* **299**, G887-97.

Celander, M. C., Goldstone, J. V., Denslow, N. D., Iguchi, T., Kille, P., Meyerhoff, R. D., Smith, B. A., Hutchinson, T. H. and Wheeler, J. R. (2011). Species extrapolation for the 21st century. *Environ Toxicol Chem* **30**, 52-63.

Cermelli, S., Ruggieri, A., Marrero, J. A., Ioannou, G. N. and Beretta, L. (2011). Circulating microRNAs in patients with chronic hepatitis C and non-alcoholic fatty liver disease. *PLoS One* **6**, e23937.

Chang, J., Nicolas, E., Marks, D., Sander, C., Lerro, A., Buendia, M. A., Xu, C., Mason, W. S., Moloshok, T., Bort, R., Zaret, K. S. and Taylor, J. M. (2004). miR-122, a mammalian liver-specific microRNA, is processed from hcr mRNA and may downregulate the high affinity cationic amino acid transporter CAT-1. *RNA Biol* **1**, 106-13.

Chen, G., Gulbranson, D. R., Hou, Z., Bolin, J. M., Ruotti, V., Probasco, M. D., Smuga-Otto, K., Howden, S. E., Diol, N. R., Propson, N. E., Wagner, R., Lee, G. O., Antosiewicz-Bourget, J., Teng, J. M. and Thomson, J. A. (2011). Chemically defined conditions for human iPSC derivation and culture. *Nat Methods* **8**, 424-9.

Chen, J., Yao, D., Zhao, S., He, C., Ding, N., Li, L. and Long, F. (2014). MiR-1246 promotes SiHa cervical cancer cell proliferation, invasion, and migration through suppression of its target gene thrombospondin 2. *Arch Gynecol Obstet*.

Chen, K. and Rajewsky, N. (2007). The evolution of gene regulation by transcription factors and microRNAs. *Nat Rev Genet* **8**, 93-103.

Chen, Q. and Cederbaum, A. I. (1998). Cytotoxicity and apoptosis produced by cytochrome P450 2E1 in Hep G2 cells. *Mol Pharmacol* **53**, 638-48.

Chen, W., Koenigs, L. L., Thompson, S. J., Peter, R. M., Rettie, A. E., Trager, W. F. and Nelson, S. D. (1998). Oxidation of acetaminophen to its toxic quinone imine and nontoxic catechol metabolites by baculovirus-expressed and purified human cytochromes P450 2E1 and 2A6. *Chem Res Toxicol* **11**, 295-301.

Chen, X. M. (2009). MicroRNA signatures in liver diseases. *World J Gastroenterol* **15**, 1665-72.

Cheng, X. and Blumenthal, R. M. (2008). Mammalian DNA methyltransferases: a structural perspective. *Structure* **16**, 341-50.

Dai, Y., Rashba-Step, J. and Cederbaum, A. I. (1993). Stable expression of human cytochrome P4502E1 in HepG2 cells: characterization of catalytic activities and production of reactive oxygen intermediates. *Biochemistry* **32**, 6928-37.

Daly, A. K., Donaldson, P. T., Bhatnagar, P., Shen, Y., Pe'er, I., Floratos, A., Daly, M. J., Goldstein, D. B., John, S., Nelson, M. R., Graham, J., Park, B. K., Dillon, J. F., Bernal, W., Cordell, H. J., Pirmohamed, M., Aithal, G. P. and Day, C. P. (2009). HLA-B*5701 genotype is a major determinant of drug-induced liver injury due to flucloxacillin. *Nat Genet* **41**, 816-9.

Danan, G. and Benichou, C. (1993). Causality assessment of adverse reactions to drugs--I. A novel method based on the conclusions of international consensus meetings: application to drug-induced liver injuries. *J Clin Epidemiol* **46**, 1323-30.

Davies, E. C., Green, C. F., Mottram, D. R., Rowe, P. H. and Pirmohamed, M. (2010). Emergency re-admissions to hospital due to adverse drug reactions within 1 year of the index admission. *Br J Clin Pharmacol* **70**, 749-55.

de Abajo, F. J., Montero, D., Madurga, M. and Garcia Rodriguez, L. A. (2004). Acute and clinically relevant drug-induced liver injury: a population based case-control study. *Br J Clin Pharmacol* **58**, 71-80.
de Longueville, F., Atienzar, F. A., Marcq, L., Dufrane, S., Evrard, S., Wouters, L., Leroux, F., Bertholet, V., Gerin, B., Whomsley, R., Arnould, T., Remacle, J. and Canning, M. (2003). Use of a low-density microarray for studying gene expression patterns induced by hepatotoxicants on primary cultures of rat hepatocytes. *Toxicol Sci* **75**, 378-92.

Duan, Y., Ma, X., Zou, W. E. I., Wang, C., Bahbahan, I. S., Ahuja, T. P., Tolstikov, V. and Zern, M. A. (2010). Differentiation and characterization of metabolically functioning hepatocytes from human embryonic stem cells. *Stem Cells* **28**, 674-686.

Eberharter, A. and Becker, P. B. (2002). Histone acetylation: a switch between repressive and permissive chromatin. Second in review series on chromatin dynamics. *EMBO Rep* **3**, 224-9.

Ek, M., Soderdahl, T., Kuppers-Munther, B., Edsbagge, J., Andersson, T. B., Bjorquist, P., Cotgreave, I., Jernstrom, B., Ingelman-Sundberg, M. and Johansson, I. (2007). Expression of drug metabolizing enzymes in hepatocyte-like cells derived from human embryonic stem cells. *Biochem Pharmacol* **74**, 496-503.

Elaut, G., Henkens, T., Papeleu, P., Snykers, S., Vinken, M., Vanhaecke, T. and Rogiers, V. (2006). Molecular mechanisms underlying the dedifferentiation process of isolated hepatocytes and their cultures. *Curr Drug Metab* **7**, 629-60.

Esau, C., Davis, S., Murray, S. F., Yu, X. X., Pandey, S. K., Pear, M., Watts, L., Booten, S. L., Graham, M., McKay, R., Subramaniam, A., Propp, S., Lollo, B. A., Freier, S., Bennett, C. F., Bhanot, S. and Monia, B. P. (2006). miR-122 regulation of lipid metabolism revealed by in vivo antisense targeting. *Cell Metab* **3**, 87-98.

Fabbri, M., Garzon, R., Cimmino, A., Liu, Z., Zanesi, N., Callegari, E., Liu, S., Alder, H., Costinean, S., Fernandez-Cymering, C., Volinia, S., Guler, G., Morrison, C. D., Chan, K. K., Marcucci, G., Calin, G. A., Huebner, K. and Croce, C. M. (2007). MicroRNA-29 family reverts aberrant methylation in lung cancer by targeting DNA methyltransferases 3A and 3B. *Proc Natl Acad Sci U S A* **104**, 15805-10.

Fausto, N. (2001). Liver regeneration: from laboratory to clinic. *Liver Transpl* **7**, 835-44.

Fontana, R. J., Seeff, L. B., Andrade, R. J., Bjornsson, E., Day, C. P., Serrano, J. and Hoofnagle, J. H. (2010). Standardization of nomenclature and causality assessment in drug-induced liver injury: summary of a clinical research workshop. *Hepatology* **52**, 730-42.

Fornari, F., Gramantieri, L., Ferracin, M., Veronese, A., Sabbioni, S., Calin, G. A., Grazi, G. L., Giovannini, C., Croce, C. M., Bolondi, L. and Negrini, M. (2008). MiR-221 controls CDKN1C/p57 and CDKN1B/p27 expression in human hepatocellular carcinoma. *Oncogene* **27**, 5651-61.

Fornari, F., Gramantieri, L., Giovannini, C., Veronese, A., Ferracin, M., Sabbioni, S., Calin, G. A., Grazi, G. L., Croce, C. M., Tavolari, S., Chieco, P., Negrini, M. and Bolondi, L. (2009). MiR-122/cyclin G1 interaction modulates p53 activity and affects doxorubicin sensitivity of human hepatocarcinoma cells. *Cancer Res* **69**, 5761-7.

Fraczek, J., Deleu, S., Lukaszuk, A., Doktorova, T., Tourwe, D., Geerts, A., Vanhaecke, T., Vanderkerken, K. and Rogiers, V. (2009). Screening of amide analogues of Trichostatin A in cultures of primary rat hepatocytes: search for potent and safe HDAC inhibitors. *Invest New Drugs* **27**, 338-46.

Fraczek, J., Bolleyn, J., Vanhaecke, T., Rogiers, V. and Vinken, M. (2013). Primary hepatocyte cultures for pharmaco-toxicological studies: at the busy crossroad of various anti-dedifferentiation strategies. *Arch Toxicol* **87**, 577-610.

Friedman, R. C., Farh, K. K., Burge, C. B. and Bartel, D. P. (2009). Most mammalian mRNAs are conserved targets of microRNAs. *Genome Res* **19**, 92-105.

Fu, H., Tie, Y., Xu, C., Zhang, Z., Zhu, J., Shi, Y., Jiang, H., Sun, Z. and Zheng, X. (2005). Identification of human fetal liver miRNAs by a novel method. *FEBS Lett* **579**, 3849-54.

Fusaki, N., Ban, H., Nishiyama, A., Saeki, K. and Hasegawa, M. (2009). Efficient induction of transgene-free human pluripotent stem cells using a vector based on Sendai virus, an RNA virus that does not integrate into the host genome. *Proc Jpn Acad Ser B Phys Biol Sci* **85**, 348-62.

Garzon, R., Liu, S., Fabbri, M., Liu, Z., Heaphy, C. E., Callegari, E., Schwind, S., Pang, J., Yu, J., Muthusamy, N., Havelange, V., Volinia, S., Blum, W., Rush, L. J., Perrotti, D., Andreeff, M., Bloomfield, C. D., Byrd, J. C., Chan, K., Wu, L. C., Croce, C. M. and Marcucci, G. (2009). MicroRNA-29b induces global DNA hypomethylation and tumor suppressor gene reexpression in acute myeloid leukemia by targeting directly DNMT3A and 3B and indirectly DNMT1. *Blood* **113**, 6411-8.

Gieseck, R. L., 3rd, Hannan, N. R., Bort, R., Hanley, N. A., Drake, R. A., Cameron, G. W., Wynn, T. A. and Vallier, L. (2014). Maturation of induced pluripotent stem cell derived hepatocytes by 3D-culture. *PLoS One* **9**, e86372.

Godoy, P., Hewitt, N. J., Albrecht, U., Andersen, M. E., Ansari, N., Bhattacharya, S., Bode, J. G., Bolleyn, J., Borner, C., Bottger, J., Braeuning, A., Budinsky, R. A., Burkhardt, B., Cameron, N. R., Camussi, G., Cho, C. S., Choi, Y. J., Craig Rowlands, J., Dahmen, U., Damm, G., Dirsch, O., Donato, M. T., Dong, J., Dooley, S., Drasdo, D., Eakins, R., Ferreira, K. S., Fonsato, V., Fraczek, J., Gebhardt, R., Gibson, A., Glanemann, M., Goldring, C. E., Gomez-Lechon, M. J., Groothuis, G. M., Gustavsson, L., Guyot, C., Hallifax, D., Hammad, S., Hayward, A., Haussinger, D., Hellerbrand, C., Hewitt, P., Hoehme, S., Holzhutter, H. G., Houston, J. B., Hrach, J., Ito, K., Jaeschke, H., Keitel, V., Kelm, J. M., Kevin Park, B., Kordes, C., Kullak-Ublick, G. A., LeCluyse, E. L., Lu, P., Luebke-Wheeler, J., Lutz, A., Maltman, D. J., Matz-Soja, M., McMullen, P., Merfort, I., Messner, S., Meyer, C., Mwinyi, J., Naisbitt, D. J., Nussler, A. K., Olinga, P., Pampaloni, F., Pi, J., Pluta, L., Przyborski, S. A., Ramachandran, A., Rogiers, V., Rowe, C., Schelcher, C., Schmich, K., Schwarz, M., Singh, B., Stelzer, E. H., Stieger, B., Stober, R., Sugiyama, Y., Tetta, C., Thasler, W. E., Vanhaecke, T., Vinken, M., Weiss, T. S., Widera, A., Woods, C. G., Xu, J. J., Yarborough, K. M. and Hengstler, J. G. (2013). Recent advances in 2D and 3D in vitro systems using primary hepatocytes, alternative hepatocyte sources and non-parenchymal liver cells and their use in investigating mechanisms of hepatotoxicity, cell signaling and ADME. *Arch Toxicol* **87**, 1315-530.

Goff, L. A., Davila, J., Swerdel, M. R., Moore, J. C., Cohen, R. I., Wu, H., Sun, Y. E. and Hart, R. P. (2009). Ago2 immunoprecipitation identifies predicted microRNAs in human embryonic stem cells and neural precursors. *PLoS One* **4**, e7192.

Goldring, C. E., Kitteringham, N. R., Jenkins, R., Lovatt, C. A., Randle, L. E., Abdullah, A., Owen, A., Liu, X., Butler, P. J., Williams, D. P., Metcalfe, P., Berens, C., Hillen, W., Foster, B., Simpson, A., McLellan, L. and Park, B. K. (2006). Development of a transactivator in hepatoma cells that allows expression of phase I, phase II, and chemical defense genes. *Am J Physiol Cell Physiol* **290**, C104-15.

Gomez-Lechon, M. J., Donato, M. T., Castell, J. V. and Jover, R. (2004). Human hepatocytes in primary culture: the choice to investigate drug metabolism in man. *Curr Drug Metab* **5**, 443-62.
Gonzalez, F., Boue, S. and Izpisua Belmonte, J. C. (2011). Methods for making induced pluripotent stem cells: reprogramming a la carte. *Nat Rev Genet* **12**, 231-42.

Greenhough, S., Medine, C. N. and Hay, D. C. (2010). Pluripotent stem cell derived hepatocyte like cells and their potential in toxicity screening. *Toxicology* **278**, 250-5.

Griffiths-Jones, S. (2004). The microRNA Registry. *Nucleic Acids Res* **32**, D109-11.

Guengerich, F. P. (2008). Cytochrome p450 and chemical toxicology. *Chem Res Toxicol* **21**, 70-83.

Guguen-Guillouzo, C. and Guillouzo, A. (2010). General review on in vitro hepatocyte models and their applications. *Methods Mol Biol* **640**, 1-40.

Hamazaki, T., Iiboshi, Y., Oka, M., Papst, P. J., Meacham, A. M., Zon, L. I. and Terada, N. (2001). Hepatic maturation in differentiating embryonic stem cells in vitro. *FEBS Letters* **497**, 15-19.

Hansel, M. C., Gramignoli, R., Blake, W., Davila, J., Skvorak, K., Dorko, K., Tahan, V., Lee, B. R., Tafaleng, E., Guzman-Lepe, J., Soto-Gutierrez, A., Fox, I. J. and Strom, S. C. (2014). Increased reprogramming of human fetal hepatocytes compared with adult hepatocytes in feeder-free conditions. *Cell Transplant* **23**, 27-38.

Harrill, A. H., Roach, J., Fier, I., Eaddy, J. S., Kurtz, C. L., Antoine, D. J., Spencer, D. M., Kishimoto, T. K., Pisetsky, D. S., Park, B. K. and Watkins, P. B. (2012). The effects of heparins on the liver: application of mechanistic serum biomarkers in a randomized study in healthy volunteers. *Clin Pharmacol Ther* **92**, 214-20.

Hay, D. C., Fletcher, J., Payne, C., Terrace, J. D., Gallagher, R. C., Snoeys, J., Black, J. R., Wojtacha, D., Samuel, K., Hannoun, Z., Pryde, A., Filippi, C., Currie, I. S., Forbes, S. J., Ross, J. A., Newsome, P. N. and Iredale, J. P. (2008). Highly efficient differentiation of hESCs to functional hepatic endoderm requires ActivinA and Wnt3a signaling. *Proc Natl Acad Sci U S A* **105**, 12301-6.

Hay, D. C., Zhao, D., Fletcher, J., Hewitt, Z. A., McLean, D., Urruticoechea-Uriguen, A., Black, J. R., Elcombe, C., Ross, J. A., Wolf, R. and Cui, W. (2008). Efficient differentiation of hepatocytes from human embryonic stem cells exhibiting markers recapitulating liver development in vivo. *Stem Cells* **26**, 894-902.

Hay, D. C., Pernagallo, S., Diaz-Mochon, J. J., Medine, C. N., Greenhough, S., Hannoun, Z., Schrader, J., Black, J. R., Fletcher, J., Dalgetty, D., Thompson, A. I., Newsome, P. N., Forbes, S. J., Ross, J. A., Bradley, M. and Iredale, J. P. (2011). Unbiased screening of polymer libraries to define novel substrates for functional hepatocytes with inducible drug metabolism. *Stem Cell Res* **6**, 92-102.

Hengstler, J. G., Brulport, M., Schormann, W., Bauer, A., Hermes, M., Nussler, A. K., Fandrich, F., Ruhnke, M., Ungefroren, H., Griffin, L., Bockamp, E., Oesch, F. and von Mach, M. A. (2005). Generation of human hepatocytes by stem cell technology: definition of the hepatocyte. *Expert Opin Drug Metab Toxicol* **1**, 61-74.

Henkens, T., Papeleu, P., Elaut, G., Vinken, M., Rogiers, V. and Vanhaecke, T. (2007). Trichostatin A, a critical factor in maintaining the functional differentiation of primary cultured rat hepatocytes. *Toxicol Appl Pharmacol* **218**, 64-71.

Hewitt, N. J., Lechon, M. J., Houston, J. B., Hallifax, D., Brown, H. S., Maurel, P., Kenna, J. G., Gustavsson, L., Lohmann, C., Skonberg, C., Guillouzo, A., Tuschl, G., Li, A. P., LeCluyse, E., Groothuis, G. M. and Hengstler, J. G. (2007). Primary hepatocytes: current understanding of the regulation of metabolic enzymes and transporter proteins, and pharmaceutical practice for the use of hepatocytes in metabolism, enzyme induction, transporter, clearance, and hepatotoxicity studies. *Drug Metab Rev* **39**, 159-234.

Hou, P., Li, Y., Zhang, X., Liu, C., Guan, J., Li, H., Zhao, T., Ye, J., Yang, W., Liu, K., Ge, J., Xu, J., Zhang, Q., Zhao, Y. and Deng, H. (2013). Pluripotent stem cells induced from mouse somatic cells by small-molecule compounds. *Science* **341**, 651-4.

Huangfu, D., Maehr, R., Guo, W., Eijkelenboom, A., Snitow, M., Chen, A. E. and Melton, D. A. (2008). Induction of pluripotent stem cells by defined factors is greatly improved by small-molecule compounds. *Nat Biotechnol* **26**, 795-7.

James, L. P., Mayeux, P. R. and Hinson, J. A. (2003). Acetaminophen-induced hepatotoxicity. *Drug Metab Dispos* **31**, 1499-506.

Jenkins, R. E., Meng, X., Elliott, V. L., Kitteringham, N. R., Pirmohamed, M. and Park, B. K. (2009). Characterisation of flucloxacillin and 5-hydroxymethyl flucloxacillin haptenated HSA in vitro and in vivo. *Proteomics Clin Appl* **3**, 720-9.

Jia, F., Wilson, K. D., Sun, N., Gupta, D. M., Huang, M., Li, Z., Panetta, N. J., Chen, Z. Y., Robbins, R. C., Kay, M. A., Longaker, M. T. and Wu, J. C. (2010). A nonviral minicircle vector for deriving human iPS cells. *Nat Methods* **7**, 197-9.

Jiang, Q., Wang, Y., Hao, Y., Juan, L., Teng, M., Zhang, X., Li, M., Wang, G. and Liu, Y. (2009). miR2Disease: a manually curated database for microRNA deregulation in human disease. *Nucleic Acids Res* **37**, D98-104.

Jigorel, E., Le Vee, M., Boursier-Neyret, C., Parmentier, Y. and Fardel, O. (2006). Differential regulation of sinusoidal and canalicular hepatic drug transporter expression by xenobiotics activating drug-sensing receptors in primary human hepatocytes. *Drug Metab Dispos* **34**, 1756-63.

Jopling, C. (2012). Liver-specific microRNA-122: Biogenesis and function. *RNA Biol* **9**, 137-42.

Kaji, K., Norrby, K., Paca, A., Mileikovsky, M., Mohseni, P. and Woltjen, K. (2009). Virus-free induction of pluripotency and subsequent excision of reprogramming factors. *Nature* **458**, 771-5.

Kajiwara, M., Aoi, T., Okita, K., Takahashi, R., Inoue, H., Takayama, N., Endo, H., Eto, K., Toguchida, J., Uemoto, S. and Yamanaka, S. (2012). Donor-dependent variations in hepatic differentiation from human-induced pluripotent stem cells. *Proc Natl Acad Sci U S A* **109**, 12538-43.

Kakizaki, S., Takizawa, D., Tojima, H., Horiguchi, N., Yamazaki, Y. and Mori, M. (2011). Nuclear receptors CAR and PXR; therapeutic targets for cholestatic liver disease. *Front Biosci (Landmark Ed)* **16**, 2988-3005.

Kalgutkar, A. S. and Soglia, J. R. (2005). Minimising the potential for metabolic activation in drug discovery. *Expert Opin Drug Metab Toxicol* **1**, 91-142.

Kechavarzi, B. and Janga, S. C. (2014). Dissecting the expression landscape of RNA-binding proteins in human cancers. *Genome Biol* **15**, R14.

Khetani, S. R. and Bhatia, S. N. (2008). Microscale culture of human liver cells for drug development. *Nat Biotechnol* **26**, 120-6.

Kia, R., Sison, R. L., Heslop, J., Kitteringham, N. R., Hanley, N., Mills, J. S., Park, B. K. and Goldring, C. E. (2013). Stem cell-derived hepatocytes as a predictive model for drug-induced liver injury: are we there yet? *Br J Clin Pharmacol* **75**, 885-96.

Kibbe, W. A. (2007). OligoCalc: an online oligonucleotide properties calculator. *Nucleic Acids Res* **35**, W43-6.

Kim, D., Kim, C. H., Moon, J. I., Chung, Y. G., Chang, M. Y., Han, B. S., Ko, S., Yang, E., Cha, K. Y., Lanza, R. and Kim, K. S. (2009). Generation of human induced pluripotent stem cells by direct delivery of reprogramming proteins. *Cell Stem Cell* **4**, 472-6.

Kim, K., Doi, A., Wen, B., Ng, K., Zhao, R., Cahan, P., Kim, J., Aryee, M. J., Ji, H., Ehrlich, L. I., Yabuuchi, A., Takeuchi, A., Cunniff, K. C., Hongguang, H., McKinney-Freeman, S., Naveiras, O., Yoon, T. J., Irizarry, R. A., Jung, N., Seita, J., Hanna, J., Murakami, P., Jaenisch, R., Weissleder, R., Orkin, S. H., Weissman, I. L., Feinberg, A. P. and Daley, G. Q. (2010). Epigenetic memory in induced pluripotent stem cells. *Nature* **467**, 285-90.

Kim, K., Zhao, R., Doi, A., Ng, K., Unternaehrer, J., Cahan, P., Huo, H., Loh, Y. H., Aryee, M. J., Lensch, M. W., Li, H., Collins, J. J., Feinberg, A. P. and Daley, G. Q. (2011). Donor cell type can influence the epigenome and differentiation potential of human induced pluripotent stem cells. *Nat Biotechnol* **29**, 1117-9.

Kim, N., Kim, H., Jung, I., Kim, Y., Kim, D. and Han, Y. M. (2011). Expression profiles of miRNAs in human embryonic stem cells during hepatocyte differentiation. *Hepatol Res* **41**, 170-83.

Kmiec, Z. (2001). Cooperation of liver cells in health and disease. *Adv Anat Embryol Cell Biol* **161**, III-XIII, 1-151.

Krichevsky, A. M. and Gabriely, G. (2009). miR-21: a small multi-faceted RNA. *J Cell Mol Med* **13**, 39-53.

Krol, J., Loedige, I. and Filipowicz, W. (2010). The widespread regulation of microRNA biogenesis, function and decay. *Nat Rev Genet* **11**, 597-610.

Krutzfeldt, J., Rajewsky, N., Braich, R., Rajeev, K. G., Tuschl, T., Manoharan, M. and Stoffel, M. (2005). Silencing of microRNAs in vivo with 'antagomirs'. *Nature* **438**, 685-9.

Krutzfeldt, J. and Stoffel, M. (2006). MicroRNAs: a new class of regulatory genes affecting metabolism. *Cell Metab* **4**, 9-12.

Kuhlmann, W. D. and Peschke, P. (2006). Hepatic progenitor cells, stem cells, and AFP expression in models of liver injury. *Int J Exp Pathol* **87**, 343-59.

Kutay, H., Bai, S., Datta, J., Motiwala, T., Pogribny, I., Frankel, W., Jacob, S. T. and Ghoshal, K. (2006). Downregulation of miR-122 in the rodent and human hepatocellular carcinomas. *J Cell Biochem* **99**, 671-8.

Kyriakis, J. M. and Avruch, J. (2001). Mammalian mitogen-activated protein kinase signal transduction pathways activated by stress and inflammation. *Physiol Rev* **81**, 807-69.

Lagos-Quintana, M., Rauhut, R., Lendeckel, W. and Tuschl, T. (2001). Identification of novel genes coding for small expressed RNAs. *Science* **294**, 853-8.

Lagos-Quintana, M., Rauhut, R., Yalcin, A., Meyer, J., Lendeckel, W. and Tuschl, T. (2002). Identification of tissue-specific microRNAs from mouse. *Curr Biol* **12**, 735-9.

Landgraf, P., Rusu, M., Sheridan, R., Sewer, A., Iovino, N., Aravin, A., Pfeffer, S., Rice, A., Kamphorst, A. O., Landthaler, M., Lin, C., Socci, N. D., Hermida, L., Fulci, V., Chiaretti, S., Foa, R., Schliwka, J., Fuchs, U., Novosel, A., Muller, R. U., Schermer, B., Bissels, U., Inman, J., Phan, Q., Chien, M., Weir, D. B., Choksi, R., De Vita, G., Frezzetti, D., Trompeter, H. I., Hornung, V., Teng, G., Hartmann, G., Palkovits, M., Di Lauro, R., Wernet, P., Macino, G., Rogler, C. E., Nagle, J. W., Ju, J., Papavasiliou, F. N., Benzing, T., Lichter, P., Tam, W., Brownstein, M. J., Bosio, A., Borkhardt, A., Russo, J. J., Sander, C., Zavolan, M. and Tuschl, T. (2007). A mammalian microRNA expression atlas based on small RNA library sequencing. *Cell* **129**, 1401-14.

Lappalainen, K., Jaaskelainen, I., Syrjanen, K., Urtti, A. and Syrjanen, S. (1994). Comparison of cell proliferation and toxicity assays using two cationic liposomes. *Pharm Res* **11**, 1127-31.

Laudadio, I., Manfroid, I., Achouri, Y., Schmidt, D., Wilson, M. D., Cordi, S., Thorrez, L., Knoops, L., Jacquemin, P., Schuit, F., Pierreux, C. E., Odom, D. T., Peers, B. and Lemaigre, F. P. (2012). A feedback loop between the liver-enriched transcription factor network and miR-122 controls hepatocyte differentiation. *Gastroenterology* **142**, 119-29.

LeCluyse, E. L. (2001). Human hepatocyte culture systems for the in vitro evaluation of cytochrome P450 expression and regulation. *Eur J Pharm Sci* **13**, 343-68.

LeCluyse, E. L., Alexandre, E., Hamilton, G. A., Viollon-Abadie, C., Coon, D. J., Jolley, S. and Richert, L. (2005). Isolation and culture of primary human hepatocytes. *Methods Mol Biol* **290**, 207-29.

LeCluyse, E. L., Witek, R. P., Andersen, M. E. and Powers, M. J. (2012). Organotypic liver culture models: meeting current challenges in toxicity testing. *Crit Rev Toxicol* **42**, 501-48.

Lee, E. W., Lai, Y., Zhang, H. and Unadkat, J. D. (2006). Identification of the mitochondrial targeting signal of the human equilibrative nucleoside transporter 1 (hENT1): implications for interspecies differences in mitochondrial toxicity of fialuridine. *J Biol Chem* **281**, 16700-6.

Lee, R. C., Feinbaum, R. L. and Ambros, V. (1993). The C. elegans heterochronic gene lin-4 encodes small RNAs with antisense complementarity to lin-14. *Cell* **75**, 843-54.

Lee, S. B., Seo, D., Choi, D., Park, K. Y., Holczbauer, A., Marquardt, J. U., Conner, E. A., Factor, V. M. and Thorgeirsson, S. S. (2012). Contribution of hepatic lineage stage-specific donor memory to the differential potential of induced mouse pluripotent stem cells. *Stem Cells* **30**, 997-1007.

Lee, W. M. (2004). Acetaminophen and the U.S. Acute Liver Failure Study Group: lowering the risks of hepatic failure. *Hepatology* **40**, 6-9.

Lefebvre, P., Chinetti, G., Fruchart, J. C. and Staels, B. (2006). Sorting out the roles of PPAR alpha in energy metabolism and vascular homeostasis. *J Clin Invest* **116**, 571-80.

Leite, S. B., Wilk-Zasadna, I., Zaldivar, J. M., Airola, E., Reis-Fernandes, M. A., Mennecozzi, M., Guguen-Guillouzo, C., Chesne, C., Guillou, C., Alves, P. M. and Coecke, S. (2012). Three-dimensional HepaRG model as an attractive tool for toxicity testing. *Toxicol Sci* **130**, 106-16.

Lewis, B. P., Burge, C. B. and Bartel, D. P. (2005). Conserved seed pairing, often flanked by adenosines, indicates that thousands of human genes are microRNA targets. *Cell* **120**, 15-20.

Li, Z. and Rana, T. M. (2014). Therapeutic targeting of microRNAs: current status and future challenges. *Nat Rev Drug Discov* **13**, 622-38.

Li, Z. Y., Xi, Y., Zhu, W. N., Zeng, C., Zhang, Z. Q., Guo, Z. C., Hao, D. L., Liu, G., Feng, L., Chen, H. Z., Chen, F., Lv, X., Liu, D. P. and Liang, C. C. (2011). Positive regulation of hepatic miR-122 expression by HNF4alpha. *J Hepatol* **55**, 602-11.

Lindow, M. and Kauppinen, S. (2012). Discovering the first microRNA-targeted drug. *J Cell Biol* **199**, 407-12.

Litovitz, T. L., Klein-Schwartz, W., Rodgers, G. C., Jr., Cobaugh, D. J., Youniss, J., Omslaer, J. C., May, M. E., Woolf, A. D. and Benson, B. E. (2002). 2001 Annual report of the American Association of Poison Control Centers Toxic Exposure Surveillance System. *Am J Emerg Med* **20**, 391-452.

Liu, D., Fan, J., Mei, M., Ingvarsson, S. and Chen, H. (2009). Identification of miRNAs in a liver of a human fetus by a modified method. *PLoS One* **4**, e7594.

Liu, H., Kim, Y., Sharkis, S., Marchionni, L. and Jang, Y. Y. (2011). In vivo liver regeneration potential of human induced pluripotent stem cells from diverse origins. *Sci Transl Med* **3**, 82ra39.

Liu, H., Ye, Z., Kim, Y., Sharkis, S. and Jang, Y. Y. (2010). Generation of endoderm-derived human induced pluripotent stem cells from primary hepatocytes. *Hepatology* **51**, 1810-9.

Livak, K. J. and Schmittgen, T. D. (2001). Analysis of relative gene expression data using real-time quantitative PCR and the 2(-Delta Delta C(T)) Method. *Methods* **25**, 402-8.

Lopez-Romero, P. (2011). Pre-processing and differential expression analysis of Agilent microRNA arrays using the AgiMicroRna Bioconductor library. *BMC Genomics* **12**, 64.

Lumelsky, N., Blondel, O., Laeng, P., Velasco, I., Ravin, R. and McKay, R. (2001). Differentiation of embryonic stem cells to insulin-secreting structures similar to pancreatic islets. *Science* **292**, 1389-94.

Macarthur, C. C., Fontes, A., Ravinder, N., Kuninger, D., Kaur, J., Bailey, M., Taliana, A., Vemuri, M. C. and Lieu, P. T. (2012). Generation of human-induced pluripotent stem cells by a nonintegrating RNA Sendai virus vector in feeder-free or xeno-free conditions. *Stem Cells Int* **2012**, 564612.

Malarkey, D. E., Johnson, K., Ryan, L., Boorman, G. and Maronpot, R. R. (2005). New insights into functional aspects of liver morphology. *Toxicol Pathol* **33**, 27-34.

Maria, V. A. and Victorino, R. M. (1997). Development and validation of a clinical scale for the diagnosis of drug-induced hepatitis. *Hepatology* **26**, 664-9.

Marquez, R. T., Wendlandt, E., Galle, C. S., Keck, K. and McCaffrey, A. P. (2010). MicroRNA-21 is upregulated during the proliferative phase of liver regeneration, targets Pellino-1, and inhibits NF-kappaB signaling. *Am J Physiol Gastrointest Liver Physiol* **298**, G535-41.

Meier, Y., Cavallaro, M., Roos, M., Pauli-Magnus, C., Folkers, G., Meier, P. J. and Fattinger, K. (2005). Incidence of drug-induced liver injury in medical inpatients. *Eur J Clin Pharmacol* **61**, 135-43.

Mikkelsen, T. S., Hanna, J., Zhang, X., Ku, M., Wernig, M., Schorderet, P., Bernstein, B. E., Jaenisch, R., Lander, E. S. and Meissner, A. (2008). Dissecting direct reprogramming through integrative genomic analysis. *Nature* **454**, 49-55.

Mitchell, J. R., Jollow, D. J., Potter, W. Z., Davis, D. C., Gillette, J. R. and Brodie, B. B. (1973). Acetaminophen-induced hepatic necrosis. I. Role of drug metabolism. *J Pharmacol Exp Ther* **187**, 185-94.

Miyoshi, N., Ishii, H., Nagano, H., Haraguchi, N., Dewi, D. L., Kano, Y., Nishikawa, S., Tanemura, M., Mimori, K., Tanaka, F., Saito, T., Nishimura, J., Takemasa, I., Mizushima, T., Ikeda, M., Yamamoto, H., Sekimoto, M., Doki, Y. and Mori, M. (2011). Reprogramming of mouse and human cells to pluripotency using mature microRNAs. *Cell Stem Cell* **8**, 633-8.

Mizuguchi, T., Mitaka, T., Hirata, K., Oda, H. and Mochizuki, Y. (1998). Alteration of expression of liver-enriched transcription factors in the transition between growth and differentiation of primary cultured rat hepatocytes. *J Cell Physiol* **174**, 273-84.

Monshi, M. M., Faulkner, L., Gibson, A., Jenkins, R. E., Farrell, J., Earnshaw, C. J., Alfirevic, A., Cederbrant, K., Daly, A. K., French, N., Pirmohamed, M., Park, B. K. and Naisbitt, D. J. (2013). Human leukocyte antigen (HLA)-B*57:01-restricted activation of drug-specific T cells provides the immunological basis for flucloxacillin-induced liver injury. *Hepatology* **57**, 727-39.

Mosmann, T. (1983). Rapid colorimetric assay for cellular growth and survival: application to proliferation and cytotoxicity assays. *J Immunol Methods* **65**, 55-63.

Naiki, T., Nagaki, M., Shidoji, Y., Kojima, H. and Moriwaki, H. (2004). Functional activity of human hepatoma cells transfected with adenovirus-mediated hepatocyte nuclear factor (HNF)-4 gene. *Cell Transplant* **13**, 393-403.

Neely, M. D., Tidball, A. M., Asad, A. A., Ess, K. C. and Bowman, A. B. (2011). Induced pluripotent stem cells (iPSCs): an emerging model system for the study of human neurotoxicology. In: Cell culture techniques (Neuromethods) (Aschner, M., Sunol, S. and Bal-Price, A., Eds.), pp. 27-61. Humana Press, New York City, NY.

Nelson, S. D. (1990). Molecular mechanisms of the hepatotoxicity caused by acetaminophen. *Semin Liver Dis* **10**, 267-78.

O'Brien, P. J., Irwin, W., Diaz, D., Howard-Cofield, E., Krejsa, C. M., Slaughter, M. R., Gao, B., Kaludercic, N., Angeline, A., Bernardi, P., Brain, P. and Hougham, C. (2006). High concordance of drug-induced human hepatotoxicity with in vitro cytotoxicity measured in a novel cell-based model using high content screening. *Arch Toxicol* **80**, 580-604.
Okita, K., Ichisaka, T. and Yamanaka, S. (2007). Generation of germline-competent induced pluripotent stem cells. *Nature* **448**, 313-7.

Olsen, A. K. and Whalen, M. D. (2009). Public perceptions of the pharmaceutical industry and drug safety: implications for the pharmacovigilance professional and the culture of safety. *Drug Saf* **32**, 805-10.

Osafune, K., Caron, L., Borowiak, M., Martinez, R. J., Fitz-Gerald, C. S., Sato, Y., Cowan, C. A., Chien, K. R. and Melton, D. A. (2008). Marked differences in differentiation propensity among human embryonic stem cell lines. *Nat Biotechnol* **26**, 313-5.

Padgham, C. R., Boyle, C. C., Wang, X. J., Raleigh, S. M., Wright, M. C. and Paine, A. J. (1993). Alteration of transcription factor mRNAs during the isolation and culture of rat hepatocytes suggests the activation of a proliferative mode underlies their de-differentiation. *Biochem Biophys Res Commun* **197**, 599-605.

Paine, A. J. and Andreakos, E. (2004). Activation of signalling pathways during hepatocyte isolation: relevance to toxicology in vitro. *Toxicol In Vitro* **18**, 187-93.

Pan, W., Zhu, S., Yuan, M., Cui, H., Wang, L., Luo, X., Li, J., Zhou, H., Tang, Y. and Shen, N. (2010). MicroRNA-21 and microRNA-148a contribute to DNA hypomethylation in lupus CD4+ T cells by directly and indirectly targeting DNA methyltransferase 1. *J Immunol* **184**, 6773-81.

Park, B. K., Kitteringham, N. R., Maggs, J. L., Pirmohamed, M. and Williams, D. P. (2005). The role of metabolic activation in drug-induced hepatotoxicity. *Annu Rev Pharmacol Toxicol* **45**, 177-202.

Park, B. K., Laverty, H., Srivastava, A., Antoine, D. J., Naisbitt, D. and Williams, D. P. (2011). Drug bioactivation and protein adduct formation in the pathogenesis of drug-induced toxicity. *Chem Biol Interact* **192**, 30-6.

Patten, C. J., Thomas, P. E., Guy, R. L., Lee, M., Gonzalez, F. J., Guengerich, F. P. and Yang, C. S. (1993). Cytochrome P450 enzymes involved in acetaminophen activation by rat and human liver microsomes and their kinetics. *Chem Res Toxicol* **6**, 511-8.

Pfeifer, A. M., Cole, K. E., Smoot, D. T., Weston, A., Groopman, J. D., Shields, P. G., Vignaud, J. M., Juillerat, M., Lipsky, M. M., Trump, B. F. and et al. (1993). Simian virus 40 large tumor antigen-immortalized normal human liver epithelial cells express hepatocyte characteristics and metabolize chemical carcinogens. *Proc Natl Acad Sci U S A* **90**, 5123-7.

Polo, J. M., Liu, S., Figueroa, M. E., Kulalert, W., Eminli, S., Tan, K. Y., Apostolou, E., Stadtfeld, M., Li, Y., Shioda, T., Natesan, S., Wagers, A. J., Melnick, A., Evans, T. and Hochedlinger, K. (2010). Cell type of origin influences the molecular and functional properties of mouse induced pluripotent stem cells. *Nat Biotechnol* **28**, 848-55.

Prescott, L. F. (1980). Hepatotoxicity of mild analgesics. *Br J Clin Pharmacol* **10 Suppl 2**, 373S-379S.

Pritchard, C. C., Cheng, H. H. and Tewari, M. (2012). MicroRNA profiling: approaches and considerations. *Nat Rev Genet* **13**, 358-69.

Ramos-Mejia, V., Melen, G. J., Sanchez, L., Gutierrez-Aranda, I., Ligero, G., Cortes, J. L., Real, P. J., Bueno, C. and Menendez, P. (2010). Nodal/Activin signaling predicts human pluripotent stem cell lines prone to differentiate toward the hematopoietic lineage. *Mol Ther* **18**, 2173-81.

Rashid, S. T., Corbineau, S., Hannan, N., Marciniak, S. J., Miranda, E., Alexander, G., Huang-Doran, I., Griffin, J., Ahrlund-Richter, L., Skepper, J., Semple, R., Weber, A., Lomas, D. A. and Vallier, L. (2010). Modeling inherited metabolic disorders of the liver using human induced pluripotent stem cells. *J Clin Invest* **120**, 3127-36.

Rausch, O. (2006). High content cellular screening. *Curr Opin Chem Biol* **10**, 316-20.

Richert, L., Liguori, M. J., Abadie, C., Heyd, B., Mantion, G., Halkic, N. and Waring, J. F. (2006). Gene expression in
human hepatocytes in suspension after isolation is similar to the liver of origin, is not affected by hepatocyte cold storage and cryopreservation, but is strongly changed after hepatocyte plating. *Drug Metab Dispos* **34**, 870-9.

Rodriguez-Antona, C., Donato, M. T., Boobis, A., Edwards, R. J., Watts, P. S., Castell, J. V. and Gomez-Lechon, M. J. (2002). Cytochrome P450 expression in human hepatocytes and hepatoma cell lines: molecular mechanisms that determine lower expression in cultured cells. *Xenobiotica* **32**, 505-20.

Rossi, E. (2005). Hepcidin--the iron regulatory hormone. *Clin Biochem Rev* **26**, 47-9.

Rowe, C., Goldring, C. E., Kitteringham, N. R., Jenkins, R. E., Lane, B. S., Sanderson, C., Elliott, V., Platt, V., Metcalfe, P. and Park, B. K. (2010). Network analysis of primary hepatocyte dedifferentiation using a shotgun proteomics approach. *J Proteome Res* **9**, 2658-68.

Rowe, C., Gerrard, D. T., Jenkins, R., Berry, A., Durkin, K., Sundstrom, L., Goldring, C. E., Park, B. K., Kitteringham, N. R., Hanley, K. P. and Hanley, N. A. (2013). Proteome-wide analyses of human hepatocytes during differentiation and dedifferentiation. *Hepatology* **58**, 799-809.

Russo, M. W., Galanko, J. A., Shrestha, R., Fried, M. W. and Watkins, P. (2004). Liver transplantation for acute liver failure from drug induced liver injury in the United States. *Liver Transpl* **10**, 1018-23.

Saldana-Ruiz, S., Soler-Martin, C. and Llorens, J. (2012). Role of CYP2E1-mediated metabolism in the acute and vestibular toxicities of nineteen nitriles in the mouse. *Toxicol Lett* **208**, 125-32.

Salminen, W. F., Yang, X., Shi, Q. and Mendrick, D. L. (2011). Using microRNA as biomarkers of drug-induced liver injury. *J Mol Biomark Diagn* **2**, 119.

Sancho-Bru, P., Najimi, M., Caruso, M., Pauwelyn, K., Cantz, T., Forbes, S., Roskams, T., Ott, M., Gehling, U., Sokal, E., Verfaillie, C. M. and Muraca, M. (2009). Stem and progenitor cells for liver repopulation: can we standardise the process from bench to bedside? *Gut* **58**, 594-603.

Seki, T., Yuasa, S. and Fukuda, K. (2012). Generation of induced pluripotent stem cells from a small amount of human peripheral blood using a combination of activated T cells and Sendai virus. *Nat Protoc* **7**, 718-28.

Sempere, L. F., Freemantle, S., Pitha-Rowe, I., Moss, E., Dmitrovsky, E. and Ambros, V. (2004). Expression profiling of mammalian microRNAs uncovers a subset of brain-expressed microRNAs with possible roles in murine and human neuronal differentiation. *Genome Biol* **5**, R13.

Sgro, C., Clinard, F., Ouazir, K., Chanay, H., Allard, C., Guilleminet, C., Lenoir, C., Lemoine, A. and Hillon, P. (2002). Incidence of drug-induced hepatic injuries: a French population-based study. *Hepatology* **36**, 451-5.

Shan, J., Schwartz, R. E., Ross, N. T., Logan, D. J., Thomas, D., Duncan, S. A., North, T. E., Goessling, W., Carpenter, A. E. and Bhatia, S. N. (2013). Identification of small molecules for human hepatocyte expansion and iPS differentiation. *Nat Chem Biol* **9**, 514-20.

Shi, L., Reid, L. H., Jones, W. D., Shippy, R., Warrington, J. A., Baker, S. C., Collins, P. J., de Longueville, F., Kawasaki, E. S., Lee, K. Y., Luo, Y., Sun, Y. A., Willey, J. C., Setterquist, R. A., Fischer, G. M., Tong, W., Dragan, Y. P., Dix, D. J., Frueh, F. W., Goodsaid, F. M., Herman, D., Jensen, R. V., Johnson, C. D., Lobenhofer, E. K., Puri, R. K., Schrf, U., Thierry-Mieg, J., Wang, C., Wilson, M., Wolber, P. K., Zhang, L., Amur, S., Bao, W., Barbacioru, C. C., Lucas, A. B., Bertholet, V., Boysen, C., Bromley, B., Brown, D., Brunner, A., Canales, R., Cao, X. M., Cebula, T. A., Chen, J. J., Cheng, J., Chu, T. M., Chudin, E., Corson, J., Corton, J. C., Croner, L. J., Davies, C., Davison, T. S., Delenstarr, G., Deng, X., Dorris, D., Eklund, A. C., Fan, X. H., Fang, H., Fulmer-Smentek, S., Fuscoe, J. C., Gallagher, K., Ge, W., Guo, L., Guo, X., Hager, J., Haje, P. K., Han, J., Han, T., Harbottle, H. C., Harris, S. C., Hatchwell, E., Hauser, C. A., Hester, S., Hong, H., Hurban, P., Jackson, S. A., Ji, H., Knight, C. R., Kuo, W. P., LeClerc, J. E., Levy, S., Li, Q. Z., Liu, C., Liu, Y., Lombardi, M. J., Ma, Y., Magnuson, S. R., Maqsodi, B., McDaniel, T., Mei, N., Myklebost, O., Ning, B., Novoradovskaya, N., Orr, M. S., Osborn, T. W., Papallo, A., Patterson, T. A., Perkins, R. G., Peters, E. H., Peterson, R., Philips, K. L., Pine, P. S., Pusztai, L., Qian, F., Ren, H., Rosen, M., Rosenzweig, B. A., Samaha, R. R., Schena, M., Schroth, G. P., Shchegrova, S., Smith, D. D., Staedtler, F., Su, Z., Sun, H., Szallasi, Z., Tezak, Z., Thierry-Mieg, D., Thompson, K. L., Tikhonova, I., Turpaz, Y., Vallanat, B., Van, C., Walker, S. J., Wang, S. J., Wang, Y., Wolfinger, R., Wong, A., Wu, J., Xiao, C., Xie, Q., Xu, J., Yang, W., Zhong, S., Zong, Y. and Slikker, W., Jr. (2006). The MicroArray Quality Control (MAQC) project shows inter- and intraplatform reproducibility of gene expression measurements. *Nat Biotechnol* **24**, 1151-61.

Shiraki, N., Umeda, K., Sakashita, N., Takeya, M., Kume, K. and Kume, S. (2008). Differentiation of mouse and human embryonic stem cells into hepatic lineages. *Genes Cells* **13**, 731-46.

Sison-Young, R. L., Kia, R., Heslop, J., Kelly, L., Rowe, C., Cross, M. J., Kitteringham, N. R., Hanley, N., Park, B. K. and Goldring, C. E. (2012). Human pluripotent stem cells for modeling toxicity. *Adv Pharmacol* **63**, 207-56.

Sjogren, A. K., Liljevald, M., Glinghammar, B., Sagemark, J., Li, X. Q., Jonebring, A., Cotgreave, I., Brolen, G. and Andersson, T. B. (2014). Critical differences in toxicity mechanisms in induced pluripotent stem cell-derived hepatocytes, hepatic cell lines and primary hepatocytes. *Arch Toxicol* **88**, 1427-37.

Slater, K. (2001). Cytotoxicity tests for high-throughput drug discovery. *Curr Opin Biotechnol* **12**, 70-4.

Smyth, G. K. (2004). Linear models and empirical bayes methods for assessing differential expression in microarray experiments. *Stat Appl Genet Mol Biol* **3**, Article3.

Soderdahl, T., Kuppers-Munther, B., Heins, N., Edsbagge, J., Bjorquist, P., Cotgreave, I. and Jernstrom, B. (2007). Glutathione transferases in hepatocyte-like cells derived from human embryonic stem cells. *Toxicol In Vitro* **21**, 929-37.

Starkey Lewis, P. J., Dear, J., Platt, V., Simpson, K. J., Craig, D. G., Antoine, D. J., French, N. S., Dhaun, N., Webb, D. J., Costello, E. M., Neoptolemos, J. P., Moggs, J., Goldring, C. E. and Park, B. K. (2011). Circulating microRNAs as potential markers of human drug-induced liver injury. *Hepatology* **54**, 1767-76.

Staudinger, J. L., Madan, A., Carol, K. M. and Parkinson, A. (2003). Regulation of drug transporter gene expression by nuclear receptors. *Drug Metab Dispos* **31**, 523-7.

Subramanian, K., Owens, D. J., Raju, R., Firpo, M., O'Brien, T. D., Verfaillie, C. M. and Hu, W. S. (2014). Spheroid culture for enhanced differentiation of human embryonic stem cells to hepatocyte-like cells. *Stem Cells Dev* **23**, 124-31.

Sullivan, G. J., Hay, D. C., Park, I. H., Fletcher, J., Hannoun, Z., Payne, C. M., Dalgetty, D., Black, J. R., Ross, J. A., Samuel, K., Wang, G., Daley, G. Q., Lee, J. H., Church, G. M., Forbes, S. J., Iredale, J. P. and Wilmut, I. (2010). Generation of functional human hepatic endoderm from human induced pluripotent stem cells. *Hepatology* **51**, 329-35.

Sumantran, V. N. (2011). Cellular chemosensitivity assays: an overview. *Methods Mol Biol* **731**, 219-36.

Szabo, G. and Bala, S. (2013). MicroRNAs in liver disease. *Nat Rev Gastroenterol Hepatol* **10**, 542-52.

Szkolnicka, D., Farnworth, S. L., Lucendo-Villarin, B., Storck, C., Zhou, W., Iredale, J. P., Flint, O. and Hay, D. C. (2014). Accurate prediction of drug-induced liver injury using stem cell-derived populations. *Stem Cells Transl Med* **3**, 141-8.

Szkolnicka, D., Zhou, W., Lucendo-Villarin, B. and Hay, D. C. (2013). Pluripotent stem cell-derived hepatocytes: potential and challenges in pharmacology. *Annu Rev Pharmacol Toxicol* **53**, 147-59.

Takagi, S., Nakajima, M., Mohri, T. and Yokoi, T. (2008). Post-transcriptional regulation of human pregnane X receptor by micro-RNA affects the expression of cytochrome P450 3A4. *J Biol Chem* **283**, 9674-80.

Takahashi, K., Tanabe, K., Ohnuki, M., Narita, M., Ichisaka, T., Tomoda, K. and Yamanaka, S. (2007). Induction of pluripotent stem cells from adult human fibroblasts by defined factors. *Cell* **131**, 861-72.

Takahashi, K. and Yamanaka, S. (2006). Induction of pluripotent stem cells from mouse embryonic and adult fibroblast cultures by defined factors. *Cell* **126**, 663-76.

Takebe, T., Sekine, K., Enomura, M., Koike, H., Kimura, M., Ogaeri, T., Zhang, R. R., Ueno, Y., Zheng, Y. W., Koike, N., Aoyama, S., Adachi, Y. and Taniguchi, H. (2013). Vascularized and functional human liver from an iPSC-derived organ bud transplant. *Nature* **499**, 481-4.

Thummel, K. E., Lee, C. A., Kunze, K. L., Nelson, S. D. and Slattery, J. T. (1993). Oxidation of acetaminophen to N-acetyl-p-aminobenzoquinone imine by human CYP3A4. *Biochem Pharmacol* **45**, 1563-9.

Tokusumi, T., Iida, A., Hirata, T., Kato, A., Nagai, Y. and Hasegawa, M. (2002). Recombinant Sendai viruses expressing different levels of a foreign reporter gene. *Virus Res* **86**, 33-8.

Ukairo, O., McVay, M., Krzyzewski, S., Aoyama, S., Rose, K., Andersen, M. E., Khetani, S. R. and Lecluyse, E. L. (2013). Bioactivation and toxicity of acetaminophen in a rat hepatocyte micropatterned coculture system. *J Biochem Mol Toxicol* **27**, 471-8.

Ulvestad, M., Nordell, P., Asplund, A., Rehnstrom, M., Jacobsson, S., Holmgren, G., Davidson, L., Brolen, G., Edsbagge, J., Bjorquist, P., Kuppers-Munther, B. and Andersson, T. B. (2013). Drug metabolizing enzyme and transporter protein profiles of hepatocytes derived from human embryonic and induced pluripotent stem cells. *Biochem Pharmacol* **86**, 691-702.

Vergoulis, T., Vlachos, I. S., Alexiou, P., Georgakilas, G., Maragkakis, M., Reczko, M., Gerangelos, S., Koziris, N., Dalamagas, T. and Hatzigeorgiou, A. G. (2012). TarBase 6.0: capturing the exponential growth of miRNA targets with experimental support. *Nucleic Acids Res* **40**, D222-9.

Verma, S. and Kaplowitz, N. (2009). Diagnosis, management and prevention of drug-induced liver injury. *Gut* **58**, 1555-64.

Vinken, M., Papeleu, P., Snykers, S., De Rop, E., Henkens, T., Chipman, J. K., Rogiers, V. and Vanhaecke, T. (2006). Involvement of cell junctions in hepatocyte culture functionality. *Crit Rev Toxicol* **36**, 299-318.

Vittet, D., Prandini, M. H., Berthier, R., Schweitzer, A., Martin-Sisteron, H., Uzan, G. and Dejana, E. (1996). Embryonic stem cells differentiate in vitro to endothelial cells through successive maturation steps. *Blood* **88**, 3424-31.

Wang, K., Zhang, S., Marzolf, B., Troisch, P., Brightman, A., Hu, Z., Hood, L. E. and Galas, D. J. (2009). Circulating microRNAs, potential biomarkers for drug-induced liver injury. *Proc Natl Acad Sci U S A* **106**, 4402-7.

Ward, J., Kanchagar, C., Veksler-Lublinsky, I., Lee, R. C., McGill, M. R., Jaeschke, H., Curry, S. C. and Ambros, V. R. (2014). Circulating microRNA profiles in human patients with acetaminophen hepatotoxicity or ischemic hepatitis. *Proc Natl Acad Sci U S A* 10.1073/pnas.1412608111.

Warren, L., Manos, P. D., Ahfeldt, T., Loh, Y. H., Li, H., Lau, F., Ebina, W., Mandal, P. K., Smith, Z. D., Meissner, A., Daley, G. Q., Brack, A. S., Collins, J. J., Cowan, C., Schlaeger, T. M. and Rossi, D. J. (2010). Highly efficient reprogramming to pluripotency and directed differentiation of human cells with synthetic modified mRNA. *Cell Stem Cell* **7**, 618-30.

Watkins, P. B. (2005). Idiosyncratic liver injury: challenges and approaches. *Toxicol Pathol* **33**, 1-5.

Weber, J. A., Baxter, D. H., Zhang, S., Huang, D. Y., Huang, K. H., Lee, M. J., Galas, D. J. and Wang, K. (2010). The microRNA spectrum in 12 body fluids. *Clin Chem* **56**, 1733-41.

Wilke, R. A., Lin, D. W., Roden, D. M., Watkins, P. B., Flockhart, D., Zineh, I., Giacomini, K. M. and Krauss, R. M. (2007). Identifying genetic risk factors for serious adverse drug reactions: current progress and challenges. *Nat Rev Drug Discov* **6**, 904-16.

Winbanks, C. E., Wang, B., Beyer, C., Koh, P., White, L., Kantharidis, P. and Gregorevic, P. (2011). TGF-beta regulates miR-206 and miR-29 to control myogenic differentiation through regulation of HDAC4. *J Biol Chem* **286**, 13805-14.

Wobus, A. M., Guan, K., Yang, H. T. and Boheler, K. R. (2002). Embryonic stem cells as a model to study cardiac, skeletal muscle, and vascular smooth muscle cell differentiation. *Methods Mol Biol* **185**, 127-56.

Wobus, A. M. and Loser, P. (2011). Present state and future perspectives of using pluripotent stem cells in toxicology research. *Arch Toxicol* **85**, 79-117.

Woltjen, K., Michael, I. P., Mohseni, P., Desai, R., Mileikovsky, M., Hamalainen, R., Cowling, R., Wang, W., Liu, P., Gertsenstein, M., Kaji, K., Sung, H. K. and Nagy, A. (2009). piggyBac transposition reprograms fibroblasts to induced pluripotent stem cells. *Nature* **458**, 766-70.

Xiao, F., Zuo, Z., Cai, G., Kang, S., Gao, X. and Li, T. (2009). miRecords: an integrated resource for microRNA-target interactions. *Nucleic Acids Res* **37**, D105-10.

Xu, J., Wu, C., Che, X., Wang, L., Yu, D., Zhang, T., Huang, L., Li, H., Tan, W., Wang, C. and Lin, D. (2011). Circulating microRNAs, miR-21, miR-122, and miR-223, in patients with hepatocellular carcinoma or chronic hepatitis. *Mol Carcinog* **50**, 136-42.

Yan, Z., Li, J., Huebert, N., Caldwell, G. W., Du, Y. and Zhong, H. (2005). Detection of a novel reactive metabolite of diclofenac: evidence for CYP2C9-mediated bioactivation via arene oxides. *Drug Metab Dispos* **33**, 706-13.

Yasunaga, M., Tada, S., Torikai-Nishikawa, S., Nakano, Y., Okada, M., Jakt, L. M., Nishikawa, S., Chiba, T. and Era, T. (2005). Induction and monitoring of definitive and visceral endoderm differentiation of mouse ES cells. *Nat Biotechnol* **23**, 1542-50.

Ye, J., Coulouris, G., Zaretskaya, I., Cutcutache, I., Rozen, S. and Madden, T. L. (2012). Primer-BLAST: a tool to design target-specific primers for polymerase chain reaction. *BMC Bioinformatics* **13**, 134.

Yi, F., Liu, G. H. and Izpisua Belmonte, J. C. (2012). Human induced pluripotent stem cells derived hepatocytes: rising promise for disease modeling, drug development and cell therapy. *Protein Cell* **3**, 246-50.

Yildirimman, R., Brolen, G., Vilardell, M., Eriksson, G., Synnergren, J., Gmuender, H., Kamburov, A., Ingelman-Sundberg, M., Castell, J., Lahoz, A., Kleinjans, J., van Delft, J., Bjorquist, P. and Herwig, R. (2011). Human embryonic stem cell derived hepatocyte-like cells as a tool for in vitro hazard assessment of chemical carcinogenicity. *Toxicol Sci* **124**, 278-90.

Yu, J., Hu, K., Smuga-Otto, K., Tian, S., Stewart, R., Slukvin, II and Thomson, J. A. (2009). Human induced pluripotent stem cells free of vector and transgene sequences. *Science* **324**, 797-801.

Yusa, K., Rad, R., Takeda, J. and Bradley, A. (2009). Generation of transgene-free induced pluripotent mouse stem cells by the piggyBac transposon. *Nat Methods* **6**, 363-9.

Zhao, J., Lammers, P., Torrance, C. J. and Bader, A. G. (2013). TP53-independent function of miR-34a via HDAC1 and p21(CIP1/WAF1.). *Mol Ther* **21**, 1678-86.

Zhou, H., Wu, S., Joo, J. Y., Zhu, S., Han, D. W., Lin, T., Trauger, S., Bien, G., Yao, S., Zhu, Y., Siuzdak, G., Scholer, H. R., Duan, L. and Ding, S. (2009). Generation of induced pluripotent stem cells using recombinant proteins. *Cell Stem Cell* **4**, 381-4.

Zhu, S., Li, W., Zhou, H., Wei, W., Ambasudhan, R., Lin, T., Kim, J., Zhang, K. and Ding, S. (2010). Reprogramming of human primary somatic cells by OCT4 and chemical compounds. *Cell Stem Cell* **7**, 651-5.